April 1982
R82AEB285

ENERGY EFFICIENT ENGINE

COMPONENT DEVELOPMENT & INTEGRATION

NAS3-20643

SEMIANNUAL REPORT No. 8

October 1, 1981 - March 31, 1982

Prepared for

NATIONAL AERONAUTICS AND SPACE ADMINISTRATION
LEWIS RESEARCH CENTER
21000 BROOKPARK ROAD
CLEVELAND, OHIO 44135

GENERAL ELECTRIC

AIRCRAFT ENGINE BUSINESS GROUP
ADVANCED ENGINEERING AND
TECHNOLOGY PROGRAMS DEPARTMENT
CINCINNATI, OHIO 45215

NAS3-20643
April 1982
R82AEB285

ENERGY EFFICIENT ENGINE COMPONENT DEVELOPMENT & INTEGRATION PROGRAM

SEMIANNUAL REPORT No. 8

October 1, 1981 - March 31, 1982

General Electric Project Manager

R.W. Bucy

Prepared for

NATIONAL AERONAUTICS AND SPACE ADMINISTRATION
LEWIS RESEARCH CENTER
21000 BROOKPARK ROAD
CLEVELAND, OHIO 44135

Carl C. Ciepluch - NASA Project Manager

General Electric Company
Aircraft Engine Business Group
Advanced Engineering and Technology Programs Department
Cincinnati, Ohio 45215

FOREWORD

This contract effort is being conducted by NASA as part of the Energy Efficient Engine project. It is managed by the NASA Lewis Research Center, with Carl C. Ciepluch serving as the NASA Project Manager and Peter G. Batterton serving as the NASA Assistant Project Manager responsible for this contract.

This semiannular report covers the work performed under Contract NAS3-20643 for the period of October 1, 1981 through March 31, 1982. It is published for technical information only and does not necessarily represent recommendations, conclusions, or the approval of NASA. The data generated under this contract are being disseminated with the U.S. in advance of general publication in order to accelerate domestic technology transfer. Since all data reported herein are preliminary, they should not be published by the recipients prior to general publication of the data by either the Contractor or NASA.

Selected portions of the data (that is, those data pertaining to specific component design details) are considered to have significant early commercial potential. As such, these data are designated as Category 2 Data under NASA FEDD (For Early Domestic Dissemination) policy and are restricted from foreign dissemination for at least two years from the date of this report. Category 2 data may be duplicated and used by the recipient with the expressed limitation that the data will not be published or released to foreign parties during this period without the expressed permission of the General Electric Company and appropriate export licenses. Release of Category 2 data to other domestic parties shall only be made subject to the stipulation that all recipients must agree, prior to receiving these data, to abide by the limitations of the FEDD legend on the cover of this report.

TABLE OF CONTENTS

TABLE OF CONTENTS (Continued)

TABLE OF CONTENTS (Continued)

TABLE OF CONTENTS (Continued)

TABLE OF CONTENTS (Concluded)

LIST OF ILLUSTRATIONS

LIST OF ILLUSTRATIONS (Continued)

LIST OF ILLUSTRATIONS (Continued)

LIST OF ILLUSTRATIONS (Continued)

LIST OF ILLUSTRATIONS (Continued)

LIST OF ILLUSTRATIONS (Continued)

LIST OF ILLUSTRATIONS (Concluded)

LIST OF TABLES

LIST OF TABLES (Concluded)

INTRODUCTION

This is the eighth semiannual report under Contract NAS3-20643 - NASA Energy Efficient Engine (E^3) Component Development and Integration Program. The report covers the period October 1, 1981 through March 31 1982.

The program objective is the development of technology that will improve the energy efficiency of propulsion systems for subsonic commercial aircraft of the late 1980's or early 1990's. The following goals have been established.

- Fuel Consumption - A reduction in Flight Propulsion System (FPS) cruise installed specific fuel consumption (sfc) of at least 12% compared to the reference CF6-50 engine. (Cruise is defined as Mach 0.8 and 35,000 feet on a standard day at maximum cruise power without bleed or power extraction.)

- Direct Operation Cost (DOC) - A DOC reduction of at least 5% based on advanced aircraft with E^3 compared to scaled CF6-50C.

- Noise - FAR Part 36 (as amended July 1978) with provision for engine growth corresponding to future engine application.

- Emissions - EPA new engine standards, January 1981:

CO	(lbm/1000 lbf-hr per cycle)	3.0
HC	(lbm/1000 lbf-hr per cycle)	0.5
NO_x	(lbm/1000 lbf-hr per cycle)	3.0
Smoke	(SAE-SN)	20.0

General Electric is projecting a reduction of 14.4% in cruise installed sfc and a DOC reduction in excess of the 5% goal. Noise and emissions projections are consistent with the established goals.

In addition to the foregoing, growth of the FPS is being considered from the outset. A minimum installed-thrust level of 36,500 lbf has been established for the FPS at takeoff. A planned growth of 20% maximum-climb thrust over the baseline rating is desired without compromise of the foregoing goals. Components of the engine are to be designed with consideration for growth and the competitiveness of the initial engine.

Commercial transport engine requirements will be factored into the development effort, as appropriate, with the objectives of (1) making the resulting

technology useful for subsequent commercial application and (2) normalizing the risk of any future commercial developments.

Four major technical tasks have been established for the E^3 program. Task 1 addresses the design and evaluation of the E^3 Flight Propulsion System; this propulsion system is designed to meet the requirements for commercial service and includes a flight nacelle. The Task 1 results will establish the requirements for the experimental test hardware including the components, core, and integrated core/low spool. Task 2 consists of the design, fabrication, and testing of the components and includes supporting technology efforts. These supporting technology efforts are to be performed where required to provide verification of advanced concepts included in the propulsion system design. In addition, more advanced technologies that are not specifically included in the propulsion system design but which provide the potential for further performance improvements are also to be explored. Task 3 involves the design, fabrication, and test evaluation of the core engine consisting of the compressor, combustor, and high-pressure turbine. Task 4 comprises integration of the core with the low-spool components and test evaluation of the integrated core/low spool (ICLS). At the conclusion of the program, the latest performance of the experimental hardware (integrated core/low spool and concurrent core and component efforts) will be factored into a final propulsion system/aircraft evaluation (as part of continual, ongoing evaluations in Task 1) to determine achievable performance as compared to program goals. Task 5 is a nontechnical task that encompasses the Project/Program Management and Control System established for the contract. The Master Program/Project Schedule is shown in Figure 1.

This report provides a review of the work accomplished during the first 51 months of the E^3 contract, with emphasis on accomplishments during the past 6 months. It is a progress report, and the data contained herein are subject to change during the remaining period of performance. The report is responsive to and consistent with the requirements of the Statement of Work.

Summary of Progress - The first 60 days under contract were devoted to planning the program. This period culminated in the Work Plan, the basis of which is the Work Breakdown Stuctures (WBS) established in accordance with

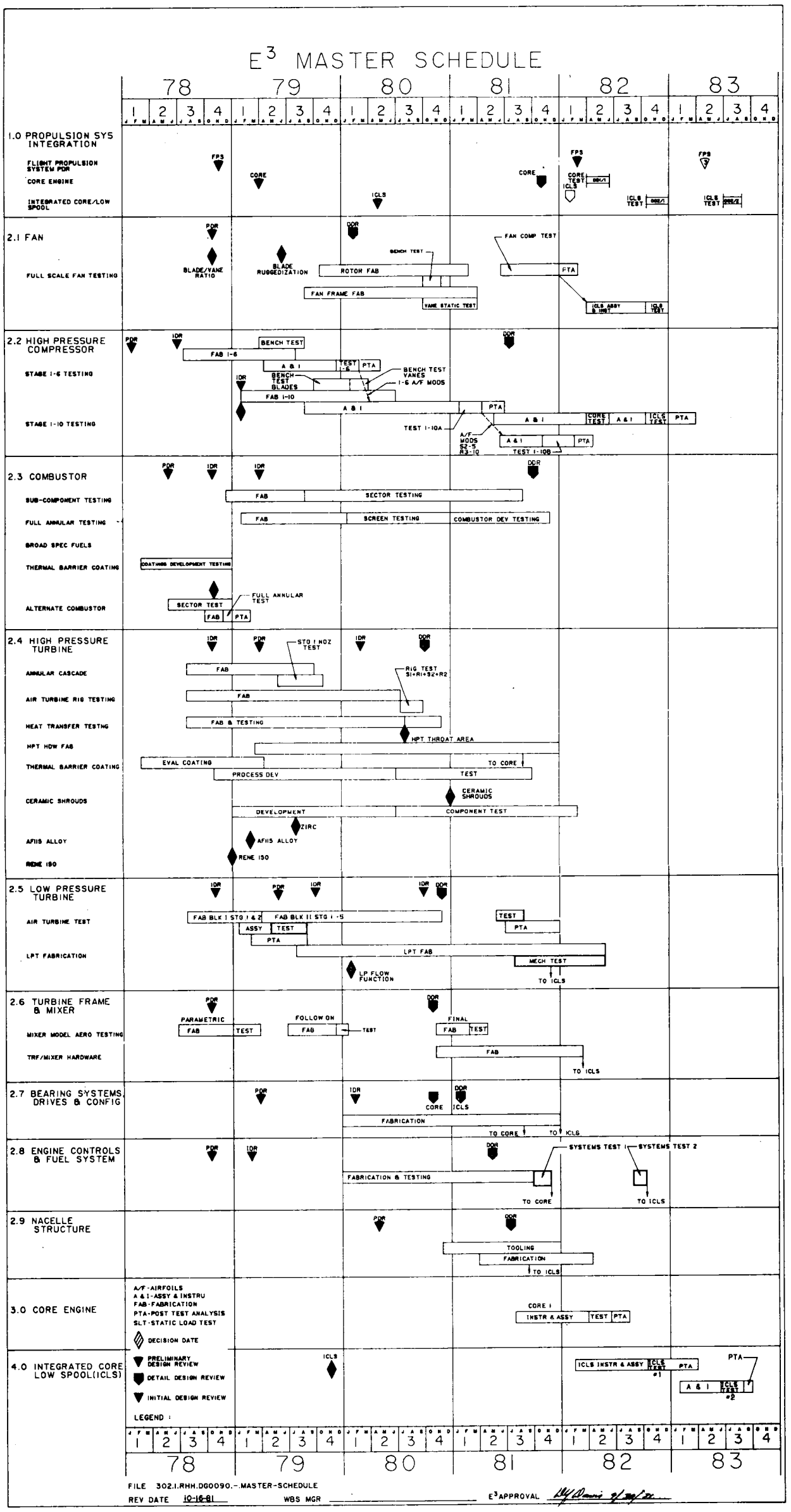

Figure 1. Master Program Schedule.

the elements contained in the contract Statement of Work. The WBS is presented in Table I in an abbreviated form. Program and design highlights, progress, and overall perspective are reported herein for the systems and components. All WBS items in which work was performed during this report period are documented. Some of the highlights during this report period are:

- All core engine hardware has been received. Long-Lead, critical items were accelerated and assembly sequences changed so that core assembly is currently projected to be complete on or before 6/30/82.
- Approximately 75% of the ICLS hardware has been received.
- Trial assembly of the nacelle, pylon, and mounts with a dummy engine is underway.
- Fan rig testing has been completed. Performance map data show the max-cruise efficiencies are 1.5% above the rig target for the fan bypass and 1.3% for the fan hub booster. These efficiencies are respectively 0.5% and 0.3% above the FPS engine goal.
- Testing of the 10B compressor rig is in progress. Stall margin and efficiency have improved over the 10A rig. A further variation in the compressor will be tested in the core engine.
- All combustor rig testing has been completed. All performance and emissions goals except NO_x have been met for the core engine combustor. With further tuning of dilution flow, NO_x is expected to be met in the FPS combustor.
- The low pressure turbine (LPT) rig exceeded the ICLS efficiency goal by 0.3%. An additional 0.25% gets credited for the flaired flowpath in the FPS.
- The combustor detailed design review (DDR) was presented, completing all component DDR's.
- The core DDR was presented.
- The FPS design and benefits were updated.
- The 30-item/20-item screening has been completed for the post-FPS technology cost-benefit study.

Table I. Work Breakdown Structure.

1.0	Task 1 - Propulsion System Analysis, Design, and Integration
1.1	Propulsion System
1.2	Cycle and Performance
1.3	Materials and Processes
1.4	Acoustic Development
1.5	Propulsion System Aircraft Integration and Development
1.6	Benefit/Cost Study
2.0	Task 2 - Component Analysis, Design, and Development
2.1	Fan
2.2	Compressor
2.3	Combustor
2.4	High Pressure Turbine
2.5	Low Pressure Turbine
2.6	Turbine Frame and Mixer
2.7	Bearings, Systems, Drives, and Configuration
2.8	Engine Controls and Fuel System
2.9	Nacelle Structure
3.0	Task 3 - Core Testing
3.1	Initial Core Build
3.2	Second Core Build
3.3	Core Posttest Analysis
4.0	Task 4 - Integrated Core/Low Spool (ICLS) Testing
4.1	ICLS Engineering and Analysis
4.2	ICLS Fabrication
4.3	ICLS Assembly and Instrumentation
4.4	ICLS Test Facilities Engineering
4.5	ICLS Testing
4.6	ICLS Posttest Analysis
4.7	Follow-on ICLS Testing
5.0	Task 5 - Management
5.1	Project Management
5.2	Configuration Management
5.3	Reporting

1.0 TASK 1 - PROPULSION SYSTEM ANALYSIS, DESIGN, AND INTEGRATION

Overall Objectives

The primary objectives of this task are to provide the preliminary design of the flight propulsion system and to evaluate the progress of the FPS to ensure that NASA program goals are being met. In addition, periodic updates and reassessments of the FPS will be conducted to ensure that FPS projections contain the most current information available from the component-technology program. Periodic preliminary design reviews (PDR) based on material and data developed under this task will be conducted to provide program status information.

As part of this task, cycle decks and performance projections for the FPS will be developed and kept current. All system-integration efforts are conducted through this task, such as FPS layouts, overall assembly drawings, parts lists, and design-change monitoring. All aspects of the system, including acoustic evaluation, aircraft integration, engine dynamics, reliability, life management, and fan and compressor compatibility, are coordinated; the results are incorporated under Task 1. Other results are the evaluation of the system benefits of the FPS and a determination as to whether direct operating cost and fuel savings goals are being met. Another objective of this task is to conduct a supporting material-technology program and to provide the reviews of the material selected for use in the program.

Task 1 also has the objectives of providing preliminary core engine and integrated core/low spool designs, appropriate efforts to integrate the designs, and hardware support for core/ICLS testing. In addition, core and ICLS PDR's and DDR's will be conducted based on the data generated during the task.

Development Approach

Evaluation and updates of the FPS will be accomplished by blending information that becomes available from the preliminary design phases of the FPS, core, and ICLS with information that becomes available from Tasks 2, 3, and 4 as the program proceeds.

Initially, layouts and system characteristics were developed from the proposal FPS and any subsequent modifications that occurred before and after the first FPS PDR. Information from the supporting efforts under the Propulsion System Design effort will be combined with that from the other Task 1 efforts, such as aircraft integration and evaluation, and acoustic studies to update the FPS status.

As changes and new estimates of component and system performance become available, new layouts and system-evaluation updates will be generated for the appropriate FPS PDR.

Continual monitoring of the core and ICLS designs and hardware, along with implementation of the system-integration responsibility, will ensure that accurate knowledge of the FPS configurations and characteristics is always available. It also ensures that changes to the core and ICLS, which could adversely affect the performance of the FPS, will be known and that action will be taken, when necessary, to prevent FPS degration.

As the program proceeds, all important aspects of core and ICLS performance and characteristics will be translated into meaningful information for FPS PDR's. Final program results and a final FPS projection will be obtained and communicated in this manner.

Flight Propulsion System Description

General Electric's proposed E^3 Flight Propulsion System is a high-bypass, dual-rotor, axial-flow turbofan with a fan pressure ratio of 1.65 and an overall pressure ratio of 38 at maximum climb, the power-matching point. At maximum cruise, the bypass ratio is approximately 7. For the sea level takeoff (SLTO) maximum thrust rating of 36,500 lbf, the combustion temperature for the FPS is projected to be 2450° F. A symmetrical nacelle with a long-duct, mixed-flow nozzle complete the installation. A cross section of the proposed installed engine is shown in Figure 2.

The major engine components are the fan rotor and stator module; the core engine, consisting of the compressor, combustor, and two-stage turbine; the LPT module, mounting provisions, and exhaust mixer; and the core-mounted accessories.

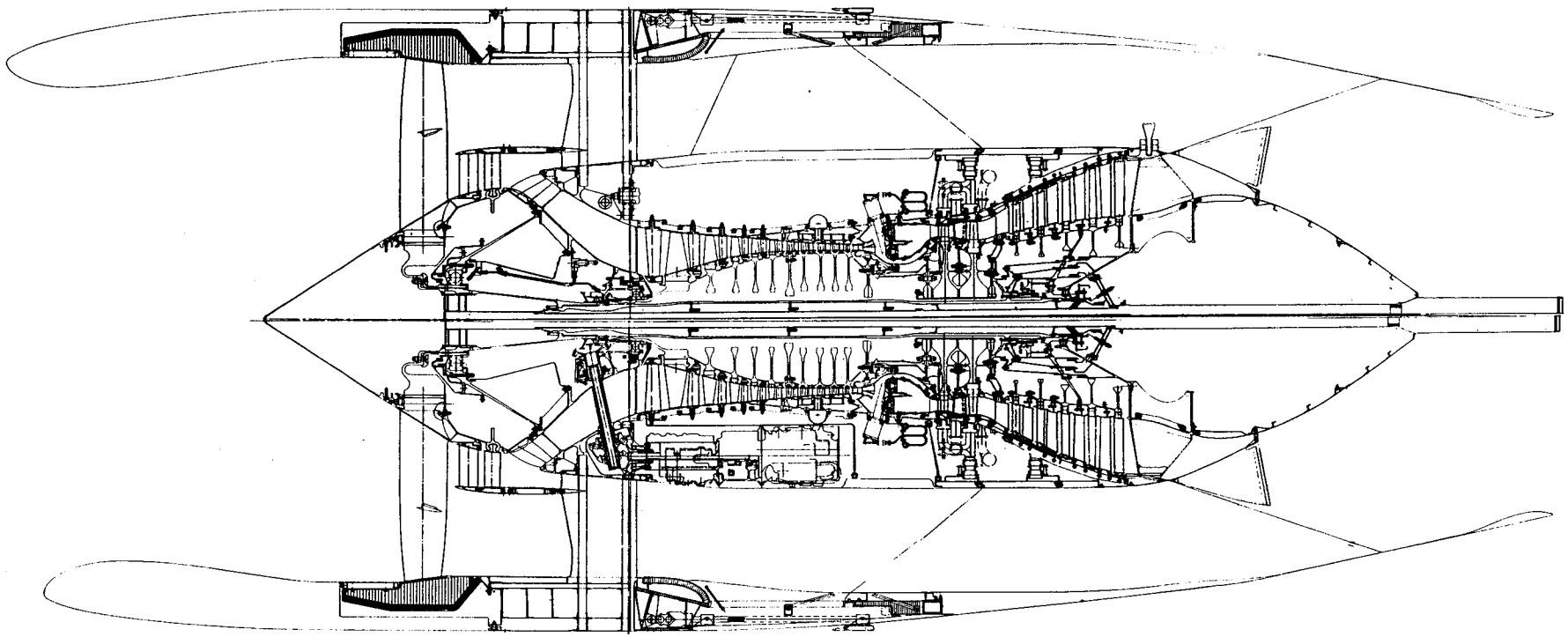

Figure 2. E^3 Propulsion System.

The fan rotor, consisting of a 32-blade fan stage and a 56-blade quarter stage for core compressor supercharging, is driven by a five-stage turbine. Titanium was utilized for blading to provide foreign object damage (FOD) ruggedness. The quarter stage provides approximately 1.7 times as much air as the core requires. The excess air is bypassed into the fan exhaust duct, providing automatic flow matching and FOD separation. The fan turbine uses tip shrouds and blade/vane root overlap to reduce leakage and aerodynamic losses. A circumferentially continuous fan turbine casing (coupled with modulated casing cooling) provides active clearance control. Increased blade numbers are used in the next-to-last fan turbine stage to raise pure-tone frequencies and reduce perceived noise.

The fan frame is integrated with the fan outer duct and nacelle to provide a stiff, lightweight structure. The outer frame and duct are constructed of graphite-epoxy materials; the inner frame is aluminum. Containment for the fan blades is provided by a hybrid system of steel backed by wrapped Kevlar.

The core compressor has 10 stages of rugged, low-aspect-ratio blading to reduce stress levels and erosion, and it provides a compression ratio of 23 at the maximum-climb matching point. The last five stages of the compressor have active clearance control and a separate aft casing support to improve running clearances. There are five stages of variable-geometry vanes to improve matching and efficiency at off-design conditions, and seventh-stage bleed is available for starting.

The combustor is a double-annular design for low emissions and is patterned after the combustor developed under a NASA low-emissions combustor development program based on the CF6 engine. A shingle liner configuration is employed; the hot, shingle liner is nonstructural (except for cooling and pressure loads) while the cool, outer liner is used for all combustor support and positioning functions. The outer combustor nozzles are used for low-thrust conditions; as thrust is increased, the inner set of main nozzles begins to function.

A two-stage turbine completes the core engine configuration. Advanced, directionally solidified (DS) René 150 is used for the Stage 1 and 2 blading

and the Stage 2 vanes. The Stage 1 vanes are constructed of an oxide-dispersion-solidified (ODS) material that has provided good service in other high-temperature nozzle applications. Both turbine disks are boltless designs with smooth side plates for low windage losses. For increased thermodynamic efficiency, the cooling-air circuits have been configured to provide the coolest air possible with no excess pressure losses or leakage. The cooling circuit for the Stage 1 blade also provides a cooling layer over the compressor and turbine interconnecting shaft. Active clearance control over the turbine is achieved with an engine control function that selectively cools the support rings of the shrouds, permitting blade running clearance to be changed thermally under transient and steady-state conditions to permit minimum blade-to-shroud average clearances.

A double-wall design is used in the hot aft sump to ensure that the inner sump is adequately cooled. Two separate sources of cooling air purge the outer and inner walls of the aft sump to prevent any inadvertent overheating. A center vent system exhausts the sump pressurization air back through the exhaust cone to the engine nozzle region.

The engine accessory gearbox is located in the engine core compartment. This location allows the nacelle diameter to be smaller and results in lower nacelle drag. The basic engine design will accommodate an alternate accessory location on the fan case if that arrangement is ultimately preferred by some users.

The engine nacelle is a symmetrical, long-duct, mixed-flow design that makes extensive use of lightweight composites to reduce cost and weight. Sound suppression is integrated into the inner walls of the inlet, fan frame, fan duct, core cowl, and nozzle. The thrust reverser is a directed-cascade type with no links crossing through the fan duct. When deployed, cooling-air slots are opened to allow cool ambient air to enter the region aft of the blocker doors to prevent the composite material from overheating due to hot, recirculating, core-exhaust gas. No thrust reverser is used for the core stream since the core thrust is effectively spoiled by the overexpansion of mixer exhaust into the fan nozzle when the fan air is blocked off.

Mounting provisions permit the point mount loads to be transferred into the engine in a smooth, attenuated manner. Thrust side and vertical loads are transferred into the forward engine frame; roll side and vertical loads are taken out by the aft mount attached to the LPT frame.

1.1 PROPULSION SYSTEM DESIGN

1.1.1 System Integration

Technical Progress

The final mixer benefit was identified. A 2.9% improvement in sfc is attributed to the FPS mixer. This is a projection of a reasonable goal based on mixer tests. It could be achieved by further tuning (flattening temperature profiles) of demonstrated mixer technology.

The FPS hot flowpath was updated to include the flaired LPT and the final mixer.

A decision was made that thermal-barrier coating will be incorporated into the final FPS. The exact configuration and benefits will be determined later and are not included in the current FPS.

The FPS materials drawing is shown in Figure 3, and the cooling-air and secondary-flow drawing is shown in Figure 4.

A general update of the FPS was completed and submitted to NASA. This covered changes in design, weight, emissions, acoustics, performance, and economic benefits from the original PDR to the present. The effect of escalated fuel price was included. Component test experience has been very successful; several components have demonstrated performance substantially above target levels. Because compressor testing and the analysis of fan rig performance are currently underway, credits for improved design-point performance were not taken in the update. Therefore, sfc is not significantly different from levels in the previous review. DOC improvement of the E^3 relative to current production engines is substantially better than it was in the previous review. In the update, the improvement in DOC was mainly due to higher fuel prices. The updated FPS exceeds performance, emissions, acoustic, and economic goals.

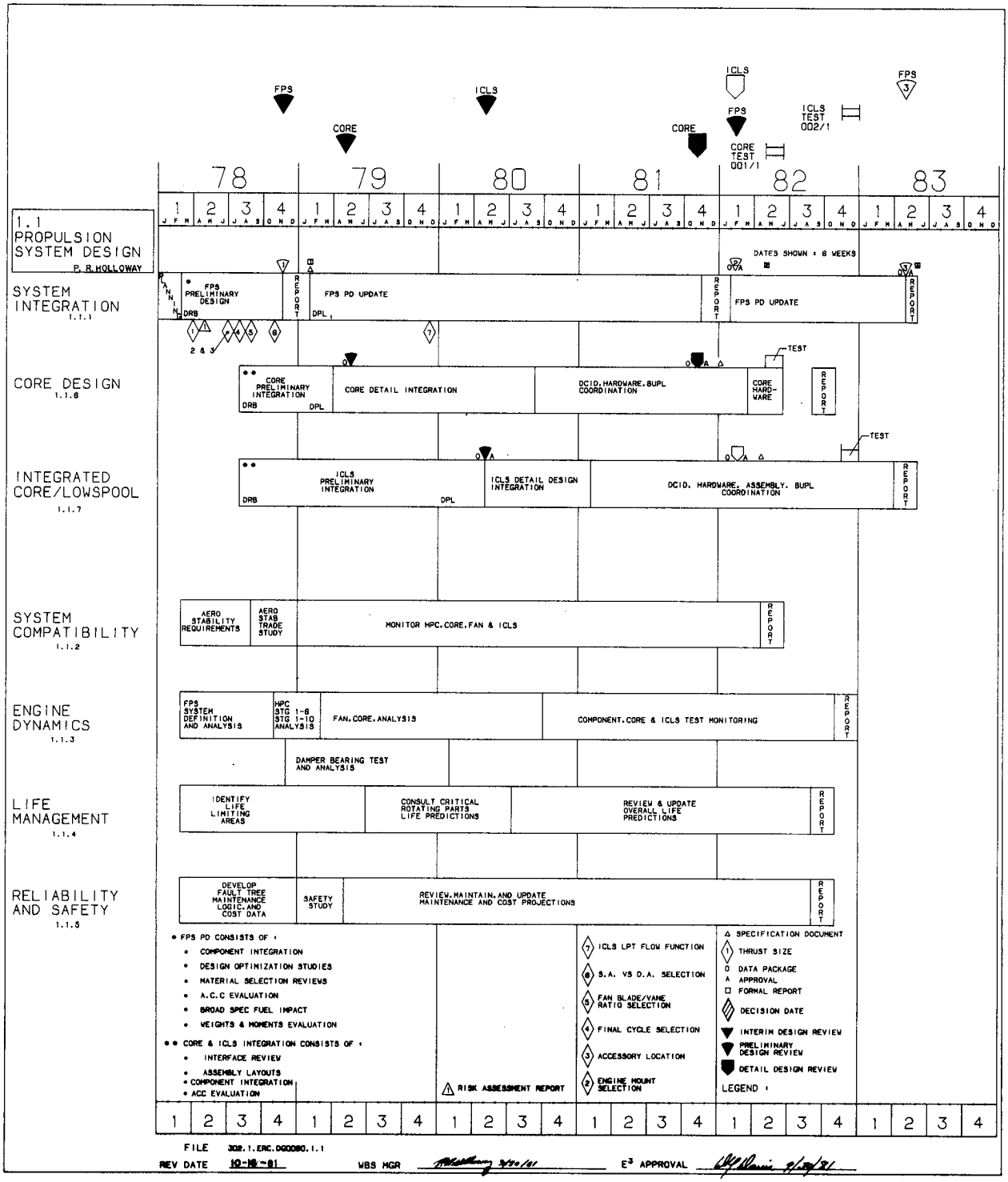
1.1 PROPULSION SYSTEM DESIGN
P. R. HOLLOWAY
SYSTEM INTEGRATION 1.1.1
CORE DESIGN 1.1.6
INTEGRATED CORE/LOWSPOOL 1.1.7
SYSTEM COMPATIBILITY 1.1.2
ENGINE DYNAMICS 1.1.3
LIFE MANAGEMENT 1.1.4
RELIABILITY AND SAFETY 1.1.5
78
79
80
81
82
83
FPS
ICLS
CORE
CORE TEST 001/1
ICLS TEST 002/1
DATES SHOWN = 6 WEEKS
FPS PRELIMINARY DESIGN
FPS PD UPDATE
CORE PRELIMINARY INTEGRATION
CORE DETAIL INTEGRATION
DCID, HARDWARE, &UPL COORDINATION
CORE HARDWARE
ICLS PRELIMINARY INTEGRATION
ICLS DETAIL DESIGN INTEGRATION
DCID, HARDWARE, ASSEMBLY, BUPL COORDINATION
AERO STABILITY REQUIREMENTS
AERO STAB TRADE STUDY
MONITOR HPC, CORE, FAN & ICLS
FPS SYSTEM DEFINITION AND ANALYSIS
HPC STG 1-8 STG 1-10 ANALYSIS
FAN, CORE, ANALYSIS
COMPONENT, CORE & ICLS TEST MONITORING
DAMPER BEARING TEST AND ANALYSIS
IDENTIFY LIFE LIMITING AREAS
CONSULT CRITICAL ROTATING PARTS LIFE PREDICTIONS
REVIEW & UPDATE OVERALL LIFE PREDICTIONS
DEVELOP FAULT TREE MAINTENANCE LOGIC AND COST DATA
SAFETY STUDY
REVIEW, MAINTAIN, AND UPDATE MAINTENANCE AND COST PROJECTIONS
REPORT
DRB
DPL
TEST
* FPS PD CONSISTS OF :
COMPONENT INTEGRATION
DESIGN OPTIMIZATION STUDIES
MATERIAL SELECTION REVIEWS
A.C.C EVALUATION
BROAD SPEC FUEL IMPACT
WEIGHTS & MOMENTS EVALUATION
** CORE & ICLS INTEGRATION CONSISTS OF :
INTERFACE REVIEW
ASSEMBLY LAYOUTS
COMPONENT INTEGRATION
ACC EVALUATION
RISK ASSESSMENT REPORT
ICLS LPT FLOW FUNCTION
S.A. VS D.A. SELECTION
FAN BLADE/VANE RATIO SELECTION
FINAL CYCLE SELECTION
ACCESSORY LOCATION
ENGINE MOUNT SELECTION
SPECIFICATION DOCUMENT
THRUST SIZE
DATA PACKAGE
APPROVAL
FORMAL REPORT
DECISION DATE
INTERIM DESIGN REVIEW
PRELIMINARY DESIGN REVIEW
DETAIL DESIGN REVIEW
LEGEND :
FILE 302.1.ERC.DGOOBO.1.1
REV DATE 10-16-81
WBS MGR
E³ APPROVAL

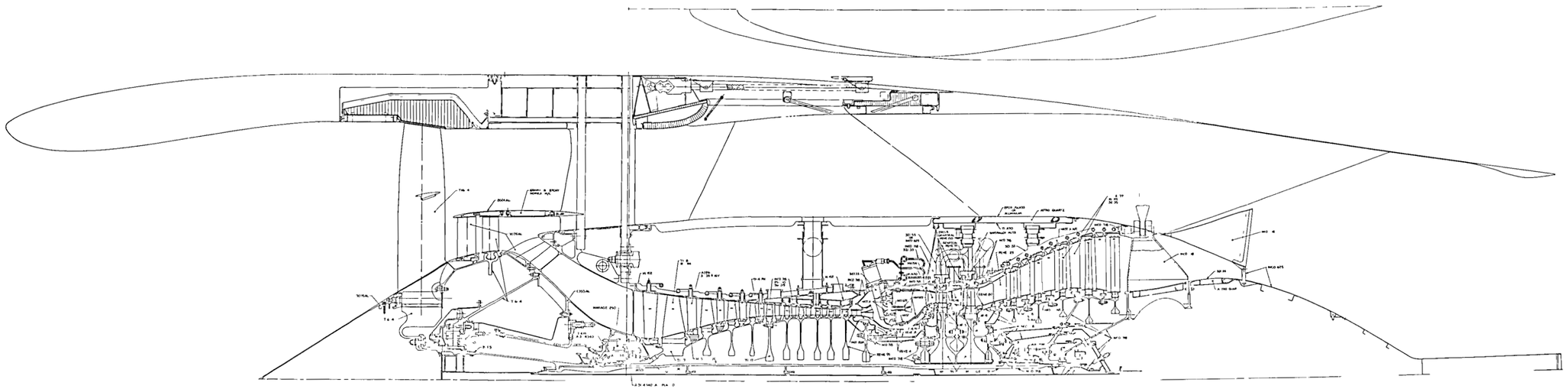

Figure 3. FPS Material Identification.

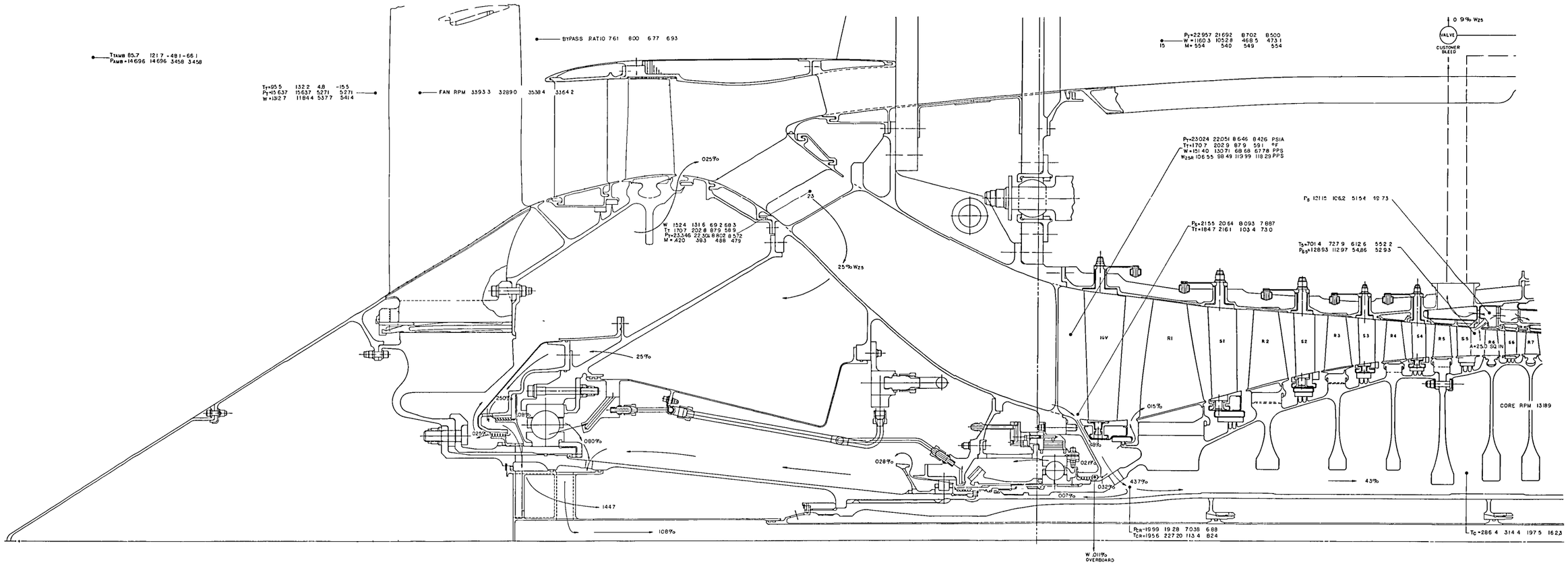

Figure 4. FPS Operating Parameters and Cooling-Supply System.

Work Planned

Complete the Preliminary Analysis and Design Report No. 2 and update the FPS Configuration Document. Incorporate component rig results into the FPS.

1.1.2 System Compatibility

Technical Progress

Test plans were prepared and coordinated with the Compressor Aero Design Group for the 10B compressor component distortion test. Interstage dynamic pressure data were also monitored during all compressor stalls.

The distortion testing was conducted with three screens which provided basic total-pressure distortion patterns. The tip radial and hub radial screens have been tested at corrected compressor speeds of 92.5, 95.0, 97.5, and 100%. The 180° 1/rev screen was tested at speeds of 92.5, 95.5, and 97.5%. This screen produced a distortion level higher than the design intent. A new 180° 1/rev screen with lower distortion was designed and is planned for testing at speeds of 97.5 and 100%.

Dynamic-pressure data were recorded during many compressor stalls. The data covered a wide range of compressor speeds and stator schedules for both clean and distorted flow testing.

Work Planned

The distortion data will be analyzed to determine compressor sensitivities to radial and circumferential distortions. The stability characteristics of the compressor will be determined using these sensitivities.

The waveforms acquired during the compressor stall tests wil be analyzed to identify the compressor stalling stage and to characterize the sequence of events near stall and at stall.

1.1.3 Engine Dynamics

Full-Scale, 10-Stage Compressor Rig

The second full-scale, 10-stage HP compressor test was initiated. Vibration levels were low and within limits at all speeds up to and including the

maximum speed of 12,000 rpm. The vibration signature was similar to that of the first build, and the frequency-response characteristics agreed with pre-test analytical projections.

The second compressor vehicle employed the same soft-mount suspension system and squeeze-film damper configuration that was used for the first build. The suspension system provided for rotor vibration isolation, and squeeze-film dampers located at the No. 1 and No. 2 bearings were utilized to dissipate the vibration energy associated with the rigid-body modes. The soft mounts allowed the rotor to run in a dynamically stiff configuration; i.e., rotor bending did not occur over the operating-speed range. The combined effect of the suspension system and dampers resulted in a rotor that had a very low sensitivity to unbalance. Figure 5 illustrates the frequency-response characteristics at the soft side of the No. 1 bearing support from a representative test run.

Full-Scale Fan Rig

The full-scale fan test program was completed after successfully field balancing the vehicle. Vibration-response characteristics were acceptable throughout the speed range encountered which included a maximum physical speed of 3922 rpm. The field balance was required due to the higher than anticipated response of the outer duct and forward containment case. The high response was associated with the Lynn test facility interface and is not expected to be a problem during ICLS testing.

Work Planned

- Complete full-scale HP compressor 10B test and posttest data reduction/analysis correlation
- Conduct core demonstrator test program and correlate test results with analysis
- Continued evaluation of FPS and ICLS

1.1.6 Core Analysis and Design

General Electric will test the E^3 core during the third quarter of 1982. The core-test engine uses a flight-design compressor, combustor, and HPT with

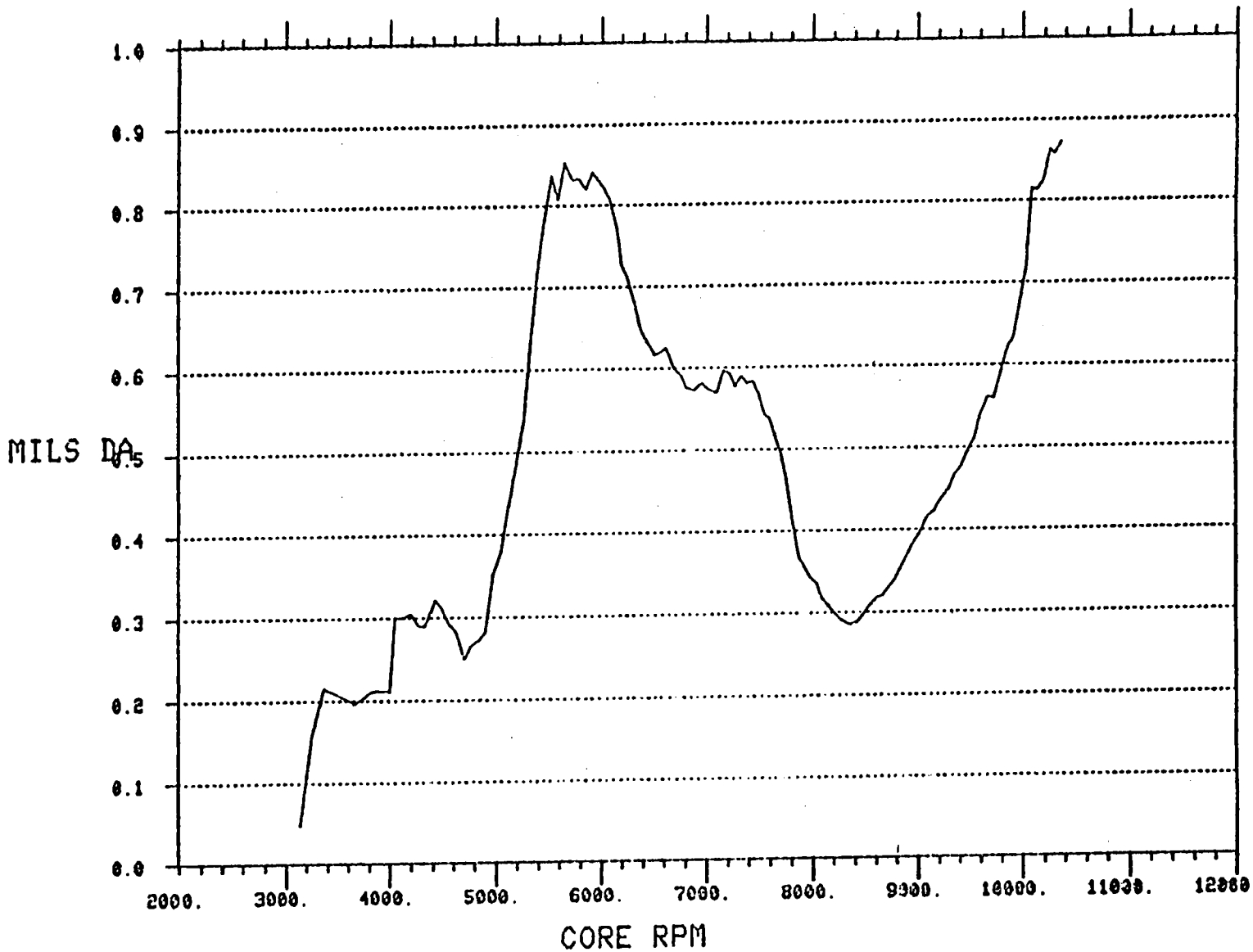

Figure 5. Ten-Stage HPC Rig Synchronous Vibration Response on the Forward-Bearing Damper Housing.

the associated key cooling, clearance control, secondary flow, and bleed circuits. Nonflight front and rear frames, inlet, exhaust, gearbox, and digital engine control are used. The engine is heavily instrumented and is configured for development testing by employing two extra variable compressor stages and variable exhaust nozzle area that can be changed to vary the operating line.

The purposes of testing the core engine are to determine core performance, component performance in an engine environment, mechanical integrity, aeromechanical characteristics, system dynamics, and thermal characteristics. This provides an evaluation of the FPS design and establishes core readiness for the ICLS test.

The core will be tested in a cell with ram inlet capability and extensive inlet-flow instrumentation. Testing the core independently from the fan and LPT allows simulation of altitude flight conditions which cannot be accomplished in a turbofan engine test at sea level static conditions. Separate core testing allows the instrumentation and flow measurements necessary to determine component performance in the engine.

Technical Progress

The core cross section is shown in Figure 6, materials are shown in Figure 7, and external piping is shown in Figure 8. The cooling and secondary-flow drawing was updated to reflect increased HPT Stage 1 shroud leakage. The drawing is shown in Figure 9. Increased HPT Vane 2 cooling flows due to hardware deviations were defined after the drawing was issued and will be incorporated in a subsequent update.

The core clearance assembly drawing, which specifies limits on clearances and fits, was issued. A review of sign-offs of interfaces between design groups was completed. The engine/facility interface drawing, which specifies locations and orientations of connections between the engine and the facility, was updated. The core stackup drawing was issued following the issuing of the last of the component stackup drawings. The core stackup drawing defines areas of responsibility and lists component stackup drawings. It had served as a working document prior to formal issue.

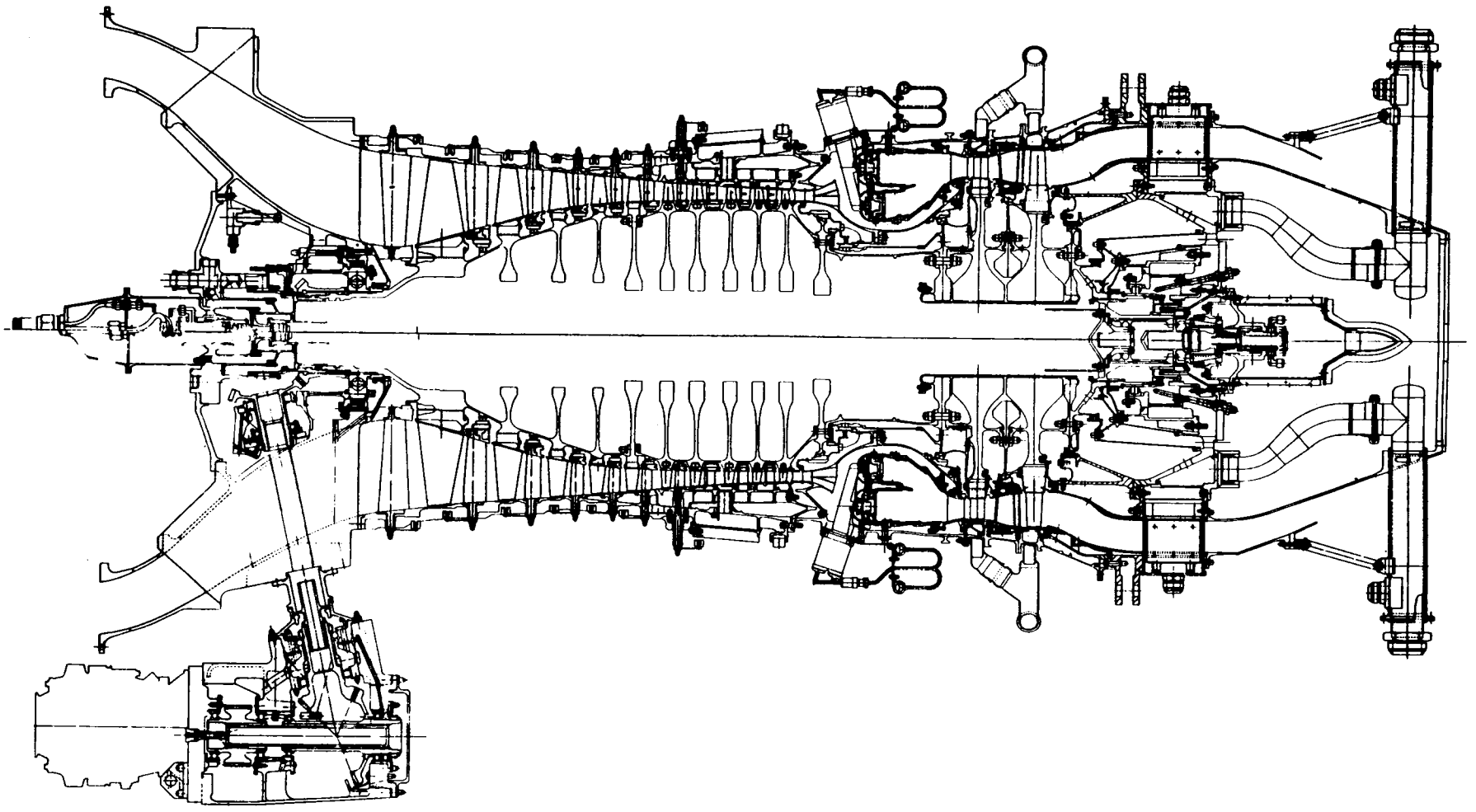

Figure 6. Core Engine.

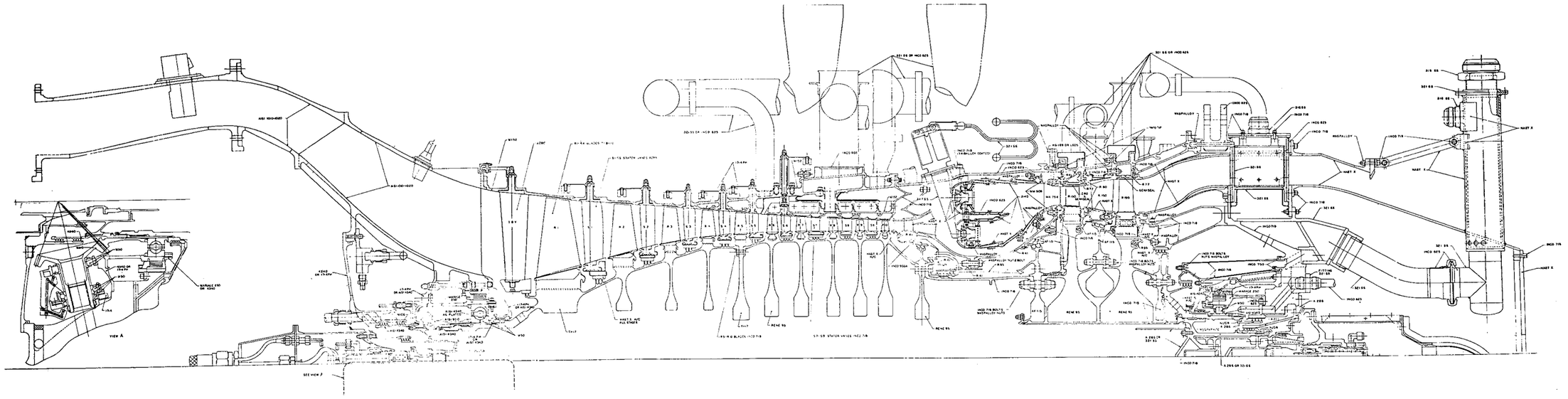

Figure 7. Core Engine Materials Identification.

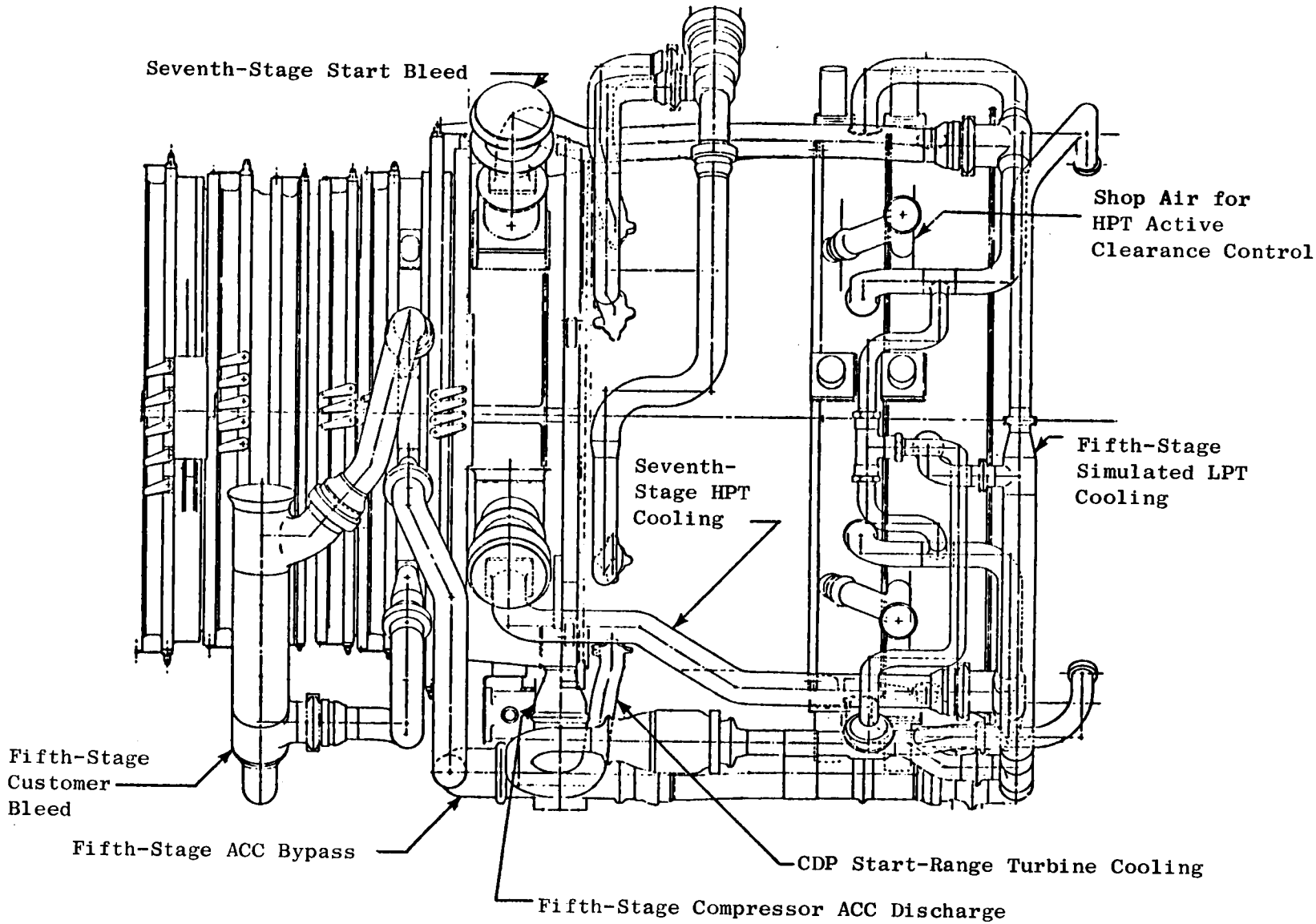

Figure 8. Core Engine Piping.

The core shell stack and centerline grind operation was very successful. This was a sequential assembly of all core engine frames and casings and the machining of key flanges and bearing bores on a single, vertical turret lathe setup. Maximum runout was 0.002 in.

General Electric conducted an internal audit of "E^3 Core Readiness to Test." This was an in-depth review of systems-related considerations which traditionally tend to be problem areas in the first test of an engine. The audit was conducted by an engineer, from outside the E^3 Program, who is highly experienced in engine design and testing. Engine design, dynamics, and hardware and facility hardware, instrumentation, build-up, and test planning were addressed. The audit concluded that the E^3 core program was being well executed. Several action items were recommended and have been or are being executed. The audit was very worthwhile; it suggested some areas where further work was warranted, and it improved confidence of a successful engine test program.

The core Detailed Design Review was presented to NASA on November 9, 1981. The Core Specification Document was subsequently completed and presented to NASA.

Test preparations are currently underway. The test plan covers mechanical, thermal, and dynamic checkout and start optimization, compressor active clearance control, HPT active clearance control, compressor stator schedule tuning, bleed effects, alternate exhaust nozzle areas, windmilling, ambient inlet performance, and ram inlet performance.

The core hardware has been manufactured; instrumentation is well underway, and components are currently being assembled. Blade tip and seal grinding processes have largely been completed.

Work Planned

- Complete core buildup and test preparations
- Test the core engine

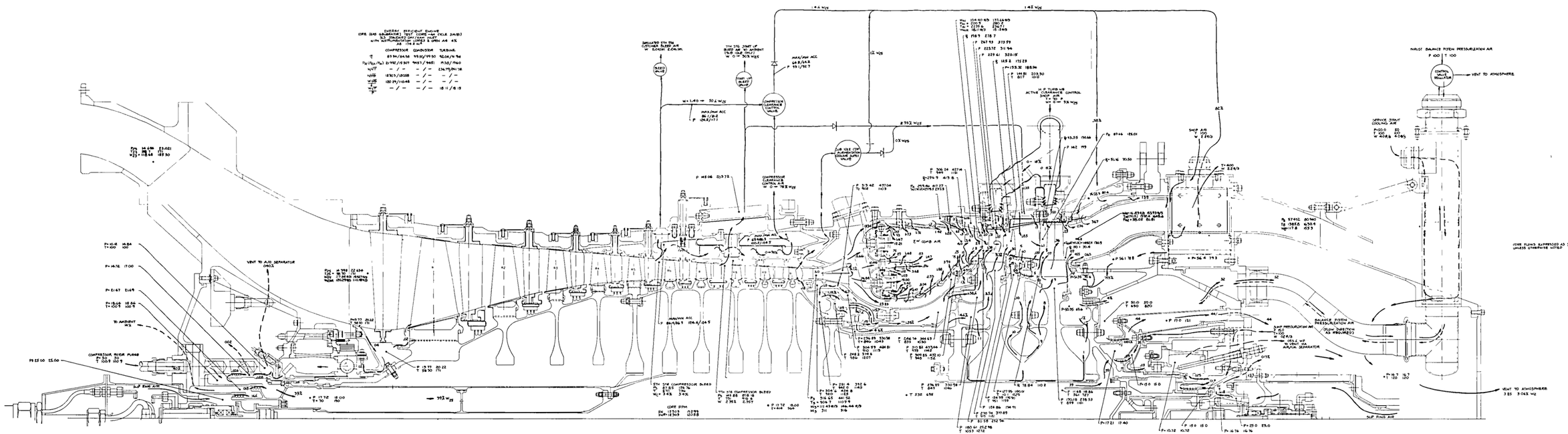

Figure 9. Core Engine Cooling and Secondary Airflows.

1.1.7 ICLS Analysis and Design

General Electric will test the E^3 turbofan in early 1983. The ICLS flight-design components will be the fan from the component rig; the compressor, combustor, and HPT from the core engine; and new LPT, rear frame, mixer, and digital engine control. The inlet, nacelle, exhaust nozzle, and front frame will be nonflight hardware. The engine will be run in an outdoor test facility.

Technical Progress

The ICLS cross section is shown in Figure 10. The operating parameters and cooling supply drawing is shown in Figure 11, and the materials drawing is shown in Figure 12.

In the interest of significant time and cost savings, the decision was made to not disassemble the HPT between the core and ICLS engine tests. This requires that the damper tube in the HPT disk bore not be removed. In order to accomplish this, instrumentation wiring carried by the tube cannot be fully removed and will be clipped following core test. The LP shaft design was modified to clear the instrumentation.

Drafting checks for interferences were made in the ICLS cowl area. Some interferences and near interferences were found and have been corrected.

The ICLS engine/facility interface drawing was completed. This drawing specifies the location and orientation of connections between the engine and facility.

Of the total number of ICLS drawings, 96% have been issued. Much of the hardware has been received, and trial fitting is underway.

Work Planned

- Conduct the ICLS DDR
- Prepare for ICLS test and start ICLS buildup

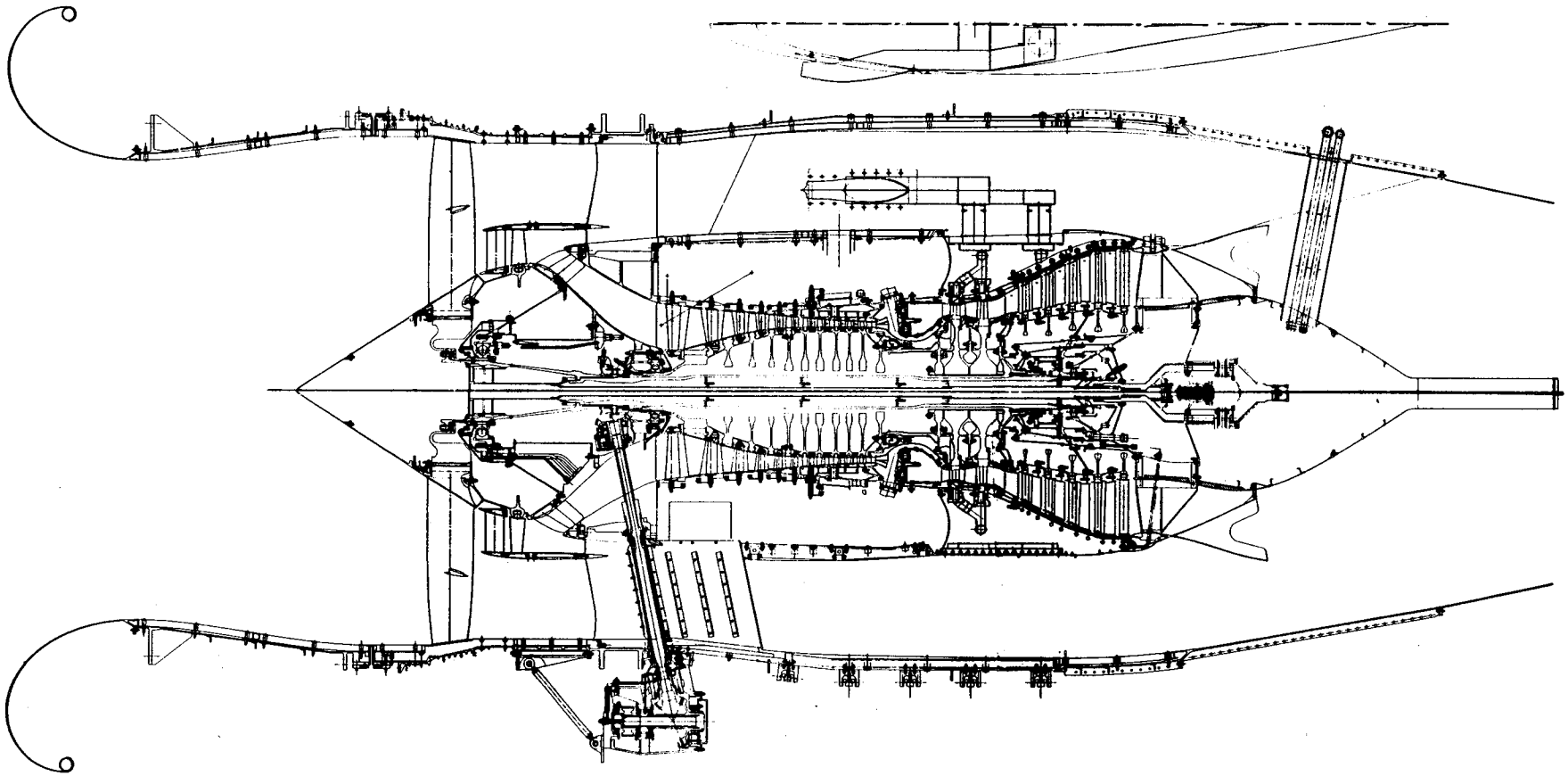

Figure 10. ICLS Cross Section.

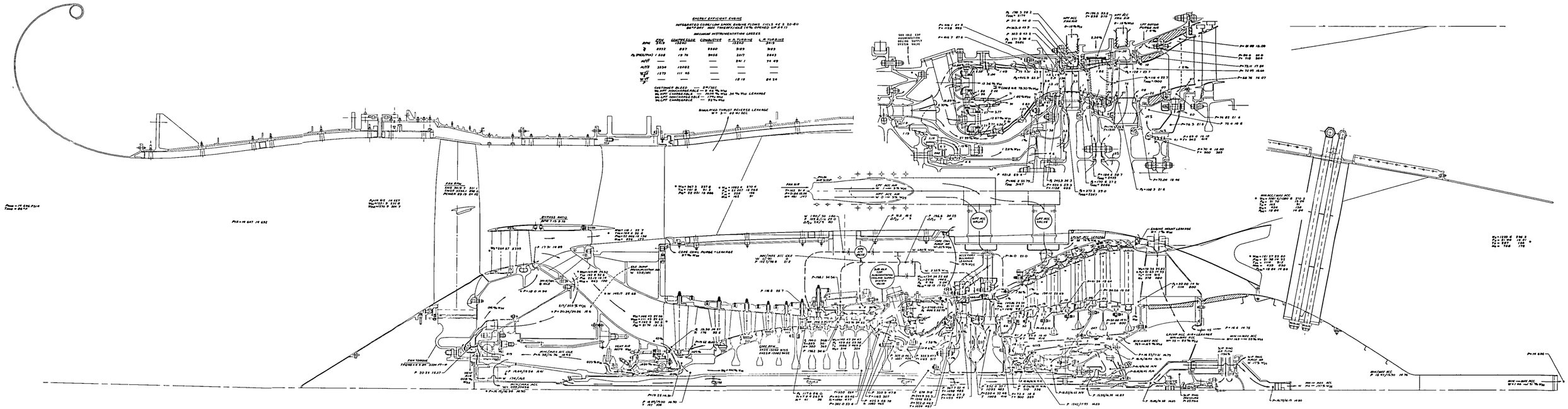

Figure 11. ICLS Operating Parameters and Cooling-Supply System.

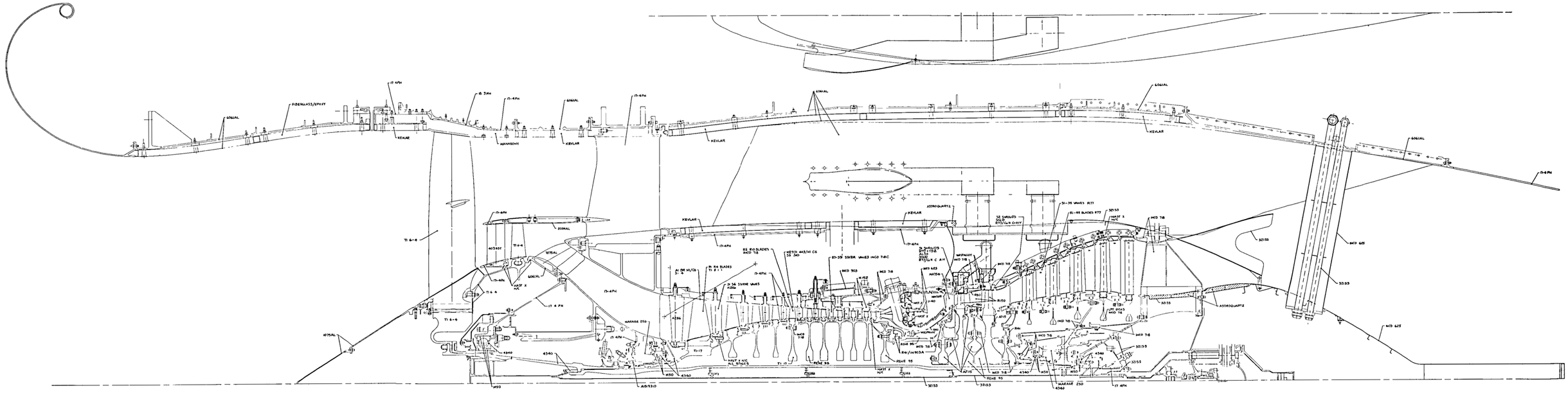

Figure 12. ICLS Material Identification.

1.2 CYCLE AND PERFORMANCE

Work is continuing on the ICLS engine status cycle deck and core engine test planning tasks. Development of the Phase II performance analysis program was initiated and three other tasks completed during this past reporting period.

Status Cycle Deck

Checkout of the HPC and HPT active clearance control (ACC) modeling was completed and found to agree closely with the detailed transient model. After exercising the models at various flight conditions, the data were reviewed by component designers. There were questions on the HPT stage-to-stage variation, and it was found that some minor revisions to the cycle-deck model should be made prior to using it for core pretest predictions. The HPC model was made of the ninth stage; however, clearance measurements will be made on the third, fifth, and tenth stages. The cycle model will be modified to reflect the tenth stage instead of the ninth stage.

An update of the mixer-model logic is in progress. Comparisons of cycle-deck pressure losses for the mixer bypass and core streams are being made with actual mixer-model test data. One concern is the proper modeling of the engine bypass ratio at part power as a function of flight Mach number. This effort will be completed prior to the ICLS DDR.

The final mixer-model test data evaluated the exhaust system nozzle and flow coefficient for simulated reverse-thrust operation. These new data were used to update the cycle deck reverse-thrust performance. This completed the modeling of the reverse-thrust mode for the FPS engine.

The LPT map fit was completed and will be incorporated into the next ICLS and FPS cycle updates. The ICLS-5 status data shown in Table II is the same as reported in semiannual report No. 6. The FPS data shown in Table II, however, have been updated based on the FPS-5 customer deck discussed below.

The fan rig test was completed, and analyses of all the data are in process. Analysis of the fan bypass and booster pumping interaction with bypass ratio variation suggests that the current cycle-deck logic may need revision.

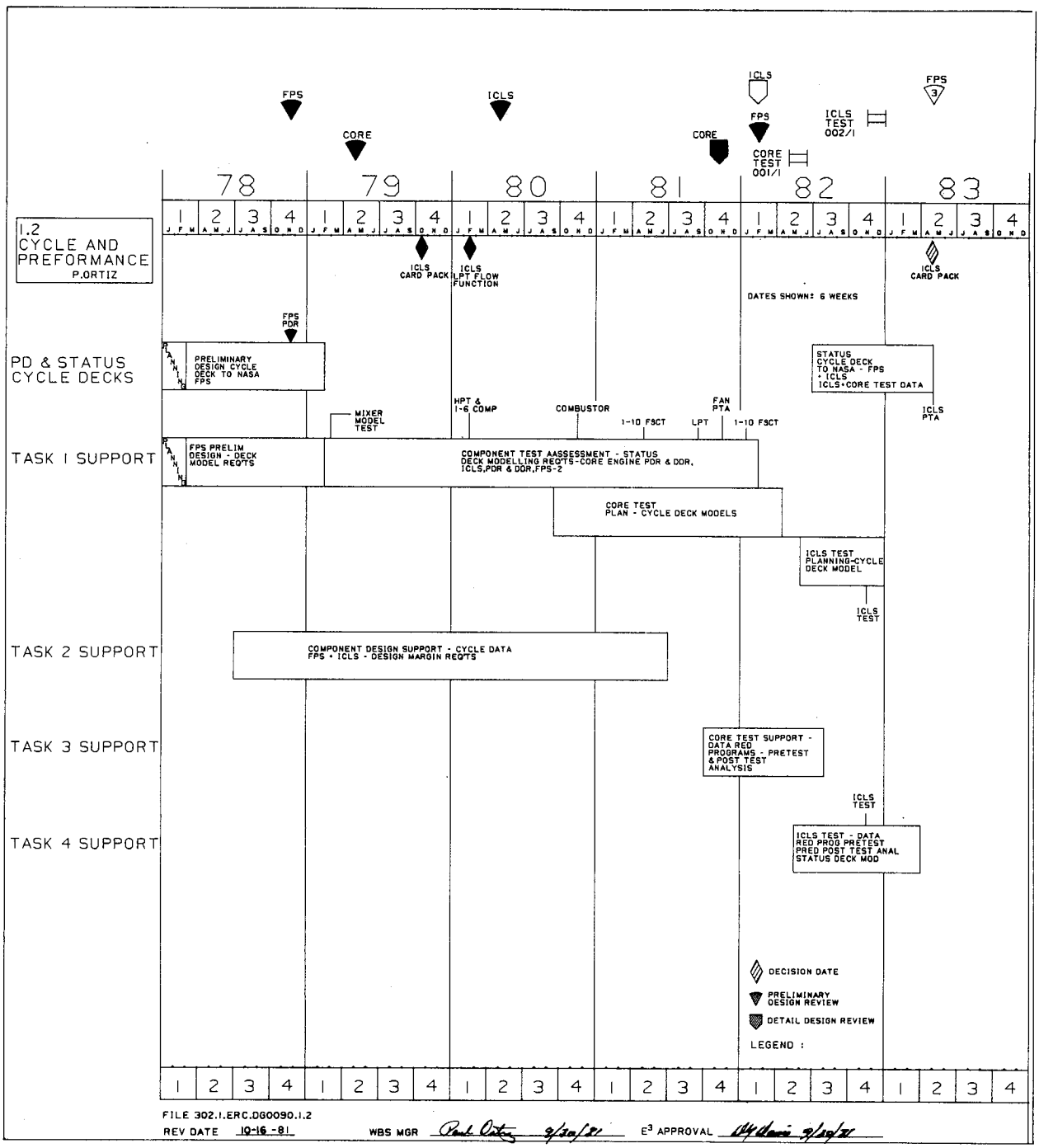
1.2
CYCLE AND
PREFORMANCE
P.ORTIZ
78
79
80
81
82
83
FPS
CORE
ICLS
CORE
FPS
ICLS
CORE
TEST
001/1
ICLS
TEST
002/1
FPS
3
ICLS
CARD PACK
ICLS
LPT FLOW
FUNCTION
ICLS
CARD PACK
DATES SHOWN± 6 WEEKS
FPS
PDR
PD & STATUS
CYCLE DECKS
PRELIMINARY
DESIGN CYCLE
DECK TO NASA
FPS
STATUS
CYCLE DECK
TO NASA - FPS
- ICLS
ICLS+CORE TEST DATA
ICLS
PTA
MIXER
MODEL
TEST
HPT &
1-6 COMP
COMBUSTOR
1-10 FSCT
LPT
FAN
PTA
1-10 FSCT
TASK 1 SUPPORT
FPS PRELIM
DESIGN - DECK
MODEL REQTS
COMPONENT TEST AASSESSMENT - STATUS
DECK MODELLING REQTS-CORE ENGINE PDR & DDR,
ICLS,PDR & DDR,FPS-2
CORE TEST
PLAN - CYCLE DECK MODELS
ICLS TEST
PLANNING-CYCLE
DECK MODEL
ICLS
TEST
TASK 2 SUPPORT
COMPONENT DESIGN SUPPORT - CYCLE DATA
FPS - ICLS - DESIGN MARGIN REQTS
TASK 3 SUPPORT
CORE TEST SUPPORT -
DATA REQ
PROGRAMS - PRETEST
& POST TEST
ANALYSIS
ICLS
TEST
TASK 4 SUPPORT
ICLS TEST - DATA
REQ,PROG PRETEST
PRED POST TEST ANAL
STATUS DECK MOD
DECISION DATE
PRELIMINARY
DESIGN REVIEW
DETAIL DESIGN REVIEW
LEGEND :
FILE 302.1.ERC.DG0090.1.2
REV DATE 10-16-81
WBS MGR
E3 APPROVAL

Table II. FPS and ICLS Maximum Cruise Cycle Comparison.

- 35,000 Feet/Mach 0.8/Standard Day + 18° F.

Parameter	FPS-4	ICLS-5A* Forecast
Uninstalled Performance		
Net Thrust, lb	8425	8425
SFC (Standard Day)	0.542	0.554
Bypass Ratio	6.94	6.94
Fan		
Corrected Flow, lb/sec	1396	1396
Bypass Pressure Ratio	1.61	1.61
Hub Pressure Ratio	1.63	1.64
Compressor		
Corrected Flow, lb/sec	117.5	117.3
Pressure Ratio	22.4	22.3
HP Turbine		
Flow Function, $W\sqrt{T}/P$	17.6	17.6
Rotor Inlet Temperature, ° F	2274	2319
LP Turbine		
Flow Function, $W\sqrt{T}/P$	80.3 (Base)	80.8 (+0.6%)
Nozzle Inlet Temperature, ° F	1436	1464

*ICLS-5A is a flight engine properly matched for the component performance levels defined.

This is being evaluated prior to fitting the fan and booster maps within the current deck logic.

Core Test Planning

Support of the core test planning activity continued. All secondary-flow circuits have been reviewed relative to impact on performance and planned circuits calibration. The defined test points are being evaluated relative to ambient or pressurized data runs. Instrumentation loss factors are being evaluated as each rake assembly design is completed.

Core DDR

The core DDR presentation was made in November of 1981. Core data analysis methodology had the primary emphasis of the performance section of the presentation.

FPS-5 Customer Deck

An FPS-5 Customer Deck for use on the IBM-370 computer was sent to NASA Lewis in January of 1982. This FPS model did not affect the high-corrected-speed region at max climb and max cruise, so the performance is essentially the same as the FPS-4 cycle reported in the last semiannular report. The update of the engine representation did change in the part-power operation of the engine. Table III shows the key FPS-5 cycle points, and they are essentially the same as the FPS-4. The takeoff temperature on this cycle rematch is about 9° F lower than previously shown.

Specific changes included are as follows:

- HPT map from the rig test
- Modified HPC flow/speed and efficiency/flow characteristics based on compressor rig test data
- Improved fan performance at low speed
- Revision of the nacelle drag model to reflect a more realistic drag and an improved installed thrust and sfc; a comparison with the FPS-4 data is shown in Table IV.

Table III. FPS-5 Performance Parameters.

Parameter	Maximum Climb 35,000 feet/ 0.8 M/+18° F	Maximum Cruise 35,000 feet/ 0.8 M/+18° F	Takeoff SLS/+27° F
Net Thrust, lb	9040	8425	36,500
SFC (Standard Day)	0.546	0.542	0.293
Bypass Ratio	6.77	6.94	7.32
Overall Pressure Ratio	37.7	35.8	29.8
Fan Bypass Pressure Ratio	1.65	1.61	1.50
Compressor Corrected Airflow, lb/sec	120.0	117.5	108.4
Compressor Pressure Ratio	23.0	22.4	20.0
HPT Rotor Inlet Temperature, ° F	2345	2274	2441

Table IV. FPS Installed Performance Comparison.

Parameter	Maximum Cruise 35,000 ft/Mach 0.8/Standard Day	
	FPS-4	FPS-5
Installed Net Thrust, lbf	7982	8089
Installed SFC	0.572	0.564

Phase II Performance Analysis Program

Work has begun on development of the Phase II program for use on the core engine test. The approach is to develop the full ICLS Phase II program with a switch that allows the program to be used for a core engine only.

Starting Sensitivity Study

A starting sensitivity study was conducted to evaluate the effects of HPC and HPT efficiency, HPT nozzle and core nozzle areas, and HPC flow/speed deviations on the predicted starting schedule. Of concern was the impact on HPC stall margin (SM) and start time. Results indicated that only the HPT nozzle area had a significant effect on stall margin for a given fuel schedule, and the sensitivity coefficient was about 1% in SM for a 1% change in HPT nozzle area. The efficiency perturbation of -5% on the HPT and HPC showed an impact of less than -0.5% on the stall margin. A core nozzle change of 25% changed the SM by only 1%.

The impact on starting time for all the perturbations was shown to be less than 4 seconds for a 45-second starting schedule.

The results from the study indicate that significant deviations in these parameters will not have a serious impact on starting schedule. The most sensitive parameter, the HPT nozzle area, is expected to be within 1.5% of predicted value and should not present a problem. In any case, the fuel schedule can easily be modified to accommodate these variables for optimum starting.

Work Planned

- Continue with the status deck and core test planning activities
- Complete development of the Phase II program
- Support the core test conduction and perform posttest performance analysis
- Prepare presentation for the ICLS DDR

1.3 MATERIALS AND PROCESSES

1.3.1 Materials and Processes Component Support

The metallurgical support activities for each component will be described individually. All component tests, other than the HP compressor 1-10 rig, are complete.

HP Compressor 1-10 Rig Test

The rig has been rebuilt and returned to test. An in situ cleaning procedure was identified and implemented when some oil contamination occurred in the test cell.

Full-Scale Fan

All testing is complete. Posttest washing and cleaning procedures were provided prior to rework required for the ICLS.

Combustor Test Rig

Combustor rig testing was completed. Some cracking was observed on the turbines, but visual examination indicated this cracking was limited to the thermal-barrier coating, and the combustor was suitable for running in the core.

LP Air Turbine

Test is complete; no additional materials support was required.

Work Planned

Support on component tests is complete except for any required posttest evaluation of the HPC 1-10.

1.3.2 Materials and Processes Engine Support

This section describes the technical progress accomplished in support of the core, ICLS, and FPS engines. The major items of technical support are as follows:

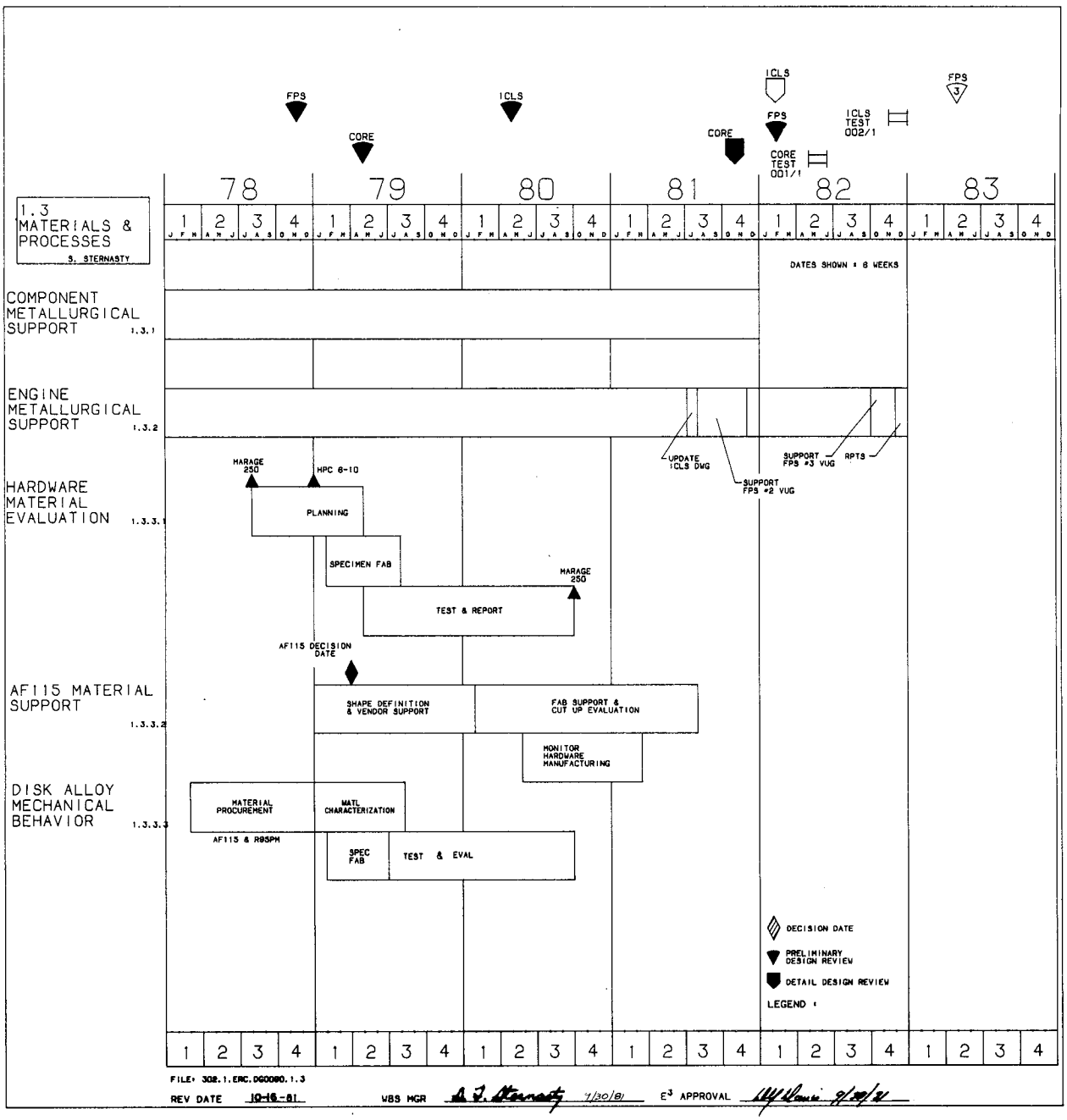
1.3 MATERIALS & PROCESSES
S. STERNASTY
78
79
80
81
82
83
FPS
CORE
ICLS
FPS
CORE
ICLS
FPS
ICLS TEST 002/1
CORE TEST 001/1
DATES SHOWN = 8 WEEKS
COMPONENT METALLURGICAL SUPPORT 1.3.1
ENGINE METALLURGICAL SUPPORT 1.3.2
HARDWARE MATERIAL EVALUATION 1.3.3.1
MARAGE 250
HPC 8-10
PLANNING
SPECIMEN FAB
MARAGE 250
TEST & REPORT
UPDATE ICLS DWG
SUPPORT FPS #2 VUG
SUPPORT FPS #3 VUG
RPTS
AF115 DECISION DATE
AF115 MATERIAL SUPPORT 1.3.3.2
SHAPE DEFINITION & VENDOR SUPPORT
FAB SUPPORT & CUT UP EVALUATION
MONITOR HARDWARE MANUFACTURING
DISK ALLOY MECHANICAL BEHAVIOR 1.3.3.3
MATERIAL PROCUREMENT
MATL CHARACTERIZATION
AF115 & R95PH
SPEC FAB
TEST & EVAL
DECISION DATE
PRELIMINARY DESIGN REVIEW
DETAIL DESIGN REVIEW
LEGEND :
FILE: 302.1.ERC.DG0080.1.3
REV DATE 10-16-81
WBS MGR
E³ APPROVAL

Material Selection

There were no changes in the materials for the engines during this reporting period.

Support Activities

Material and process drawing definitions continued to be provided for the engines. Over 100 drawings were signed off; this activity dropped significantly in the latter part of this reporting period. The detail drawings were primarily in the areas of configurations, controls, and accessories.

The manufacture of hardware for the engines was monitored; some of the specific support activities required were:

- Provided support on the correction of dimensional discrepancies, weld repair, activated diffusion healing, hot isostatic pressing, and inspection of the cast Inco 718 diffuser and OGV which were the pacing items on the core buildup.
- Demonstrated the repair of a discontinuity in the airflow path of the HP Stage 2 nozzle using plasma-sprayed NiCrAlY.
- Evaluated methods of reducing trailing-edge holes (and airflow) in Stage 2 HP nozzles. Demonstrated that activated diffusion bonding, followed by redrilling trailing-edge holes by electrodischarge machining (EDM), was a satisfactory rework procedure.
- Recognized discrepant compressor clearance-control coating, evaluated effect on wear rates, and recommended corrective action (strip and recoat).
- Identified descaling procedure for A286 inlet guide vanes (IGV's).

Coordination was provided between Design Engineering and the Material and Process Technology Laboratories on supporting technology programs; capsule status of the programs not previously reported complete are as follows (details of the programs are in the appropriate WBS section):

- WBS 2.2.7.1 Variable Stator Vane Bushing - The data and conclusions presented in this semiannular complete the program; a report has been issued.

- WBS 2.4.7.1.1 Ceramic Shroud Process - Completion of nondestructive evaluation (NDE), reported in this semiannual, finishes this activity. Evaluation of thermal-shock tests will be reported in the future in WBS 2.4.7.1.2, Component Test of Ceramic Shrouds.

- WBS 2.4.7.2.1 Thermal Barrier Process - The report is written and has been reviewed internally.

Work Planned

Provide metallurgical support for the core and ICLS manufacture and buildup as required.

1.4 ACOUSTIC DEVELOPMENT

1.4.1 System Acoustic Prediction

Technical Progress

Projections of E^3 noise levels have been made reflecting advances in estimation procedure due to recent full-scale engine noise measurements. These projections confirm that the E^3 is still expected to meet or exceed program goals for all aircraft, with at least 2 to 4 EPNdB margin to FAR36 Stage 3 at approach and 4 to 8 EPNdB margin at takeoff, depending on the aircraft.

The advances in estimation procedures are primarily due to improved source-isolation techniques in noise measurements on commercial full-scale engine tests. Utilization of noise-isolation barriers, directional-microphone arrays, and advanced narrowband analysis are prime examples of these improved source-isolation techniques.

Work Planned

Refinements of the projected levels will be made reflecting acoustic treatment advancements.

1.4.5 ICLS Acoustic Testing

Technical Progress

No activity during this reporting period.

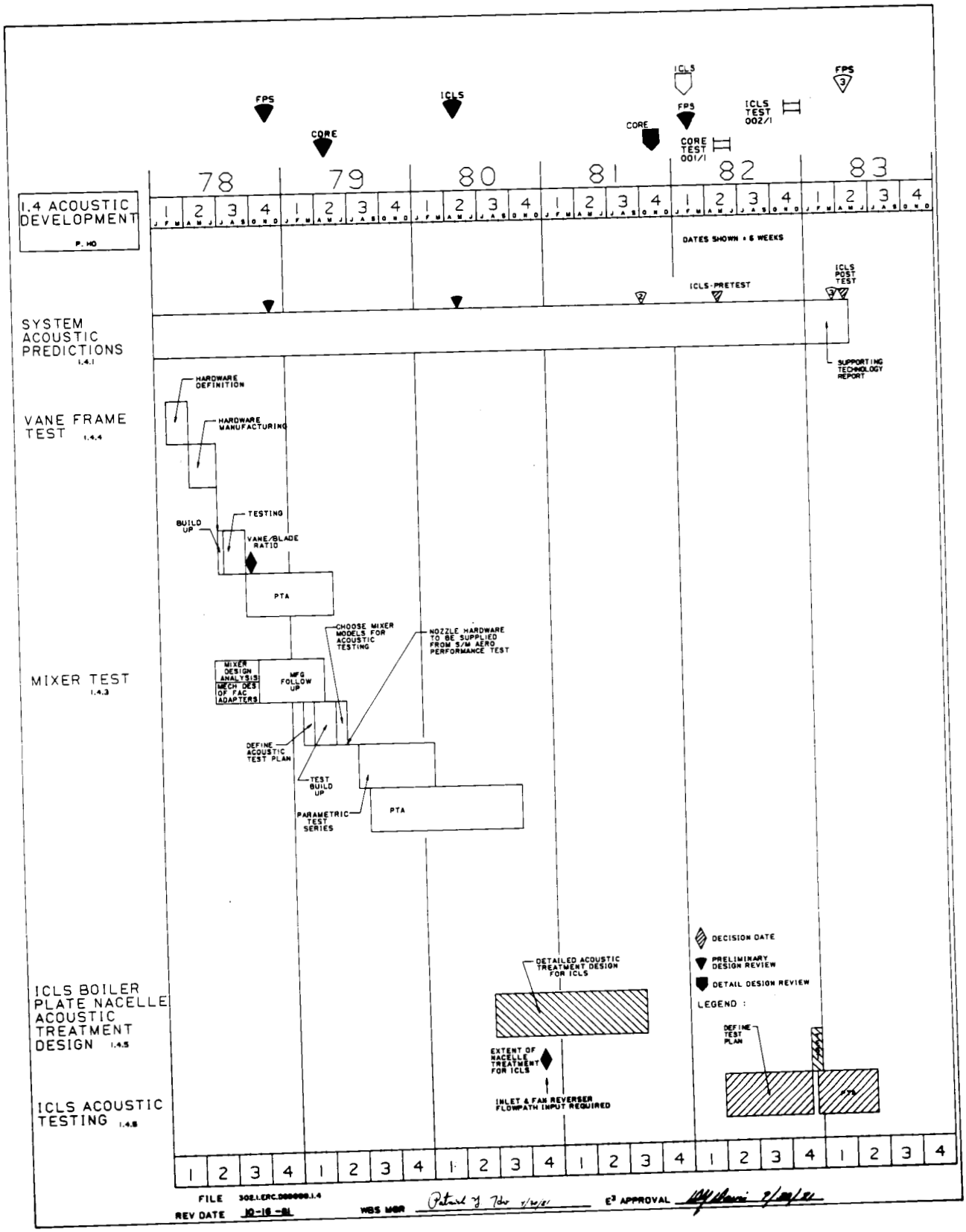
1.4 ACOUSTIC DEVELOPMENT
P. HO
78
79
80
81
82
83
FPS
CORE
ICLS
CORE
FPS
ICLS
FPS
CORE TEST 001/1
ICLS TEST 002/1
DATES SHOWN ± 6 WEEKS
ICLS-PRETEST
ICLS POST TEST
SYSTEM ACOUSTIC PREDICTIONS 1.4.1
SUPPORTING TECHNOLOGY REPORT
VANE FRAME TEST 1.4.4
HARDWARE DEFINITION
HARDWARE MANUFACTURING
BUILD UP
TESTING
VANE/BLADE RATIO
PTA
MIXER TEST 1.4.3
CHOOSE MIXER MODELS FOR ACOUSTIC TESTING
NOZZLE HARDWARE TO BE SUPPLIED FROM S/M AERO PERFORMANCE TEST
MIXER DESIGN ANALYSIS MECH DES OF FAC ADAPTERS
MFG FOLLOW UP
DEFINE ACOUSTIC TEST PLAN
TEST BUILD UP
PARAMETRIC TEST SERIES
PTA
ICLS BOILER PLATE NACELLE ACOUSTIC TREATMENT DESIGN 1.4.5
DETAILED ACOUSTIC TREATMENT DESIGN FOR ICLS
EXTENT OF NACELLE TREATMENT FOR ICLS
INLET & FAN REVERSER FLOWPATH INPUT REQUIRED
ICLS ACOUSTIC TESTING 1.4.6
DECISION DATE
PRELIMINARY DESIGN REVIEW
DETAIL DESIGN REVIEW
LEGEND :
DEFINE TEST PLAN
PTA
FILE 302.1.ERC.000000.1.4
REV DATE 10-16-81
WBS MGR
E³ APPROVAL

Work Planned

Define ICLS Acoustic Test Plan.

1.5.1.1 Economics and Design

Technical Progress

In support of the FPS update, the Boeing 1980 E^3 economic analysis was expanded to cover current and future fuel prices for two flight lengths. This was used to reevaluate the E^3 FPS. Higher fuel prices have magnified the benefits of the E^3.

Work Planned

None.

1.5.1.3 Nacelle Performance Evaluation, Langley

Technical Progress

A final draft of the calibration report was prepared and sent to NASA Langley for approval. The report includes results from the TPS calibration tests at the Boeing Flight Simulation Chamber from both the Phase I and the Phase II tests.

Preparation of a data memo summarizing the major results of the wind tunnel test program was initiated. A final evaluation of the data at design-point conditions is being conducted as part of the data memo preparation.

Work Planned

Complete the data memo, the final task of this WBS item.

1.6 BENEFIT/COST STUDY

Technical Progress

To date, 183 raw concepts have been identified for potential application. The screening, evaluation, and concept-integration process has been implemented through the definition of three conceptual energy-efficient

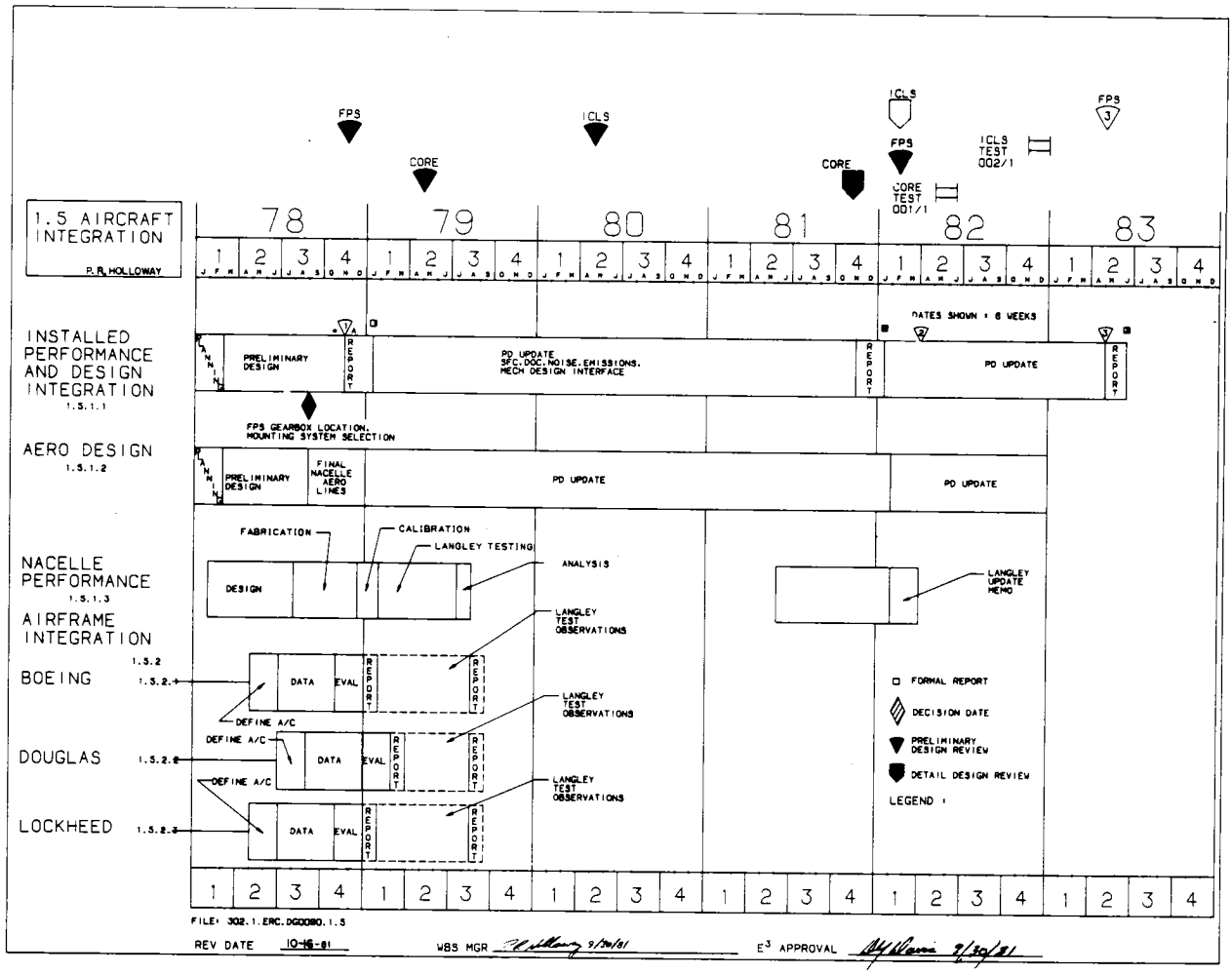
1.5 AIRCRAFT INTEGRATION
P.R. HOLLOWAY
78
79
80
81
82
83
FPS
CORE
ICLS
CORE
FPS
CORE TEST 001/1
ICLS
FPS
ICLS TEST 002/1
DATES SHOWN : 6 WEEKS
INSTALLED PERFORMANCE AND DESIGN INTEGRATION
1.5.1.1
PRELIMINARY DESIGN
REPORT
PD UPDATE SFC, DOC, NOISE, EMISSIONS, MECH DESIGN INTERFACE
REPORT
PD UPDATE
REPORT
FPS GEARBOX LOCATION, MOUNTING SYSTEM SELECTION
AERO DESIGN
1.5.1.2
PRELIMINARY DESIGN
FINAL NACELLE AERO LINES
PD UPDATE
PD UPDATE
NACELLE PERFORMANCE
1.5.1.3
FABRICATION
CALIBRATION
LANGLEY TESTING
DESIGN
ANALYSIS
LANGLEY UPDATE MEMO
AIRFRAME INTEGRATION
1.5.2
BOEING
1.5.2.1
DATA
EVAL
REPORT
REPORT
LANGLEY TEST OBSERVATIONS
DEFINE A/C
DOUGLAS
1.5.2.2
DEFINE A/C
DATA
EVAL
REPORT
REPORT
LANGLEY TEST OBSERVATIONS
DEFINE A/C
LOCKHEED
1.5.2.3
DATA
EVAL
REPORT
REPORT
LANGLEY TEST OBSERVATIONS
FORMAL REPORT
DECISION DATE
PRELIMINARY DESIGN REVIEW
DETAIL DESIGN REVIEW
LEGEND :
FILE: 302.1.ERC.DG0080.1.5
REV DATE 10-16-81
WBS MGR
E3 APPROVAL

propulsion systems for certification in both the near- and far-term time spans.

Representative trends in installed sfc and fuel burn for selectively integrated, advanced, low-drag, lightweight technology concepts are presented in Figure 13. These approximate trends cover the propulsive-efficiency range developed by fan pressure ratios from 1.65 through 1.25. Core and low-spool improvements appear about equally split at moderate fan pressure ratios, and significant installation improvements are indicated. The gains represented by the migration from an overall pressure ratio (OPR) of 38 to 45 are somewhat limited. This is because an objective evaluation requires that the OPR increase be made at constant metal temperature and constant turbine rotor inlet temperature. These trend curves are derived from approximations of 85% summations of individual-concept, derivative-based evaluations. As such, they are qualitive in nature and are intended for overview purposes only.

Work Planned

Refined assessment of selected concepts and systems will continue, and technology-demonstration plans will be prepared.

- Reference Turbine Metal Temperature = E^3 FPS-4 + 50° F (N5 Material)
- Reference T_{41} = Constant 2450° F

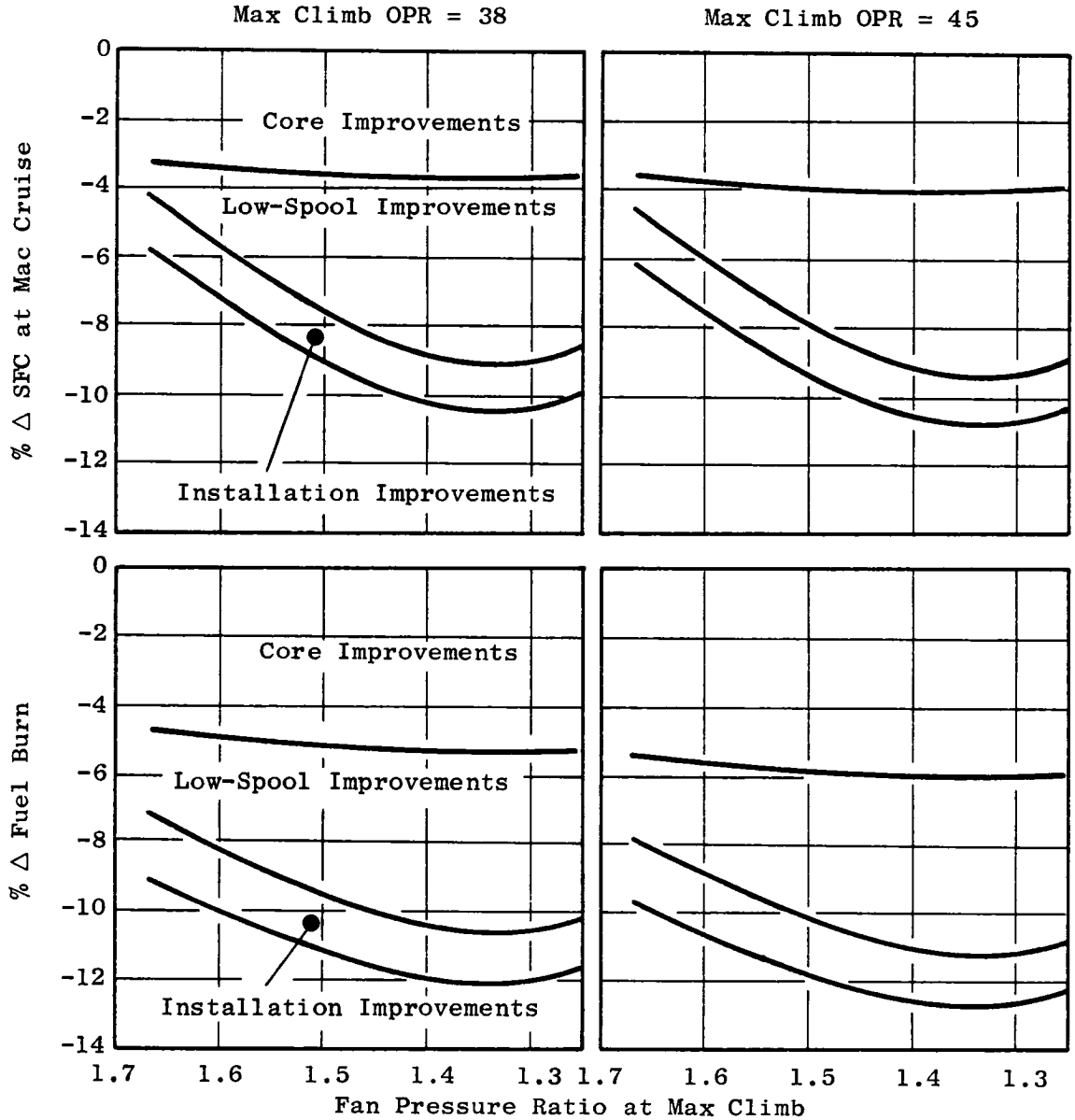

Figure 13. Trends in Installed SFC and Fuel Burn for Advanced, Low-Drag, Lightweight Technology.

2.0 TASK 2 - COMPONENT ANALYSIS DESIGN AND DEVELOPMENT

2.1 FAN

Overall Objective

The primary objective of the fan development effort is to evolve a high-technology design able to meet or exceed all commercial certification requirements for noise, performance, life, and bird or ice ingestion. The general configuration of the fan (Figure 14) will incorporate a high-bypass fan stage with a part-span shroud followed by a quarter stage to provide additional supercharging to the core compressor. The design of the quarter stage, and passages aft of it, will minimize foreign-object ingestion into the high-pressure compressor. The quarter stage will also provide good distortion attenuation and tolerance to bypass variation without variable geometry.

Blades will be solid titanium construction to provide the lightest weight fan capable of meeting the operational environment imposed by bird-ingestion requirements. The fan will have no life-limiting conditions for the expected operation in commercial service including crosswinds, thrust reversals, and tip rubs. The FPS fan efficiency goals are 0.882 bypass and 0.892 hub at Mach 0.8, 35,000-feet altitude, standard day, maximum power setting.

Preliminary mechanical design studies were conducted to establish the general fan configuration with the best potential for meeting the overall program objectives. In June 1979, the fan-blade parameters related to bird-ingestion tolerance were evaluated based on commercial service experience with improved blade designs now in production. The objective of this selection was to ensure that the E^3 fan blading design was compatible with commercial engine certification requirements.

The final aerodynamic design of the fan rotor was completed during the third quarter of 1979. The final mechanical design was completed in the fourth quarter of 1979 with an Interim Design Review (IRD) in 1979 leading to the fan Detail Design Review (DDR) in February 1980; design parameters are shown in Table V. Concurrent with the above effort, the final aerodynamic

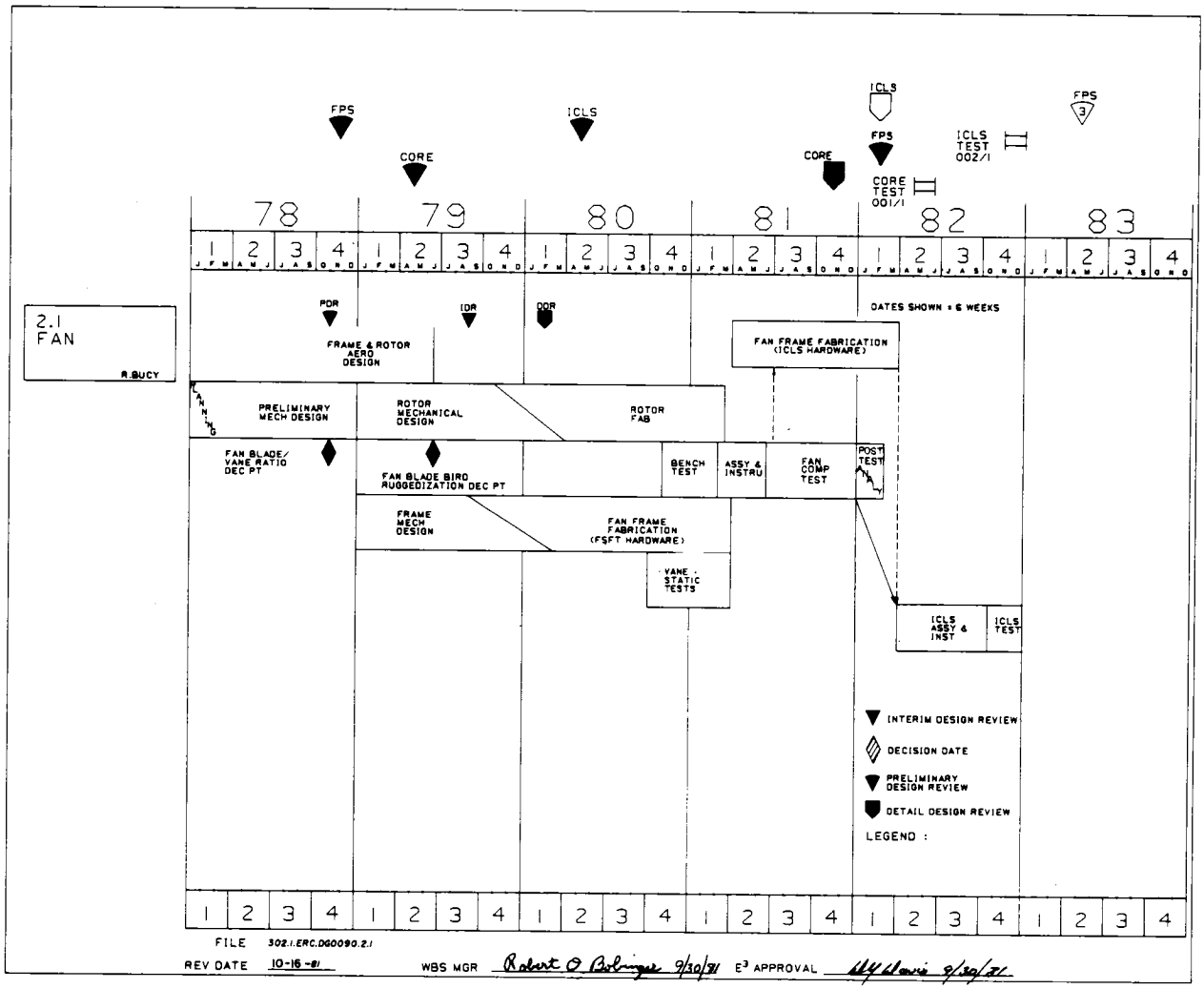
2.1
FAN
R.BUCY
78
79
80
81
82
83
FPS
CORE
ICLS
CORE
FPS
ICLS
TEST
002/1
CORE
TEST
001/1
FPS
3
PDR
IDR
DDR
DATES SHOWN ± 6 WEEKS
FRAME & ROTOR AERO DESIGN
FAN FRAME FABRICATION (ICLS HARDWARE)
PRELIMINARY MECH DESIGN
ROTOR MECHANICAL DESIGN
ROTOR FAB
FAN BLADE/ VANE RATIO DEC PT
FAN BLADE BIRD RUGGEDIZATION DEC PT
BENCH TEST
ASSY & INSTRU
FAN COMP TEST
POST TEST
FRAME MECH DESIGN
FAN FRAME FABRICATION (FSFT HARDWARE)
VANE STATIC TESTS
ICLS ASSY & INST
ICLS TEST
INTERIM DESIGN REVIEW
DECISION DATE
PRELIMINARY DESIGN REVIEW
DETAIL DESIGN REVIEW
LEGEND :
FILE 302.1.ERC.DG0090.2.1
REV DATE 10-16-81
WBS MGR Robert O Bolinger 9/30/81
E³ APPROVAL 9/30/81

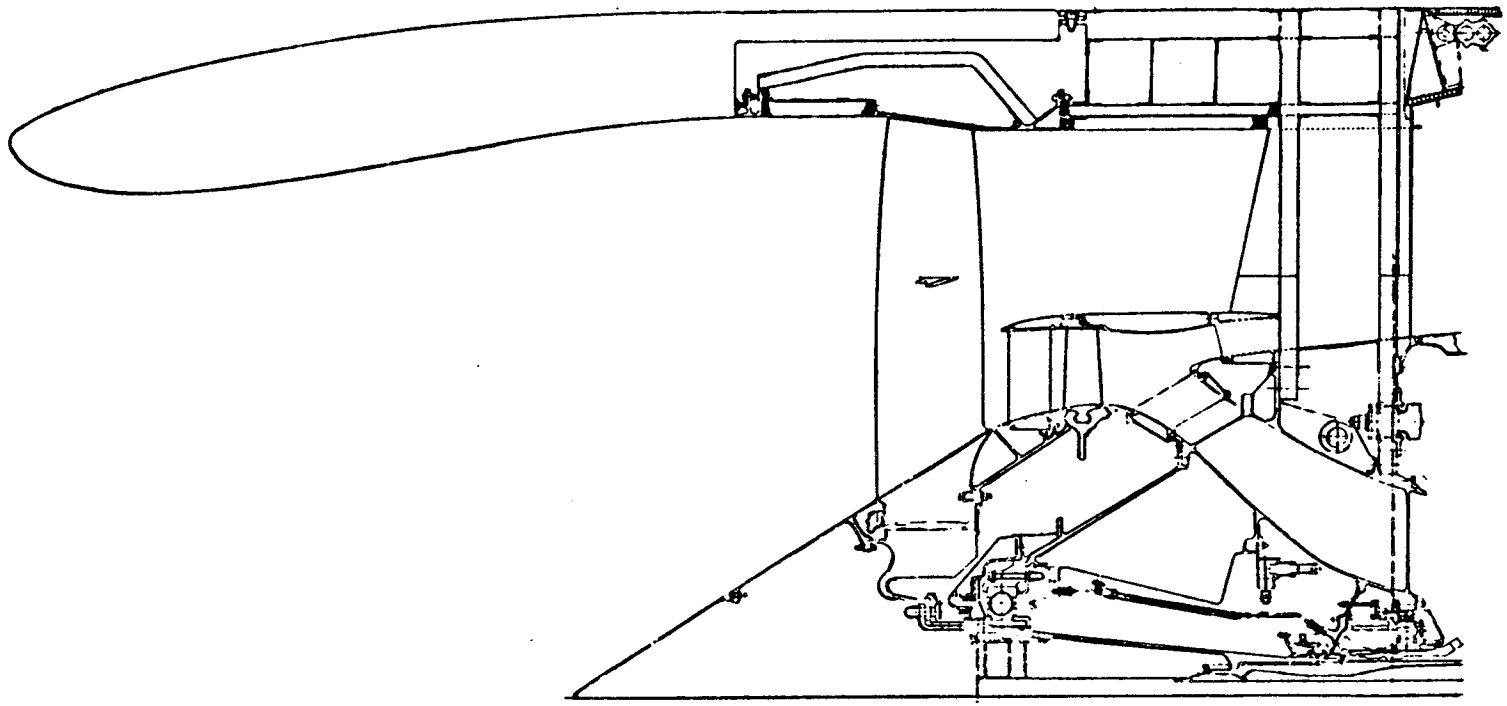

Figure 14. Fan Module Cross Section.

design of the frame structures was also completed during the last quarter of 1979. The final frame mechanical design was initiated at the beginning of 1979 and conducted during the latter part of 1979. The slave frame design was reviewed in an informal IDR on September 12, 1979 to allow an early start on the relatively long procurement cycle of the slave frame. Fabrication of the slave frame was completed during the first quarter of 1981.

Fan rotor hardware and the slave frame were available to initiate the component test buildup by the end of the first quarter of 1981. Following the instrumentation and buildup cycle, the fan component test was initiated in late September 1981. After a few days of testing, high vibration levels were encountered. The vibration was traced to the facility steam-turbine drive system. Repairs were made, and testing resumed on November 4, 1981. Testing was completed on November 19, 1981 after a total of 201 data points had been taken. Final analysis of the test data continues at this time.

Table V. Fan Aerodynamic Design Parameters.

Parameters	Maximum Climb	Maximum Cruise	Takeoff
	35,000 feet/Mach 0.8/+18° F		SLS/+27° F
Corrected Tip Speed, ft/sec	1350	1311	1198
Corrected Airflow, lbm/sec	1419	1396	1274
Flow/Annulus Area, lbm/sec-ft^2	42.8	42.1	38.4
Bypass Pressure Ratio	1.65	1.61	1.50
Bypass Adiabatic Efficiency, percent	87.9	88.7	90.0
Core Pressure Ratio	1.67	1.63	1.51
Core Adiabatic Efficiency, percent	88.5	89.2	89.7
Bypass Ratio	6.8	6.9	7.3

2.1.1. Fan Aerodynamic Design

Fan Aerodynamic Test Results

The E^3 fan was tested as a component in the General Electric Large Fan Test Facility (LFTF) in Lynn, Massachusetts. The test was completed on November 17, 1981 after 81.6 hours of operation. Clean-inlet performance test data readings were taken at fan speeds ranging from 40% to 105% of the corrected design speed. Several data points were recorded at each speed line from a low operating line to a near-stall point. Stalls were intentionally induced by throttling the fan with closure of the bypass discharge valve at speeds from 40% to 95%. At speeds above 95%, test vehicle operation was limited by the available drive-turbine horsepower; therefore, stalls and near-stall data points were not possible. Most of the test readings were taken with design or near-design bypass ratios; a separate portion of the test was carried out with off-design bypass ratios at 90 and 95% corrected speeds. Radial traverses taken ahead of and behind the fan rotor and at the quarter-stage rotor exit plane provided complete radial distributions of pressure, temperature, and flow angle. Dynamic-pressure measurements over the fan rotor tip were recorded at several high-speed conditions in order to provide data for analyzing the rotor tip flow field and shock patterns.

A cross section of the test configuration flowpath is shown in Figure 15. Flow enters the bellmouth, located 1.25 fan diameters upstream of the fan rotor blade, after exiting the inlet stack and 90° turning vanes far upstream. The bellmouth flow-measurement station (Plane 10) is located 0.62 diameters from the fan. The total flow enters the fan rotor and is split by the quarter-stage island such that 23% of the flow passes through the booster. The booster flow is then split with the inner 60% flow entering the transition duct to the core flow-measuring section. The outer 40% of the booster flow passes underneath the island and then back into the bypass duct, mixing with the outer-bypass flow.

The main instrumentation planes used for defining the overall fan performance are:

1. Inlet Screen (Plane 2) — Twenty-four thermocouples judiciously positioned over the entire screen to provide a representative temperature sampling of the total inlet flow.

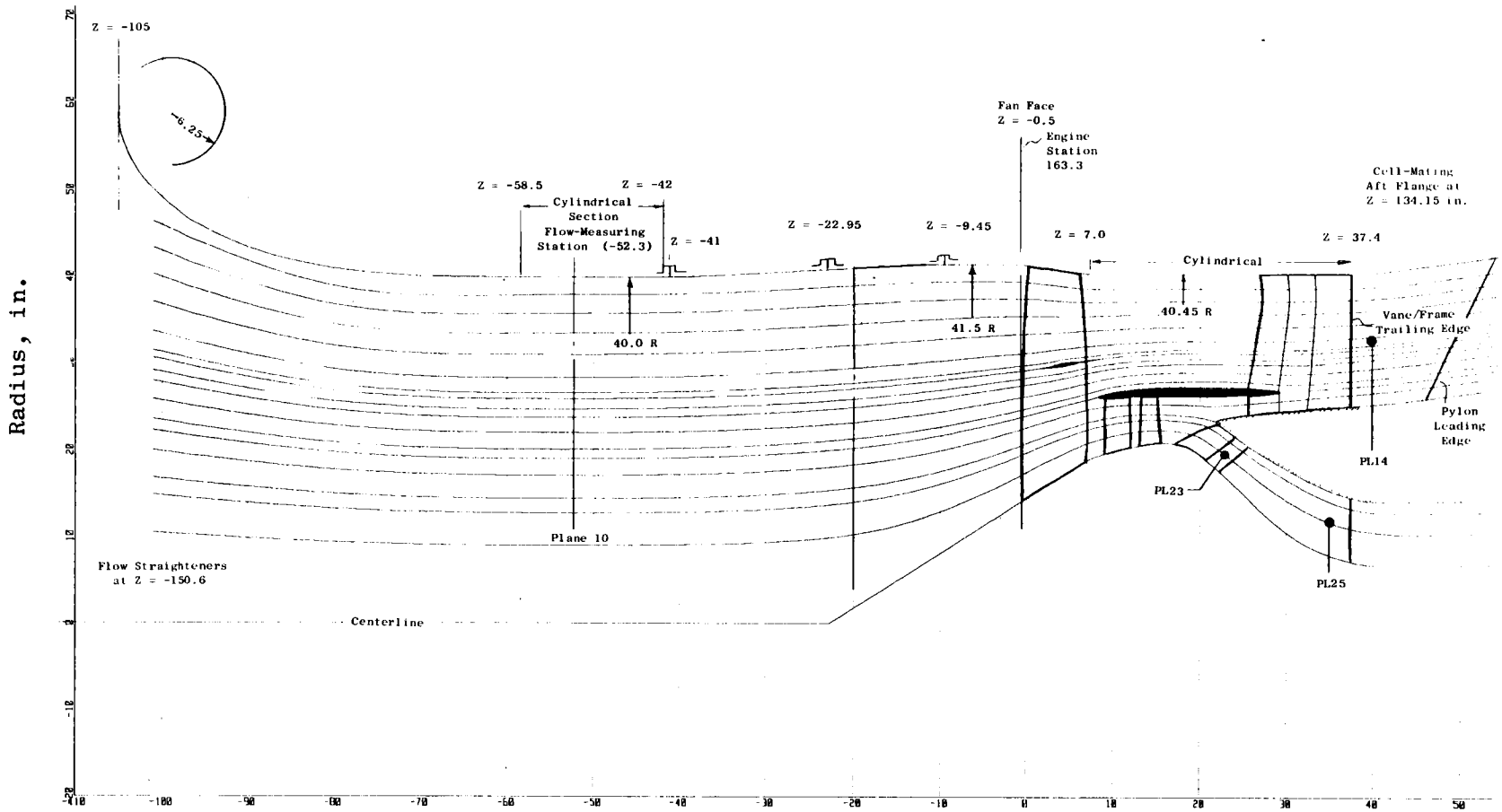

Figure 15. Fan Component-Test Rig Flowpath.

2.	Inlet Plane	Four 6-element pitot-static rakes, located at the bellmouth throat, used to measure total fan flow and inlet total pressure.
3.	Bypass OGV exit (PL14)	Seven 11-element arc rakes and seven 7-element radial rakes located ≈ 1/2 chord length behind bypass OGV's. Arc rakes alone are used to define fan bypass performance.
4.	Core OGV exit (PL23)	Five 11-element arc rakes located between inner OGV's and the core frame struts.

Other instrumentation is located on the vane leading edges, the flowpath walls, and the core duct exit (compressor inlet, Plane 25). A boundary-layer rake at the fan rotor inlet (Plane 12) was used to measure the total-pressure gradient near the outer wall and to determine the total-pressure loss in the duct between Plane 10 and Plane 12. This loss was calculated for several data points, and an adjustment of approximately +0.6 points in efficiency was then applied to the test-measured, Plane 14 efficiency for each reading.

Fan Bypass and Core-Stream Performance

The fan bypass performance may is shown in Figure 16. The sea level and altitude cruise (Mach 0.8, 35,000 ft) operating lines are shown for reference. The abscissa scale is the total fan airflow corrected by Plane 12 average conditions. The ordinate scale is the fan bypass pressure ratio calculated from the average total pressure at Plane 12 and the average arc-rake total pressure at Plane 14.

The measured total airflow is higher than predicted at all speeds by 1.5 to 3.5%. The design airflow of 1419.2 lbm/sec was reached at 97% corrected speed at the design pressure ratio of 1.65. Test-measured stall points were determined for all speed lines up through 95% corrected speed. The target stall line was exceeded at all speeds by approximately 3.0 to 5.0%. The stall margin available at the sea level takeoff condition is approximately 15% at a constant airflow.

Detailed analysis of the fan test data has produced flows, pressure ratios, and bypass efficiencies slightly different from the actual measured

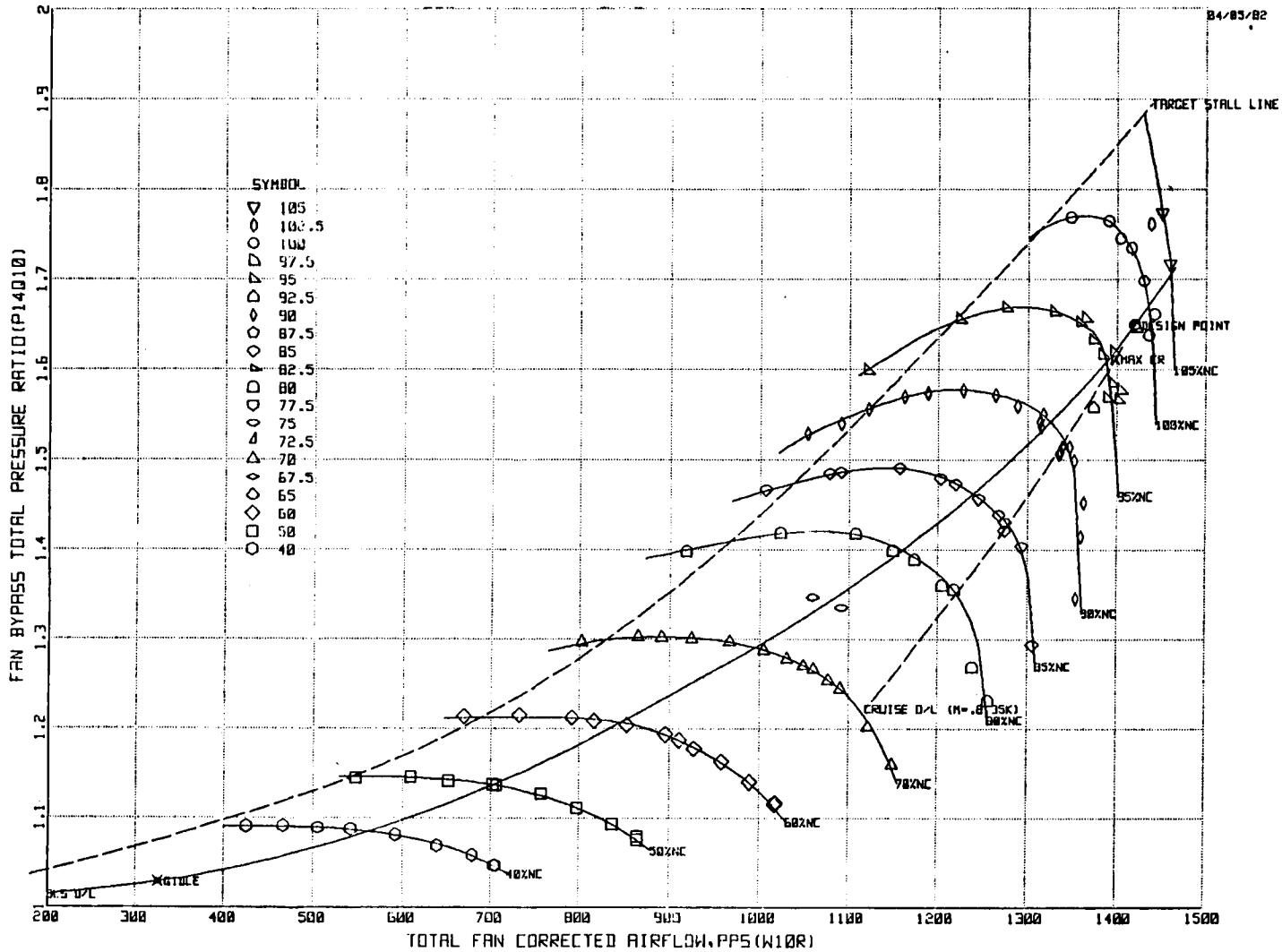

Figure 16. Fan Bypass Performance Map.

values. The total corrected airflows and bypass pressure ratios were adjusted for the difference in total pressure between Plane 10 and Plane 12 (fan face) caused by the inlet duct wall-friction loss. The bypass efficiencies were further adjusted to account for momentum averaging and circumferential sampling variations at Plane 14. The core-stream pressures and efficiencies were not adjusted since the inlet wall-friction loss and and momentum-averaging method do not apply.

The core-stream performance map is shown in Figure 17. The core-stream corrected airflow plotted on the abscissa is the flow which enters the core-flow measuring section, corrected to Plane 10. The pressure ratio plotted on the ordinate is the Plane 23 arc rake average total pressure, ratioed to the Plane 10 inlet total pressure. Each numbered symbol represents the aerodynamic performance reading taken during the component test. The operating lines and predicted stall line are shown. The points of rotating stall at 90 and 95% speeds are shown at approximately 10% pressure-rise above the predicted stall line. The bypass migration test points are shown at 90 and 95% speed lines. The high bypass ratios (7 to 13) occur above the predicted stall line when the core discharge valve is well-closed relative to the nominal position; the low bypass ratios (4 to 6) occur when the core valve is wide open and the bypass valve is closed. The nominal discharge-valve position produces the design bypass ratio near the engine operating line. A summary of the fan bypass (with adjustments) and core-steam performance at the important engine cycle conditions max climb, max cruise, and takeoff is shown in Table VI.

The fan efficiencies, summarized relative to the component test goals, and the fully developed FPS fan goals are shown in Table VII.

These test efficiencies exceed the component test goals at all of the important engine operating conditions. Relative to the FPS engine goals, the fan bypass efficiency is higher by 0.7 points at max cruise and 0.5 points at max climb. At takeoff, the bypass efficiency is 0.7 points lower than the FPS goal. The core-stream efficiency is 0.7 points greater than the FPS goal at max climb, 0.3 points greater at max cruise, and 0.1 points greater at takeoff.

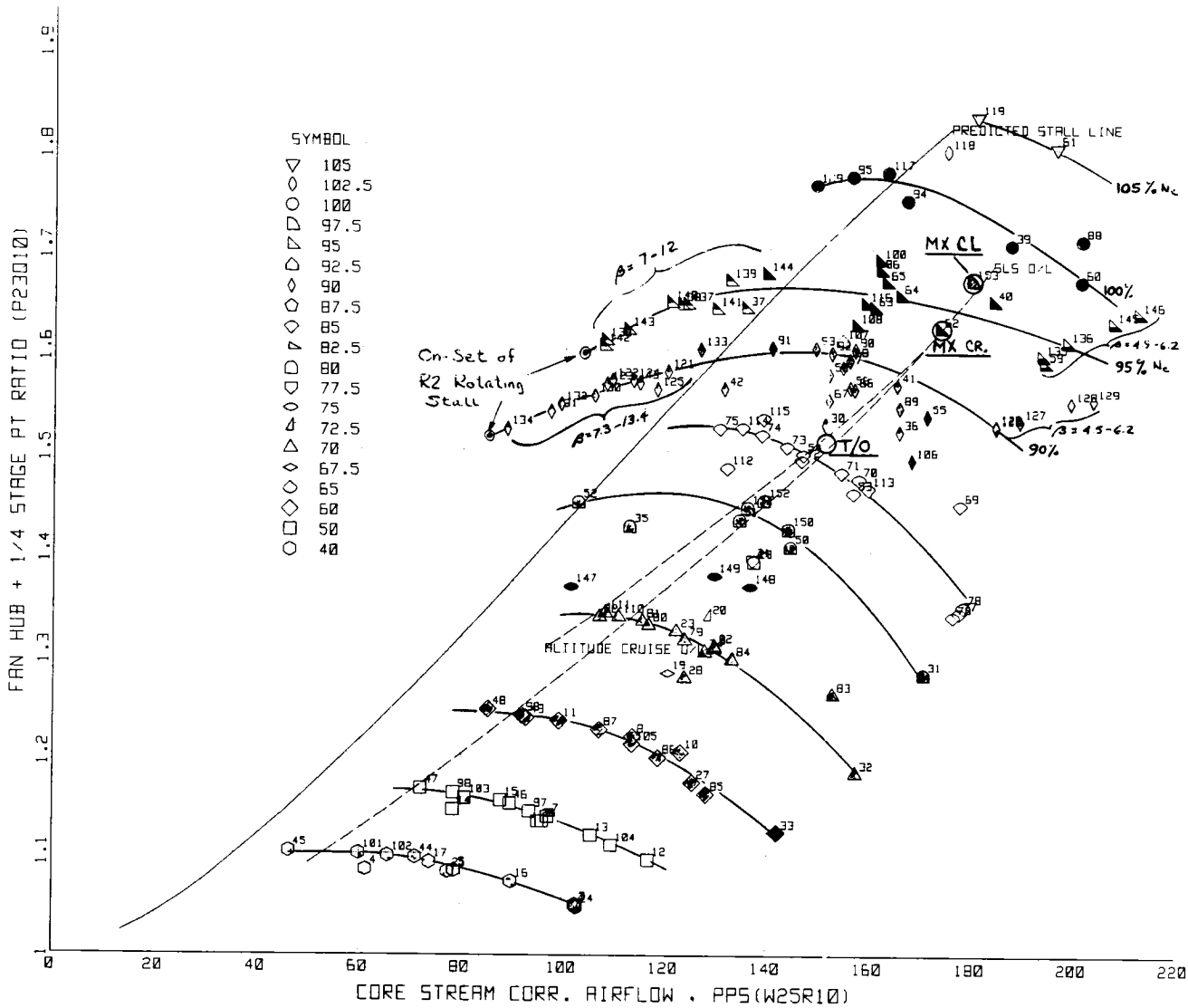

Figure 17. Fan Hub and Quarter-Stage Performance Map.

Table VI. Performance Results.

Parameter	Max Climb	Max Cruise	Takeoff
Corrected Tip Speed, ft/sec	1316	1283	1175
Corrected Total Fan Airflow, lbm/sec	1420	1395	1270
Flow/Annulus Area, lbm/sec-ft^2	42.8	42.1	38.4
Bypass Total-Pressure Ratio, P14/P10	1.65	1.61	1.50
Bypass Adiabatic Efficiency, η_{14}	0.886	0.892	0.893
Core-Stream Total-Pressure Ratio, P23/P10	1.67	1.62	1.53
Core-Stream Adiabatic Efficiency, η_{23}	0.892	0.895	0.898
Bypass Ratio	6.9	7.0	7.4

Table VII. Fan Efficiency Summary.

Parameter	Max Climb	Max Cruise	Takeoff
Bypass Adiabatic Efficiency			
Full-Scale Fan Test	0.869	0.877	0.890
FPS Goal	0.879	0.887	0.900
Full-Scale Fan Test (Adjusted)	0.886	0.892	0.893
Core-Stream Adiabatic Efficiency			
Full-Scale Fan Test Goal	0.875	0.882	0.887
FPS Goal	0.885	0.882	0.887
Full-Scale Fan Test Measured	0.892	0.895	0.898

Work Planned

Detailed data analysis of the fan test data will continue. The final performance report will be written, and preparation for the ICLS engine test will continue.

2.1.2 Fan Rotor Mechanical Design

2.1.2.1 Fan Rig Rotor Mechanical Design

Technical Progress

During this reporting period, the mechanical checkout, performance mapping, and bypass ratio excursions of the full-scale fan test have been completed. A maximum speed of 3930 rpm (105.4% physical) was reached, and 12 intentional and 2 unintentional stalls were sustained. Normal fan operation produced a maximum blade response of 18% of limits for Stage 1 and 17% of limits for Stage 2. The highest stress level seen during a stall (at 100% speed) was 50% of limits for Stage 1 and 65% of limits for Stage 2.

The fan rotor blade response during normal operation was very well-behaved. The Stage 1 blade first-flexural mode 3/rev crossing at 2150 rpm produced a response only 16% of limits. The first- and second-system modes were seen but were at levels below 21% of limits. At a near-stall setting at 70% speed (2610 rpm), the second-system mode responded at 25% of limits but died away to less than 10% when the fan was returned toward the operating line. The two-stripe mode was seen at the 12/rev crossing (3720 rpm) but only responed at 6% of limits.

The Stage 2 blades were equally well-behaved. The stage maximum response occured at 90% speed (3350 rpm) when the blade first-flexural mode reacted with a 5/rev crossing to produce a response that was 17% of limits. The two-stripe mode responds to a crossing with 120/rev (2 times Stator 1) at 2800 rpm to 16% of limits. At 3370 rpm, 180/rev (3 times Stator 1) excites a complex mode at 10.08 kHz to 11% of limits. During the bypass excursion testing at 90 and 95% speeds, the Stage 2 blade experienced separated-flow vibration of 28% of limits. At these test points, the bypass ratio was in the 14 to 16 range. During the bypass excursion testing, the Stage 1 blade remained quiet.

Intentional-stall testing was conducted at 40, 50, 60, 70, 80, 85, 90, and 95% speed points. Two additional stalls at each of the 90 and 95% speed points were obtained at different bypass ratios. The highest response to these stalls was 48% of limits for Stage 1 and 44% for Stage 2, both in first flex.

Two unintentional stalls were also encountered. One, at 100% speed, occurred with the bypass discharge valve (BDV) open 100%. It was initiated when the main discharge valve (MDV) was being closed to the 75% position. The Stage 1 blade responded to 50% of limits (first flex) and the Stage 2 blade to 65% of limits (first flex). The other unintentional stall occurred after taking a steady-state reading at a 90% speed, near-stall condition. Table VIII details the stresses and operating conditions of all of the stall events.

Table VIII. Stall Events.

% Nc	RPM	MDV, % Position	BDV, % Position	Blade Response, % Limits	
				Stage 1	Stage 2
40	1481	40	17.0	18	8
50(1)	1854	50	17.6	-	-
60	2219	50	18.8	38	12
70	2612	60	24.8	38	16
80	2968	50	25.2	40	26
85(1)	3178	64	28.3	-	-
90	3345	75	29.2	43	33
90	3360	100	29.0	38	31
90	3360	56	29.7	48	41
90(1,2)	3360	56	31.0	-	-
95	3550	70	31.2	38	44
95	3535	60	30.0	43	41
95	3535	100	32.7	40	28
100(2)	3732	75.4	100	50	65

(1) Blade stress levels at these points were not reduced.

(2) Inadvertant stalls

Blade initability was not encountered at any condition during the test. A time/spectral-frequency plot of the stall at 80% speed is shown in Figure 18 for the Stage 1 fan blade and is typical of the response seen during stall testing. Figure 19 depicts the stability plot for the Stage 1 fan blade using actual blade frequencies, incidence angles, and relative velocities measured during the test.

Work Planned

None

2.1.2.2 ICLS Fan Rotor

Technical Progress

Manufacture of the forward fan shaft is approximately 95% complete. The fan rotor assembly drawing has been issued.

Work Planned

- Follow hardware procurement
- Follow ICLS buildup

2.1.3 Fan Stator Mechanical Design

2.1.3.1 Frame Interface Design

Technical Progress

The fan stator vanes (Stage 1, core OGV, and bypass) were safety-monitored during the entire fan test program. Due to manpower changes, the backlog in the data-reduction facility, and the planning effort required for the ICLS fan stator modifications, the data from the fan test has not been completely reduced. The data to be reduced is primarily the stall responses which will be used to verify the stress levels and modes recorded from visual observations during the testing. In general, the bypass vanes were very quiet during the testing, as expected, with very minor responses during all operating conditions including stall. The Stage 1 vanes were the next quietest,

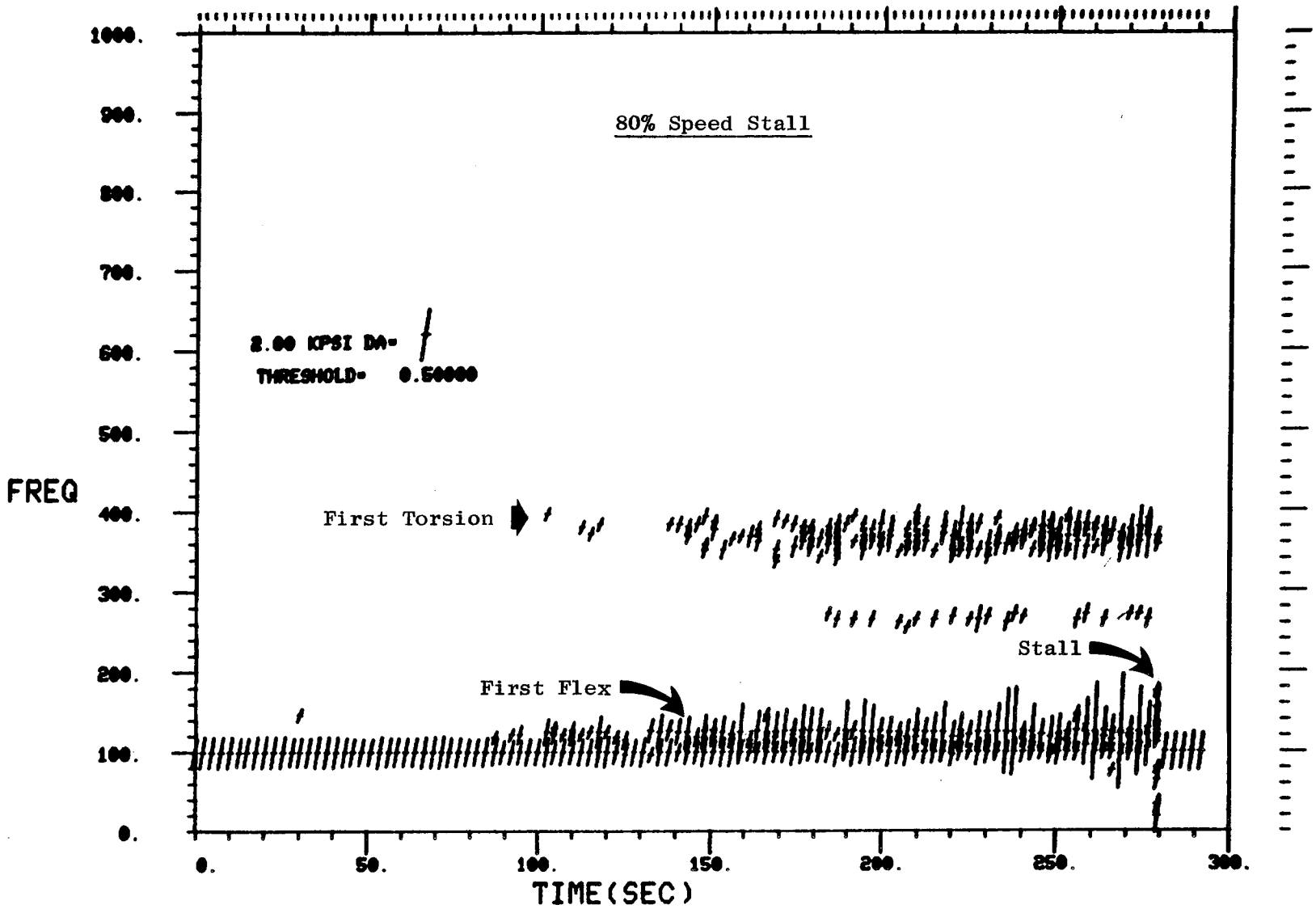

Figure 18. Stage 1 Fan Blade Campbell Diagram.

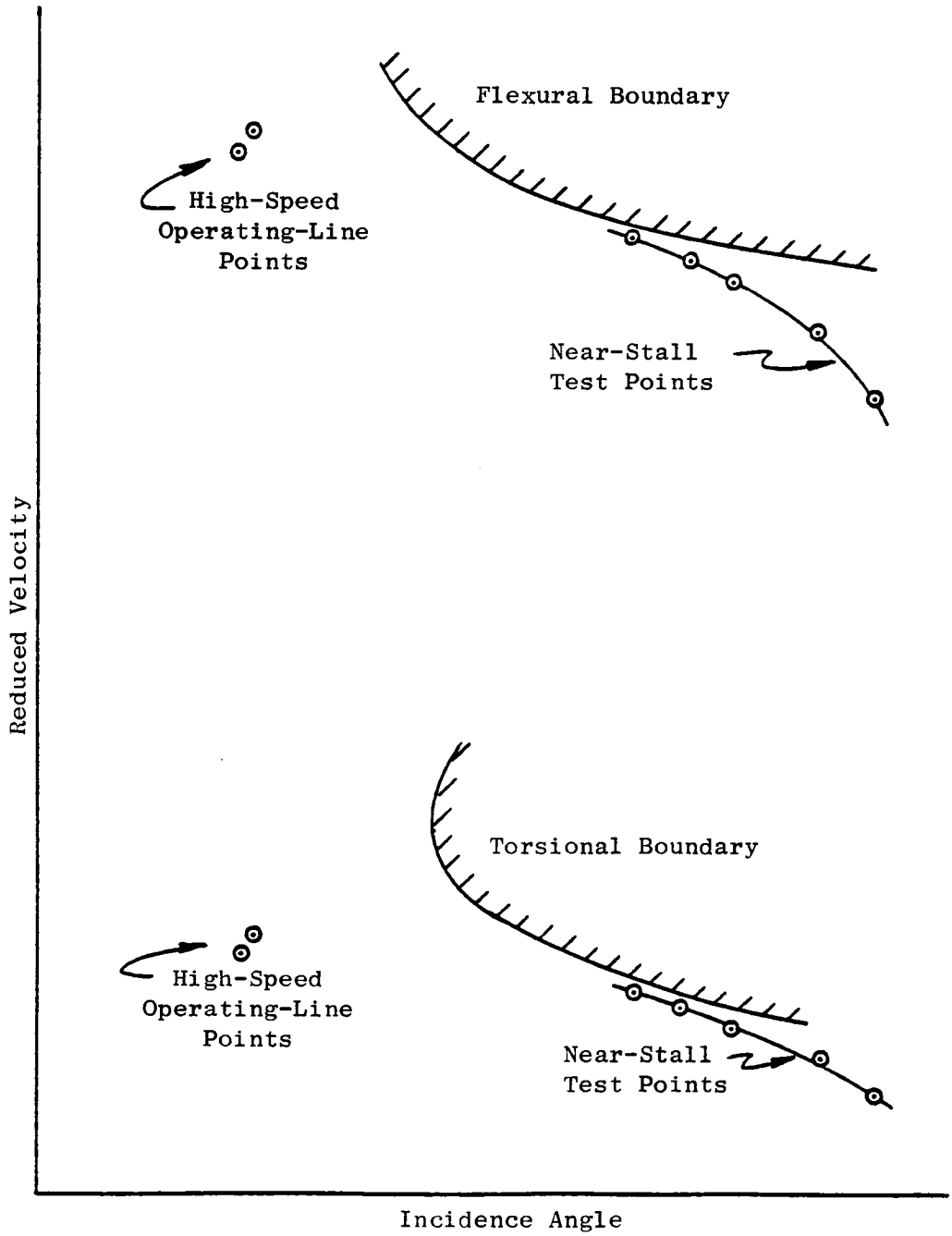

Figure 19. Stage 1 Fan Blade Stability Plot.

responding with all nonstall condition stresses below 20% limits except for the anticipated resonance of the first-torsional (1T) mode with the fan blade-passing frequency of 32/rev. This resonance at approximately 70% design corrected fan speed (Nf) produced a maximum response of 34% of limits. The stall-condition response of the vanes was observed to be well within limits at all stall conditions. The fan stator vanes located aft of the fan booster rotor, designated the core OGV's, exhibited a natural frequency response in 1T to the fan rotor 32/rev excitation. This response varied with fan speed due to slight differences in the natural frequencies of the individual vanes. For the five vanes monitored in the vane row, the responses which occurred in the 95 to 100% N_f (3500 to 3700 rpm) range reached 50 to 75% of the allowable limits (subject to complete data reduction). The response at all other operating conditions was well below these values. The observed stall stress responses were also within limits throughout the entire operating regime. The core OGV response in 1T at the 95 to 100% N_f range was higher than expected but still within limits. The anticipated maximum fan speed for the ICLS engine test is below 3500 rpm. This reduction in maximum operating speed during ICLS testing should eliminate the only significant vane response during the engine testing.

Following the fan test, work was resumed in support of the hardware fabrication for ICLS. All the components and associated hardware have been identified and ordered with delivery scheduled well before required dates for initiation of the assembly and instrumentation cycle. The major effort required to modify the fan frame was planned during December 1981 through February 1982 and initiated in March 1982. The machining of the fan frame should be completed by June 1982; at that time the frame will be ready for assembly.

Work Planned

Follow the fan frame rework and hardware fabrication and complete the reduction of fan test data.

2.1.3.5 Frame Mechanical Design

Technical Program

The acoustic panel design for the fan splitter was completed and sent to Mojave for fabrication. The detail drawing (4013284-208) describing the required fan frame machining for the ICLS hardware was also completed. This concludes the design effort required for the fan stator.

Work Planned

None

2.1.6 Full-Scale Fan Testing

2.1.6.1 Component Development and Evaluation

Technical Progress

Evaluation engineering direction was provided in the following areas during the full-scale fan test:

- Vehicle mapping and bypass ratio migration testing (November 4, 5, and 6, 1981)
- Radial traverse probe and dynamic-pressure sensor hardware installation and setup (November 9 and 16, 1981).
- Removal of the fan vehicle from the test cell and shipment to Evendale.

Work Planned

All work has been completed.

2.1.6.2 Evendale Test Facilities Engineering

Technical Progress

Engineering support was provided as it was needed during the fan vehicle performance testing conducted during the month of November 1981 and also during removal of the fan vehicle hardware from the Lynn test facility during the latter part of November and December 1981.

Work Planned

All work has been completed.

2.1.6.3 Instrumentation Design

Technical Progress

Engineering support was provided to monitor the aerodynamic rake stresses during the fan vehicle performance testing conducted in November 1981. Engineering support was also provided during the installation and setup of the radial traverse probes and dynamic pressure sensors followed by the monitoring of this instrumentation during the fan vehicle test runs of November 17 and 18, 1981. Engineering support and direction were provided for the post-test calibration of the cobra radial traverse probes and during the removal and storgae of the aerodynamic instrumentation rakes.

Work Planned

All work has been completed.

2.1.6.4 Test Facilities Engineering - Lynn

Technical Progress

Engineering support was provided during the month of October 1981 to direct the disassembly, repair, and reassembly of the high-pressure steam turbine to correct the high vibration levels encountered during the initial fan vehicle test runs in September 1981. Engineering support continued during the remaining fan vehicle performance testing conducted in November 1981.

Work Planned

All work has been completed.

2.6.6.7 Lynn Testing

Technical Progress

During the month of October 1981, effort was directed toward the disassembly, repair, and reassembly of the Lynn test facility high-pressure steam

turbine. This effort was expended in order to locate and correct the cause of the high vibration levels encountered on the steam-turbine drive system during the fan testing conducted on September 21, 22, 23, and 24, 1981. Repair of the steam turbine was completed on November 2, 1981; fan vehicle performance testing was resumed on November 4, 1981. Performance map and bypass ratio migration data were obtained during three test runs on November 4, 5, and 6, 1981. Testing was completed by November 19, 1981. Removal of the fan vehicle hardware from the test facility was completed on December 11, 1981, and all hardware was returned to Evendale. A total of 201 data points were taken during a total test time of 81 hours and 36 minutes.

Work Planned

All work has been completed.

2.1.7 Fan Fabrication

2.1.7.2 Fan Stator

Technical Progress

During this reporting period, the hardware required for the fan stator during the ICLS engine testing was procured. This hardware included engine mount and gearbox brackets, nacelle cowl door seal rings, radial driveshaft oil tube and adapter bracket, fan splitter acoustic panels, and associated hardware. Hardware still to be completed is the bottom vane extension and stiffeners. This hardware is currently being fabricated and will be completed in time for the ICLS frame buildup. The nacelle cowl door seal rings and a set of engine mount brackets were sent to Mojave for trail fitting with the test facility engine mount beam and dummy engine. This trail fitting will be completed in April 1982.

Work Planned

Follow fabrication of the bottom vane extension hardware and trail assembly of the mount brackets and cowl door rings to the Test Facility hardware at Mojave.

2.2 HIGH PRESSURE COMPRESSOR

Overall Objectives

The primary objective of the compressor development effort is to evolve a 10-stage, high-performance, high-stage-loading design (Figure 20) capable of achieving a pressure ratio of 23:1 at the maximum-climb design point. The primary aerodynamic design challenge is to provide adequate levels of stall margin at part-speed operation while maintaining the high efficiency required for this compressor. The FPS compressor efficiency goal is 0.861 at Mach 0.8, 35,000 feet, standard day, maximum-cruise power setting.

The mechanical design requirements include the development of an active clearance-control system for the rear block of compressor stages to achieve tip clearance at cruise compatible with efficiency and stall margin goals and to enhance performance retention. The compressor has fewer, longer chord airfoils (low aspect ratio) to increase blade and vane life and general ruggedness and to reduce performance deterioration and operational costs. The compressor is short and stiff and, in conjunction with the short combustor and HPT, permits the use of only two bearings to support the core rotor.

A sequential arrangement of the tests will allow refinements of the design to be introduced throughout the compressor development test program. The test program will culminate with the ICLS test in 1983.

Development Approach

Precontract aerodynamic design studies were completed in sufficient detail to allow the detailed aerodynamic design to commence at contract initiation. The initial contract efforts were devoted to the detail design and testing of the first six stages of the compressor. The PDR for the compressor was, therefore, completed very early in the program (February 1978). An IDR was held in July 1978 before committing to the hardware fabrication cycle for a 1-6 stage component test shown in Figure 21. Following instrumentation and assembly, the 1-6 stage component test was completed during the month of February 1980, and posttest analysis of the data has been completed.

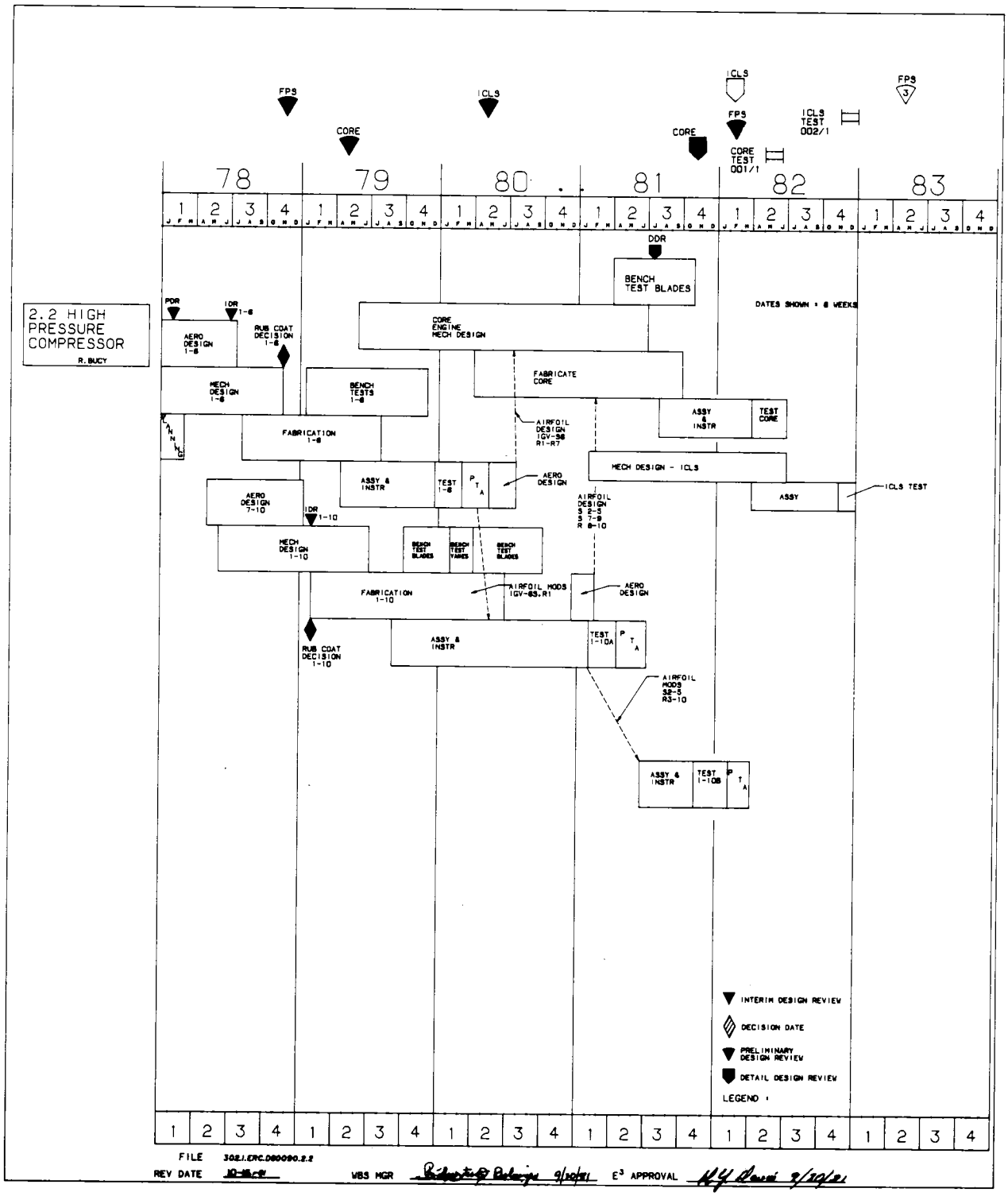
2.2 HIGH PRESSURE COMPRESSOR
R. BUCY
78
79
80
81
82
83
FPS
ICLS
CORE
CORE TEST 001/1
ICLS TEST 002/1
DDR
BENCH TEST BLADES
DATES SHOWN ± 6 WEEKS
PDR
IDR 1-6
AERO DESIGN 1-6
RUB COAT DECISION 1-6
CORE ENGINE MECH DESIGN
MECH DESIGN 1-6
BENCH TESTS 1-6
FABRICATE CORE
ASSY & INSTR
TEST CORE
FABRICATION 1-6
AIRFOIL DESIGN IGV-S6 R1-R7
MECH DESIGN - ICLS
ASSY
ICLS TEST
AERO DESIGN 7-10
IDR 1-10
AERO DESIGN
AIRFOIL DESIGN S2-S R7-8 R8-10
MECH DESIGN 1-10
BENCH TEST BLADES
BENCH TEST VANES
FABRICATION 1-10
AIRFOIL MODS IGV-S3, R1
RUB COAT DECISION 1-10
ASSY & INSTR
TEST 1-10A
AIRFOIL MODS S2-S R3-10
TEST 1-10B
INTERIM DESIGN REVIEW
DECISION DATE
PRELIMINARY DESIGN REVIEW
DETAIL DESIGN REVIEW
LEGEND :
FILE
REV DATE
WBS MGR
E³ APPROVAL

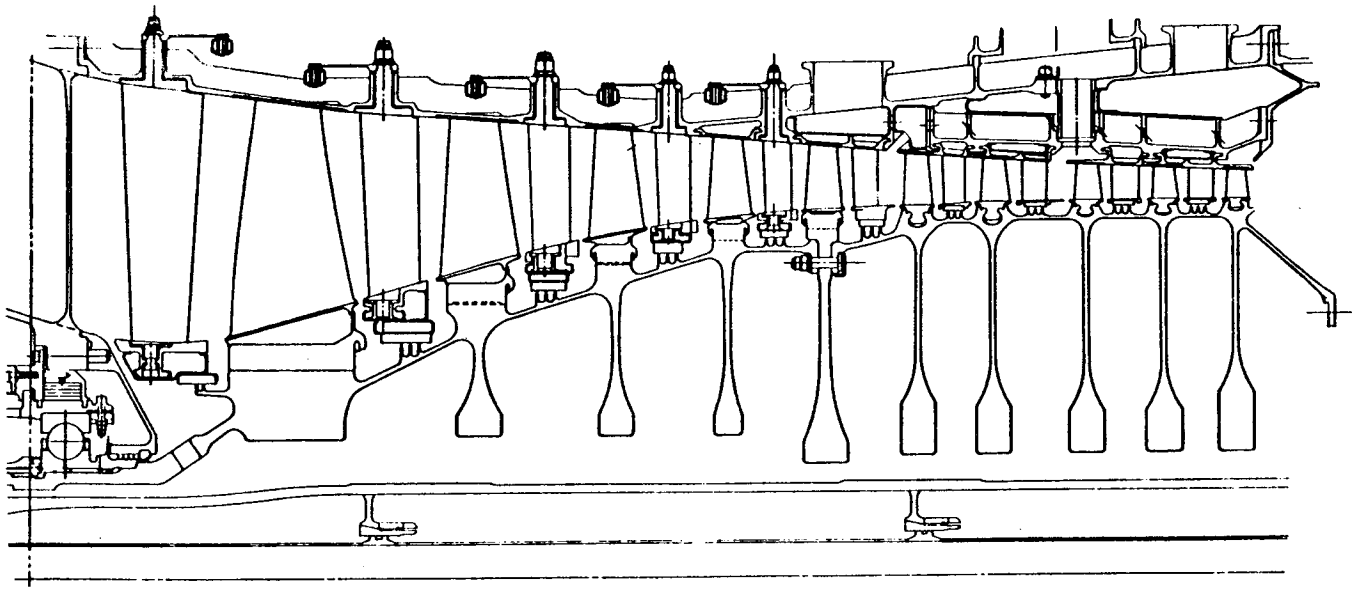

- Efficiency - MXCR - 86.1%
- 10 Stage, 23:1 PR-MXCL
- Low Aspect Ratio, Rugged Blades
- Steel Casing
- Inertial Welded Spools
- Ti 17 Forward, R95 Aft Spool
- Digital Control of Variable Stators
- Active Clearance Control Stages 6-10
- Adequate Stall Margin

Figure 20. HP Compressor Cross Section.

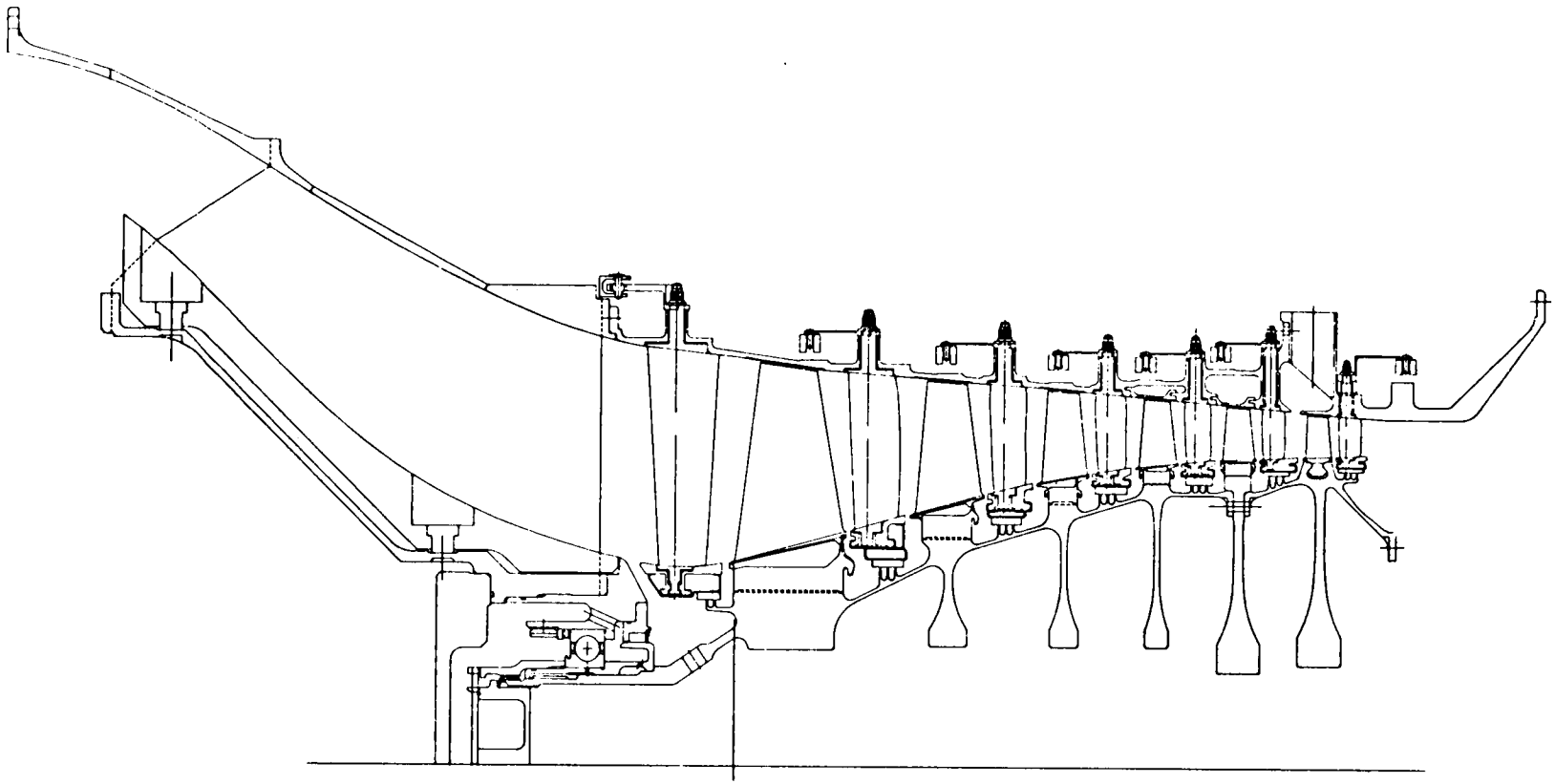

Figure 21. Stages 1 Through 6 Compressor Rig,

The detailed aerodynamic and mechanical design of the rear stages of the compressor was completed in the first quarter of 1979 during the procurement cycle for the first six stages. This permitted an additional IDR for the entire 10-stage compressor in late January 1979; compressor aerodynamic design parameters are shown in Table IX. Upon successful completion of this IDR, the hardware for the last four stages of the compressor was released for procurement.

Table IX. Compressor Aerodynamic Design Parameters.

Parameter	Maximum Climb 35,000 ft/0.8 Mach/+18° F	Maximum Cruise SLS/+27° F	Takeoff
Corrected Speed, % Design	100.0	99.5	97.7
Corrected Airflow, lbm/sec	120.0	118.0	108.8
Total Pressure Ratio	23.0	22.4	20.0
Adiabatic Efficiency	0.857	0.861	0.865
Polytropic Efficiency	0.903	0.905	0.908
Inlet Temperature, ° R	547.9	542.5	621.6
Inlet Pressure, psia	8.65	8.42	21.84

Appropriate hardware from the 1-6 stage vehicle was merged with the hardware procured for the aft stages to complete the 1-10 stage component buildup shown in Figure 22. The first 1-10 stage component test was completed during the first quarter of 1981. The compressor DDR was held at NASA Lewis in July 1981.

Following detailed analysis of the 10-stage test data, refinements in the mechanical and aerodynamic design were executed in the hardware for the second 10-stage component test. Testing of the 10B rig was initiated in December 1981 and is continuing in the first quarter of 1982.

A complete new set of hardware, refinements for which were defined based on the first 1-10 test, will be introduced into the first core engine test

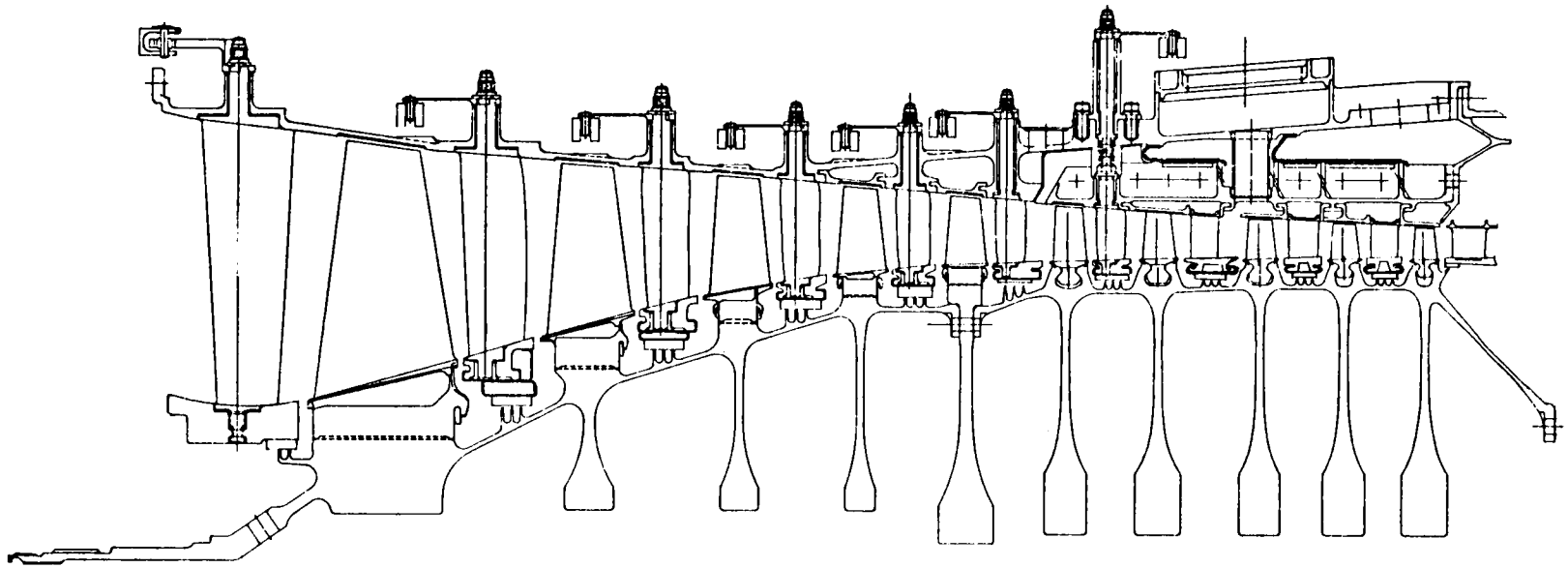

Figure 22. Stages 1 Through 10 Compressor Rig.

planned for the third quarter of 1982. Upon successful completion of this test, the low-pressure system will be added to the core and built into the ICLS to be tested in early 1983.

2.2.1 Aerodynamic Design

Technical Progress

Testing of the second build of the 10-stage compressor began in December 1981, and the mechanical checkout was completed during January 1982. Through the end of January, six test runs were made; 42 data points and 3 intentional stalls were recorded. Testing continued in February with an additional 11 test runs, 246 steady-state data points, and 58 intentional stalls.

Undistorted inlet data were obtained at speeds from 40 to 102.5% of design speed, and intentional stalls were performed up to 100% of design speed. The Stage 5 and Stage 7 bleeds were set to simulate the amount required for turbine blade cooling in the turbofan engine. The Stage 5 ACC bleed and the rotor-bore cooling flows were exercised during the early testing and then set at flows which resulted in acceptable rotor tip clearances. Several stator schedules were tested for each speed. The effects of the Stage 7 bleed flow, with amounts up to 16.8%, were studied at 60% speed for engine-starting requirements. The effect of the Stage 5 customer bleed on the compressor performance at high speeds and on the stall margin at low speeds was also studied. Two locked-stator decels were performed, one at 92.5% and the other at 97.5% of design speed.

A peak adiabatic efficiency of 0.832 was measured near the operating line at 90.3% of the design flow (97.5% speed); this is approximately the takeoff point. The highest efficiency recorded near the max cruise operating point was 0.827. The peak efficiencies at each speed occurred near the FPS operating line, and the efficiency island was quite wide. Adjustments totaling about 2 points in efficiency are believed to be appropriate to account for extensive instrumentation, inlet duct loss, extra variable stator rows, and some hardware variances. The demonstrated stall margin was 14% at design flow and 17% at takeoff flow. The stall margin in the low-speed region was

equal to or better than that required for a 45-second engine start without utilizing either Stage 5 or Stage 7 bleed. The data also indicated that substantial improvement of stall margin at low speeds could be achieved with moderate Stage 5 or Stage 7 bleed if needed.

Distortion testing was started in early March. The data indicated that only a small loss of stall margin resulted from a hub radial distortion and that very little change in stall margin resulted from a tip radial distortion. The stall margin sensitivity measured with a 180°, 2/rev distortion screen was comparable to that of a current-production, highly loaded, high-speed, core compressor.

Radial traversing, additional stator optimization, and final performance mapping with the selected stator schedule will be performed during March, and it is expected that the second full 10-stage compressor test will be completed by the first week of April 1982.

Preparation of the core engine test was carried out, and the aerodynamic definition of the instrumentation locations for the core engine compressor was also completed. Aerodynamic coverage of the core engine test vehicle buildup was provided to assure that hardware and instrumentation quality were consistent with the design intent.

Work Planned

- Detailed data analysis of the second 10-stage test will be completed, and the component performance test report for the core compressor will be written. The instrumentation plan and the test plan documentation will be prepared for the core engine test.
- Data-acquistion/data-reduction computer programs will be prepared for the core engine.
- The core engine test will be run in the second half of 1982.
- Preparation for the ICLS turbofan engine test will continue.

2.2.2 Rotor Mechanical Design

2.2.2.3 Design of Second 1-10 Rig

Technical Progress

The completed compressor rotor was assembled into the test vehicle and installed in the General Electric Full-Scale Compressor Test Facility in Lynn, Massachusetts. Instrumentation and control-system connections to the facility monitoring equipment were completed, and testing commenced. Rotor mechanical performance data have been recorded for the following:

- Mechanical Checkout - Steady-state and transient conditions at 0 to 87.5% corrected speeds, ambient inlet, full range of bleed and rotor cooling valve settings
- Ambient Inlet - Steady-state, transient, and stall conditions at 40% to 92.5% corrected speeds for several variable-stator-vane angle settings
- Refrigerated Inlet - Steady-state, transient, and stall conditions at 40% to 102.5% corrected speeds for several variable-stator-vane angle settings

The testing completed to date has revealed the following preliminary information about the mechanical behavior of this second Stage 1-10 rig:

- Blade natural frequencies observed during test correlate well with predictions.
- Recorded rotor temperatures are closer to predictions than was the case for the first 1-10 rig test.
- Borescope inspection showed that Stages 3, 4, 7 blades have experienced tip rubs. This airfoil distress was observed after off-design stalls caused by variable-stator-vane-controls malfunction.

Work Planned

- Complete rig testing and data analysis
- Complete vehicle removal, teardown inspection, and posttest reporting

2.2.2.4 Design of Core HPC

Technical Progress

During this reporting period all E^3 core compressor rotor hardware was received including the Stages 8, 9, and 10 Mod C blades. All hardware items except the instrumentation-leadout duct have been incorporated in the buildup. All rotor stages have been bladed and the axial dovetails sealed except Stage 1 which will be sealed after final balance. A new sealant compound will be tested in the Stage 5 disk assembly. This compound has a higher allowable operating temperature than that used on the forward stages, and the viability will be assessed at teardown. The rotor has completed assembly to the point of final balancing.

Rotor instrumentation application and checkout has been completed. Airfoil strain gage calibration data have been recorded and used to calculate maximum allowable operating stresses. The limit clearance and the assembly stackup drawings have also been issued.

The design modifications identified to increase the sensitivity of the clearanceometers used on the second Stage 1-10 rig were prototype tested and found to be very effective. These modifications have, therefore, been incorporated in the core clearanceometers along with improvements in the electronic signal conditioning.

Work Planned

- Complete rotor final balancing
- Complete installation of the instrumentation-leadout duct and instrumentation-lead routing and tie-down
- Complete assembly of compressor rotor into core engine
- Monitor core engine testing

2.2.3 Stator Mechanical Design

2.2.3.3 Design of 1-10 Rig, Build II

Technical Progress

- Completed engineering support of the vehicle assembly

- Continued engineering support of procurement of spare cast-vane sectors
- Provided safety monitoring during vehicle test

Work Planned

- Continue to provide safety monitoring of vehicle test
- Analyze test data and prepare summary of vane stresses observed during test

2.2.3.4 Design of Core Engine

Technical Progress

- Calculated rotor/stator operating and buildup clearances
- Issued clearance and stator grind drawings
- Issued compressor stator assembly drawings
- Completed engineering support of hardware procurement
- Initiated engineering support of engine assembly

Work Planned

- Complete engineering support of engine assembly and test-cell installation
- Provide safety monitoring during engine test
- Analyze test data and prepare summary of vane stresses observed during test

2.2.3.5 Design of ICLS Engine

Technical Progress

- Completed design and issued detail drawings of IGV actuation linkage
- Conducted an internal design review of torsion bar actuation system
- Continued engineering support of hardware procurement

Work Planned

- Complete engineering support of hardware procurement
- Trial assembly and checkout of actuation system on reworked 1-10B compressor stator prior to ICLS assembly
- Provide engineering support during vehicle assembly

2.2.4 Rotor Design Testing

Technical Progress

The impulse-vibration bench test of the core compressor rotor instrumentation-leadout duct has been completed. The results show good agreement between predicted resonant frequencies and those determined during the bench test.

Work Planned

No further effort is planned.

2.2.6 Full-Scale Compressor Testing

2.2.6.1 Component Development and Evaluation

Technical Progress

Engineering direction was provided for the final assembly of the 10B compressor vehicle completed on November 10, 1981. The vehicle was shipped to Lynn and arrived there on November 12, 1981. Engineering direction was provided at Lynn during the test-cell installation of the compressor vehicle initiated on November 13, 1981 and completed on December 17, 1981. Compressor vehicle testing was initiated on December 18, 1981 and continued during the months of January, February, and March of 1982.

Work Planned

Engineering direction will be provided at Lynn during the remaining compressor vehicle testing and the test cell removal activity that will follow the completion of the vehicle testing. Engineering direction will then be

provided during disassembly of the compressor after it is returned to the Evendale plant.

2.2.6.2 Test Facilities Engineering

Technical Progress

Engineering support was provided during the final assembly of the 10B compressor vehicle and during the Lynn test cell installation and performance-testing activities.

Work Planned

- Provide engineering support as required during the remaining 10B compressor test program.
- Provide engineering support as required during the disassembly of the 10B compressor vehicle.

2.2.6.3 Instrumentation

2.2.6.3.1 Instrumentation Application

Technical Progress

Instrumentation shop support was provided during the main compressor vehicle buildup and during final vehicle instrumentation termination. Support was also provided, as required, during the Lynn test cell installation and compressor testing activities.

Work Planned

Provide instrumentation shop support during disassembly of the 10B compressor vehicle following the completion of all Lynn test and cell-removal activity.

2.2.6.3.2 Instrumentation Design

Technical Progress

Engineering support was provided during the final assembly and instrumentation termination activities on the 10B compressor vehicle. Support was also

provided at the Lynn test facility during the installation, hookup, and checkout of the clearanceometers and touch probes. On-test monitoring of the aerodynamic rake, strain gage, and rotor tip-clearance data from the clearanceometers and touch probes also provided during the compressor testing.

Work Planned

- Provide engineering support as required during the remaining 10B compressor vehicle test activity
- Provide engineering support during disassembly of the 10B compressor vehicle after it is returned from Lynn.

2.2.6.4 Development Assembly

Technical Progress

Development assembly manpower was provided to complete the final assembly cycle on the 10B compressor vehicle. The 10B compressor vehicle buildup was completed on November 10, 1981, and the vehicle was shipped to Lynn.

Work Planned

Provide the necessary manpower for disassembly of the 10B compressor vehicle after it is returned from Lynn.

2.2.6.5 Lynn Testing

2.2.6.5.1 Test Facilities Engineering

Technical Progress

Preparations to the Lynn test facility were completed, and engineering support was provided during the test-cell installation of the 10B compressor vehicle. Support was also provided during testing of the 10B compressor vehicle to assure the proper operation of the various facility systems and the inlet refrigeration system.

Work Planned

Provide engineering support during the remaining 10B compressor vehicle test program and during removal from the Lynn test facility.

2.2.6.5.4 Stage 1-10 Compressor Testing

Technical Progress

Test cell installation preparations were completed, and installation of the 10B compressor vehicle into the Lynn test facility was initiated on November 13, 1981. Test cell installation of the vehicle was completed on December 17, 1981. A mechanical checkout test run to 85% corrected speed was conducted on December 18, 1981. Aerodynamic performance testing was initiated on January 11, 1982, and five test runs were made during January 1982 with a total test time of 22 hours and 11 minutes. An extensive amount of vehicle testing was conducted during the month of February 1982. During March 1982, seven additional test runs were made for a total test time of 44 hours and 21 minutes. As of the end of March 1982, the accumulated total vehicle test time was 192 hours and 4 minutes during which 404 data points were taken.

Work Planned

Complete the 10B compressor vehicle performance test program and the following removal from the test cell.

2.2.7.1 VSV Bushing Application

This program has been completed.

Synopsis

Dry bearing materials for use up to 900° F and having low friction and wear are required for variable stator vane (VSV) bushings for the compressor. This program has identified and evaluated candidate materials for all stages of the compressor for 18,000 hours of service. Based on this work, selected materials are being further evaluated in the component and engine testing. This effort was an extension of work previously performed, in support of the CF6 and F101/CFM56 programs, in which long-life VSV bushings were developed for these production engines.

Maximum operating temperatures, as determined later in the E^3 design program, are as follows (° F):

Stage	FPS		Growth	
	HDTO	Cruise	HDTO	Cruise
IGV	202	82	248	118
1	316	190	371	245
2	421	287	482	318
3	523	386	593	417
4	623	485	699	554
5	723	581	814	653
6	802	666	888	737

These represent maximum gas-path temperatures and are assumed to be worst-case bushing temperatures.

In the early phases of the program, nominal conditions for the wear tests were defined for Stages 1, 4, and 6 as representative of loading and temperature ranges for the compressor design.

A number of redirections of the original program were made as requirements of the engine were refined. In September 1978, a revised program was approved to include pressurized, wear-test-rig evaluation of candidate materials. Component friction and wear testing was increased, but simpler geometry friction and wear tests were deleted. All subsequent testing was done with bushings and washers to-print rather than with simple-geometry test blocks.

As the engine design evolved, changes to the bushing dimensions were made either to give increased wear life or to accomodate, in some cases, materials which could not be fabricated as very thin-wall bushings. Journal length, for example, on Stage 4 initially was 0.75 inches but was increased first to 1.00 inches and later to 1.25 inches. Wall thickness was increased from 0.040 to 0.060 inches to accommodate mechanical carbon-sleeve bearings.

In October 1978, a decision was made to delete testing at conditions above 700° F.

It was judged that variable stators may not be used in the final design for Stages 5 and 6.

Wear testing began in January 1979. Both test rigs in this laboratory (MPTL) and in the Component Mechanical Laboratory (CML) were utilized.

The ideal dry-bearing material has the following properties for VSV bushing applications:

- Thermal stability
- Very low wear-rate coefficient
- Low coefficient of friction
- Resistance to shock, impact, and vibration
- Forms an effective air seal
- Satisfies thin-wall dimensional requirements
- Reasonable cost

Wear-test results of some 65 tests over the three-year program are given in previous semiannual reports. Endurance wear tests results are shown in Tables X and XI.

These tests were run under simulated Stage 1, Stage 4, or Stage 5 conditions up to 2,500,000 wear cycles to substantiate the 18,000-hour expected service life of the bushing materials selected for engine tests. This was the final and most significant block of testing done on this contract. Each 2.5-million-cycle test took three weeks to complete.

Several conclusions drawn from earlier testing led to the materials, test conditions, and geometry of specimens used in these tests. It is desirable to do further testing at growth-engine conditions, but this could not be accomplished within the scope and resources of the program.

Conclusions and Recommendations

1. VSV bushing materials and geometries were developed for all stages of the compressor. Endurance wear tests were run to validate 18,000 hours. Materials selected on the basis of these tests for the VSV system are as follows:

Vane Stages	Component	Material
IGV-4	Thrust washers, outer	Composite ZX (703 resin)
IGV-4	Bushings, outer	Fabroid XV
4-6	Thrust washers, outer	PBH-20 mechanical carbon
4-6	Bushings, outer	PBH-20
IGV-3	Bushings, inner	Fabroid XV
4-5	Bushings, inner	PBH-20

Table X. Endurance Wear-Test Conditions, MPTL Pressurized Rig.

• 200,000 Cycles HDTO Plus 2,300,000 Cycles at Cruise

Test No.	Materials		Stage: (Bushing Geometry)	Stage: (Test Conditions)	Moment Load, lbf	Pressure, psia		Temperature, ° F		Remarks
	Bushing	Washer				HDTO	Cruise	HDTO	Cruise	
57	PBH-20	PBH-20	4	5	32	75	53.9	700	581	1.0-in. Bushing
58	GENR-150	Xylan NR150	4	4	34	75	39.3	623	485	0.8-in. Bushing
59	Fabroid XV	Comp. ZX(703)	1	1	62.8	30.2	12.4	316	190	-
60	PBH-20	PBH-20	4	5	30.2	75	53.9	723	581	1.25-in. Bushing
61	Comp. ZX(703)	Comp. ZX(703)	1	1	62.8	30.2	12.4	316	190	-
62	Comp. ZX(NR150)	Comp. ZX(NR150)	1	4	44.8	75	39.3	623	485	Rig failure
63	Comp. ZX(NR150)	Comp. ZX(NR150)	1	4	44.8	75	39.3	623	485	-
64	PBH-20	PBH-20*	4	5	30.2	75	53.9	723	581	1.25-in. Bushing
65	Fabroid XV	Comp. ZX(703)	4	4	34	75	39.3	623	485	1.25-in. Bushing

*Carbon wear pad washer

Table XI. Endurance Wear-Test Results.

Test No.	Materials	Stage	Cycles Run (1000's)		Max. Wear		Actuation Force, lbf	Remarks
			HDTO	Cruise	Mils	Mils/10^5 Cycles		
57	PHB-20	5	200	2,207	B 28 W 13	1.27 0.59	3.5-15	Bushing length: 1.0 in. Bushing wore through to metal backing.
60	PBH-20	5	200	2,393	B 13 W 8	0.50 0.31	1.5-2	Bushing length: 1.25 in. Metal-encased flat washer
64	PBH-20	5	250	2.250	B 12 W 11	0.48 0.44	1 - 4	Bushing length: 1.25 in. Carbon wear pad washer
58	GENR-150/ Xylan	4	200	1,012	B 32 W 31	2.6 2.6	2 - 17	Bushing length: 0.8 in. Test terminated - wear out.
59	Fabroid XV	1	200	2,300	B 10 W 5	0.40 0.20	7 - 14	Comp. ZX washer
65	Fabroid XV	4	200	2,300	B 7 W 9	0.28 0.36	0.8 - 1.0	Bushing length: 1.25 in. Comp. ZX washer delaminated on disassembly.
61	Comp. ZX (703)	1	200	2,300	B 6 W 3	0.24 0.12	4.5 - 0.8	-
62	Comp. ZX (NR150)	4	282	-	B 10 W 10	- -	-	Test terminated - rig failure and excessive HDTO cycles.
63	Comp. ZX (NR150)	4	200	1,954	B 33 W 10	1.53 0.46	2 - 4	Bushing length: 1.0 in. Bushing wore out; test terminated short.

2. Increasing bushing length from 0.8 inches to 1.0 inches and then to 1.25 inches greatly improved wear life and allows completion of 2.5-million cycles, with margin, for material selected above.

3. Mechanical carbons are the only attractive bearing materials for 700° F and above (Stages 5 and 6, and possibly essential even for Stage 4). Pure Industries PBH-20 was the best of three grades screened.

4. Useful dry bearings made from NR150 resin and capable of use to 675° F were demonstrated. However, DuPont's refusal to produce the resin long term, at reasonable price, makes GENR-150, Filimide 7X, or Composite ZX (NR150) unacceptable for E^3 (or any other advanced engine).

2.2.8 High Pressure Compressor Fabrication

2.2.8.1 Compressor Rotor

2.2.8.1.4 Core

Technical Progress

Instrumentation rework of the Stage 1-4 spool has been completed along with the addition of oil-drain holes. The Stages 8, 9, and 10 Mod C blades have been received, inspected, and incorporated in the core compressor rotor buildup.

Work Planned

None; all identified hardware has been received.

2.2.8.2 Compressor Stator

2.2.8.2.3 Stage 1-10 Rig Stator Hardware, Build II

Technical Progress

Reworked hardware as required during vehicle assembly.

Work Planned

Procure spare Stages 7 to 9 vane castings.

2.2.8.2.4 Core Stator Hardware

Technical Progress

- Completed machining of Stages 7 to 9 vane sector castings
- Procured OGV and diffuser castings
- Completed fabrication and machining of OGV/diffuser assembly
- Procurement of ICLS VSV actuation hardware continued

Work Planned

Complete procurement of ICLS VSV actuation hardware.

2.3 COMBUSTOR

Overall Objectives

The key objective of this program is to design and develop an advanced combustion system capable of meeting the stringent emissions and long-life goals of the E^3 as well as meeting all of the usual performance requirements of combustion systems for modern turbofan engines. The specific E^3 goals are the emissions standards for carbon monoxide (CO), unburned hydrocarbons (HC), oxides of nitrogen (NO_x), and smoke that have been specified by the EPA for newly certified, subsonic-aircraft engines. These very stringent CO and HC emissions goals require very high combustion efficiencies at all engine operating conditions, including idle. The FPS combustion efficiency goal is 0.995 minimum at high power settings with a total pressure drop of 5.0% maximum.

To meet these emissions goals and other performance requirements, an advanced, short, double-annular combustor concept has been selected (Figure 23). This design approach was chosen based on the low-emissions combustor design technology developed in the NASA Experimental Clean Combustor Program (ECCP) and the NASA Quiet, Clean, Short-Haul Experimental Engine (QCSEE) Program. A comparison of the key design parameters for the NASA E^3, NASA ECCP, and NASA QCSEE combustors is shown in Table XII. In these development programs it was demonstrated that low emissions levels could be obtained with the double-annular design in addition to the other combustor performance required

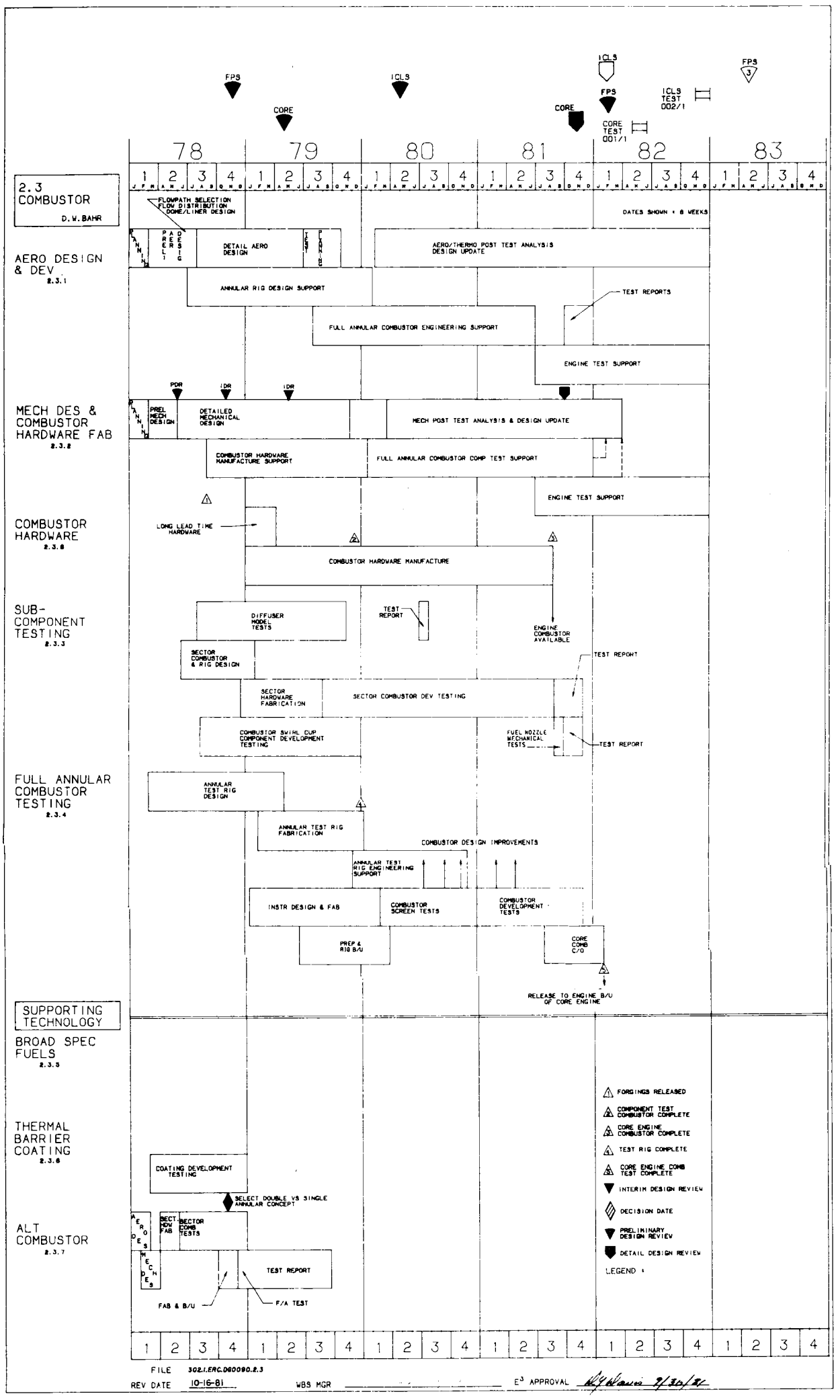

FILE 302.1.ERC.080080.2.3

REV DATE 10-16-81 WBS MGR _____ E^3 APPROVAL [signature] 9/30/81

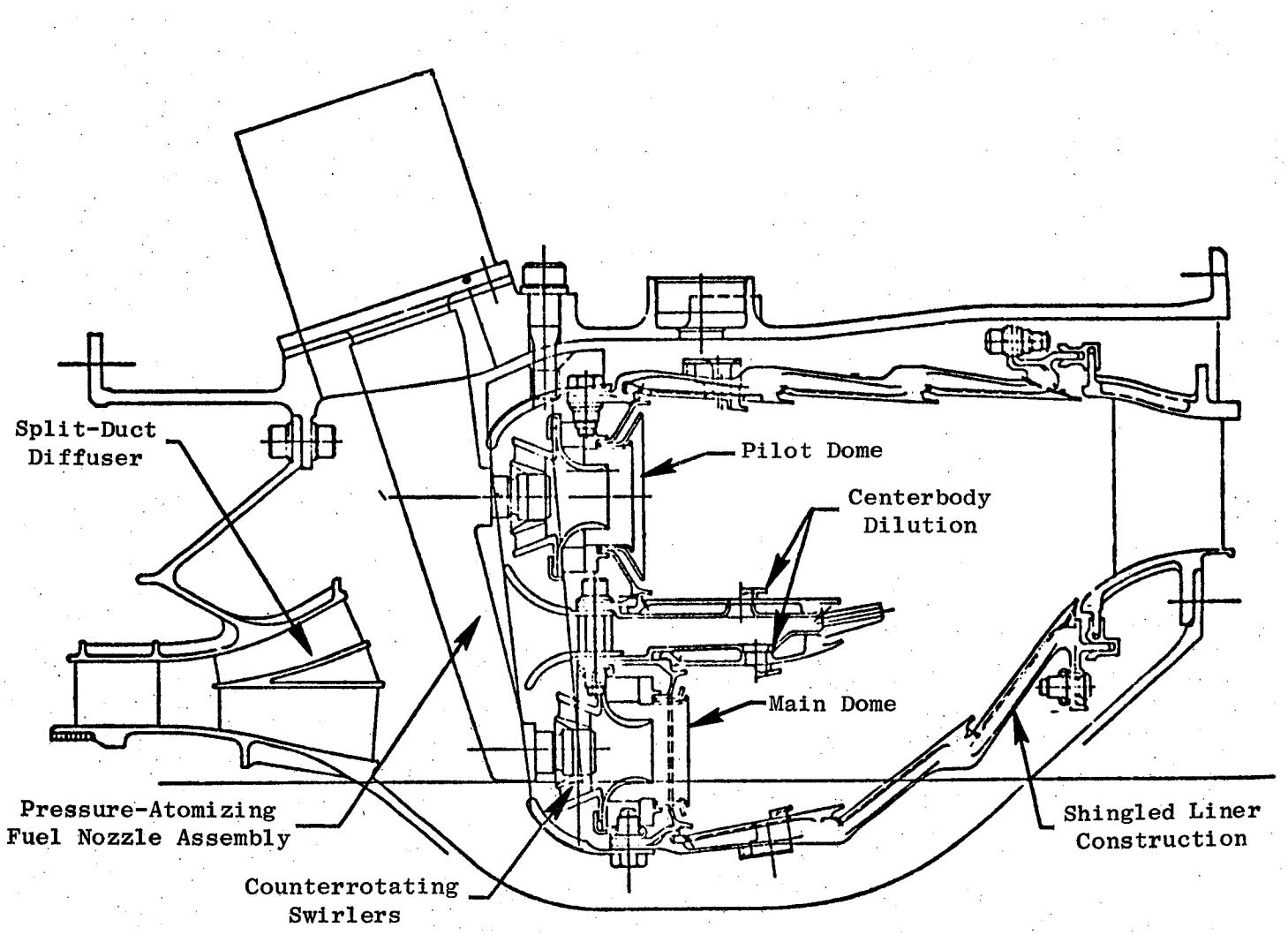

Figure 23. Combustor Design Concept

Table XII. Comparison of Double-Annular Combustors.

Combustion System	E^3	ECCP	QCSEE
Burning Length, in.	6.7	12.9	7.0
Pilot Dome Height, in.	2.4	2.7	2.3
Main Dome Height, in.	2.0	2.4	2.0
Length/Dome Height - Pilot	2.8	4.8	3.0
Length/Dome Height - Main	3.4	5.4	3.5
Number of Fuel Injectors - Pilot	30	30	20
Number of Fuel Injectors - Main	30	30	20
Reference Velocity, ft/sec	58	75	59
Space Rate, Btu/hr; ft^3-atm x 10^{-6}	7.0	5.8	8.1

for satisfactory operation. To meet the long-life goals, an advanced, double-walled, axially segmented, cooling-liner design using both impingement and film cooling has been selected. This advanced cooling-liner concept, in conjunction with the very short length, is projected to result in a combustor with the requisite long-life objectives.

Basic Development Approach (Double-Annular Combustor Design)

The overall design definition and development approach have been selected for the E^3 combustor. The aerodynamic and mechanical design features identified for the diffuser, cowling, dome, and liner were based on proven design and analytical techniques evolved from other General Electric combustor designs.

Initially, an extensive series of combustion-system aeromechanical and design tradeoff studies was conducted using existing combustor design tools and correlations to define the optimum combination of the basic combustor design parameters. These design studies included the definition of the combustor inlet diffuser, combustor cooling features, the number of fuel injectors, the swirl-cup design features, and the dilution airflow patterns. Based on the results of these design studies, combustion system performance and emission levels were estimated. The final flowpath design was then incorporated into a mechanical-design layout.

Following these initial design studies, detailed stress analysis, heat-transfer analysis, and life prediction studies were made for both steady-state and transient operation at the most adverse operating conditions.

Based on these detailed aerodynamnic and mechanical design studies, the detail features of the combustor evolved into engineering drawings for procurement of development-test hardware.

To evaluate and confirm the design analyses efforts, subcomponent tests were conducted. The purpose of these tests was to permit preliminary development and refinement of the emissions and performance characteristics of the combustor design prior to and during the full-annular combustor development testing. These subcomponent development tests included tests to develop the diffuser aerodynamic characteristics in order to obtain the required combustor inlet conditions at the various simulated engine conditions from idle to take-off, individual swirl cup tests to develop the required fuel preparation and introduction characteristics to obtain the desired combustion-zone stoichiometry, and sector-combustor tests to develop the pilot-stage dome features to meet the idle emissions goals and develop ground-start and altitude-relight capability.

The diffuser test program was conducted in a full-size, full-annular test rig and is complete. These tests were run with ambient-temperature airflow, and the diffuser was tested over a broad range of passage flow-split values with three different inlet-velocity profiles. The results of these tests (based on measured static pressure recovery and total pressure loss coefficients for the inner and outer combustor domes, the centerbody passage, and the inner and outer combustor liner passages) indicated that the diffuser would perform satisfactorily in the development combustor test rig and in the E^3.

The swirl cup spray-visualization tests were conducted to determine the effects of combustor dome pressure drop, swirl cup fuel/air ratio, and fuel/air momentum ratios on fuel spray characteristics such as spray angle, stability, and atomization. The results of these tests were utilized to select the swirl cup design features for the sector combustor and for the full-annular combustor.

The sector combustor tests were conducted with a 60° sector of the E^3 combustor design. The emissions-related aspects of these tests were primarily directed toward obtaining low CO and HC emissions levels in the pilot stage at idle operating conditions and evaluating the crossfire and fuel-staging characteristics between the pilot and main stages. Additional sector testing was conducted to evaluate the altitude-relight characteristics of this combustor design. This testing was conducted with ambient-temperature air and fuel. Pressures were reduced to subatmospheric levels to simulate altitude effects. It had been intended to evaluate the sector combustor for altitude relight with cold air and cold fuel (around -30° F); however, schedular and budgetary considerations did not permit this phase of the program to be completed.

A significant portion of the planned E^3 combustor component development effort has been performed with a full-scale, annular test vehicle that duplicates the flowpath of the engine and can accommodate full-scale combustor hardware. Testing in the combustor test vehicle was performed at both atmospheric and elevated-pressure conditions.

The exit annulus of the test rig is at the same radial location as the turbine nozzle of the engine. The test vehicle simulates the cooling flows of the turbine nozzle diaphragm and first-stage turbine blades.

The OGV/diffuser section of the full-annular test vehicle simulates the aerodynamic characteristics of the airflow delivered to the combustor from the engine compressor. Provisions to add inlet airflow profiling features to simulate compressor circumferential and radial distortion were also included. The test rig prediffuser incorporates structural features identical to those of the engine design including flowpath simulation, strut supports, and bleed capability at the prediffuser trailing edge. Pressure-measurement instrumentation was provided along the diffuser flowpath surfaces to monitor stability and performance.

The combustor section provides the structural pressure vessel to house the combustor and duplicates the flowpath of the engine combustor housing. Ignitor port locations can be incorporated at several circumferential positions to permit selection of location flexibility based on sector combustor component test data.

Two different exit-instrumentation sections were used with this test vehicle. Atmospheric-pressure tests were performed with a mechanically actuated ring mounted from the outer flange. Temperature and pressure rakes are mounted to the ring which is traversed around the combustor circumference. With this test rig setup, combustor airflow is discharged directly to the atmosphere; the reaction zone can be viewed directly from the combustor exit. For testing at elevated pressure levels, a high-pressure casing containing five internal, rotating, gas-sample rakes is used. This exit section allows operation up to pressures of 300 psia.

Two different types of full-annular combustor tests were conducted: (1) high-pressure tests to develop the emissions, performance, and durability characteristics of the combustor at various simulated engine-operating conditions from idle to takeoff and (2) atmospheric-pressure combustor tests to develop the required combustor exit temperature distributions and ground-start ignition capability. The altitude-relight capability of one combustor configuration was evaluated in an accompanying sector-combustor test.

The evaluation of the baseline combustor configuration and the first phase of development testing have been completed. The design information acquired in the baseline test in conjunction with preferred combustor design features evolved in the sector-combustor development program were incorporated into a modified version of the baseline design.

Cold-flow calibrations of this modified E^3 combustor test hardware were performed to verify that the various dome and liner cooling airflows were distributed as intended. Then full-annular tests were conducted at atmospheric pressure to provide additional data on pattern factor, profile factor, and ground-start characteristics. Following completion of the atmospheric tests, evaluation of the improved design for reduced emissions was conducted at ground idle operating conditions. A final high-pressure test was conducted to measure combustor metal temperatures at simulated high-power conditions. Following analysis of the data from this modified configuration, additional development tests were conducted to further improve the design.

Upon selection of the final design for engine installation, all of the design features evolved in the development program were incorporated into the core engine combustor. This hardware was given a complete evaluation of all

facets of combustor operation including ignition, emissions, and performance. The combustor was then released to the core engine upon satisfactory completion of the tests.

2.3.1 Aerodynamic Design

Technical Progress

The E^3 double-annular combustor concept is an advanced design approach which must meet the engine performance requirements as well as the emissions goals over a wide range of operating conditions. Some of the key operating conditions for the E^3 combustor are shown in Table XIII. Operation of the combustor at these varied conditions requires that the fuel flow be staged to the two domes as shown in Figure 24. Therefore, considerable aerodynamic development effort was anticipated to obtain satisfactory operation over this wide range of operating conditions while meeting the challenging performance and emissions goals for this engine.

At the conclusion of the last reporting period, component development of the Mod. VII development combustor configuration had been completed. This combustor was a lean-dome design similar to the Baseline, Mod. I, and Mod. VI configurations previously evaluated. Design modifications featured in the Mod. VII combustor involved moving a small amount of inner liner Panel 3 trim dilution upstream into Panel 2. In addition, new dome sleeves were fabricated for both the pilot- and the main-stage swirl cups, and the combustor hardware was refurbished to improve the quality. This rework was intended to improve the disappointing exit-temperature pattern factor and profile results obtained with the Mod. VI combustor configuration.

As noted in the last Semiannual Report, the Mod. VII combustor did demonstrate substantial improvement in pattern factor and profile. Although the pattern factor performance (0.275) was slightly above the program target goal (0.250), the results were considered acceptable. Additional hardware modifications intended to further reduce the pattern factor were not considered necessary. Instead, it was decided to proceed to evaluate the Mod. VII configuration at true engine-cycle operating conditions for ground-start ignition, staging, and low-power emissions. The results of this evaluation showed

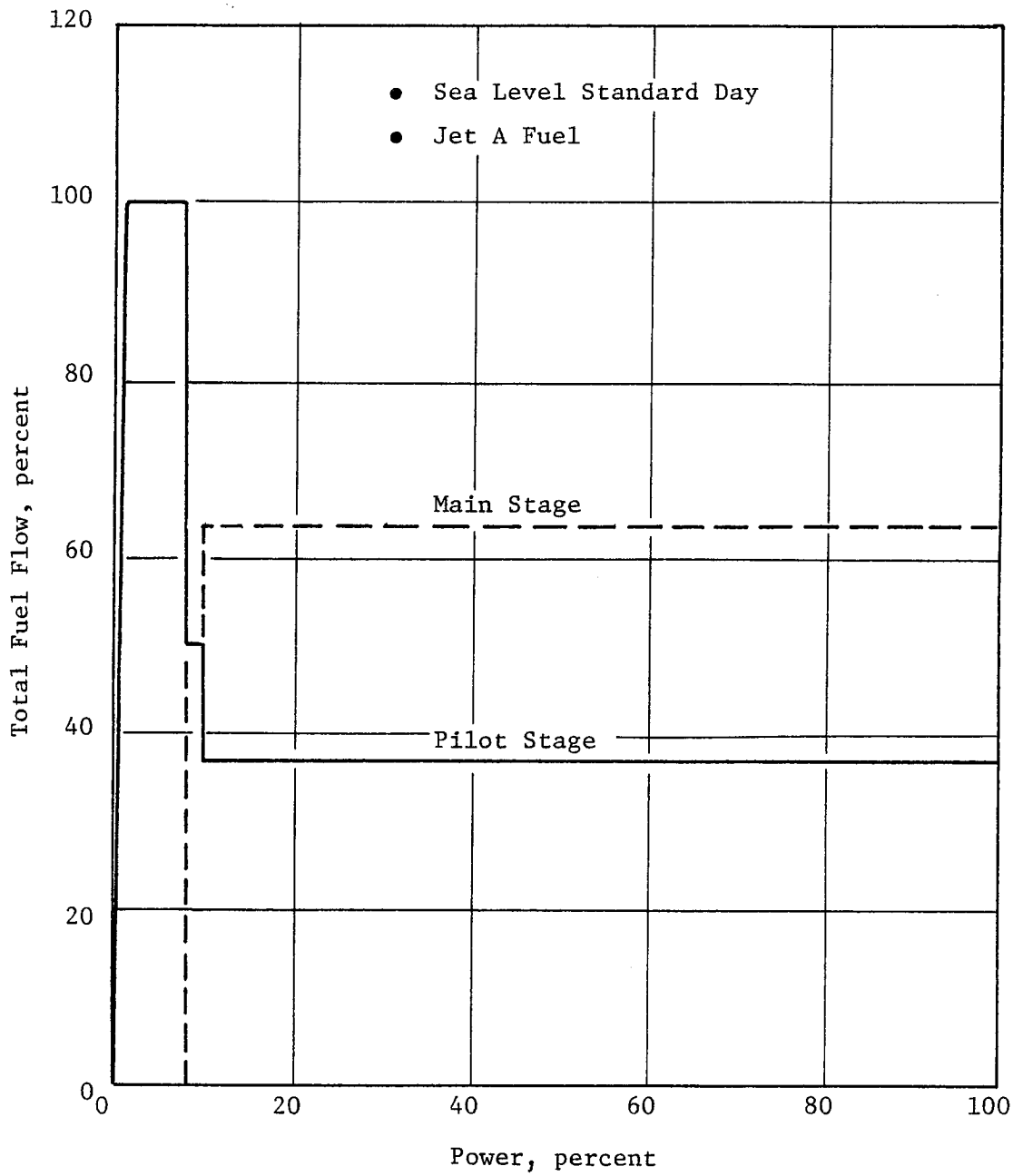

Figure 24. Fuel Flow Staging.

Table XIII. Combustor Aerodynamic Parameters.

- EPA Landing/Takeoff Cycle
- Sea Level Static/Standard Day

	SLTO	Climb	Approach	Idle	Cruise 35,000 ft/0.8 Mach/+18° F
W_3 (pps)	146.1	131.0	69.3	27.1	63.6
T_3 (° R)	1467	1409	1145	895	1408
P_3 (Psia)	438.9	382.5	175.6	63.4	189
ΔP (%)	5.02	5.08	5.34	5.0	4.97
Fuel Flow (pph)	10730	8776	2930	993	4695
Reference Velocity (fps)	58.8	58.1	54.1	46.1	57.1
Residence Time (ms)	3.3	3.4	2.8	4.3	3.3
Compressor Mach No.	0.305	0.307	0.318	0.302	0.301
Space Rate $\left(\frac{\text{Btu}}{[\text{hr-ft}^3\text{-atm}] \times 10^{-6}}\right)$	7.0	6.6	4.8	4.5	7.9

satisfactory ignition characteristics, and idle emissions levels closely approached the program goals. Because of the overall satisfactory results, no further development testing was planned. The Mod. VII combustor represented the last development configuration evaluated.

The E^3 combustor final design incorporates many of the aerodynamic features evolved from the series of development configurations evaluated, especially those of the Mod. I and Mod. VII configurations. It is a lean-main-stage design with the same internal aerodynamic flowpath as the development configurations. The hardware of the domes and centerbody assemblies is similar in design to that used in the development combustor; however, the liners are double-walled, film-plus-impingement-cooled, segmented, shingle-type construction different from the conventional film-cooled, machined-ring design used in the development combustor.

All hardware components of the engine combustor assembly were received and individually airflow calibrated to establish the effective flow areas. All major discrepancies between actual and design-intent airflows were investigated. In most cases, the problem was found to be inaccurate flow data; in some cases, fault was found with the physical aspects of the flow feature (wrong hole size and/or number of holes). In the case of the centerbody inner dilution, the thimbles were reworked to bring the thimble-hole physical diameter to the design intent. But other hardware modifications of this nature (rework) were held up, pending the outcome of component evaluations, to determine if the rework would be necessary. Upon completion of rework, the dilution thimbles were rechecked for flow area to assure that the design flow area had been obtained. Utilizing this flow data, estimates of the combustor airflow distribution were calculated and compared to the design intent. This comparison is presented in Figure 25.

Following the flow-area calibration, the combustor hardware was assembled and installed into the component test rig to evaluate the ground-start ignition and exit-temperature characteristics at atmospheric inlet conditions. The combustor demonstrated excellent ground-start ignition characteristics and a pattern factor of 0.24 at the design sea level takeoff (SLTO) operating point. However, visual observations of the combustor operating at simulated

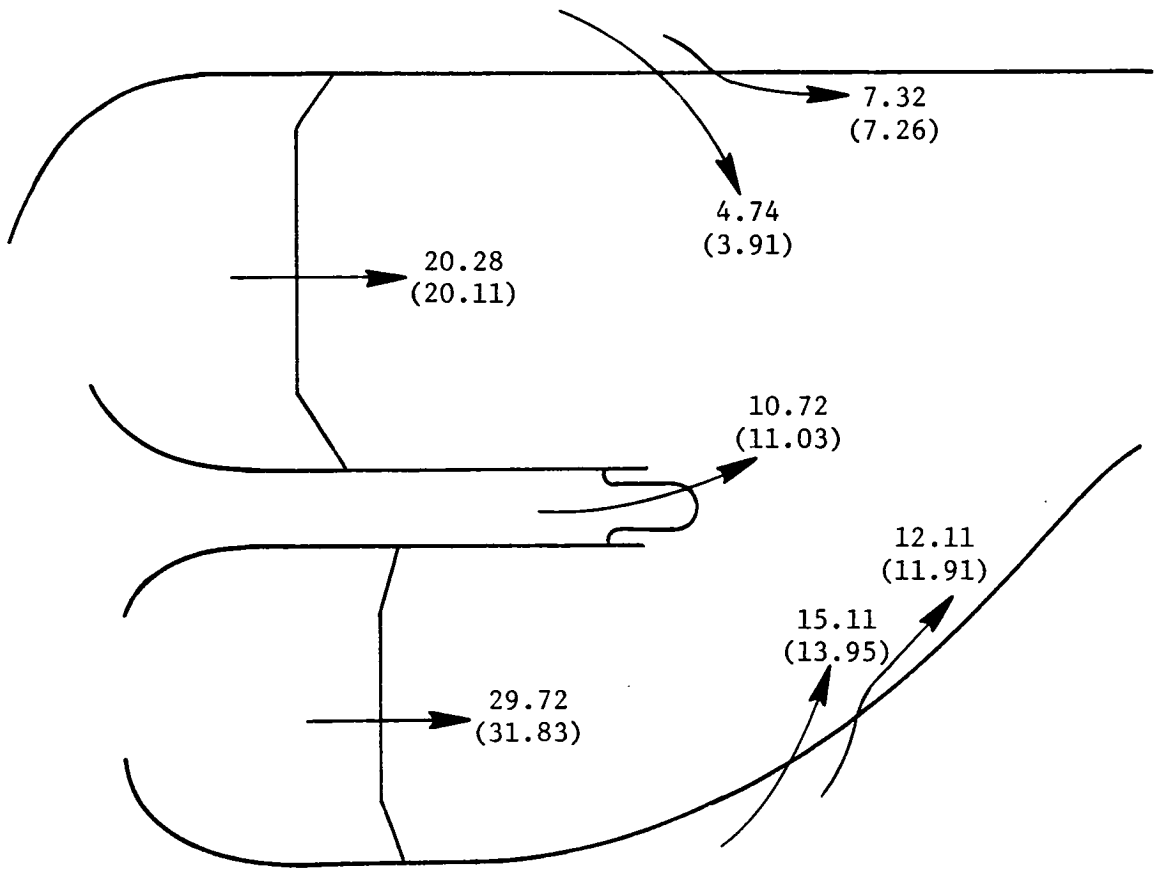

- Flows Presented in Percent $W_{Combustor}$
- Design Levels Shown in Parentheses

Figure 25. Combustor Airflow Distribution.

SLTO operating conditions suggested that the centerbody was excessively hot in line with the swirl cups. From the estimated airflow distribution, it was known that cooling flows in the centerbody structure outer and inner forward cooling rings were below design levels. Concern arose as to whether these cooling flows were sufficient to maintain the structural integrity of the centerbody when subjected to the more severe conditions associated with the component evaluation at elevated inlet pressures and the core engine test series. To correct the problem, several modifications were incorporated into the combustor hardware. These modifications involved preferentially increasing the pilot-dome, inner-cooling-ring flow and the main-dome, outer-cooling-ring flow in line with the swirl cups. In addition, a circular arc of "gill" type cooling holes was incorporated into the pilot-stage side of the centerbody structure just downstream of the two cross-fire tubes. These hardware changes are illustrated in Figure 26.

Following this rework, the combustor was reassembled and instrumented with an array of 28 static-pressure probes and 65 skin-temperature thermocouples. The combustor was installed into the component test rig to evaluate it for ground-start ignition, staging, emissions, and metal-temperature characteristics at elevated inlet pressures simulating actual engine operation. The results of this testing were very satisfactory. The combustor achieved almost all of the design objectives established in the development program. Following completion of the component evaluation, the combustor was inspected for damage, and the instrumentation was refurbished to the specifications defined in the core engine instrumentation plan. The combustor was then delivered to E^3 Evaluation Engineering for incorporation into the core engine CDN assembly.

During this reporting period, the engine fuel nozzle assemblies were received following a significant delay involving a fabrication error. The problem was corrected by the manufacturer in a satisfactory manner. All fuel nozzle assemblies were calibrated in detail at the General Electric Fuel Nozzle laboratory as a check against calibration records from the manufacturer and the design intent. The results of this independent calibration revealed that flows were lower than design intent at conditions representing high-power operation. These results were confirmed by the manufacturer during a

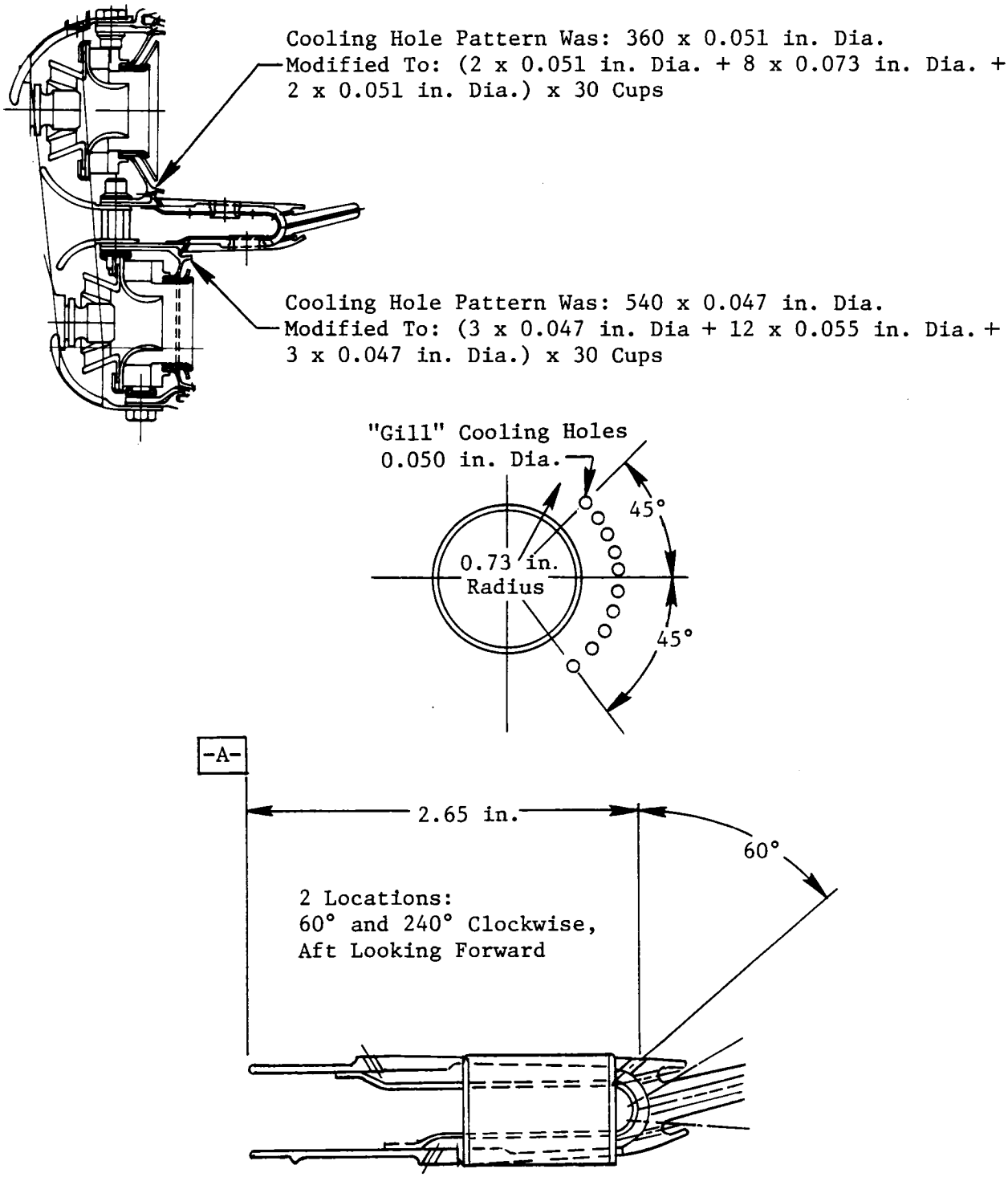

Figure 26. Centerbody Cooling Modifications.

discussion of the problem. From this discussion it was learned that, in sizing the secondary fuel-metering passages, the specified fuel flow for the secondary system was set as a total (primary plus secondary) nozzle-tip flow. Thus, the secondaries were sized for a lower flow than specified. The problem was not considered severe. There is ample pump-discharge pressure from the engine fuel-supply system to achieve the fuel flows associated with maximum-power operation. The engine fuel nozzle flow calibation was completed prior to completion of the engine combustor component evaluation. Therefore, it was decided to use the engine nozzle assemblies with the engine combustor for the component evaluation at elevated inlet pressures. During this testing, the fuel nozzle assemblies performed without any problems. A posttest inspection and flow calibration were performed on the nozzle assemblies. All assemblies were in good condition, and a complete set of fuel nozzles was delivered to E^3 Evaluation Engineering along with the combustor for incorporation into the E^3 CDN assembly.

Work Planned

Combustor aerodynamics engineering effort will be directed at following the buildup of the core engine CDN assembly and supporting the upcoming E^3 core test. In addition, a component-test memo will be compiled to summarize the results from the engine combustor component evaluations. A detailed design report will follow. The DDR will encompass the entire E^3 combustor development effort.

2.3.2 Component Fabrication and Test Support

Technical Progress

Primary activity under this task involved procuring the hardware required for the core engine combustion system. All engine combustor components have been received and assembled. Overall hardware quality is excellent, and the proper fit-up of the various components was achieved. The core engine combustor was final assembled and instrumented in January 1982. The assembled combustor is shown in forward view in Figure 27 and in aft view in Figures 28 and 29. The fuel nozzle is shown in Figure 30.

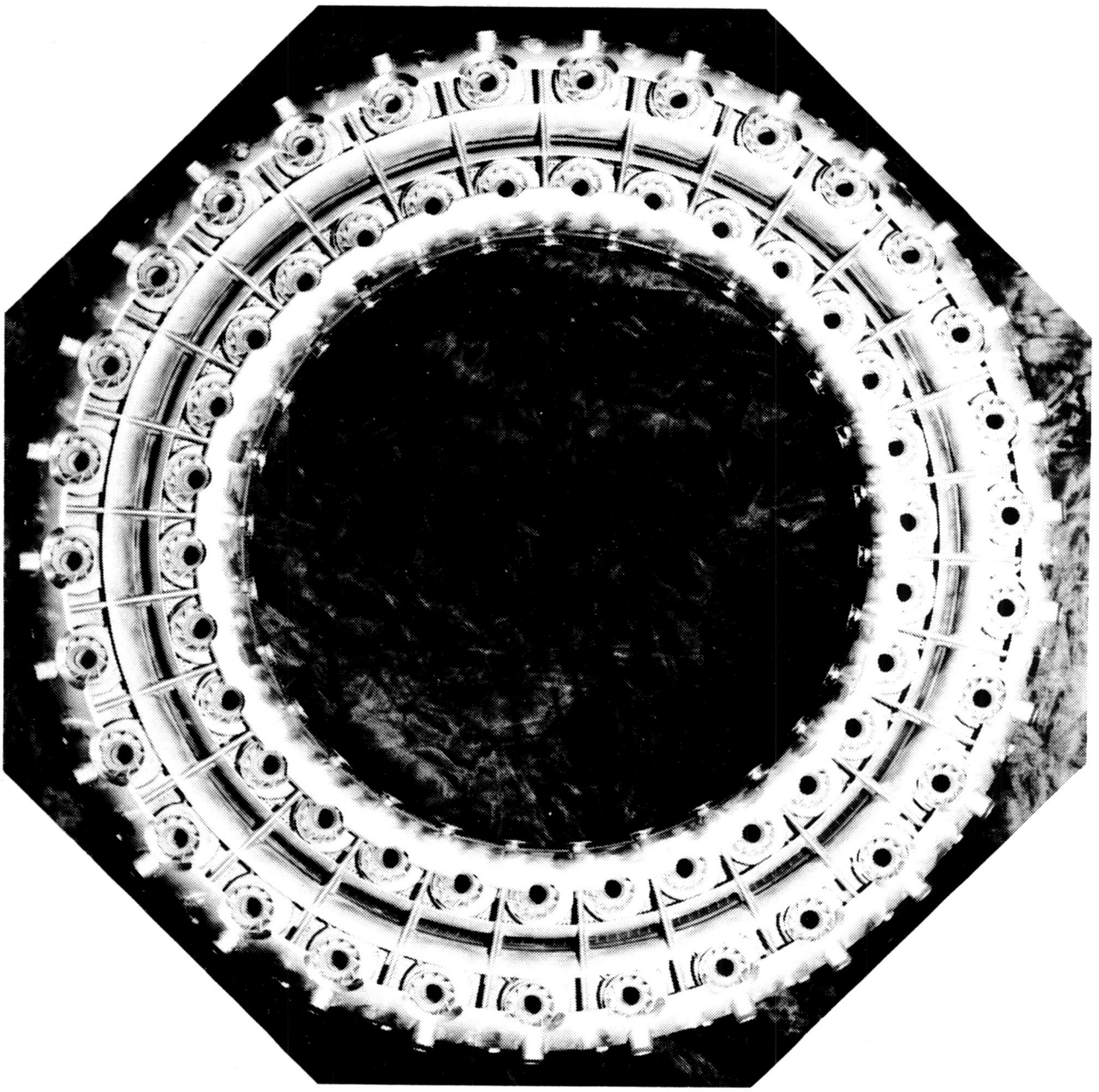

Figure 27. Engine Combustor - Forward View.

Figure 28. Engine Combustor - Aft View.

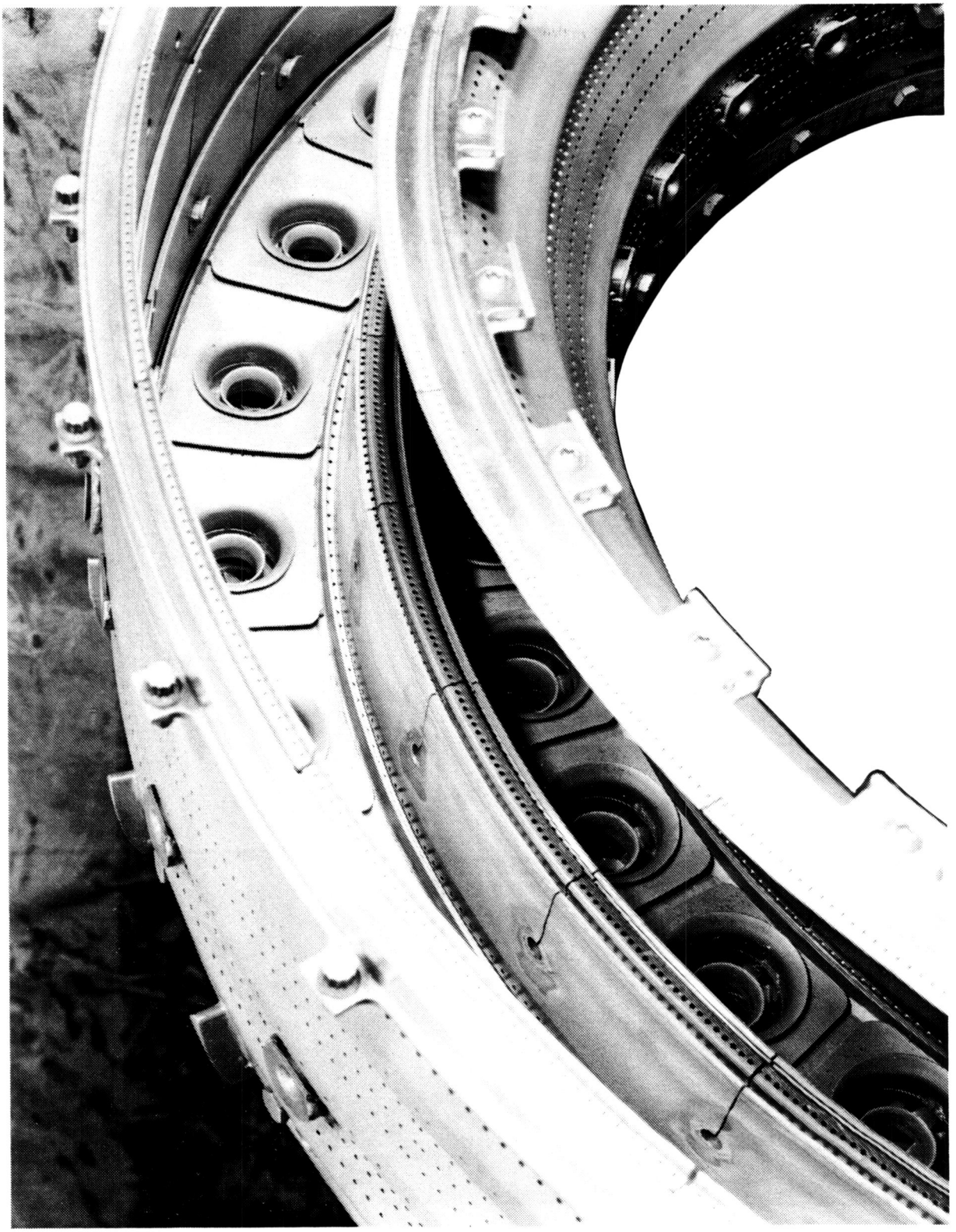

Figure 29. Engine Combustor - Aft View Closeup.

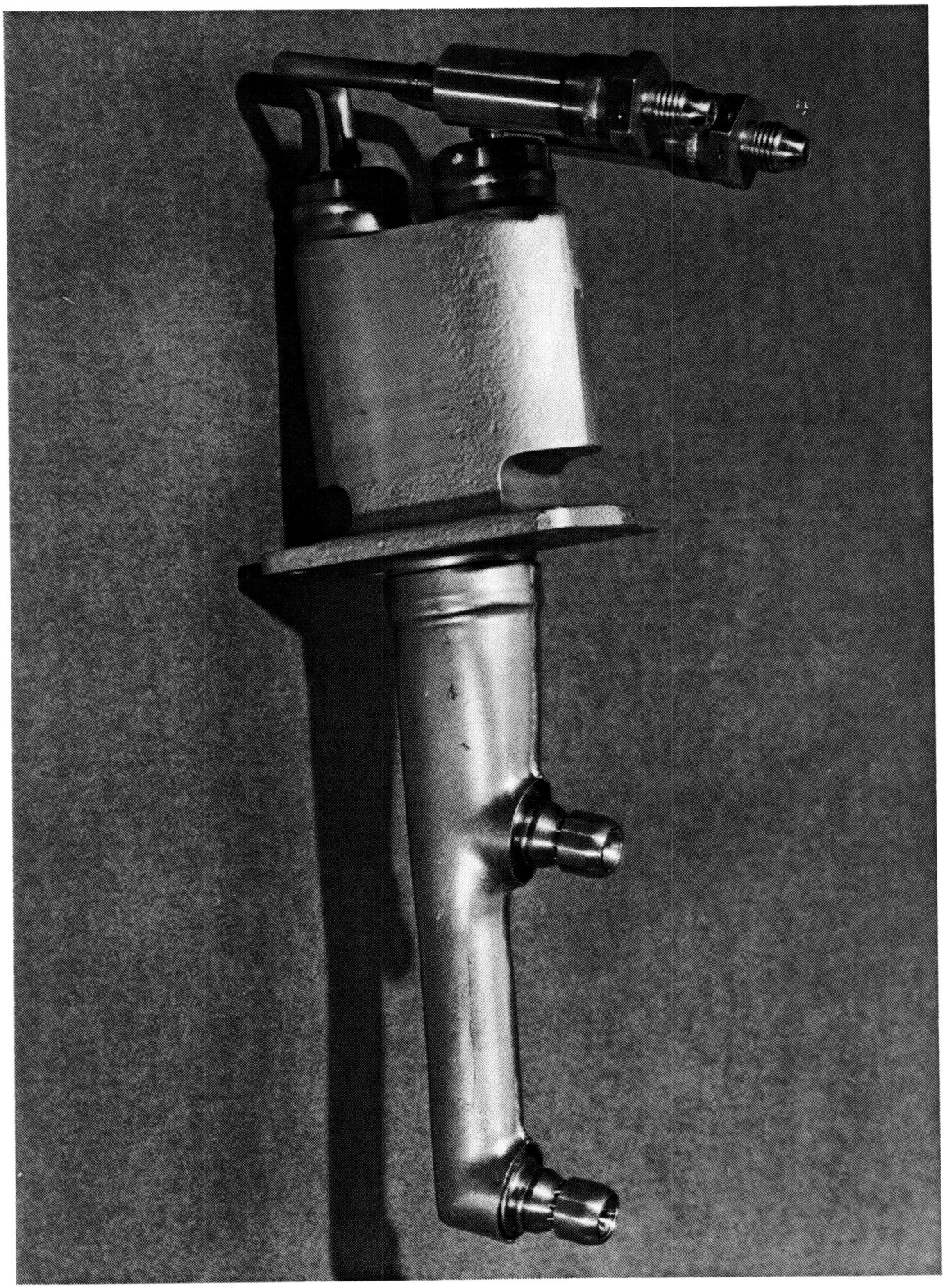

Figure 30. Engine Combustor Fuel Nozzle.

An extensive component checkout test was conducted on the double-annular combustor in February 1982. The combustor exhibited excellent mechanical and aerodynamic operating characteristics.

Detailed thermocouple measurements were monitored to determine combustor operating temperatures. The highest temperatures occurred on the forward row of inner-liner shingles. Prior heat-transfer analysis had predicted the hot-shingle location. This shingle location could utilize a thermal-barrier coating for long-term E^3 application. However, it is anticipated that the uncoated shingle will provide adequate life for the demonstrator engine test program. No other significant hot spots were detected in the skin-temperature measurements. The combustor will provide adequate engine performance, based on the measured performance parameters. A thorough visual inspection of the combustor hardware revealed no problems, and the combustor was delivered to Engine Assembly. The combustor and fuel-delivery system have been installed into the engine combustor casing. All critical interfacing features indicated the desired fit-up.

Work Planned

- Monitor final assembly of combustion system components into core engine assembly
- Provide combustor mechanical engine support of core engine testing

2.3.3 Subcomponent Tests

Technical Progress

Sector-combustor test activity was completed early in this reporting period. The final phase of testing concentrated on evaluating the pilot-stage ignition performance at simulated altitude and Mach numbers from the E^3 operating envelope. The evaluation was conducted only on the final (Mod. VI) configuration of the sector combustor using the CF6-50 engine windmilling map since the E^3 windmilling map was not yet defined.

Successful ignition was obtained for test points simulating conditions in the left portion of the windmilling envelope only, as shown in Figure 31. Initially, this was thought to be caused by low pressure drop across the fuel

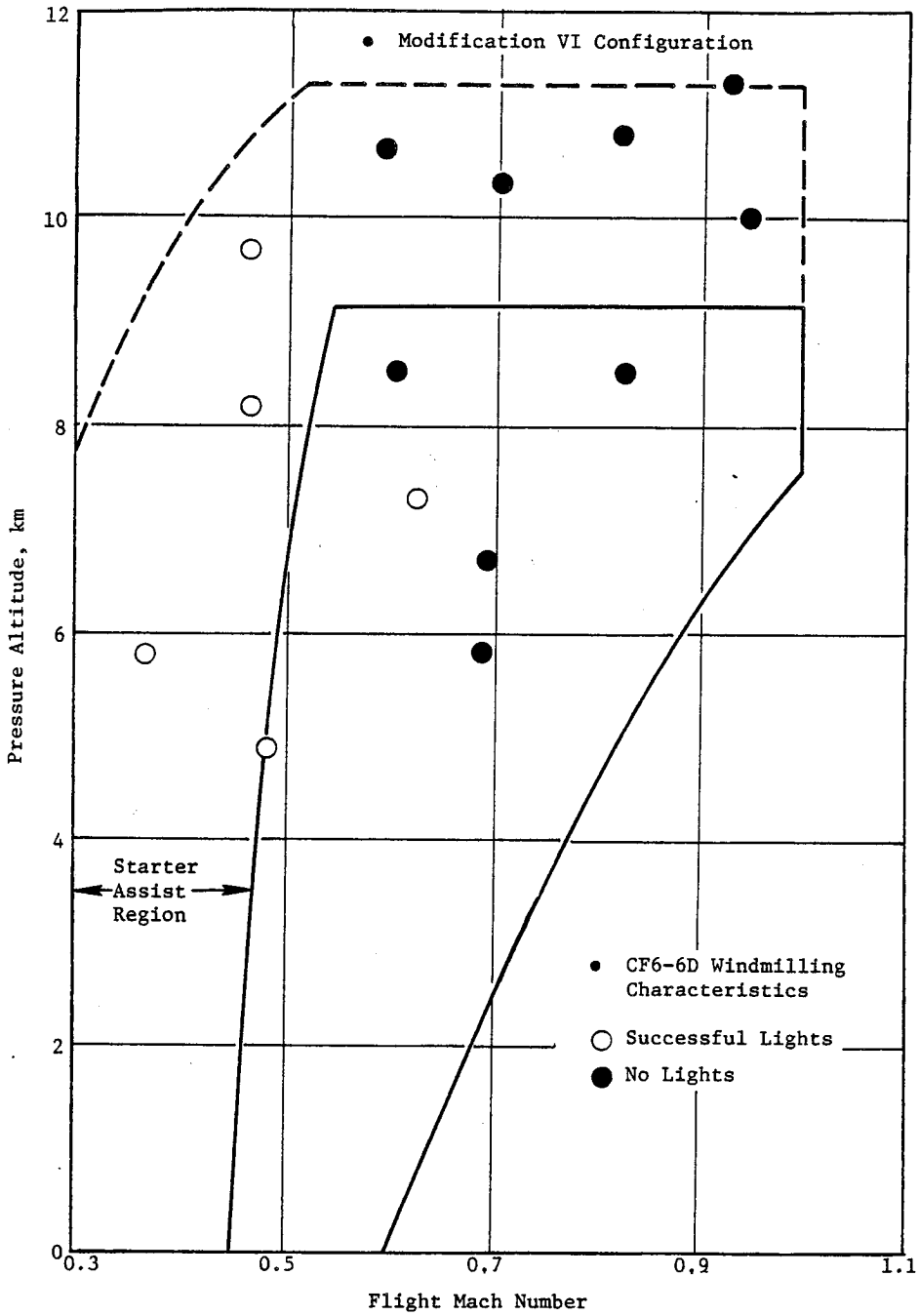

Figure 31. Sector Combustor, Altitude-Relight Tests.

nozzle tip due to the relatively high-flow-number nozzles (low fuel nozzle pressure drop usually results in poor fuel atomization). However, a repeat test with significantly lower flow fuel nozzles resulted in no improvement on the number of successful ignition points even though the ignition fuel/air ratios for these successful points was substantially reduced.

Additional altitude-ignition testing with the pilot-stage dilution flow area blocked, and using the prototype "peanut" nozzles, indicated that no further improvements in performance were attainable with the current configuration. Further investigation was still required for any effort to improve the altitude-ignition performance; however, such effort was not planned in the E^3 Sector Development Program Scope.

A draft copy of the final report on the E^3 Subcomponent Test Program was completed and submitted to NASA.

Work Planned

None - Subcomponent Program complete.

2.3.4 Full-Annular Test

Technical Progress

During this reporting period, full-annular test activities involved completion of the reduction of test data obtained from component testing of the Mod. VII development combustor configuration. In addition, a series of component tests was conducted on the engine combustor prior to release to the core engine.

Component testing of the Mod. VII configuration was conducted to evaluate the design for ground-start ignition, staging, and low-power emissions characteristics at true engine-cycle operating conditions. Test results from the ignition and staging phase of this evaluation were discussed in the last semi-annual report. The results of the idle emissions testing are presented in Figure 32. As indicated in the figure, significant reductions in CO emissions were achieved compared to levels previously demonstrated with the Mod. I configuration. At the 6% design idle operating condition, a CO level of 23.3

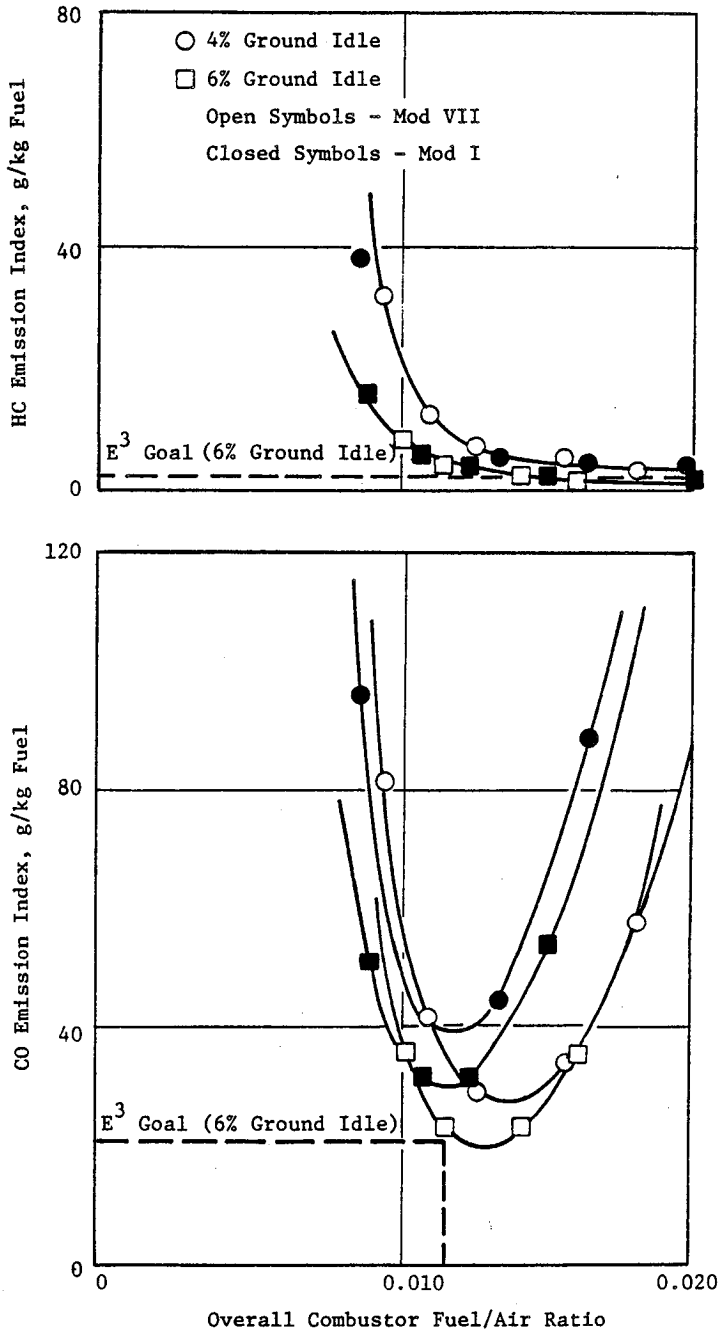

Figure 32. Development Combustor, Low-Power Emissions.

g/kg of fuel was demonstrated. This closely approached the program target level of 20.7 g/kg of fuel. A minimum level of 20 g/kg of fuel was achieved at a combustor fuel/air ratio of 0.0129, compared to the design cycle fuel/air ratio of 0.0116. Hydrocarbon emissions were nearly identical to levels previously demonstrated with the Mod. I configuration. A HC emissions level of 4.3 g/kg of fuel was obtained at the 6% design idle operating condition. The program target at this operating condition is a level of 2.8 g/kg of fuel. HC levels at or below this target level were demonstrated at 6% ground-idle operating conditions at overall fuel/air ratios greater than 0.015.

CO and HC emissions data obtained at the derated approach-power condition (30% F_N) were adjusted to correct for the low inlet total pressures using the relations:

$$EI(CO) = EI(CO)_{measured} \times (P_3/175)^{1.5}$$

$$EI(HC) = EI(HC)_{measured} \times (P_3/175)^{2.5}$$

(175 psia is the inlet pressure at actual design-cycle approach power)

The results (presented in Table XIV) show that very low levels of CO and HC emissions were demonstrated in the pilot-only operating mode. However, significantly higher levels resulted for the staged operating modes (pilot and main dome of the combustor both fueled and burning). These results are similar to those previously obtained for the baseline and Mod. I development combustor configurations evaluated at the same conditions. The reason for the high CO and HC emissions levels is related to the low overall combustion fuel/air ratio of 0.014 at this operating condition; it results in very low fuel/air ratios in the domes of the pilot and main stages.

Table XIV. Adjusted Emissions at 30% F_N (Approach).

Combustor Operating Mode	Emission Index, g/kg Fuel		
	CO	HC	NO_x
Pilot Only	2.9	0.4	10.7
40/60 Split	54.0	22.9	2.7
30/70 Split	56.0	40.7	2.2

NO_x emission data obtained at the derated approach-power operating conditions were adjusted to the correct operating conditions by using the following relation:

$$EI(NO_x) = EI(NO_x)_{measured} \ (175/P_3)^{0.37} \times (V/51.3) \times e - [(6.29 - humidity)/53.19]$$

The results for the three pilot-to-total fuel splits are also presented in Table XIV. As would be expected, the lean combustion conditions associated with fuel staging yield very low levels of NO_x; the pilot-only operating mode yields levels considerably higher. In Figure 33, the measured NO_x emission levels obtained in the staged operating mode are plotted against the E^3 design-cycle severity parameter. Also shown in this figure are data from the baseline and Mod. I combustor configurations. It is observed from this figure that the NO_x emission characteristic of the Mod. VII configuration would be expected to be very similar to the characteristics demonstrated by the baseline and Mod. I configurations. Therefore, the Mod. VII configuration should demonstrate NO_x emission levels at sea level takeoff operating conditions similar to those of the other two configurations, each of which satisfied the program target goal.

EPA parameter numbers (based on the EPA landing/takeoff cycle for CO, HC, and NO_x) were generated for combustor operation at 6% ground idle and pilot-to-total fuel splits of 1.0 and 0.35 at the approach power operating condition. Because of the lack of data at the higher power operating conditions, results obtained with the baseline combustor configuration at these conditions were used. The results are presented in Table XV and compared to the E^3 Program goals. As observed from this table, the NO_x emission levels satisfy the program goal with pilot-only or staging at the approach-power operating condition. However, both the CO and the HC emissions levels fail to meet the respective program goals with either operating mode. With the pilot-only operating mode, the CO emissions closely approach the goal, but reductions greater than 30% are required for the HC emissions. Significantly greater reductions in both CO and HC emissions are required to satisfy the program target goals for staged combustor operation at approach.

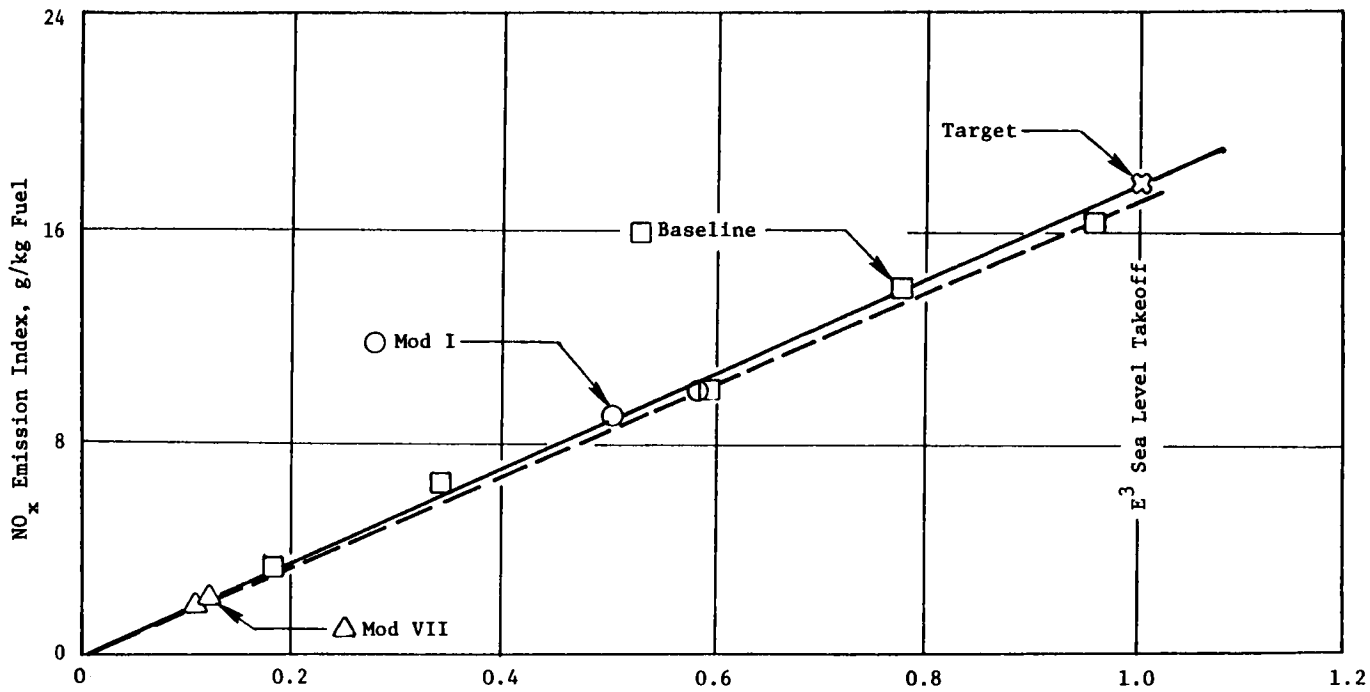

Figure 33. Combustor NO_x Emissions.

Table XV. Mod. VII E^3 Emissions Goal Comparison.

Emission	lbm Emission/1000 lbf-hr-cycle		
	Pilot Only at Approach	35/65 Split at Approach	E^3 Goals
Carbon Monoxide	3.27	6.40	3.00
Hydrocarbons	0.58	2.48	0.40
Oxides of Nitrogen	2.96	2.51	3.00

The purpose of the initial component test of the E^3 combustor was to evaluate the ignition, crossfire, and lean-extinction characteristics at selected steady-state operating points along the E^3 6/81 ground-start cycle. For the purposes of main-stage crossfire, data were also obtained at simulated steady-state conditions representing 4%, 6%, 10%, and 30% of full-rated thrust along the E^3 FPS operating line. At all test conditions, the inlet temperature matched the cycle, but the inlet total pressure was atmospheric. The combustor airflows were set so that combustor velocities duplicated the velocities at the actual cycle conditions. No prediffuser or aft bleeds were used in this test. Test point and corresponding operating conditions are presented in Table XVI.

Fuel was supplied to the combustor using the E^3 test rig fuel nozzle assemblies incorporating simplex nozzle tips rated at 26.5 lbm/hr at 100 psid in both the pilot and the main stage. A standard GE ignition system was used as in all previous development combustor testing. The ignitor was located at 240° clockwise, aft looking forward, immersed flush with the inside shingle wall of the pilot stage.

Test results from this ignition evaluation are presented in Figure 34. It is observed that the core engine combustor pilot-stage ignition and lean-blowout characteristics are considerably better than those demonstrated with the Mod. VII development combustor configuration. These ignition and blowout characteristics will satisfy the E^3 ground-start cycle fuel schedule requirements with and without bleed. Crossfire and full propagation (staging) of the

Table XVI. Core Engine Combustor Ignition Test.

- Standard day
- Atmospheric inlet pressure
- 6.85 in^2 bleed
- P_3 = 15.0 psia

Test Point	PCNHR	$W_{36}\sqrt{T_3}/P_3$	T_3, °F	W_{36}, lbm/sec	Cycle, Comments
1(1)	21.0	7.51	87	4.82	6/81, Simulated No Bleed
2(1)	21.0	7.18	87	4.61	6/81, Simulated Bleed
3(1)	24.5	8.67	98	5.50	6/81, Simulated No Bleed
4(1)	24.5	8.25	98	5.24	6/81, Simulated Bleed
5(1,2)	30.0	10.11	120	6.30	6/81, Simulated No Bleed
6(1,2)	30.0	9.70	120	6.06	6/81, Simulated Bleed
7(1)	36.9	11.61	150	7.05	6/81, Simulated No Bleed
8(1)	36.9	11.27	150	6.87	6/81, Simulated Bleed
9(2)	4% F_N	10.22	379	5.29	FPS II Cycle
10(2)	64.3	9.88	410	5.03	6/81 Cycle
11(2)	6% F_N	10.67	432	5.36	FPS II Cycle
12(2)	10% F_N	11.06	510	5.33	FPS II Cycle
13(2)	30% F_N	11.14	687	4.94	FPS II Cycle

Notes:

1. Core engine motoring combustor inlet conditions (no fuel).
2. Ignition characteristics of main stage to be investigated.

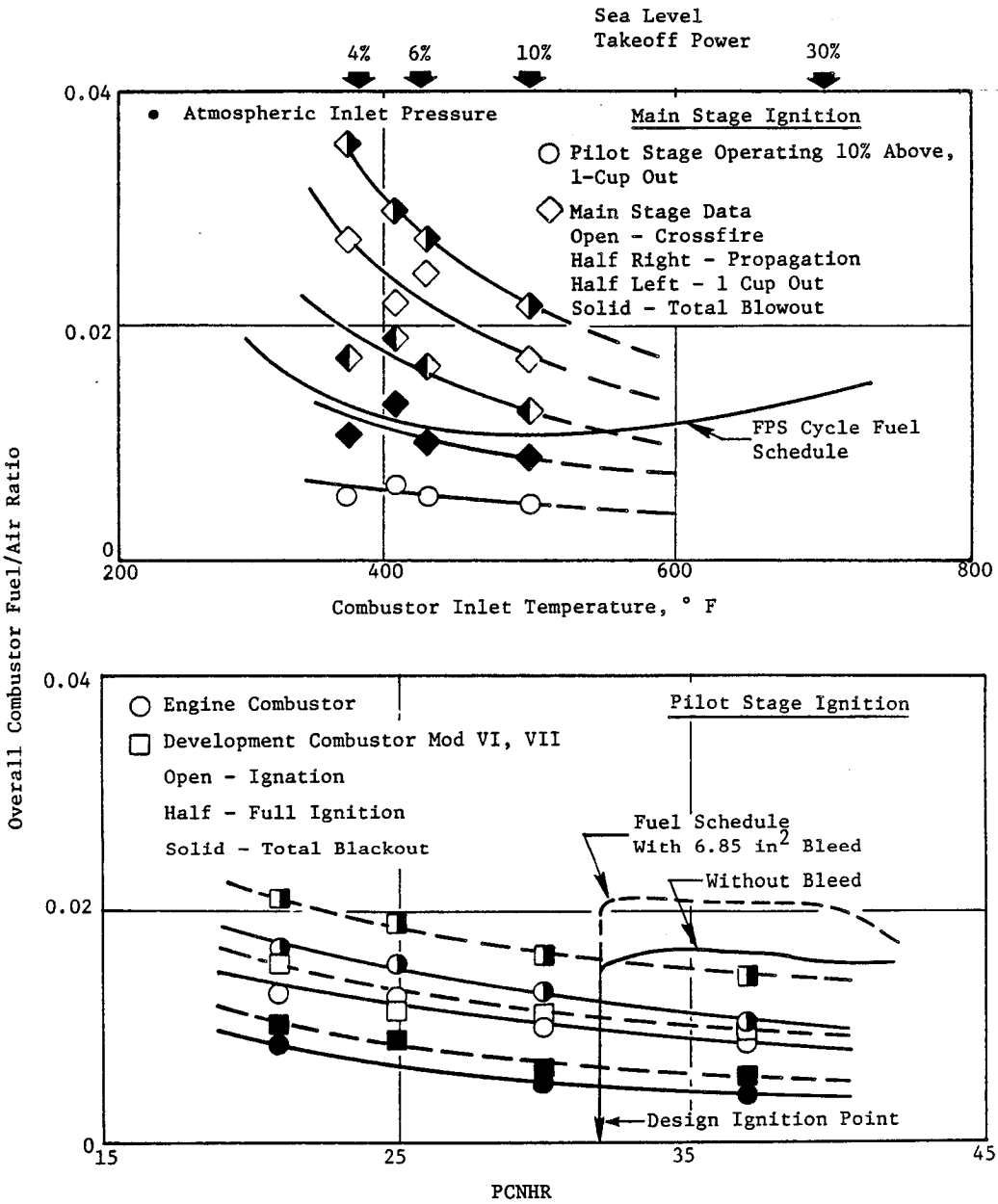

Figure 34. Engine Combustor Ground-Start Ignition Results.

core engine combustor main stage required overall combustor fuel/air ratios well above the fuel schedule defined in the E^3 FPS steady-state operating cycle. This is typical of past experience of development combustor configurations featuring lean-main-stage-dome designs. Improvements anticipated at actual cycle inlet pressures would not be sufficient to permit staging at subidle or idle operating conditions. The lean-blowout characteristics for the main stage generally fall below the FPS cycle fuel schedule. It is, therefore, possible to achieve staged combustor operation at the low-power operating conditions by initially accelerating the engine to a power level where staging can be accomplished within the cycle fuel schedule, then decelerating to the desired operating condition.

As part of this test, a dynamic ignition evaluation was conducted on the pilot and main stages. This was an attempt to determine the time required to achieve ignition and full propagation while simulating the engine fuel scheduling as a function of core speed. The pilot stage was evaluated at the simulated 30 PCNHR test condition. A constant fuel flow of 345 lbm/hr was preset in the pilot-stage fuel system. The manifold, pigtails, and nozzles were then purged of fuel. The ignitor was activated, and the pilot-stage shutoff valve was opened to introduce the surge of fuel. A time of 11 seconds was required to achieve full propagation once the valve was opened. The main stage was evaluated at the simulated 6% and 10% power test conditions. The pilot stage was ignited and set to a fuel flow of 145 lbm/hr. Constant fuel flows of 370 and 320 lbm/hr were respectively preset in the main stage at the 6% and 10% power operating conditions. These were sufficient to achieve full propagation as determined from the ignition data. The main-stage system was purged of fuel. The shutoff valve was opened, and the surge of fuel was sent to the main stage. This sudden surge caused a slight reduction in the pilot fuel flow but did not cause any cups to blow out. At the simulated 6% power operating condition, 10 seconds were required to achieve full main-stage propagation. At the simulated 10% power operating condition, 15 seconds were required to achieve full main-stage propagation.

Exit gas temperature performance testing was conducted to evaluate the combustor for pattern factor and average profile characteristics at test conditions simulating sea level takeoff power, 30% approach power, and 6% ground

idle. Combustor inlet pressure was atmospheric; inlet temperatures duplicated actual cycle T_3 conditions. Airflows were adjusted for the atmospheric inlet pressure in a manner which duplicated actual combustor velocities. Test points and corresponding operating conditions are presented in Table XVII.

Exit gas temperature data were obtained with four rakes, each with seven chromel/alumel (C/A) thermocouple elements. The thermocouple elements were equally spaced across the radial annulus as shown in Figure 35. Circumferential traverse increments of 1.5° were used at all test conditions.

Exit gas temperature performance of the core engine combustor was initiated using nozzle tips rated at 14 lbm/hr at 100 psid in both the pilot and main stage. During this test run, visual observations at the combustor exit revealed that several cups were extinguished in the pilot- and main-stage domes in the top half of the annulus at simulated sea level takeoff operating conditions. Several attempts at varying fuel splits to the pilot and main stages to achieve cup ignition were unsuccessful. Variations in inlet temperature and airflow were also investigated and found to influence the combustion performance of cups in question. If the inlet temperature was lowered to 600° F, then all cups would burn. If the airflow and fuel flow were increased by about 20%, all cups would burn at the high inlet temperature associated with the sea level takeoff operating condition. Unfortunately, many of the rake thermocouple elements were lost during the investigation period, so no meaningful exit-temperature data were obtained.

It was concluded that the problem was related to fuel vaporization within the fuel manifold and nozzle assemblies. Using the fuel nozzles selected for the performance testing, the fuel flows specified at some of the test points resulted in low system fuel pressures. This was especially true in the pilot systems where measured fuel pressures were below 10 psi at some test points. These low pressures coupled with the high operating temperatures in the test rig could cause a vaporization problem with the Jet A fuel used.

Performance testing was resumed. No changes in fuel nozzle or combustor hardware were made; however, insulating material was wrapped around the pilot and main-stage fuel manifolds and around the fuel pigtails to help shelter

Table XVII. Engine Combustor Performance Test.

- 60 Traverse Positions
- P_3 = 1 Atmosphere

Test Point	T_3, °F	Airflows, lbm/sec			Fuel/Air Ratio	Pilot/Total Fuel Flow	Fuel Flows, lbm/hr		
		W_3	Bleed	Combustor			Total	Pilot	Main
1	1007	5.31	0.34	4.97	0.0245	0.3	436	131	306
2	1007	5.31	0.34	4.97	0.0245	0.4	436	175	262
3	1007	5.31	0.34	4.97	0.0245	0.5	436	218	218
4	687	5.68	0.36	5.32	0.0143	0.4	274	110	164
5	687	5.68	0.36	5.32	0.0143	0.5	274	137	137
6	687	5.68	0.36	5.32	0.0143	1.0	274	274	0
7	432	5.72	0.36	5.36	0.0123	1.0	237	237	0
8	432	5.72	0.36	5.36	0.0200	0.5	386	193	193

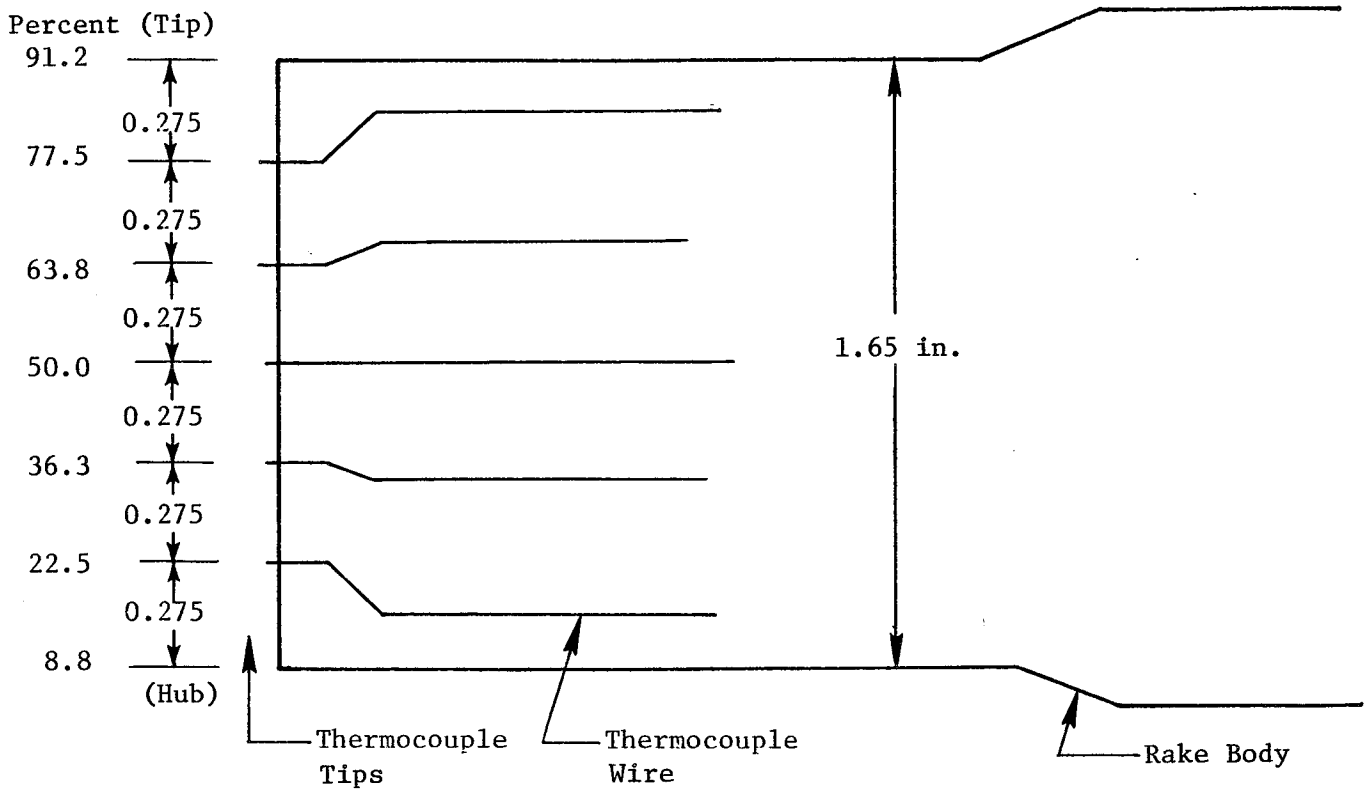

Figure 35. Rake-Element Spacing.

the fuel system from exposure to thermal radiation from the hot test rig. Despite the application of the insulation, the same nonburning cup problems were encountered as in the previous test. It also was observed (visually) that several pilot-stage swirl cups had very low fuel flow. The performance test was terminated, and a calibration of the pilot and main-stage nozzle tips was conducted. The results of this calibration identified five pilot-stage and one main-stage nozzle tips which had evidence of flow restrictions, confirming the observations. The restrictions were believed to result from fuel coking within the nozzle body and were directly linked to the fuel-vaporization problem.

The low-pressure-drop fuel-nozzle tips in the pilot stage were replaced with higher pressure-drop, simplex tips, and performance testing was resumed. This change was made to increase manifold pressure, eliminating the fuel vaporization and coking problems experienced in the previous two test runs, and to provide improved fuel atomization in the pilot stage to improve the simulation of engine operation. The coked-up nozzle tip in the main stage was replaced with another of that type. The high-pressure nozzle tips were not used in the main stage because the maximum fuel flow obtainable with these nozzles is lower than flow levels specified at several of the test points. With this nozzle change, the fuel-vaporization problem was eliminated, and good exit-gas-temperature data were obtained.

Exit gas temperatures at sea level takeoff operating conditions are presented in Figures 36 through 38. As observed from these figures, a pattern factor of 0.24 was demonstrated at a 40/60 pilot-to-main-stage fuel split. This satisfied the E^3 combustor development program target goal of 0.25. The maximum profile is relatively flat; this indicates an acceptable stoichiometric balance between the pilot and main stage at the 40/60 fuel split.

The average profile demonstrated at the 50/50 fuel split is generally within the design limit and has an outboard-peaked characteristic. At the 40/60 fuel split, the average profile is center-peaked with a profile factor of 0.11 which is within the design limit of 0.125. However, the average profile slightly exceeds the design limit from 30% to 50% of the exit annulus height. Exit-temperature traverse data in the form of isothermal contours is

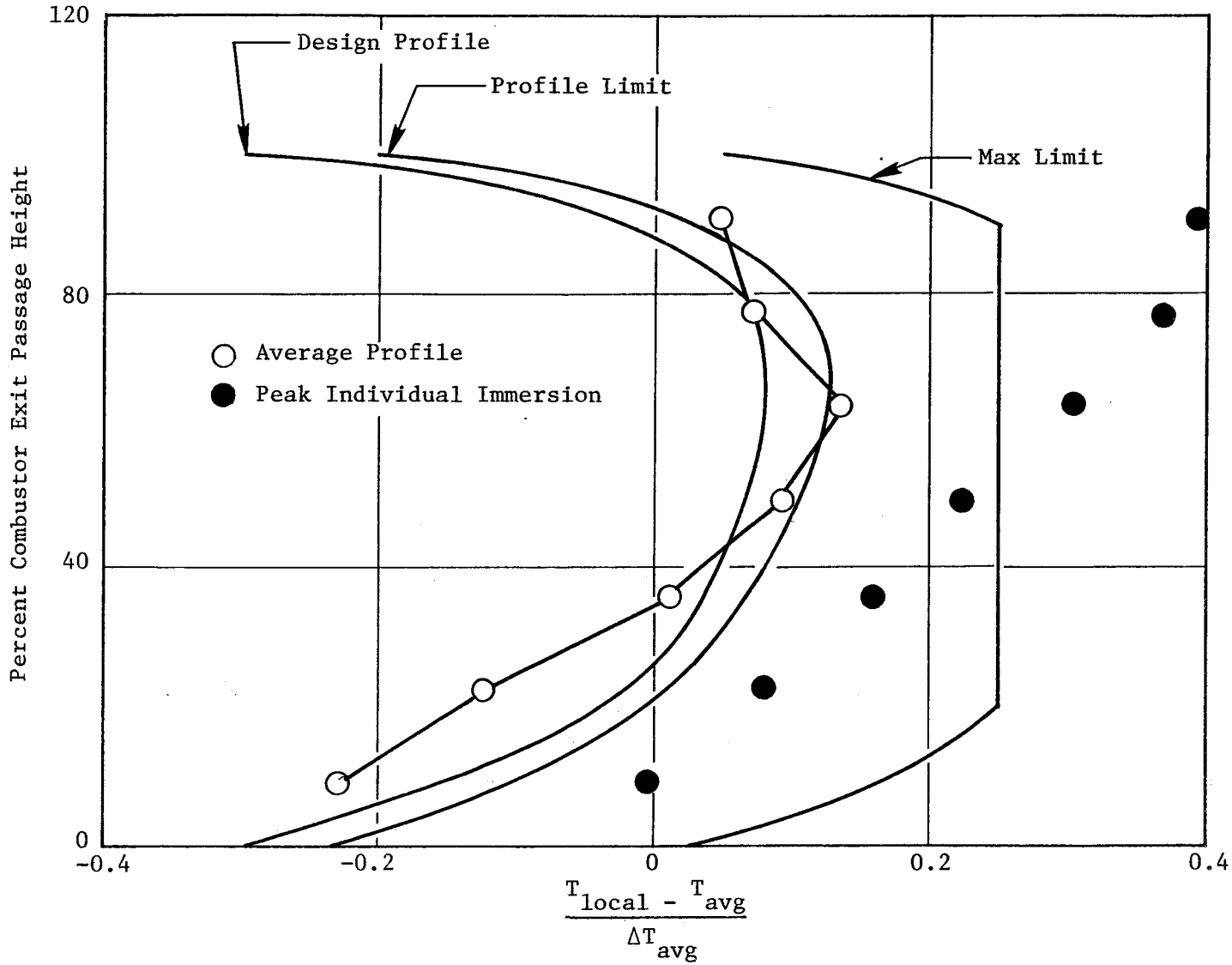

Figure 36. Development Combustor Exit Temperature Performance, 50/50 Pilot-to-Main-Stage Fuel Split.

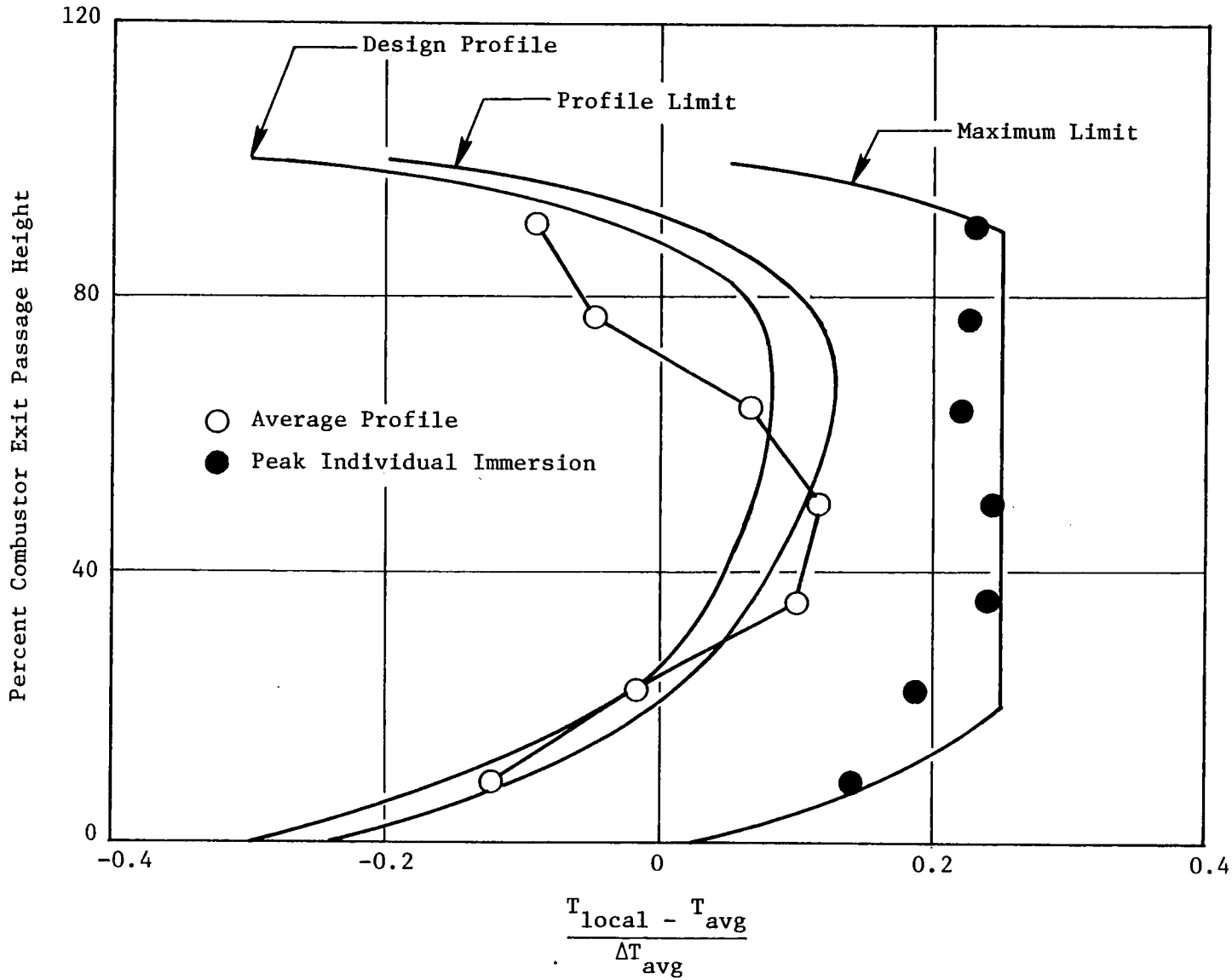

Figure 37. Development Combustor Exit Temperature Performance, 40/60 Pilot-to-Main-Stage Fuel Split.

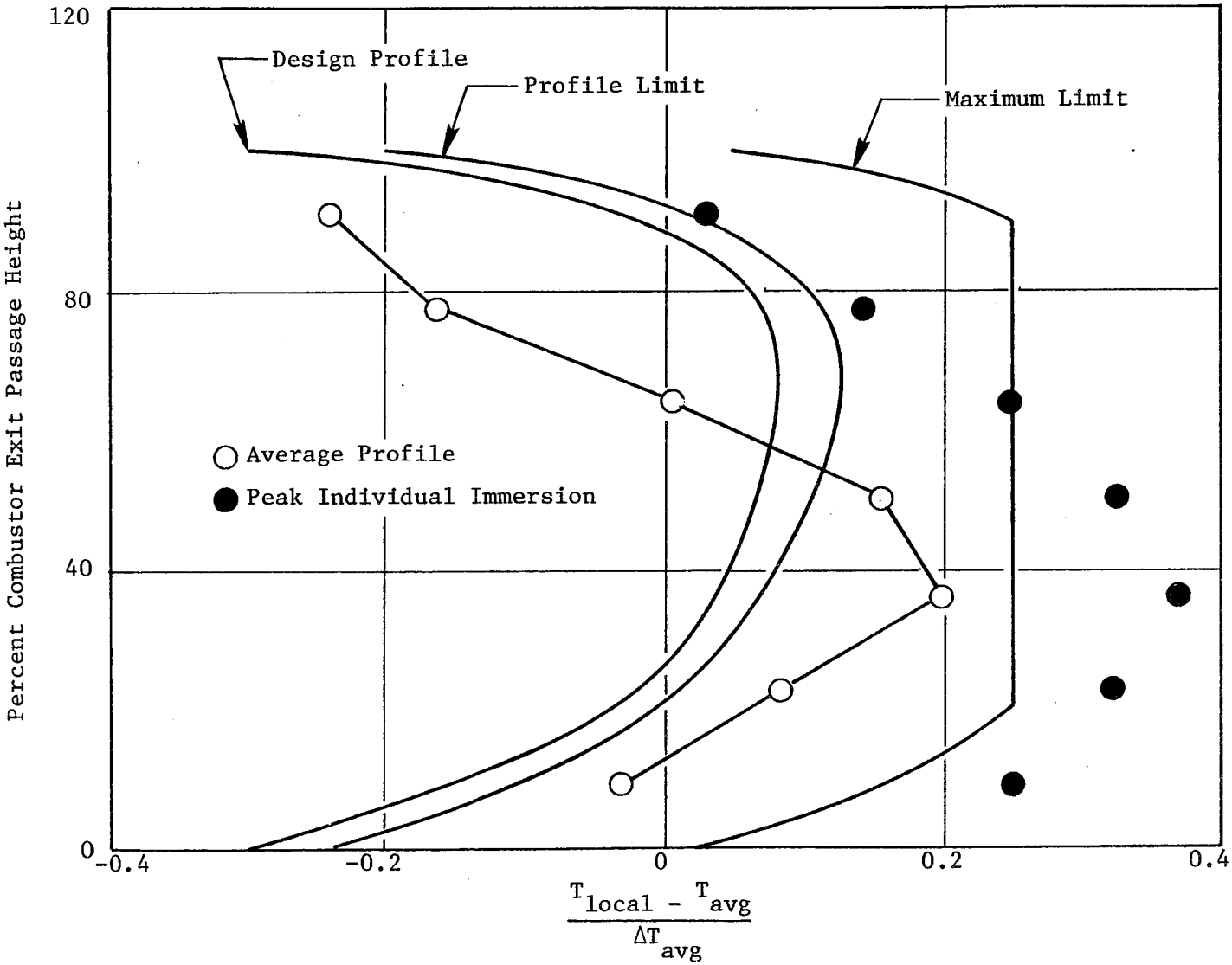

Figure 38. Development Combustor Exit Temperature Performance, 30/70 Pilot-to-Main-Stage Fuel Split.

presented in Figure 39 for the 40/60 pilot-to-main-stage fuel split at simulated sea level takeoff operating conditions.

Average and peak temperature profiles demonstrated at the simulated lower power operating conditions are presented in Figure 40. In the pilot-only mode, the combustor demonstrated a pattern factor of 1.23 at the approach-power condition and 1.36 at the ground-idle condition (6% of sea level takeoff thrust). As expected, the profiles are sharply outward-peaked. These results are similar to those demonstrated with the Mod. VII development combustor configuration at the same operating conditions. Considerably lower pattern factors were demonstrated in the staged operating mode, illustrating the exit-temperature performance advantages of this operating mode. However, as determined from the ground-start ignition test results of this combustor, staged operation at idle or subidle conditions may not be possible.

The purpose of the final test of the engine combustor was to evaluate the ground-start ignition, lean extinction, and staging characteristics at true operating conditions for selected points along the revised (6/81), E^3 ground-start operating line and the E^3 FPS design cycle operating line. In addition, the core combustor was evaluated for emissions, pressure-drop performance, and metal temperature characteristics at selected points from 4% ground idle to simulated sea level takeoff along the E^3 FPS design-cycle operating line. As a secondary effort, testing was also conducted for the purpose of obtaining a comparison, between prototype (peanut) fuel nozzles and the standard-test-rig simplex fuel nozzles, of the CO and HC emissions at ground-idle operating conditions. Combustor inlet total pressures and airflows were scaled down to the facility capacity at the higher power (above 30% power) operating conditions. Combustor inlet temperatures duplicated the design cycle while inlet total pressure and airflow were scaled down in a manner which duplicated the combustor velocities. Bleed flows from the split-duct diffuser and the outer and inner flowpaths were extracted at levels simulating actual engine operation for the emissions evaluation. No bleed flows were extracted during the ignition and staging evaluation. Test points and corresponding operating conditions are presented in Table XVIII.

Simulated Sea Level Takeoff

T_3	1000° F
P_3	1 Atm
f/a	0.0243

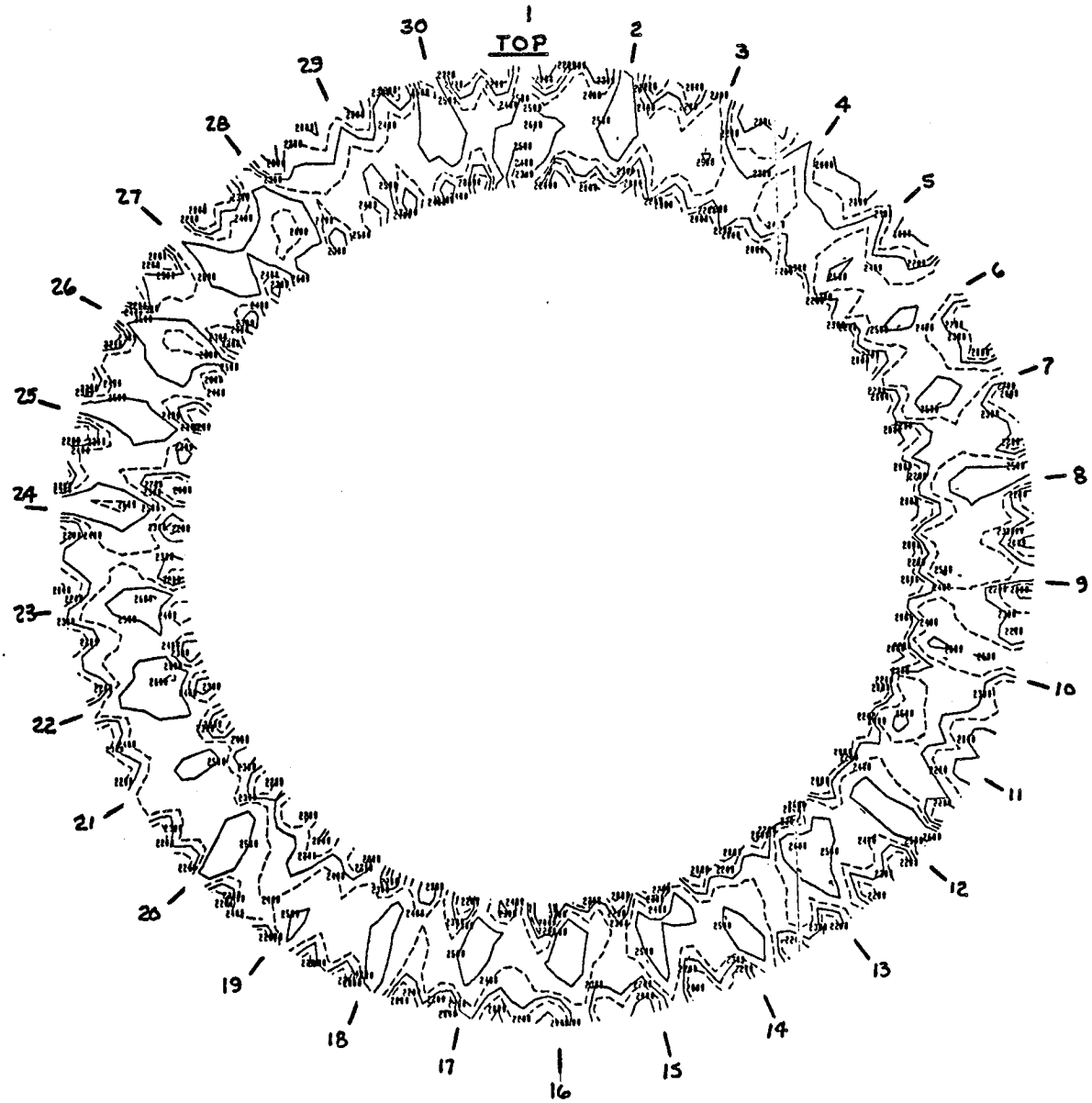

Figure 39. Development Combustor Exit-Temperature Contours at 40/60 Pilot/Main-Stage Fuel Split.

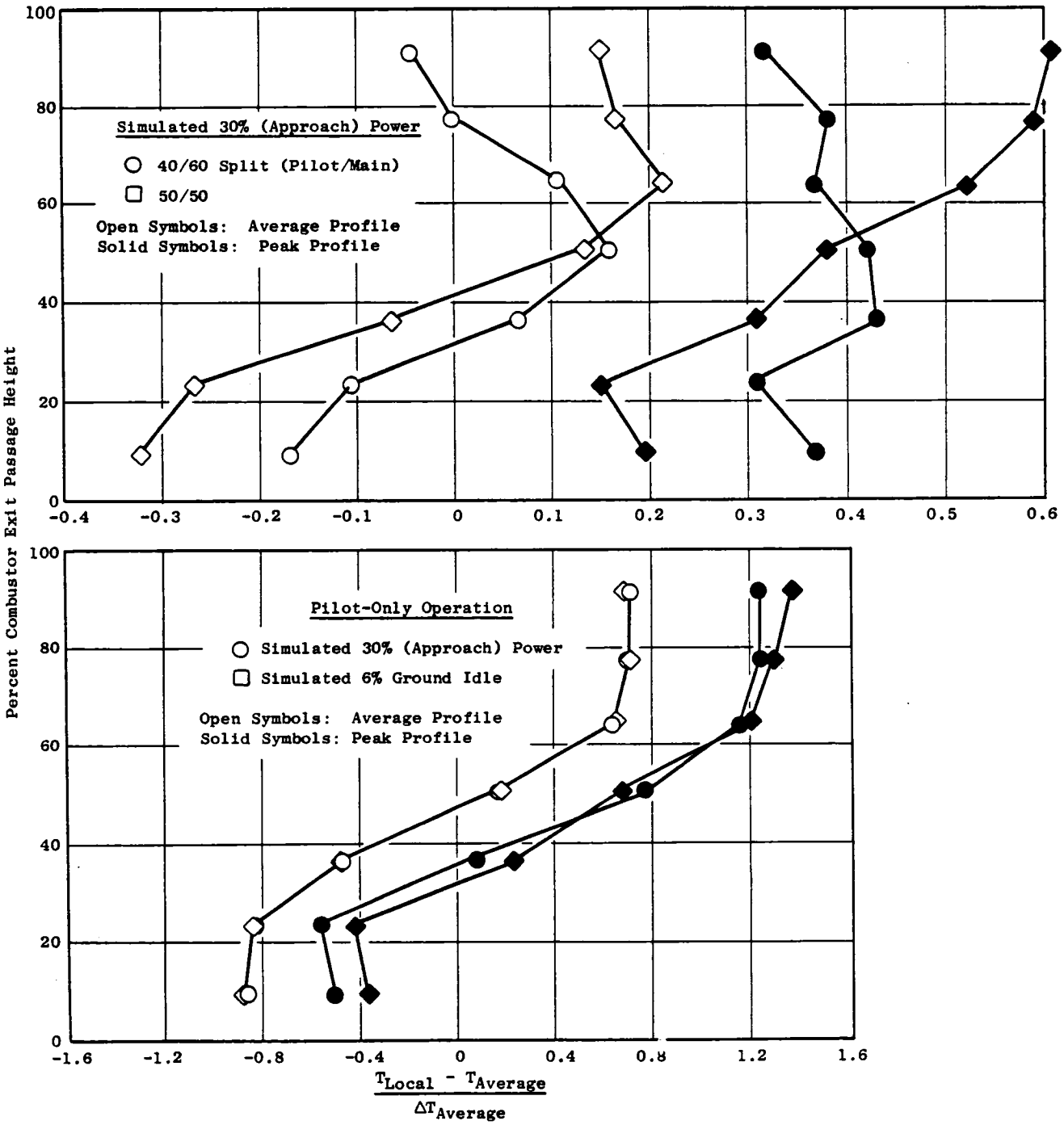

Figure 40. Combustor Thermal Signature at Part-Power Operation.

Table XVIII. Development Combustor Emissions - Ignition Test Schedule.

Test Point	Operating Condition	T_3, °F	P_3, psia	Airflows, lbm/sec					F/A Overall	Fuel Flows, lbm/hr				Sampling Mode
				W_3	Bleed, Outer	Bleed, Inner	Bleed, Prediffuser	Combustor		Total	Pilot/Total	Pilot	Main	
1	21 PCNHR	87	16.2	8.2	0	0	0	5.2						Ignition
2	24.5 PCNHR	98	16.9	6.2	0	0	0	6.2						Ignition
3	30 PCNHR	120	18.1	7.6	0	0	0	7.6						Ignition
4	37 PCNHR	173	23.3	8.2	0	0	0	8.2						Ignition
5	4% Idle	369	50.2	18.0	0	0	0	18.0						Ignition
6	6% Idle	426	63.2	22.9	0	0	0	22.9						Ignition
7	10% Idle	500	86.4	31.0	0	0	0	31.0						Ignition
8	4% Idle	369	50.2	21.7	1.25	1.15	1.38	17.9	0.0090	581	1.0	581	0	G
9		369	50.2	21.7	1.25	1.15	1.38	17.9	0.0110	710		710		G
10		369	50.2	21.7	1.25	1.15	1.38	17.9	0.0127	819		819		G, I
11		369	50.2	21.7	1.25	1.15	1.38	17.9	0.0150	968		968		G
12		369	50.2	21.7	1.25	1.15	1.38	17.9	0.0200	1290		1290		G
13	6% Idle	426	63.2	27.5	1.58	1.45	1.75	22.7	0.0080	654		654		G
14		426	63.2	27.5	1.58	1.45	1.75	22.7	0.0100	817		817		G
15		426	63.2	27.5	1.58	1.45	1.75	22.7	0.0116	946		948		G, I
16		426	63.2	27.5	1.58	1.45	1.75	22.7	0.0150	1226		1226		G
17		426	63.2	27.5	1.58	1.45	1.75	22.7	0.0200	1634		1634		G
18	30%	692	130.0	51.6	2.94	2.71	3.26	42.7	0.0140	2152		2152		G
19		692	130.0	51.6	2.94	2.71	3.26	42.7	0.0140	2152	0.4	861	1291	G
20		692	130.0	51.6	2.94	2.71	3.26	42.7	0.0140	2152	0.3	646	1506	G

Fuel was supplied to the combustor through the E^3 fuel nozzle assemblies. This was the first time that these nozzle assemblies were used. The nozzles were placed around the combustor to provide uniform fuel distribution in the pilot-stage dome for the purpose of demonstrating low emission levels at idle. The engine nozzles were used to complete the high-pressure evaluation of the combustor.

The engine fuel nozzle assemblies were then removed from the rig and replaced with the E^3 test rig fuel nozzle assemblies. The customer test rig featured a 12-cup section of prototype (peanut) nozzles and an 18-cup section of standard test rig nozzles in the pilot-stage dome. Both the peanut and the standard nozzles are rated at about 26 lbm/hr of fuel flow at 100-psi pressure drop. These two nozzle tip designs are illustrated in Figure 41. The engine idle conditions were then rerun.

Test rig instrumentation consisted of five gas-sampling rakes, each with four sampling elements, plus the standard, total-pressure and inlet-air-temperature rakes at Plane 3.0 of the test rig. Two C/A (0.06-in. wire diameter) thermocouples were strapped onto the outermost and innermost sampling elements of each of the five gas-sampling rakes. These thermocouples were connected to a "Metrascope" visual display system within the cell control room and were used in determining ignition, staging, and lean extinction of the combustor. For gas-sampling, all four elements of each gas rake were individually connected to the valving in the gas-sampling equipment. Since only ganged rake samples were desired, this approach provided the flexibility to close-off individual rake elements from the gas sample if problems occurred in any of the four elements. The gas-sampling rakes were equally spaced around the test-rig instrumentation spool. Ambient water was used to cool the rakes during testing. When taking gas samples, the rakes were traversed through 66°, in 6° increments, enabling gas samples to be obtained in-line with and between all swirl cups. For ignition and blowout evaluation, the gas-sampling rakes were positioned such that one rake was located at 240° clockwise, aft looking forward, placing two thermocouple elements directly downstream of the pilot-stage ignitor cup and one of the two pilot-stage-to-main-stage crossfire tubes.

Simplex "Peanut"

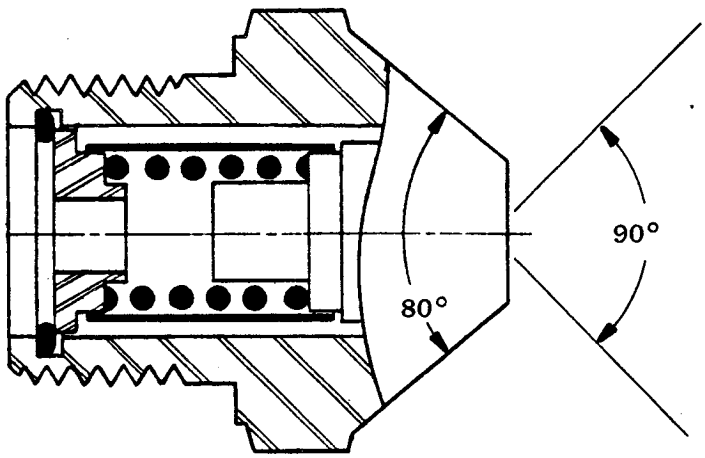

Development "Hago"

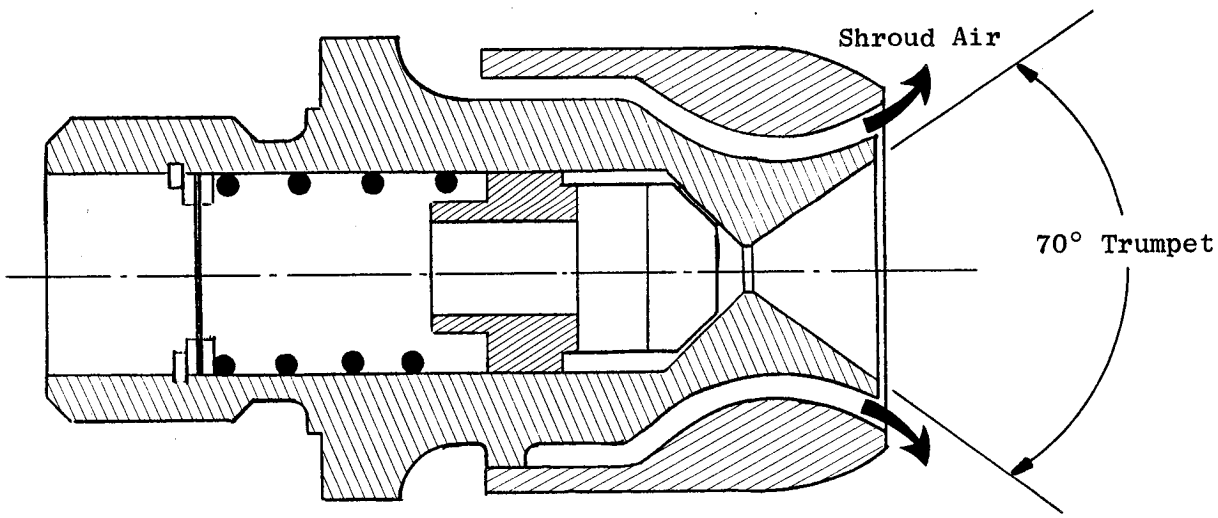

Figure 41. Sector-Combustor Fuel Nozzle Comparison.

Gas samples were analyzed using the CAROL II (Contaminates Are Read On Line) system located at the test facility. Instruments featured in this system include:

- Beckman Model 402 total hydrocarbon analyzer (flame-ionization detector)
- Beckman Model 315-B carbon monoxide and carbon dioxide analyzer (NIDR)
- Beckman Model 951-H NO_x analyzer (heated chemiluminescence with converter)

Sample flow was passed through a refrigerated trap, to remove excess water from the sample, before entering the gas-analysis instruments. Prior to testing, the CAROL II system was calibrated using gases of known concentrations. During testing, calibration spot checks of the instruments, and any necessary adjustments, were made to assure that this equipment was in good working order at all times. Inlet-air humidity was measured using an EG&G Model 440 dew-point meter.

Smoke samples were taken only at key combustor operating points in the test schedule. Smoke samples were extracted from the exhaust gases using two of the five gas-sampling rakes valved to provide a single sample. At those test points where smoke samples were taken, the rakes were initially positioned in-line with the swirl cups, then rotated 6° to between swirl cups. At both of these positions, several 0.2-ft^3 smoke samples were obtained using a standard GE smoke console located in the cell control room.

Combustor instrumentation consisted of 28 static pressures, 2 total pressures, and 65 grounded and capped chromel/alumel thermocouples. Of these thermocouples, 19 were embedded into the surface of the centerbody structure at several places around the circumference. This instrumentation provided important performance data concerning combustor pressure drops, airflow distribution, and metal temperatures. The locations of this instrumentation on the combustor hardware are illustrated in Figure 42. A dynamic-pressure probe was installed through an available test-rig port and immersed into the combustor outer flowpath. This probe was used to monitor the characteristic frequencies and fluctuations of the engine combustor.

Circumferential Location, Degrees

A	0, 48, 51, 54, 354, 357
B	6
C	0, 6, 54, 60
D	6
E	0, 45, 48, 51, 351, 357
F	6
G	60, 240
H	60, 240, 264
I	60, 240, 264
J	132, 312
K	132, 312
L	129, 135, 309, 315, 318
M	60, 120, 240
N	60, 127, 135, 240, 312, 315, 318
O	132, 309
P	60, 240
Q	60, 240, 264
R	60, 240, 264
S	252
T	150, 153, 156, 246, 249, 252
U	252
V	156, 159, 162, 252, 255, 258
W	252
X	150, 153, 156, 246, 249, 252

• Static Pressure Taps

▲ Skin Thermocouples

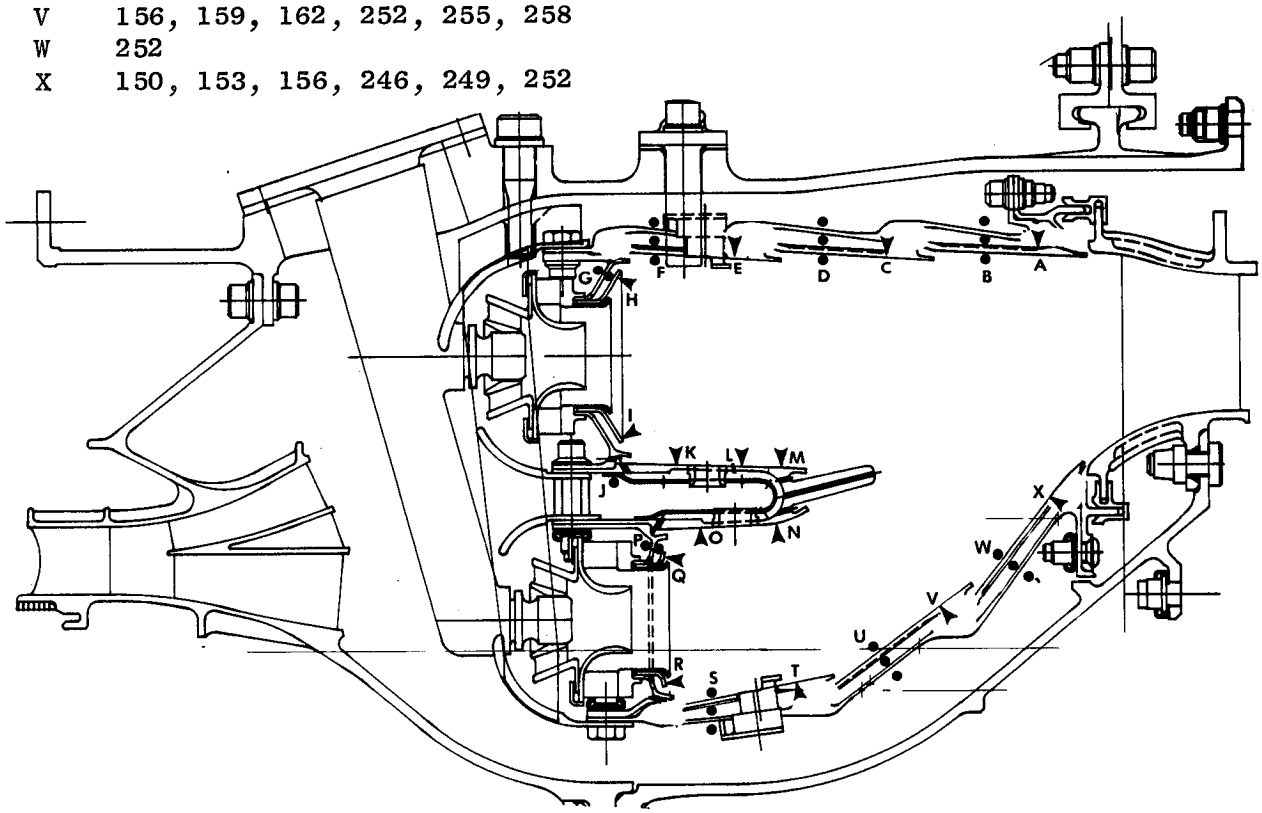

Figure 42. Engine Combustor Instrument Layout.

All emissions and instrumentation data acquisition was automatically handled by the medium-speed, digital-data-acquisition system of the test facility. From this system the data were processed through a computer which performed calculations of the various emission indices and combustor operating parameters and converted digital signals from all pressure and temperature instrumentation to engineering units. All smoke samples were obained on Wattman No. 4 filter paper. Following completion of testing, the smoke samples were analyzed on a Densichron to determine the optical density used to compute the SAE smoke number.

The ignition test results obtained on the E^3 combustor are presented in Figure 43. The pilot stage demonstrated excellent ignition and lean-extinction characteristics. Considerable margin is available against the E^3 ground-start cycle fuel schedule, with or without compressor bleed, down to 30% corrected core engine speed. These results are very similar to the pilot-stage ignition characteristics demonstrated at atmospheric inlet pressures. The anticipated improvement at true cycle inlet pressure was not demonstrated. This is most probably related to the differences in the fuel-spray characteristics between the engine fuel nozzle assemblies used in this test and the test-rig nozzle assemblies used in the atmospheric test.

Test data from the main stage suggest that it will not be possible to achieve main-stage ignition within the steady-state FPS cycle fuel schedule at engine power levels up to 10% thrust. However, taking into consideration the additional fuel available on the engine accel schedule, staging this combustor while on this accel schedule should be possible at the 10% power operating condition. The lean-extinction characteristics of the main stage are sufficient to allow staged combustor operation at conditions as low as 4% ground idle if the engine decels to that operating condition from a point where main-stage crossfire can occur.

The idle emissions obtained using the engine fuel nozzle assemblies are presented in Figure 44. As observed from this figure, the engine combustion system achieved exceptionally low levels of CO and HC emissions at both the 4% and 6% ground-idle operating conditions. At the 4% ground idle design point (f/a = 0.0123), a CO emission level of 18.2 g/kg of fuel and a HC emission level of 1.7 g/kig of fuel were demonstrated. At the 6% ground-idle

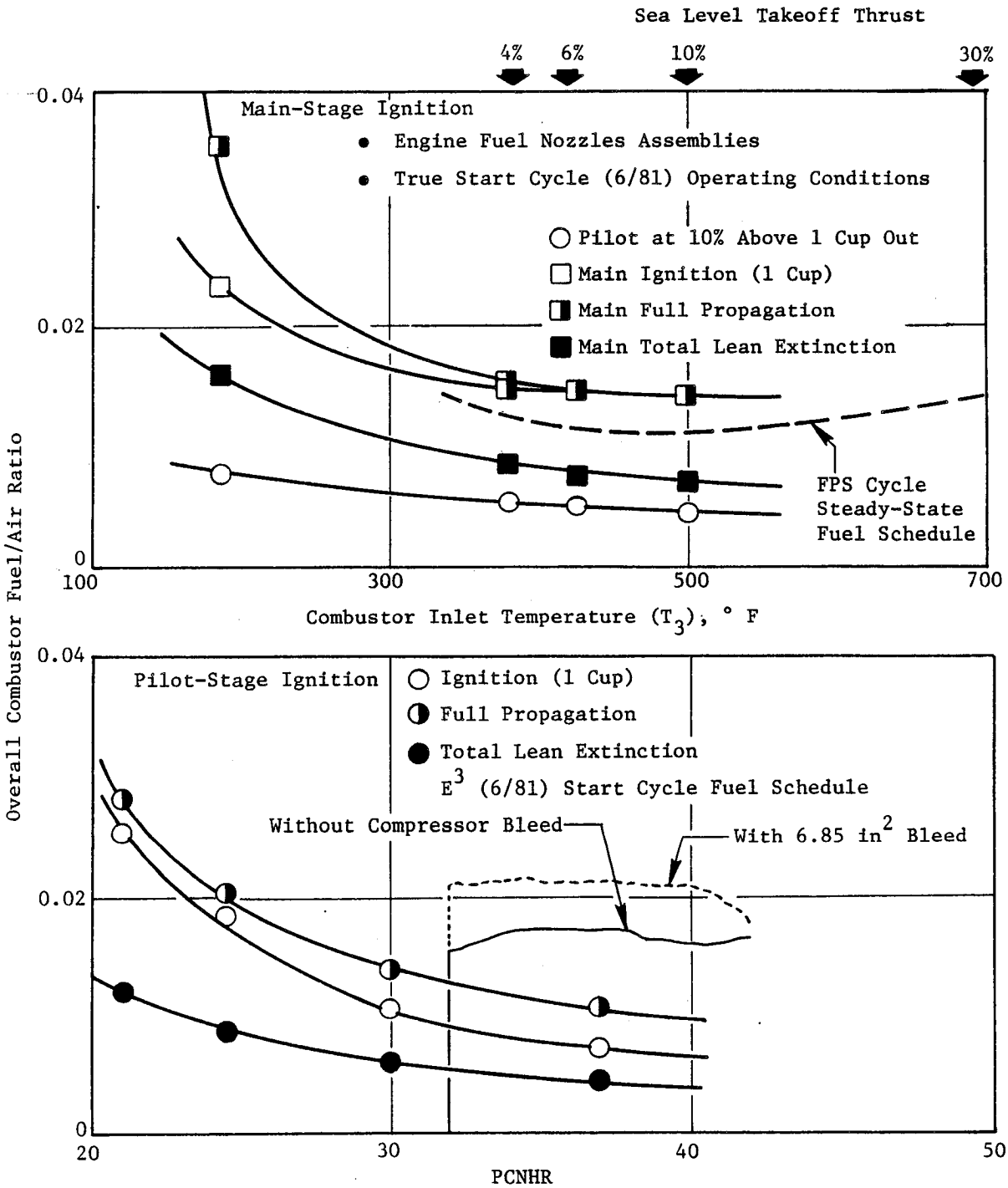

Figure 43. Engine Combustor Ground-Start Ignition Results.

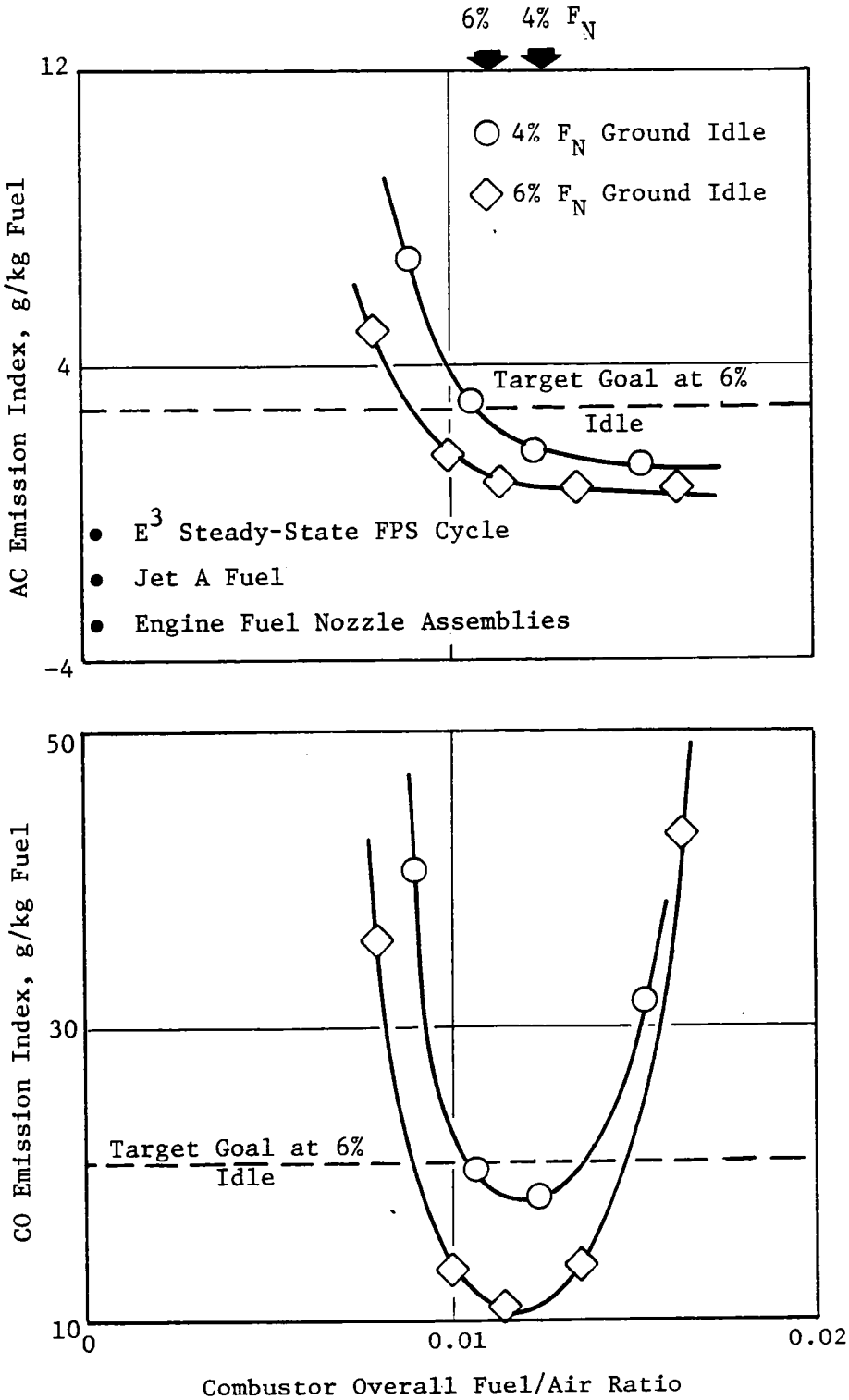

Figure 44. Engine Combustor Idle Emission Results.

design point (f/a = 0.0113), the levels demonstrated were 10.8 g/kg of fuel and 0.8 g/kg of fuel, respectively, for CO and HC emissions. The 6% levels are substantially below the program target goals of 20.7 g/kg of fuel for CO emissions and 2.8 g/kg of fuel for HC emissions estimated to satisfy the E^3 Program EPAP design goals for these emissions categories. Both emission levels remain at the goal levels or below at combustor fuel/air ratios from 0.009 to 0.0145.

Idle emissions obtained using the array of peanut and standard-test-rig fuel nozzles are presented in Figure 45. This testing was prematurely terminated because of a failure in the gas-sampling traverse system. Sufficient data were obtained to make the comparison at the 6% ground-idle operating condition. As observed from Figure 45, the peanut-type fuel nozzles demonstrated CO and HC emissions levels lower than levels obtained from the standard test rig nozzles at fuel/air ratios above 0.0110. This supports results previously obtained from E^3 sector-combustor subcomponent testing. Neither of the test-rig fuel nozzle types demonstrated CO and HC emissions levels as low as those achieved using the engine nozzle assemblies.

One of the interesting outcomes of this test involves the difference in fuel/air ratio at which each nozzle type demonstrated the minimum CO emission level. The engine nozzle assemblies achieved a minimum CO level of 10.5 g/kg of fuel at a fuel/air ratio of 0.0118; for the peanut nozzles, 12.5 g/kg of fuel resulted at a fuel/air ratio of 0.0138, and for the standard-test-rig nozzles, 15.5 g/kg of fuel resulted at 0.0129. This could be related to the differences in the fuel-spray-angle characteristics of each nozzle type. The peanut nozzles and the engine nozzle assemblies are known to have wider fuel-spray angles than the standard rig nozzles. An anticipated result is the observed lesser sensitivity of the CO emissions to fuel/air ratio demonstrated with these two nozzle types.

Emissions were measured at the 30% power (approach) operating condition at pilot-to-total fuel splits of 1.0, 0.5, 0.4, and 0.3. The effects of these fuel-staging modes on the measured CO, HC, and NO_x are presented in Table XIX. The expected trend of low CO and HC emissions and high NO_x emissions at the pilot-only operating mode is evident. In the staged operating mode, the

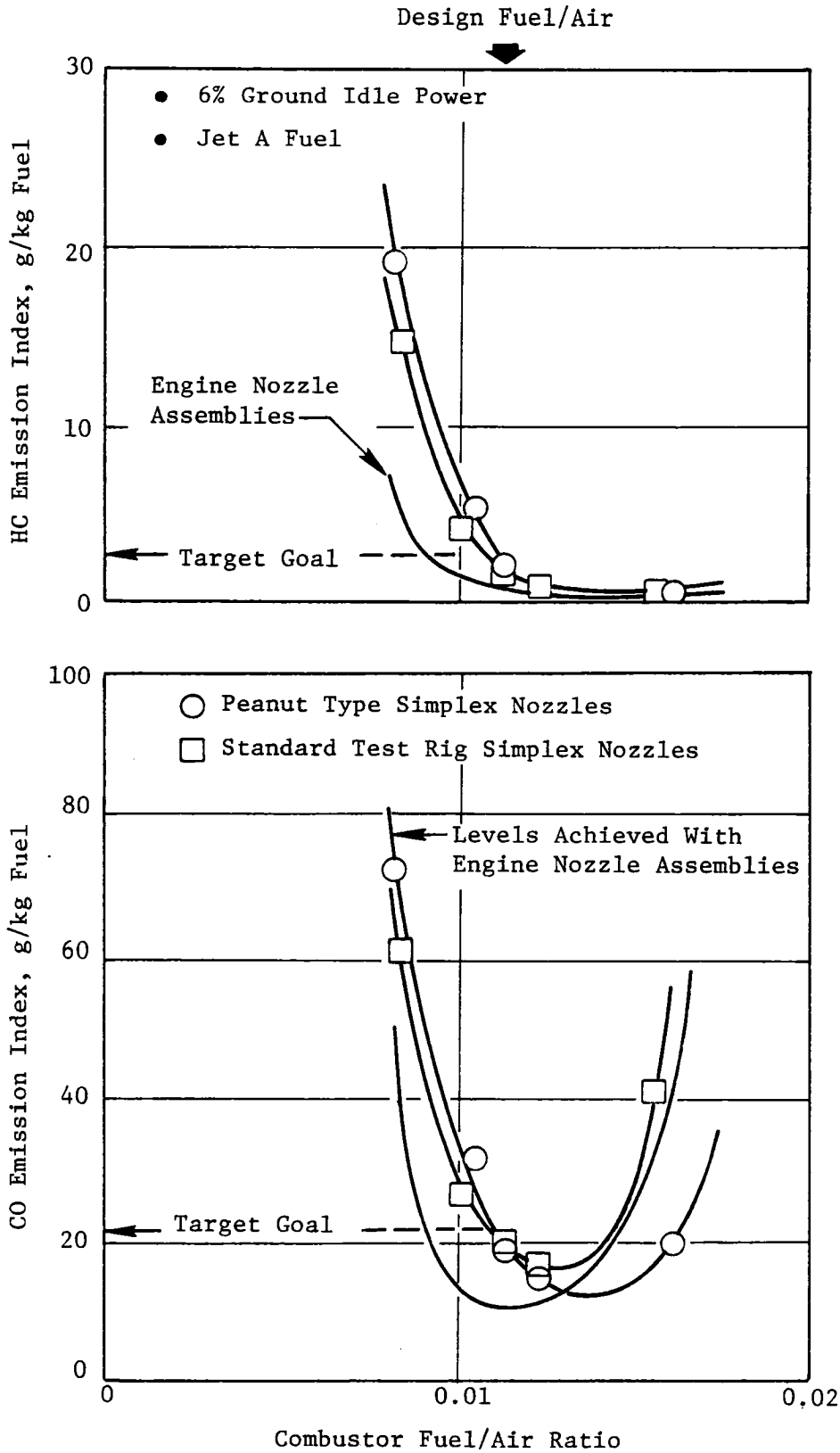

Figure 45. Engine Combustor Idle Emissions Comparison

NO_x levels are reduced, but the CO and HC emissions increase substantially. This trend has been observed in previous testing of the E^3 development combustor. In the staged operating mode at the 30% power operating condition, the low overall combustor fuel/air ratio (0.0140) of the FPS design cycle creates very lean fuel/air mixtures in both domes. These lean primary-zone conditions cause low combustion efficiencies and result in the high CO and HC emissions levels. Another contributing factor may involve the fuel-spray quality. At fuel flows associated with this operating condition and staging mode, the secondary fuel systems of the pilot- and main-stage duplex nozzle tips have just opened. This situation often produces larger fuel droplets mixed with the nozzle-tip fuel spray.

Table XIX. Emissions at 30% Approach Power.

Combustor Operating Mode	Emission Index, g/kg Fuel		
	CO	HC	NO_x
Pilot Only	2.1	0.1	16.0
50/50 Fuel Split	66.9	13.2	6.1
40/60 Fuel Split	71.7	8.8	5.2
30/70 Fuel Split	83.0	8.0	5.4

All CO and HC emissions measured at the simulated high-power operating conditions were adjusted for the scaled-down inlet conditions associated with the inability of the facility to provide the actual design-cycle inlet conditions. These adjustments were made using the following relations:

- Adjusted EI_{CO} = Measured EI_{CO} x $(P_3/P_{3ref})^{1.5}$ g/kg of fuel
- Adjusted EI_{HC} = Measured EI_{HC} x $(P_3/P_{3ref})^{2.5}$ g/kg of fuel

These relations were derived as part of the data-reduction effort for the NASA/GE Experimental Clean Combustor Program and the EPA/GE CFM56 Program. The referenced conditions represent the design-cycle values at a specific power setting. The adjusted CO and HC emissions levels as well as those measured

at the lower power operating conditions are plotted against the combustor inlet temperature along the E^3 FPS design cycle in Figure 46. In this figure, the design fuel split at the higher power operating condition is considered to be 40/60; the impact of staging is clearly illustrated.

Measured NO_x emissions in the staged combustor mode at operating conditions from 30% power up to simulated sea level takeoff are plotted against the E^3 design-cycle severity parameter in Figure 47. This adjustment technique was also developed as part of the NASA/GE ECCP and the EPA/GE CFM56 Programs. The resulting correlation yields a NO_x emission index of 28.7 g/kg of fuel at the E^3 FPS sea level takeoff condition. This level is considerably above the target of 17.5 g/kg of fuel estimated to satisfy the E^3 NO_x EPA parameter goal and well above the satisfactory levels previously demonstrated with the Baseline and Mod. I development-combustor configurations. Slightly lower NO_x levels are obtained by establishing the off-design 30/70 fuel split. A potential explanation involves the main-stage, primary-dilution flow and is addressed in more detail in the discussion of the performance results. The adjusted NO_x emission levels as well as those measured at the lower power operating conditions are plotted against the combustor inlet temperature along the E^3 FPS design cycle in Figure 48. The design fuel split at the higher power operating conditions is considered to be 40/60.

EPA parameter numbers, based on the EPA landing/takeoff cycle, for CO, HC, and NO_x emissions were generated for various combustor operating-mode combinations along the E^3 FPS design-cycle operating line. The results are compared to the E^3 Program goals in Table XX. As observed from this table, in the pilot-only operating mode at the 30% power condition the CO and HC levels satisfy the requirements with margin for both 4% and 6% thrust at ground idle. However, the NO_x levels exceed the requirements by 40% or more depending on the pilot-to-main-stage fuel split selected at the higher power operating conditions. Operating the combustor in the staged mode at the 30% power condition provides some reduction in NO_x levels. However, reductions of at least 20% are yet necessary to satisfy the requirement. In addition, the CO and HC levels increase significantly and no longer satisfy or closely approach the requirements.

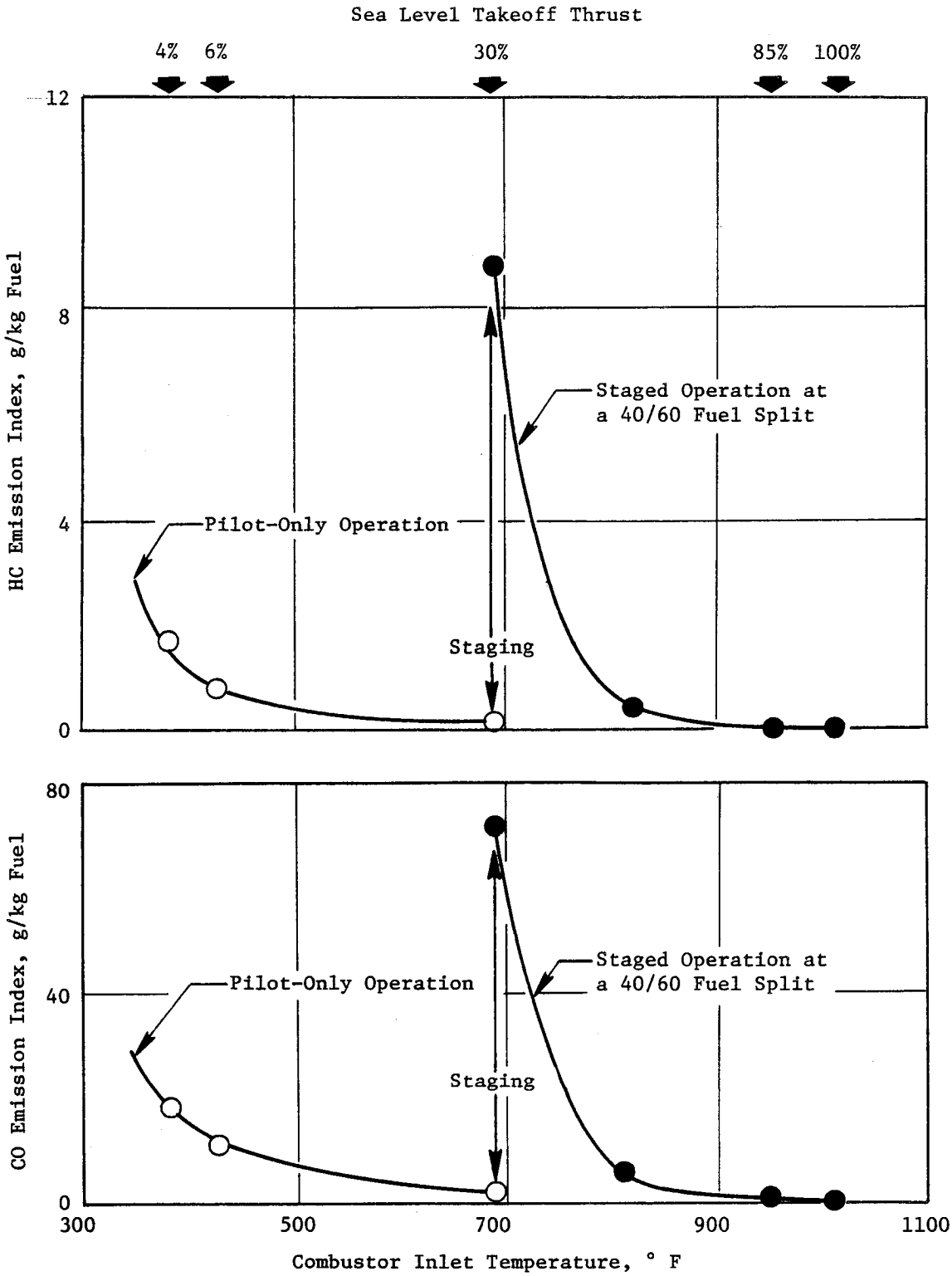

Figure 46. Engine Combustor CO and HC Emissions.

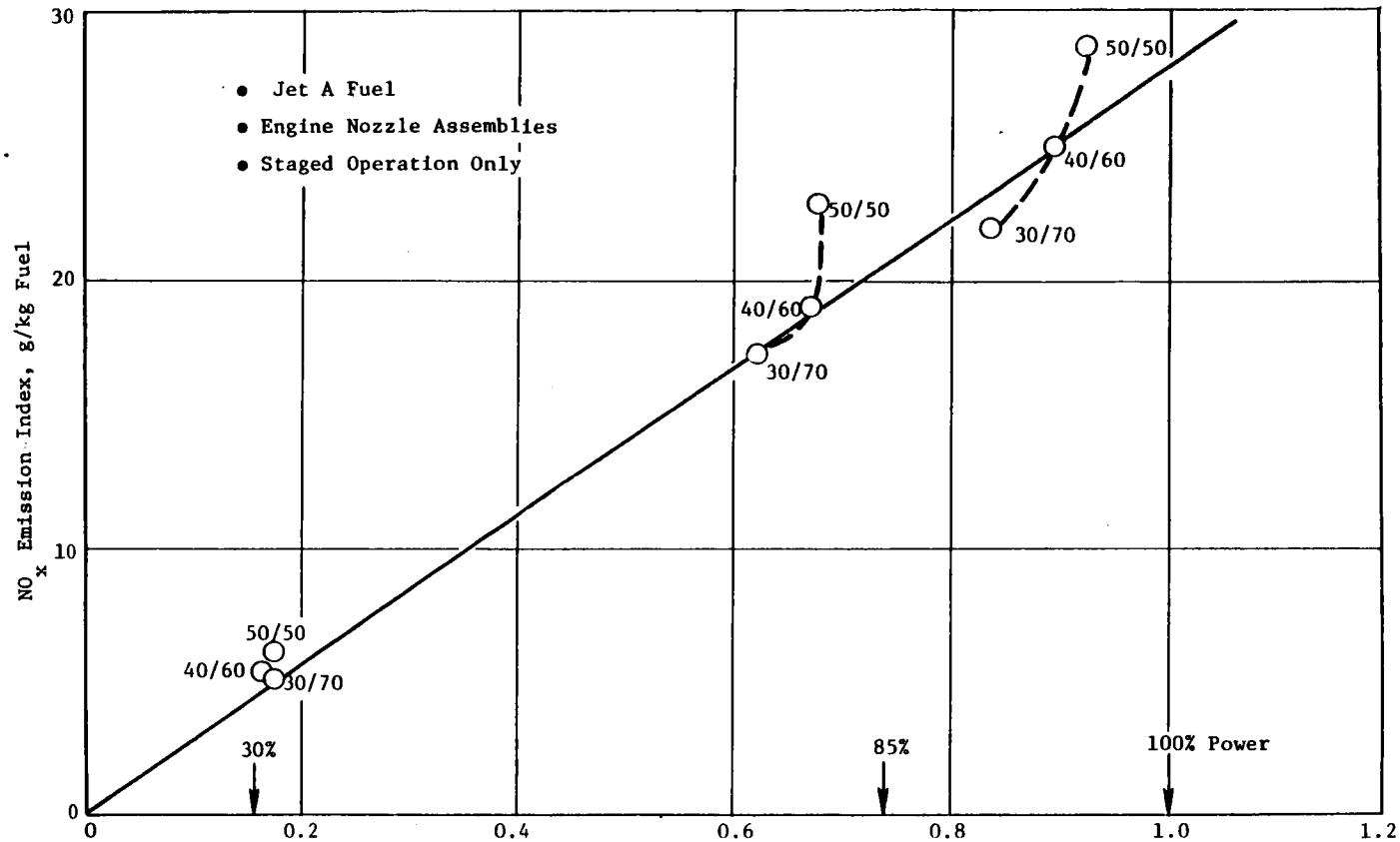

$$S = \left(\frac{P_3}{439}\right)^{0.37}\left(\frac{58.93}{V_{ref}}\right)\left(\frac{f/a\ Pilot}{0.00854}\right)^{0.65}\left(\frac{f/a\ Main}{0.01586}\right)^{0.65}\ Exp\left(\frac{T_3 - 1471}{345} + \frac{6.29 - Humidity}{53.14}\right)$$

Figure 47. Engine Combustor NO_x Emissions.

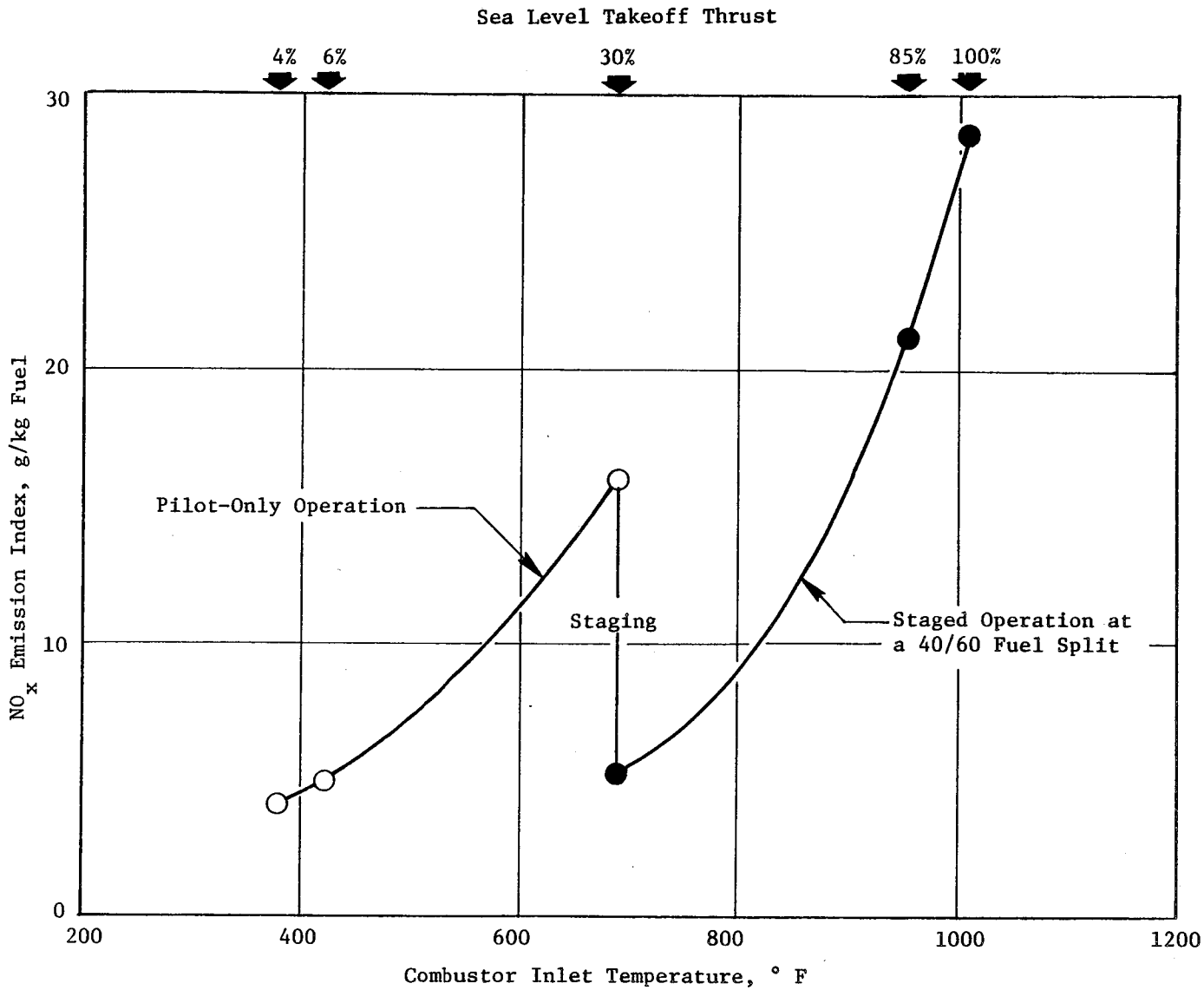

Figure 48. NO_x Emissions Corrected to FPS Cycle P_s.

Table XX. Engine Combustor EPAP Results.

- FPS Design Cycle, Steady State, Sea Level Static

Power	Operating Mode	EPAP, lbm/1000 lbf-hr-Cycle		
		CO	HC	NO_x
4% Ground Idle	Pilot Only at Approach 40/60 Split at Climb and Sea Level Takeoff	2.45	0.22	5.11
4% Ground Idle	40/60 Split at Approach 40/60 Split at Climb and Sea Level Takeoff	7.09	0.80	4.39
4% Ground Idle	Pilot Only at Approach 30/70 Split at Climb and Sea Level Takeoff	2.45	0.22	4.76
4% Ground Idle	30/70 Split at Approach 30/70 Split at Climb and Sea Level Takeoff	7.84	0.74	4.05
6% Ground Idle	Pilot Only at Approach 40/60 Split at Climb and Sea Level Takeoff	1.58	0.11	4.79
6% Ground Idle	40/60 Split Approach 40/60 Split at Climb and Sea Level Takeoff	5.76	0.63	4.15
6% Ground Idle	Pilot Only at Approach 30/70 Split and Climb and Sea Level Takeoff	1.58	0.11	4.48
6% Ground Idle	30/70 Split at Approach 30/70 Split at Climb and Sea Level Takeoff	6.44	0.58	3.84
E^3 Program Goals		3.00	0.40	3.00

Smoke levels obtained are presented, along with the combustor operating conditions at which they were measured, in Table XXI. The highest smoke level was measured at the approach operating condition in the pilot-only operating mode. Test conditions at this point exactly matched the design-cycle operating/conditions. Therefore, the measured smoke number of 16.5 would be representative of engine operation at this power setting and combustor operating mode. Slightly lower smoke levels (smoke number of 12.8) were measured at this same operating condition in the staged mode. Significantly lower smoke levels were obtained at the simulated high-power operating conditions. Although somewhat higher levels would be expected at the actual design-cycle conditions at high power, the levels should be well below the E^3 Program smoke number goal of 20.

Measured overall combustion system total pressure drop is plotted against the square of the combustor flow function parameter in Figure 49. A significant amount of data scatter is evident. Throughout this testing, problems were incurred with the transducer-scanning equipment used to read the combustor-exit total pressures. Pretest predictions of the overall loss were ≈5.3%. This tends to agree with the upper bounds of the measured data obtained. Measured static pressure drops across the domes indicate a drop of 3.3% across the pilot-stage dome and 2.9% across the main-stage dome at sea level takeoff operating conditions. Static pressure drops across the liners were between 1.1% and 1.4% for the forward panels and between 1.5% and 2.8% for the aft panels. Static pressure drops across the centerbody structure were 3.2% on the pilot-stage side and 2.3% on the main-stage side.

Using the measured combustor static pressures and measured combustor flow areas, estimates of the combustor airflow were generated for the pilot-only mode associated with low-power operation and the staged mode associated with high-power operation. The combustor flow areas were measured on a calibration test stand as part of the pretest checkout of the E^3 combustor hardware. These estimated airflow distributions are presented in Figures 50 and 51. Airflow distribution levels defined in the combustor design are also shown for comparison in Figure 51. Key areas of discrepancy occur in the primary zone of both the pilot stage and the main stage. Swirl-cup and primary-dilution flows in the pilot stage are considerably above the design intent while in the

Table XXI. Engine Combustor Measured Smoke.

P_3, psia	T_3, °F	Combustor Airflow, lbm/sec	Fuel/Air Ratio	Pilot/Total Fuel Flow	SAE Smoke Number	Comments
50.1	377	18.57	0.0123	1.0	8.5	4% Idle
63.2	423	23.20	0.0114	1.0	13.2	6% Idle
176.1	698	56.57	0.0143	1.0	16.5	30% Approach
176.3	694	56.33	0.0144	0.4	12.8	30% Approach
220.0	959	63.95	0.0215	0.4	5.2	Simulated 85% F_N
221.1	1016	60.45	0.0242	0.4	6.3	Simulated 100% F_N
E^3 Program Goal					20	

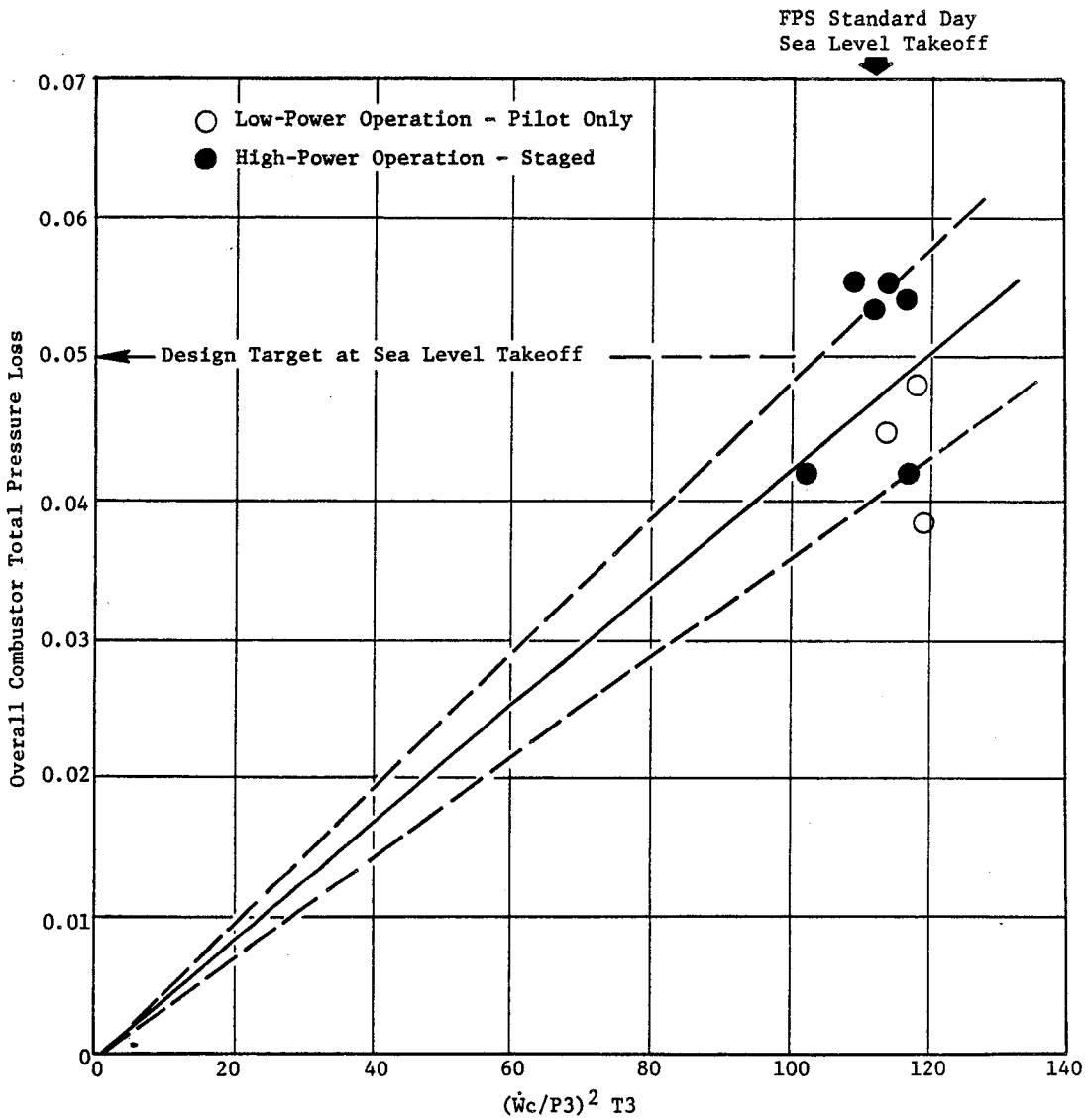

Figure 49. Measured Overall Combustion System Pressure Drop.

- Flows Presented in Percent $W_{Combustor}$

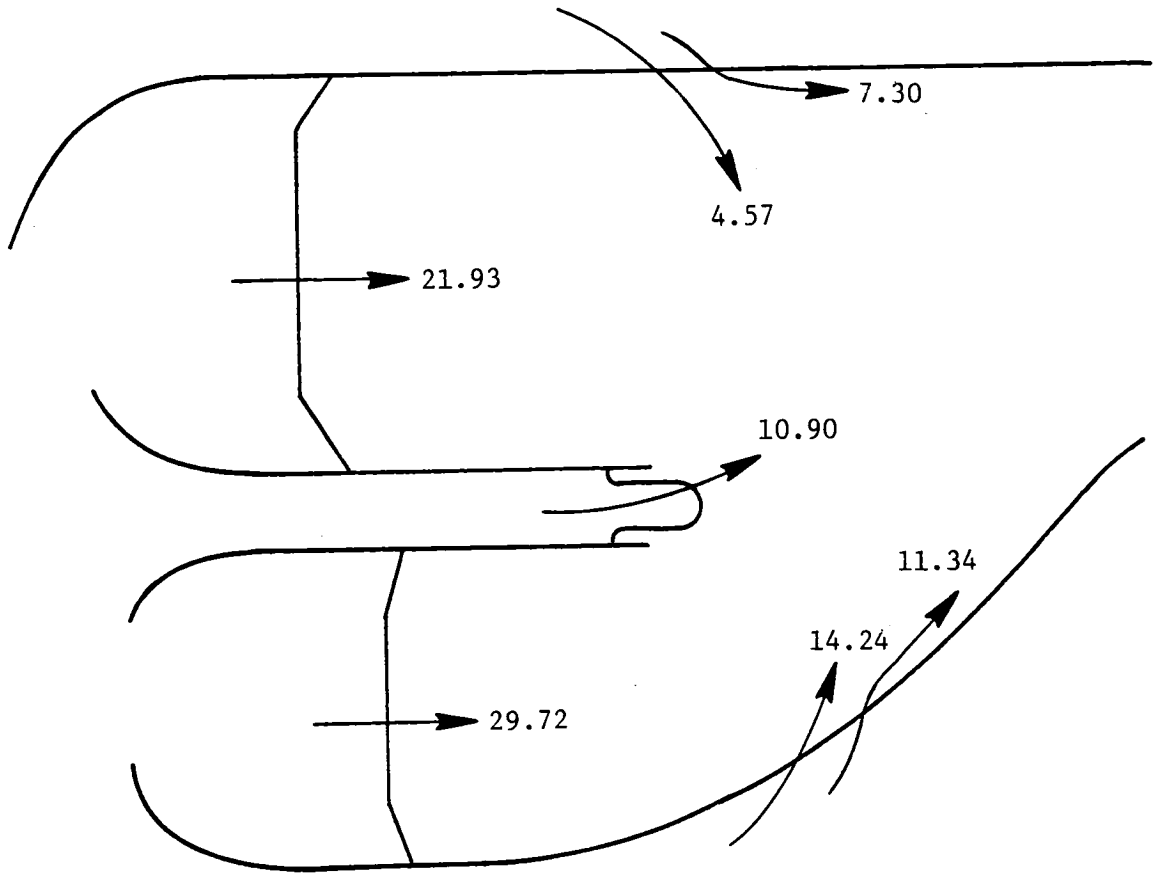

Figure 50. Engine Combustor Airflow Distribution; 6% Ground Idle, Pilot Only.

- Flows Presented in Percent $W_{Combustor}$
- Design Levels Shown in Parentheses

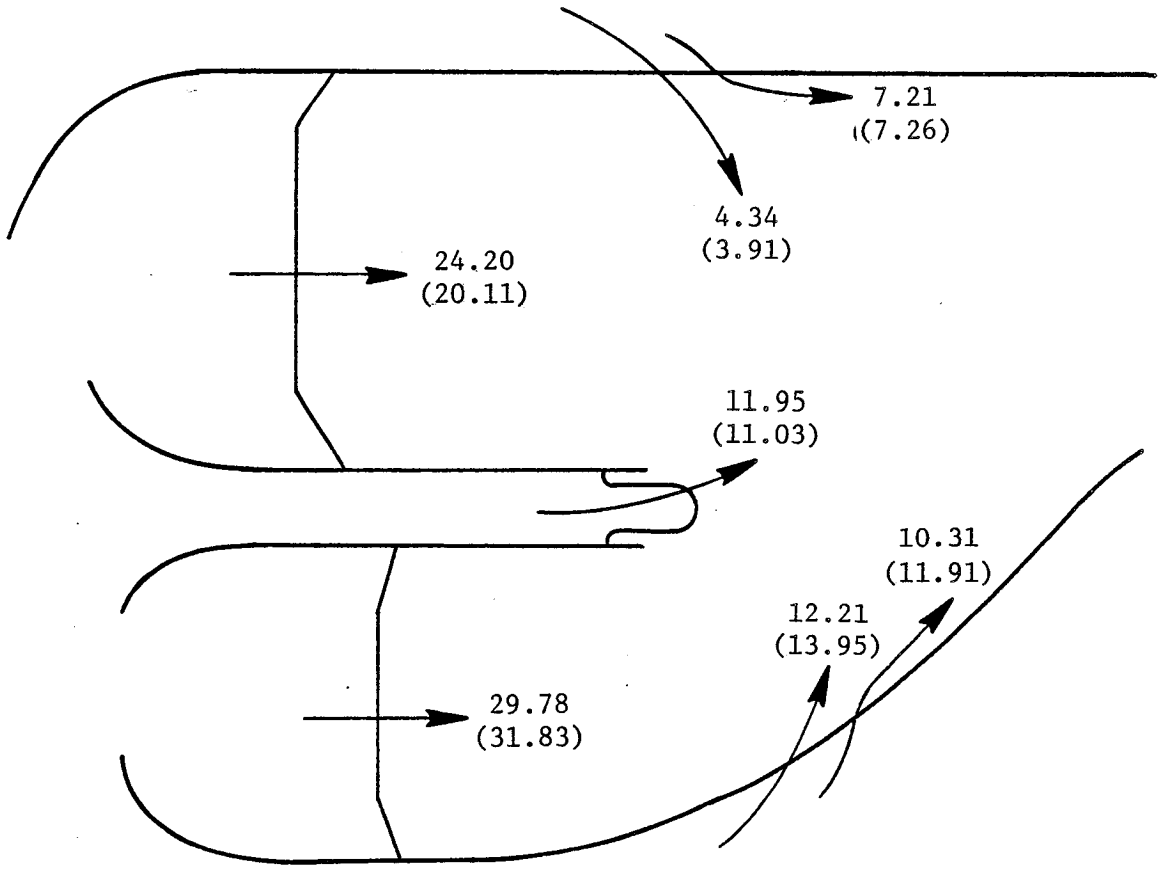

Figure 51. Engine Combustor Airflow Distribution, Simulated Sea Level Takeoff.

main stage the swirl-cup and inner-liner primary dilution, Panel 1, and Panel 2 cooling flows are below the design intent. The lower swirl-cup flow and primary-dilution flow in the main stage may be responsible for the high NO_x emission levels demonstrated. One explanation may be higher than expected pressure losses in the diffuser inner flow stream resulting from combustor inner flowpath airflow higher than the diffuser design intent. No diffuser performance data were obtained during this test to verify this hypothesis.

Indicated liner peak metal temperatures at the design-point (pilot-to-total fuel split of 0.4), simulated sea level takeoff operating conditions are compared to estimated temperatures based on the design airflow distribution in Figure 52. The highest liner temperature occurred on the inner-liner Rows 1 and 2 shingles. These hot spots are located directly in line with a swirl cup. The estimated airflow distribution indicated that both panels had cooling flows considerably below design intent. However, this condition cannot be applied to explain the higher than anticipated temperatures on outer-liner Row 1 and Row 2 shingles. Despite pretest apprehension, the centerbody structure did not exhibit excessively high metal temperatures. This is credited to the increased cooling flow incorporated into the design and the application of thermal-barrier coating to the exposed surfaces prior to the emissions test.

None of the indicated combustor metal temperatures should pose a problem during upcoming core and fan engine testing. Estimates have suggested that inner-liner Panel 1 shingle temperature will increase to ≈1820° F at full engine cycle operating conditions. The other temperatures are expected to show similar increases.

In summary, the results of the E^3 combustor component testing are very satisfactory. The combustor achieved almost all of the design objectives established for the development program. The high NO_x levels represent the only shortcoming in what was an excellent overall performance demonstration.

Besides the NO_x characteristics, two other areas stand out as requiring further development. One of these areas involves improving the main-stage crossfire characteristics to permit staging the combustor at ground idle. The other area involves improving the combustion efficiency at 30% approach power

Simulated Sea Level Takeoff: T_3 = 1016° F, P_3 = 220 psia, f/a = 0.0242

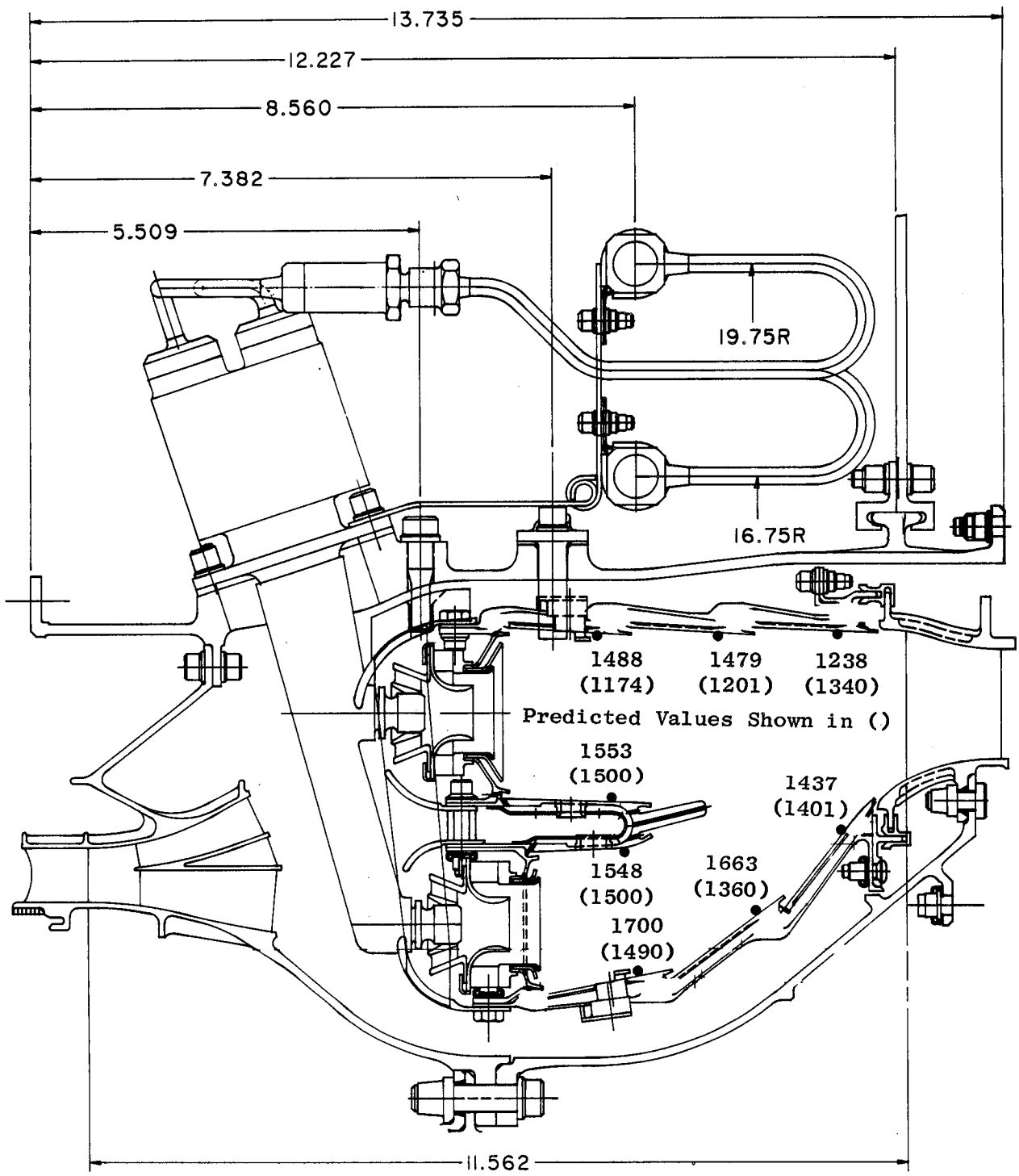

Figure 52. Engine Combustor Peak Indicated Liner Temperatures.

in the staged combustor-operating mode to get the necessary reductions in the CO and HC emissions.

Work Planned

This concludes the component development effort of the E^3 combustor. The combustor is to be turned over to the E^3 Evaluation Team for incorporation into the core engine build.

2.3.5 Combustor Fabrication

Technical Progress

All engine combustion-system hardware has been received. A complete inventory of the engine hardware is provided in Table XXII.

Work Planned

This task is complete; all combustor items have been procured. No further activity is planned.

2.4 HIGH PRESSURE TURBINE

Overall Objective

The objective of the HPT effort is to develop, evaluate, and demonstrate an efficient, two-stage turbine. The turbine design incorporates features that provide the best balance of efficiency and direct operating costs while achieving required component life.

Performance achievements will be aimed at developing high turbine efficiency using moderately loaded airfoils. The HPT efficiency goal for the fully developed FPS is 0.924 at Mach 0.8, 35,000-ft altitude, standard day, maximum cruise power setting. Additionally, the turbine incorporates an active clearance control system to achieve and maintain closer operating clearances for enhanced performance, particularly in climb and cruise operation.

Table XXII. Engine Combustor Hardware.

Item	Part Number	Quantity
Outer Impingement Liner Forging	4013267-459P02	3
Inner Impingement Liner Forging	4013267-460P02	3
Combustor Support Pins	4013249-922P01	65
Outer Aft Seal	4013249-931P01	2
Inner Aft Seal	4013249-932P01	2
Centerbody Forging	4013267-586P01	2
Shingle Castings	4013249-913/914/915/9/11	325
Outer Liner Retainer	4013249-446P01	2
Inner Liner Retainer	4013249-447P01	2
Combustor Casing Forging	4013267-466P01	2
Inner Fuel Manifold	4013279-056G01/G02	2 each
Outer Fuel Manifold	4013279-055G01/G02	2 each
Primary Fuel Manifold	4013279-055G01/G02	2 each
Primary Swirler Casting	4013267-587P01	205
Secondary Swirler Casting	4013249-442P01	205
Primary Swirler Housing Casting	4031267-585P01	205
Dilution Eyelet Casting	4013249-933P01/P02	200 each
Fuel Nozzle Seals	4013279-001P01	125
Fuel Manifold Bracket	4013279-095G01	20
Ignitor Dilution Eyelet	4013249-452P01	4
Shingle Retainer Rings	4013249-450P01/P02/P03	12
Instrumentation Seal	4013279-002P01	65
CDP Bleed Cover Plate	4013279-012P01	8
CDP Bleed Seal Plates	4013279-011P01	20
Ignitor Seal	4013204-109P01	10
Outer Support Liner	4013249-929P01	2
Inner Support Liner	4013249-930P01	2
Fuel Nozzle Forging	4013279-042P01	95
Ignitors	4013204-112P02	12
Ignition Exciter Box	910M52-P110	2
Miscellaneous Fasteners		4.5 Combustors
Outer Case Machining	4013297-050P01	1
Liner Shingle Machining	4013249-919/920/921/917	110
Outer Dome Assembly	4013267-595G01	1
Inner Dome Assembly	4013267-596G01	1
Outer Support Liner Hole Drilling	4013249-568G01	1
Inner Support Liner Hole Drilling	4013249-567G01	1
Centerbody	4013267-589G01	1
Liner Dilution Eyelets	4013 .49-933P01/P02	60
Cowl Assembly	4013297-594G03	1
Ignition Cables	4013284-325P02	6
Fuel Nozzles	4013279-050G01	48

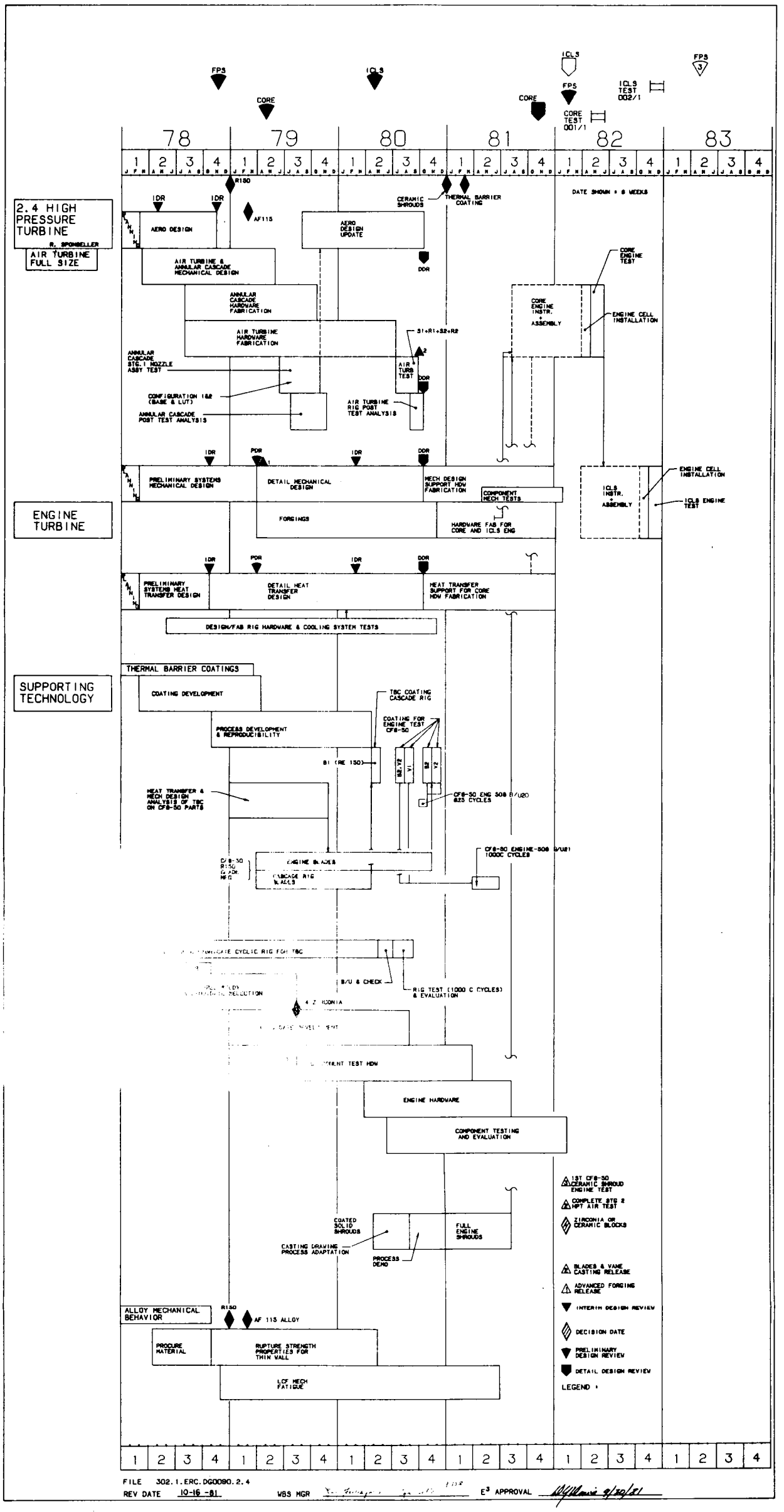
78
79
80
81
82
83
1 2 3 4
FPS
CORE
ICLS
FPS
CORE
ICLS
FPS
ICLS TEST 002/1
CORE TEST 001/1
DATE SHOWN + 6 WEEKS
2.4 HIGH PRESSURE TURBINE
R. SPONSELLER
AIR TURBINE FULL SIZE
ENGINE TURBINE
SUPPORTING TECHNOLOGY
R150
AF115
IDR
AERO DESIGN
AERO DESIGN UPDATE
CERAMIC SHROUDS
THERMAL BARRIER COATING
AIR TURBINE & ANNULAR CASCADE MECHANICAL DESIGN
ANNULAR CASCADE HARDWARE FABRICATION
AIR TURBINE HARDWARE FABRICATION
DDR
CORE ENGINE TEST
CORE ENGINE INSTR. ASSEMBLY
ENGINE CELL INSTALLATION
S1+R1+S2+R2
ANNULAR CASCADE STG.1 NOZZLE ASSY TEST
AIR TURB TEST
CONFIGURATION 1&2 (BASE & LUT)
ANNULAR CASCADE POST TEST ANALYSIS
AIR TURBINE RIG POST TEST ANALYSIS
PDR
PRELIMINARY SYSTEMS MECHANICAL DESIGN
DETAIL MECHANICAL DESIGN
MECH DESIGN SUPPORT HDW FABRICATION
COMPONENT MECH TESTS
FORGINGS
HARDWARE FAB FOR CORE AND ICLS ENG
ICLS INSTR. + ASSEMBLY
ICLS ENGINE TEST
PRELIMINARY SYSTEMS HEAT TRANSFER DESIGN
DETAIL HEAT TRANSFER DESIGN
HEAT TRANSFER SUPPORT FOR CORE HDW FABRICATION
DESIGN/FAB RIG HARDWARE & COOLING SYSTEM TESTS
THERMAL BARRIER COATINGS
COATING DEVELOPMENT
TBC COATING CASCADE RIG
PROCESS DEVELOPMENT & REPRODUCIBILITY
COATING FOR ENGINE TEST CF6-50
B1 (RE 150)
HEAT TRANSFER & MECH DESIGN ANALYSIS OF TBC ON CF6-50 PARTS
CF6-50 ENG 50B B/U20 825 CYCLES
CF6-50 ENGINE-50B B/U21 1000C CYCLES
ENGINE BLADES
CASCADE RIG BLADES
B/U & CHECK
RIG TEST (1000 C CYCLES) & EVALUATION
ENGINE HARDWARE
COMPONENT TESTING AND EVALUATION
COATED SOLID SHROUDS
FULL ENGINE SHROUDS
CASTING DRAWING PROCESS ADAPTATION
PROCESS DEMO
ALLOY MECHANICAL BEHAVIOR
AF 115 ALLOY
PROCURE MATERIAL
RUPTURE STRENGTH PROPERTIES FOR THIN WALL
LCF MECH FATIGUE
1ST CF6-50 CERAMIC SHROUD ENGINE TEST
COMPLETE STG 2 HPT AIR TEST
ZIRCONIA OR CERAMIC BLOCKS
BLADES & VANE CASTING RELEASE
ADVANCED FORGING RELEASE
INTERIM DESIGN REVIEW
DECISION DATE
PRELIMINARY DESIGN REVIEW
DETAIL DESIGN REVIEW
LEGEND :
FILE 302.1.ERC.DG00B0.2.4
REV DATE 10-16-81
WBS MGR
E3 APPROVAL

Development Approach (Reference WBS 2.4 Schedule Sheet)

The overall program plan for the HPT is to establish a turbine mechanical system and configuration that will achieve the projected levels of turbine efficiency and mechanical integrity. The aerodynamic design studies, initiated in March 1978, are devoted to the design for the air turbine and the aerodynamic airfoils definition for the core and the ICLS engine. An Intermediate Design Review was presented in November 1978 for the overall air turbine test program, the aerodynamic blade and vane airfoil definition, and the mechanical and heat transfer designs. The Preliminary Design Review was presented and approved for the aerodynamic, mechanical, and heat transfer designs in March 1979.

The detailed mechanical design began in April 1979 and consisted of an 18-month effort to integrate the experience gained from the materials program, heat transfer cascade tests, air turbine tests, and preliminary mechanical and systems design. The High Pressure Turbine Design Review was presented to NASA on October 1980 and was approved in December 1980. The review consisted of a presentation of all the technological disciplines associated with the turbine: heat transfer, mechanical, aerodynamics, and systems. After NASA approval of the design, the balance of the turbine components not yet released (as an advanced release) were authorized for manufacture. One set of hardware has been fully manufactured. This set of hardware is planned to be used for both core and ICLS engine testing. Adequate spares have been ordered, primarily for the flowpath components. Manufacturing progress for these spares is consistent with the time schedule required; the blade deliveries are planned by July 1982.

Major work accomplishments performed during the last six months were as follows:

- Issued all drawings for components requiring rework for instrumentation application.
- Performed all the necessary instrumentation rework on all parts requiring strain, pressure, and temperature measurements for the planned core and/or ICLS tests. Essentially every turbine component required some rework.

- Delivered the balance of the turbine hardware for core assembly including both stages of blades, nozzle segments, Stage 1 ceramic shrouds, and Stage 2 solid shrouds. Airflow checks were also completed for these components except for the Stage 2 shrouds.

Other work accomplishments during the last six months included airflow tests and calibration of the inducer nozzle and clearance-control manifolds plus dynamic tests for the cylindrical rotative structures and both stages of blades. Determination of the nodal variation frequencies for the rotating shaft, liner, and inner tube was necessary to assure adequate safety margin with respect to vibratory resonances within the engine operating-speed range.

The Stages 1 and 2 HPT blade natural frequencies were updated using a full dovetail form support versus the blade brazed to a block at the shank. Excellent agreement in most of the primary frequency modes was obtained between the two blade-support arrangements.

The thermal-barrier coating (TBC) program reached another major milestone with the completion of engine testing on Stage 1 nozzle segments in two CF6-50 engines. A total of 1300 "C" cycles were completed on four nozzle segments in the first engine test; a total of 750 "C" cycles, as planned, were completed on two other segments in another engine build. The TBC was applied on the bands and partially applied to the airfoil for both tests. Each test demonstrated the capability and potential payoff of TBC for reducing the cooling flow for both stages of turbine stator and rotor blading. Note that TBC blades have also been tested for 1000 "C" cycles in the first engine, and these results were reported in the last report.

Two reports covering the progress of the TBC program are in final publication. The first report is the metallurgical evaluation after the successful test in the CF6-50 engine of TBC turbine blades and vanes which were run for 1000 and 1300 "C" cycles, respectively. The second report documents the detailed TBC development program and process selection of the candidate coating.

Further accomplishments were also achieved in the ceramic-shroud development program. Ceramic shrouds were tested in a CF6-50 engine for 750 "C" cycles. A second test was completed using E^3 ceramic shrouds in a static, flame tunnel test. One thousand cycles were conducted in which the ceramic

surface was heated for three minutes to 2550° F and then rapidly air cooled for three minutes. The ceramic shrouds performed extremely well in both tests; no visible loss of the ceramic coating layer occurred.

Design Engineering has been providing support and continues to provide support to the Evaluation Engineering group during the turbine rotor and stator build-up and assembly. This work involved significant coordination, consultation, and requests for component rework, as required, to assure proper assembly and fit. Review and approval of recorded dimensional values for specific subassemblies, prior to release for engine build-up, was also provided.

2.4.1 HPT Aero Design Analysis

Technical Progress

During this reporting period, the first draft of the air turbine rig performance report was written. Currently, it is undergoing internal review.

Support was provided to mechanical, heat transfer, and instrumentation designers relative to build-up of the core engine. This support was primarily to assess the impact on performance due to hardware anomalies, assembly, instrumentation, and design changes.

Flow-area measurements taken on assembled rings indicate that the Stage 1 nozzle area is -0.2% of nominal, and the Stage 2 nozzle is -0.9% of nominal. These are within acceptable limits.

Stage 1 blade rework resulted in the unintentional cutting back of the trailing edge by 1.4 millimeters. This causes an increase in blade throat area of 2.8%, a convergent-divergent passage, and an increase in diffusion on the suction surface. A boundary-layer analysis of this blade indicates no separation.

A performance prediction update for the core engine relative to the air turbine rig was completed. This update included an increase in chargeable flow of 1.25% due to hardware deviations and 0.65% instrumentation related. Turbine efficiency is expected to be lower by 0.02% per cycle definition.

Work Planned

- Continue to support core engine build-up and monitor core engine test
- Publish the air turbine rig performance report

2.4.2 High Pressure Turbine Heat Transfer Design

Detailed design work was nearly complete at the beginning of this reporting period. The majority of the work this reporting period consisted of core engine hardware flowchecks, determination of hardware discrepancies and resultant impact on core engine test, and refining engineering specifications for successive sets of hardware. A discussion of the work during the six-month reporting period is presented here.

Stage 1 Blade

Seventy-six blades have been flowchecked during this reporting period and are now available for engine testing. There are 16 instrumented blades in this group. Coolant flow for the forward serpentine and warm-bridge circuit is at design intent, 1.63% W_{25}. The trailing-edge circuit will have a coolant flow 0.25% W_{25} greater than design intent. This was due to two deviations from the initial design. Low casting yield dictated a change in trailing-edge slot configuration. Coolant flow for those blades is 0.2% above nominal. Half of the blades in the demonstrator vehicle will have the higher flowing blades, resulting in 0.10% W_{25} increased flow. The remainder of the additional flow is due to the airfoil chord length being approximately 0.050 in. less than design intent. Gas-side aerodynamics cause a reduction in trailing-edge-slot static pressure. This will increase the trailing-edge flow by 0.15% W_{25}. Total aft serpentine and trailing-edge flow will be 1.94% W_{25}. The total blade flow will be 3.57%, rather than 3.3% W_{25}, at ICLS 86° F day maximum takeoff conditions.

Stage 2 Nozzle Assemblies

Twenty-six 2-vane nozzle assemblies were flowchecked and found to be satisfactory for engine testing. Trailing-edge casting problems precluded the

proper finished slot size. Completed vanes have nearly twice the trailing-edge-slot flow area intended. This will result in an increase in trailing-edge cooling flow from the design level of 1.1% W_{25} to 2.0% W_{25}. The inner-band metering holes were adjusted to provide the proper interstage seal purge flows. The total nozzle flow will be 2.85% W_{25} at ICLS 85° F day maximum takeoff conditions.

A procedure to obtain the correct trailing-edge slot and design flow levels has been identified. The cast holes will be completely closed by activated diffusion healing (ADH). The proper trailing-edge slot will be machined with electrodes and electrical discharge. All subsequent nozzle assemblies will have the reduced slot size with design-level flows.

Stage 2 Blades

During this period, 63 Stage 2 blades were flowchecked and found to be satisfactory for core and ICLS testing. An additional 15 instrumented blades also met the airflow and pressure-margin requirements. The results of the flowchecks indicate that coolant flow at ICLS 86° F day maximum takeoff conditions will be 0.63% W_{25}. The design coolant flow of 0.75% W_{25} was reduced due to increased turbulator height and increased serpentine friction factors. The reduction in flow would normally increase the blade bulk temperature by approximately 20° F for constant gas temperature. However, due to the increased Stage 2 vane trailing-edge flow and consequent dilution of gas temperature, the bulk temperature of the Stage 2 blade will remain at design intent.

HPT Rotor Cooling-Air Supply System

The HPT inducer was flowchecked during the previous reporting period. Information obtained from blade flowchecks indicated the desirability of resetting the inducer flow area during the current reporting period. The combination of increased blade flow (0.15% W_{25}), potential instrumentation leaks (0.15% W_{25}), and instrumentation-lead friction losses in the supply passages gave reason for a 10% increase in flow area. The inducer cold-flow check value after reset is still within the design tolerance range but now

lies on the high side of the nominal design value. This will ensure adequate Stage 1 backflow margin with the current hardware configuration.

2.4.3.4 Hardware Fabrication and Component Test Support

Technical Progress

A major effort by the HPT engineering group has been devoted to manufacturing support. This included coordination with production control on delivery schedules, engineering disposition on out-of-print manufacturing dimensions, and cost control.

All component delivery schedules and costs were met within the work scope defined under this program. The balance of the first set of turbine rotor and stator parts have been delivered for core engine build-up during the six-month effort.

Figures 53 and 54 are cross sections of the HPT rotor and stator assemblies, respectively. Cross reference with specific manufactured hardware for these components can be found in WBS 2.4.8.1 through 2.4.8.6.

Work Planned

Continue engineering support of manufacturing for the completion of spare hardware.

2.4.3.5 HPT Core/ICLS Support

Technical Progress

All HPT component rework for instrumentation application was completed. Table XXIII shows a breakdown of the type and quantity of instrumentation planned for use in monitoring HPT operation during the core engine tests. In addition, for each stage there are eight laser probes to measure blade tip clearance.

Engineering support for the core engine build-up continues. The Stage 1 nozzle (shown in Figure 55) and inducer seal subassemblies have been assembled to the compressor diffuser and to the combustor. The assembly, as shown in

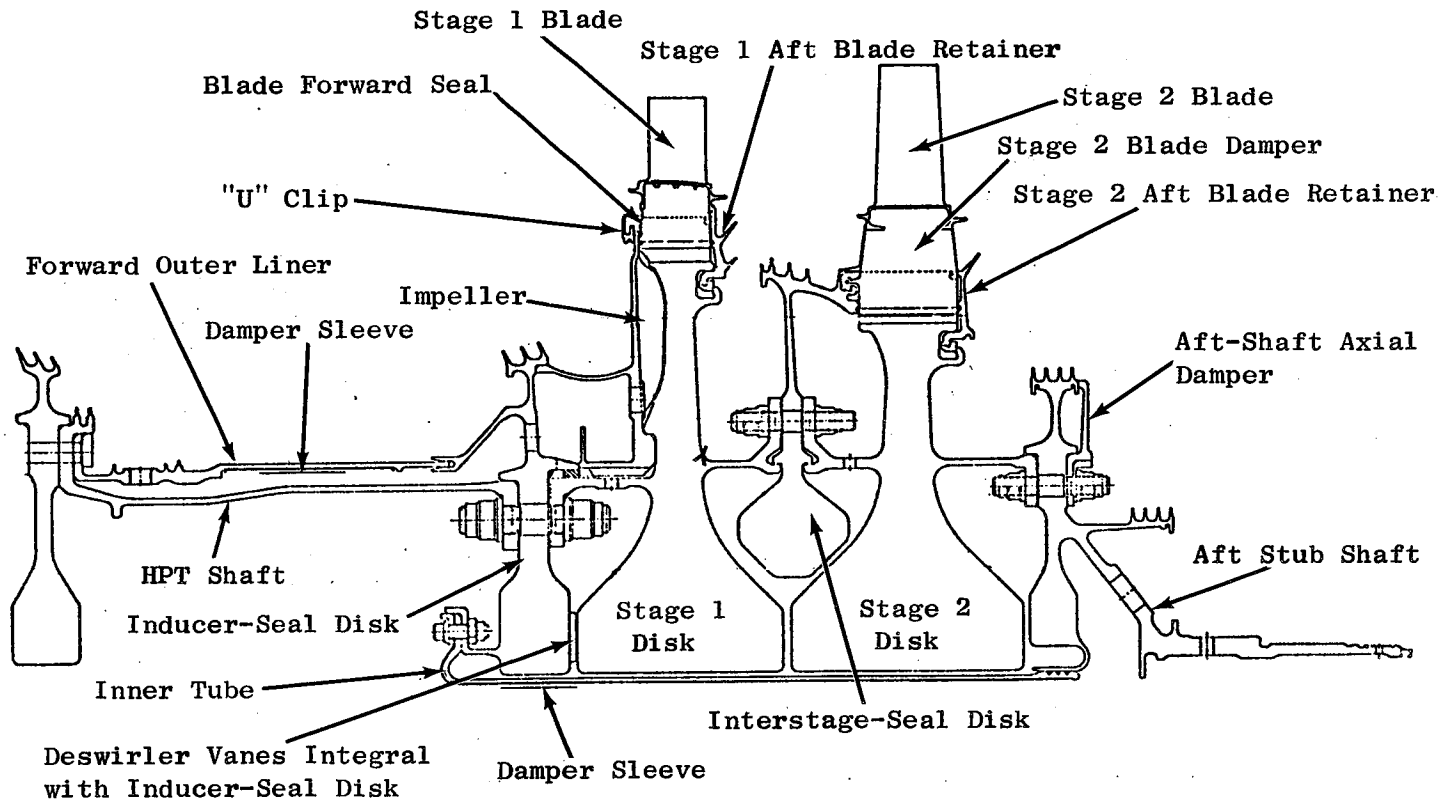

Figure 53. HPT Rotor.

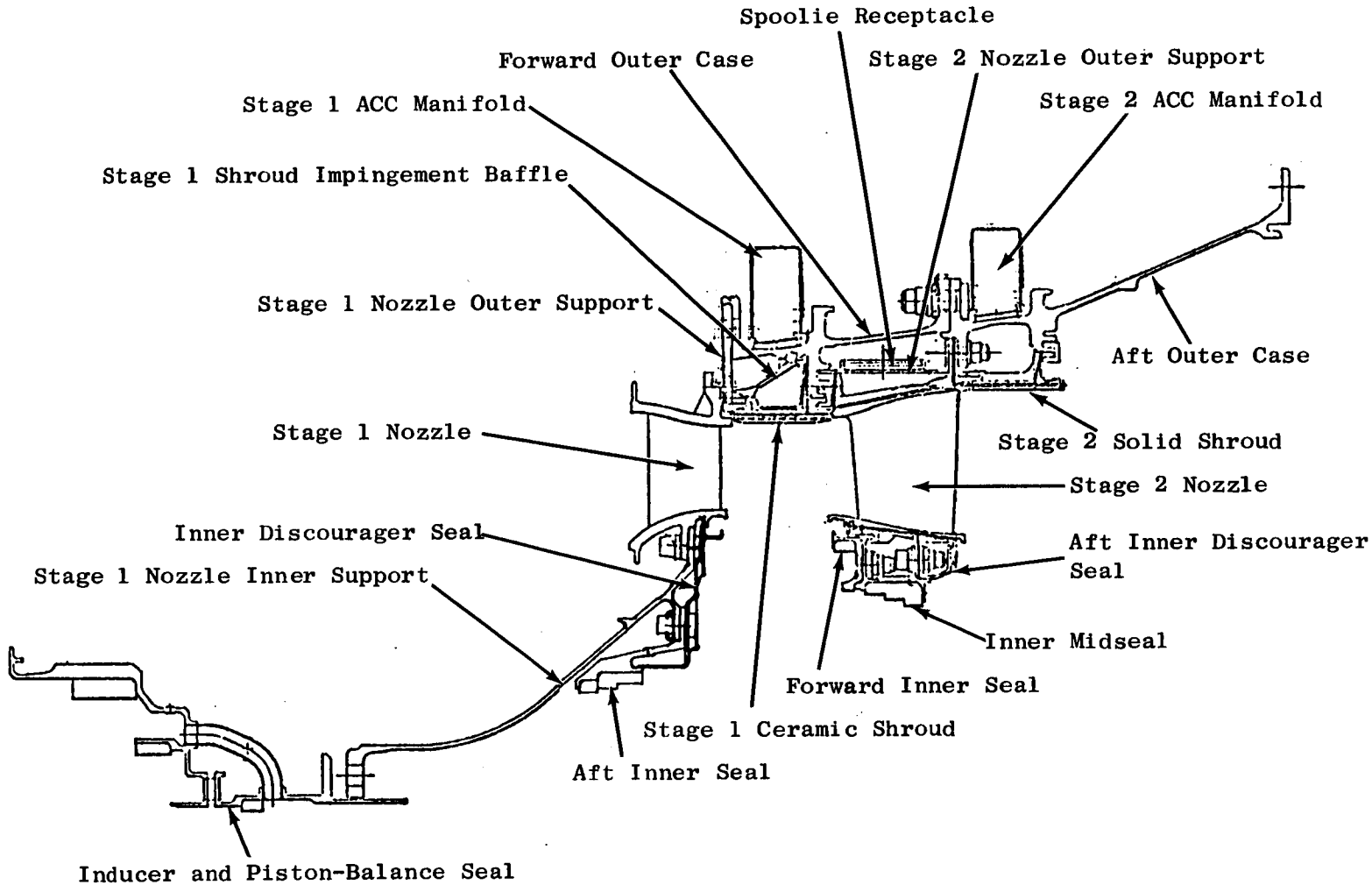

Figure 54. HPT Static Structures.

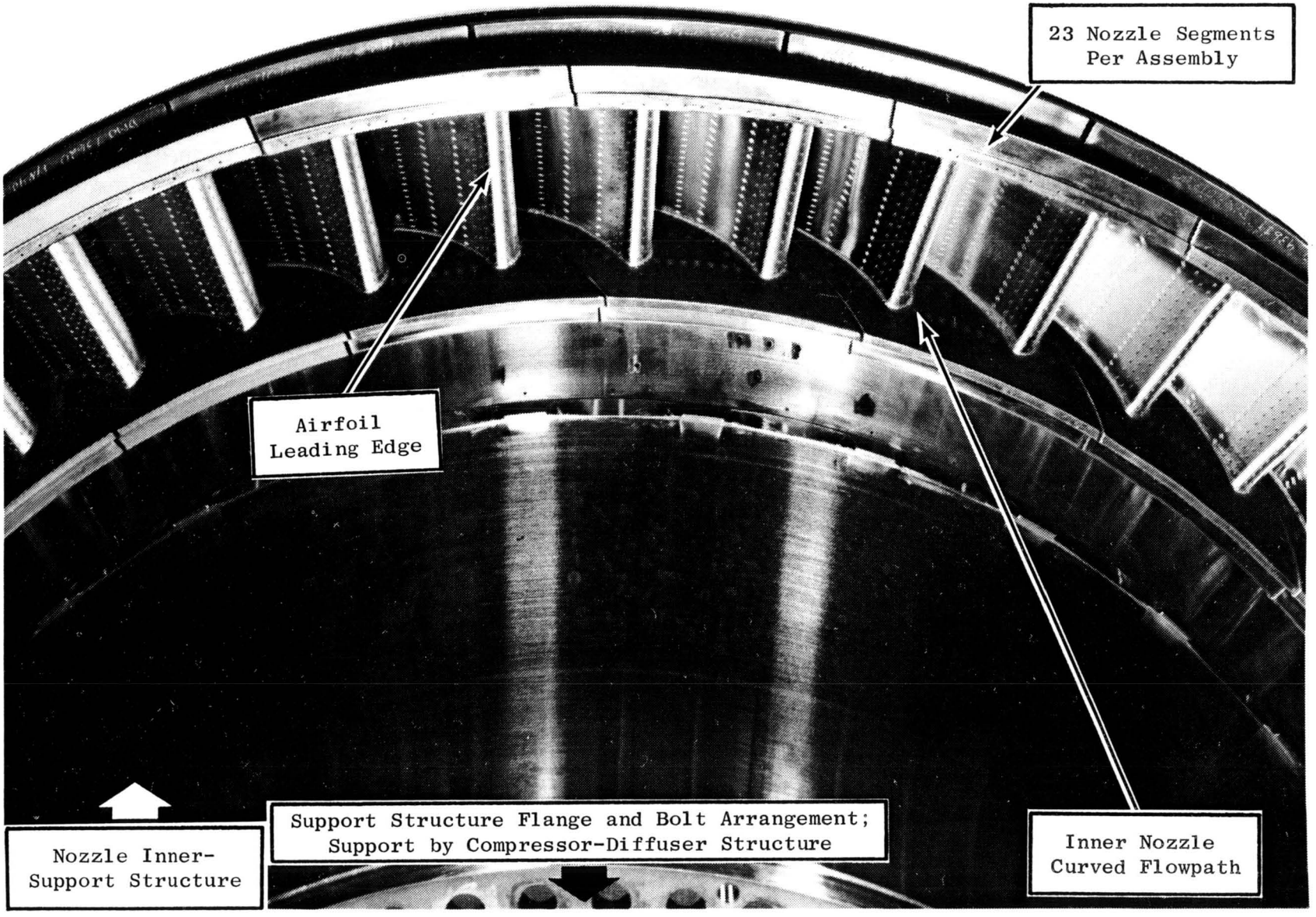

Figure 55. HPT Stage 1 Nozzle Assembly.

Table XXIII. HPT Core Engine Test Instrumentation.

Type of Sensor	Rotor	Stator	Total
Thermocouple	58	116	174
Pressure	3	49	52
Strain Gage	19	--	19
Total	80	165	245

Figure 56 and commonly called the CDN assembly, represents one of the three prime modules designed for improved maintainability in the HPT. Radial grinding was also completed for all static seals in this assembly.

The Stage 2 nozzle and shroud subassembly module is shown in Figure 57. Assembly of this module was completed. All Stage 2 nozzle segments and Stage 2 shroud-segment instrumentation leads are routed through access ports in the casing above the Stage 2 nozzles. The Stage 2 shroud instrumentation leads are routed through the aft portion of the combustor casing. This assembly module has just been completed and is in process of the shroud and seal radial grind operation.

The HPT rotor module is shown in Figure 58. The Stage 1 subassembly was completed, and all instrumentation leads were tacked down and routed through the inner pressure tube. This subassembly has been joined to the Stage 2 rotor subassembly at the interstage seal interface. Instrumentation for this stage has also been tacked down and lead out through the pressure tube. Final tiedown of all rotor instrumentation leads along the inside diameter of the pressure tube is now in process.

Engineering analysis to determine the vibratory scope limits continues. The establishment of these values is based on data to be made available from the hot, high-cycle fatigue (HCF) blade tests and vibratory blade stress distribution mapping.

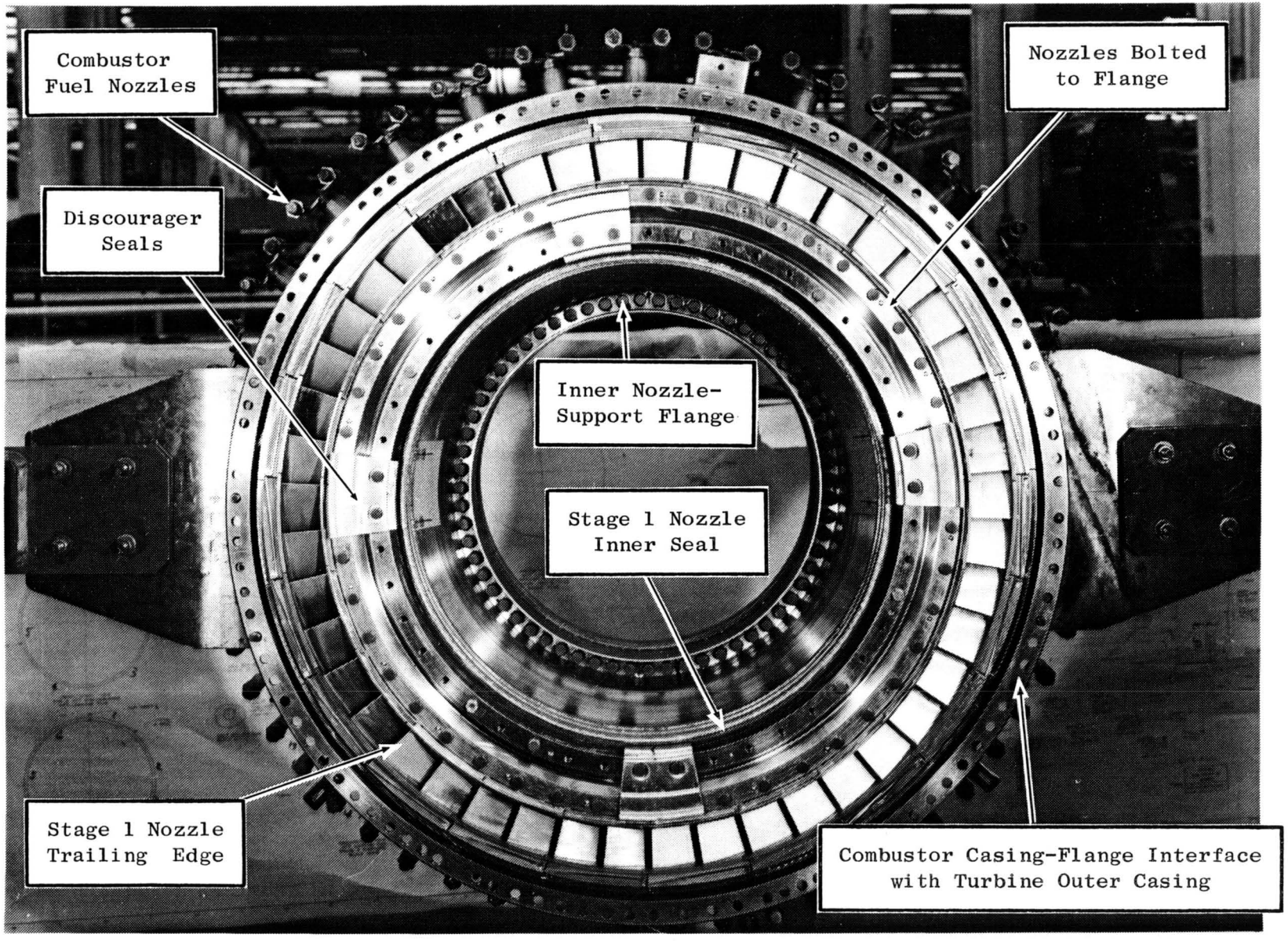

Figure 56. HPT Nozzle and Combustor Module.

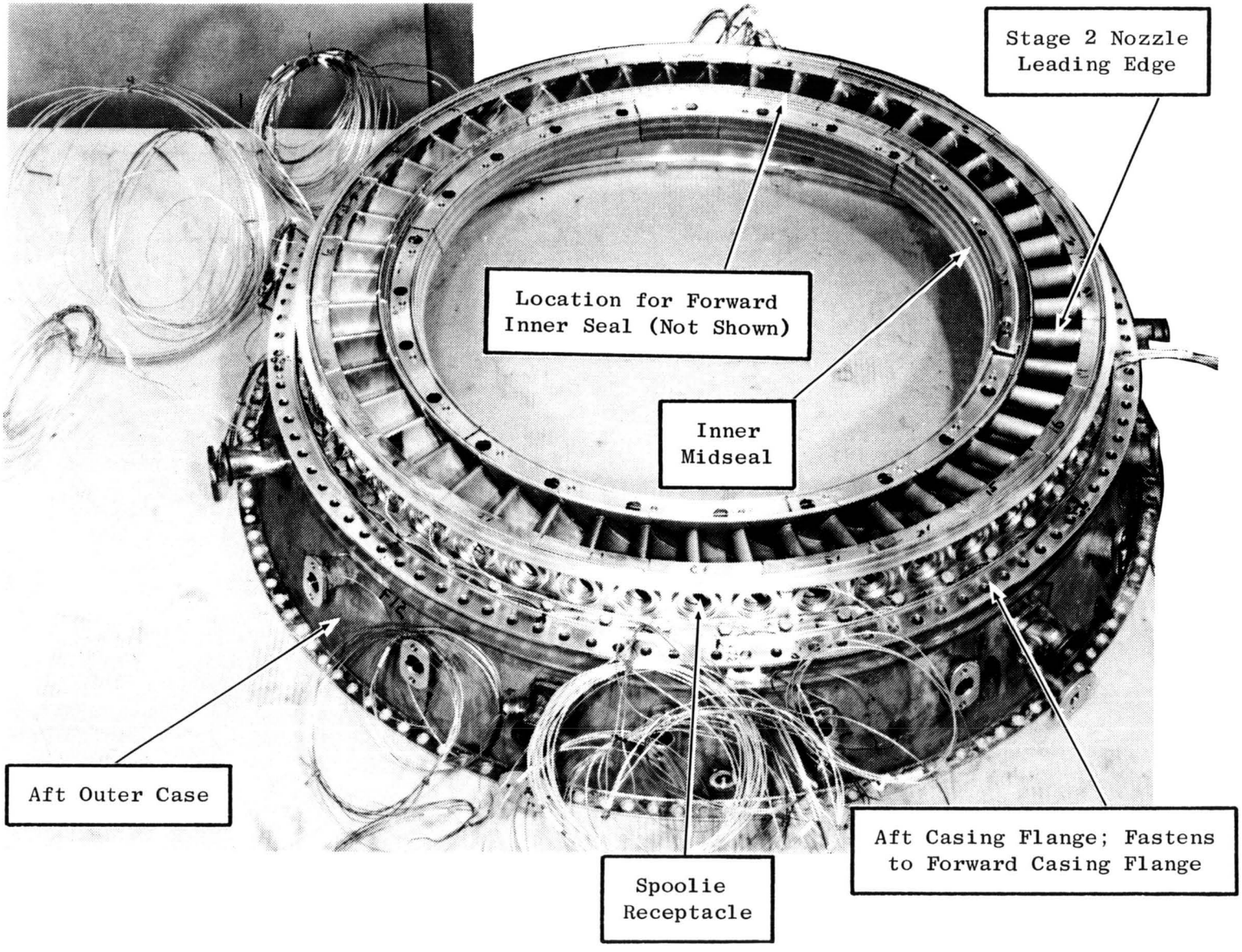

Figure 57. HPT Stage 2 Nozzle and Shroud Module (Partial).

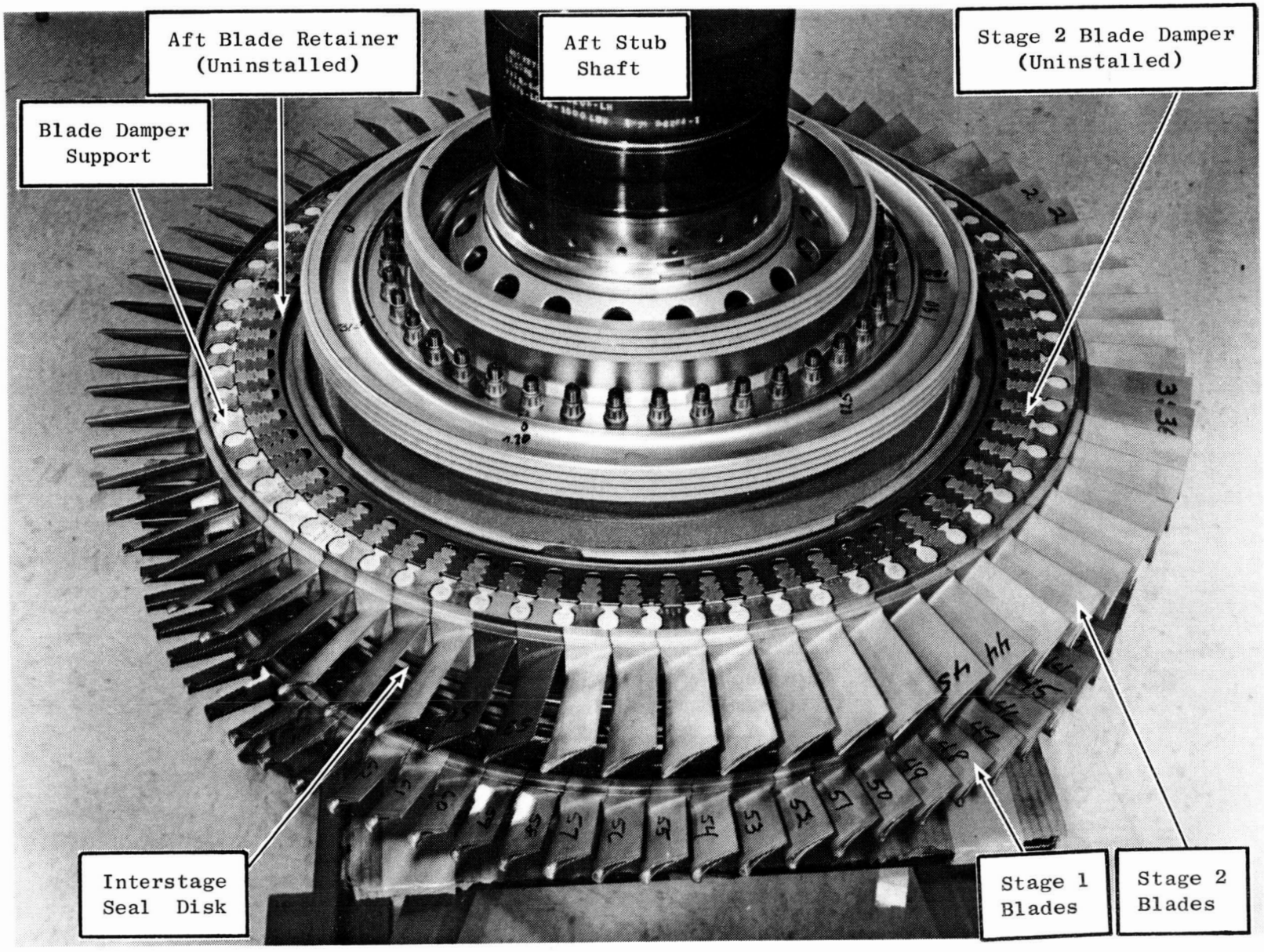

Figure 58. HPT Rotor Assembly.

Work Planned

- Complete analysis and establish blade scope limits for the engine core tests
- Complete rotor balancing
- Review all measured axial and radial assembly clearances
- Continue support of Evaluation during the core engine assembly.

2.4.4 HPT Mechanical Design Testing

Technical Progress

Static tests to determine the natural vibration frequencies for the rotating, cylindrical structures was completed. Components included in the investigations were the HPT forward shaft, forward shaft outer liner, and the inner pressure tube.

Figure 59 is a Campbell diagram comparison between the analysis results and bench tests for the HPT shaft. Very good agreement was found for the N = 4 nodal pattern representing the lowest critical engine speed for this component.

Figures 60 and 61 are Campbell diagrams for the inner tube and forward outer liner, respectively. Both parts in the engine assembly have one end fixed by means of a bolted flange while the other end is only supported radially. However, during a dynamic system mode, the radially supported end may not behave as a fully supported system around the entire circumference. This is due to the nodal displacement behavior comprising outward radial motion as well as inward motion. This type of system therefore behaves as a system with a frequency boundary which is higher than that of a cantilevered end but lower than a radially supported end (pinned).

The vibrational behavior and frequency for the inner tube, based on the static test, results in a safety margin substantially higher than the 115% required for safe engine operation. The dynamic behavior of the forward outer liner at the aft end is similar to that described for the inner tube, and the safety margin is also higher than the requirements.

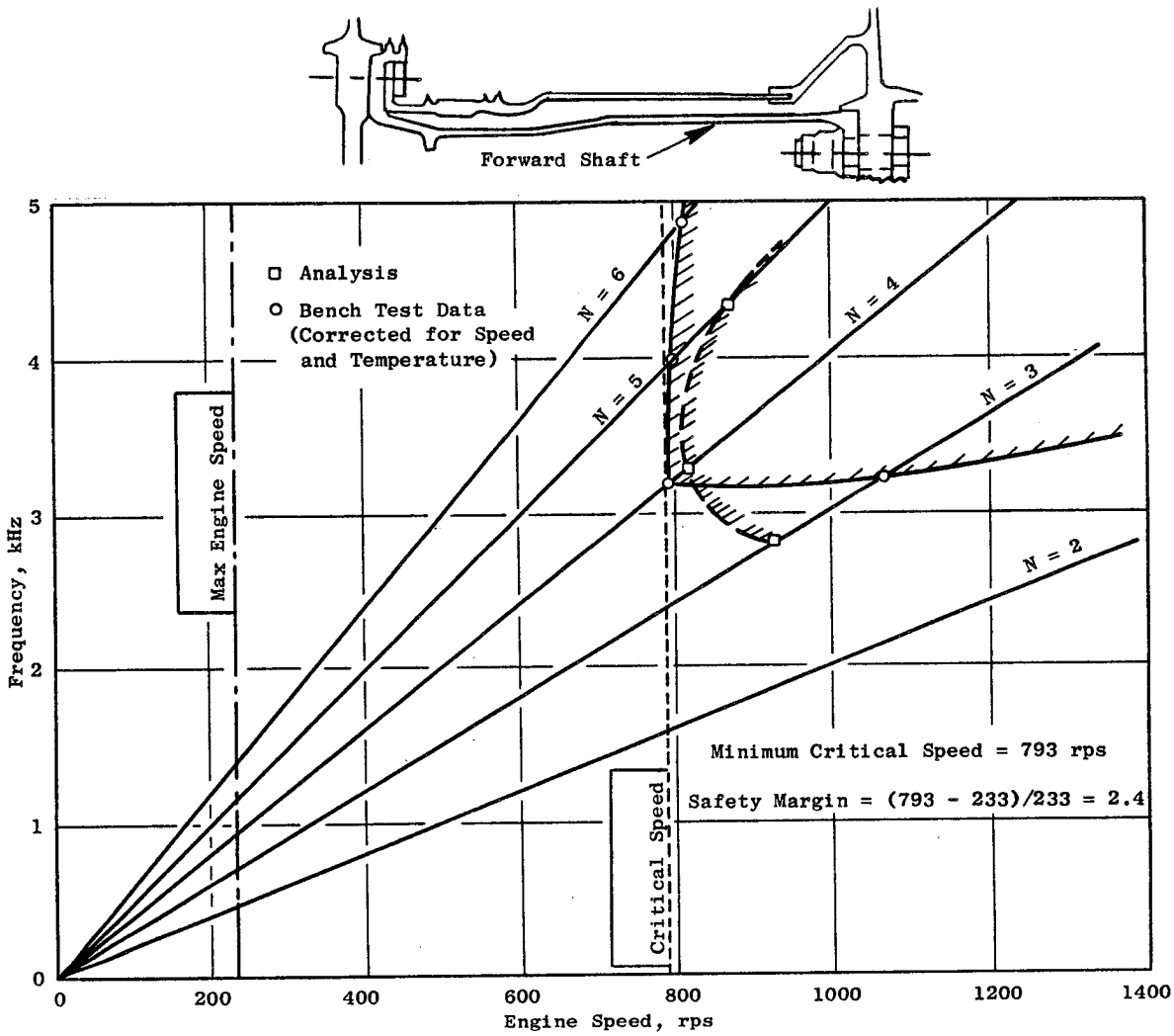

Figure 59. Campbell Diagram for HPT Forward Shaft.

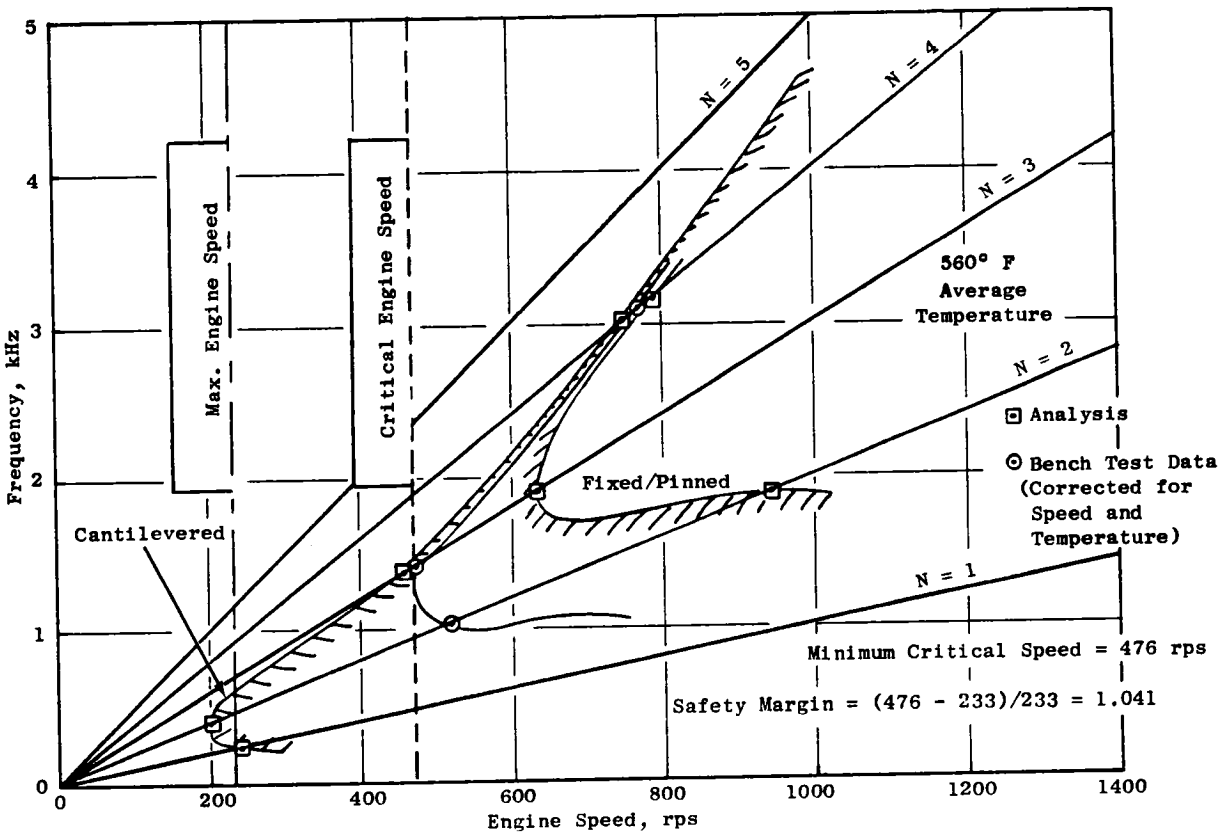

Figure 60. Campbell Diagram for HPT Inner Tube.

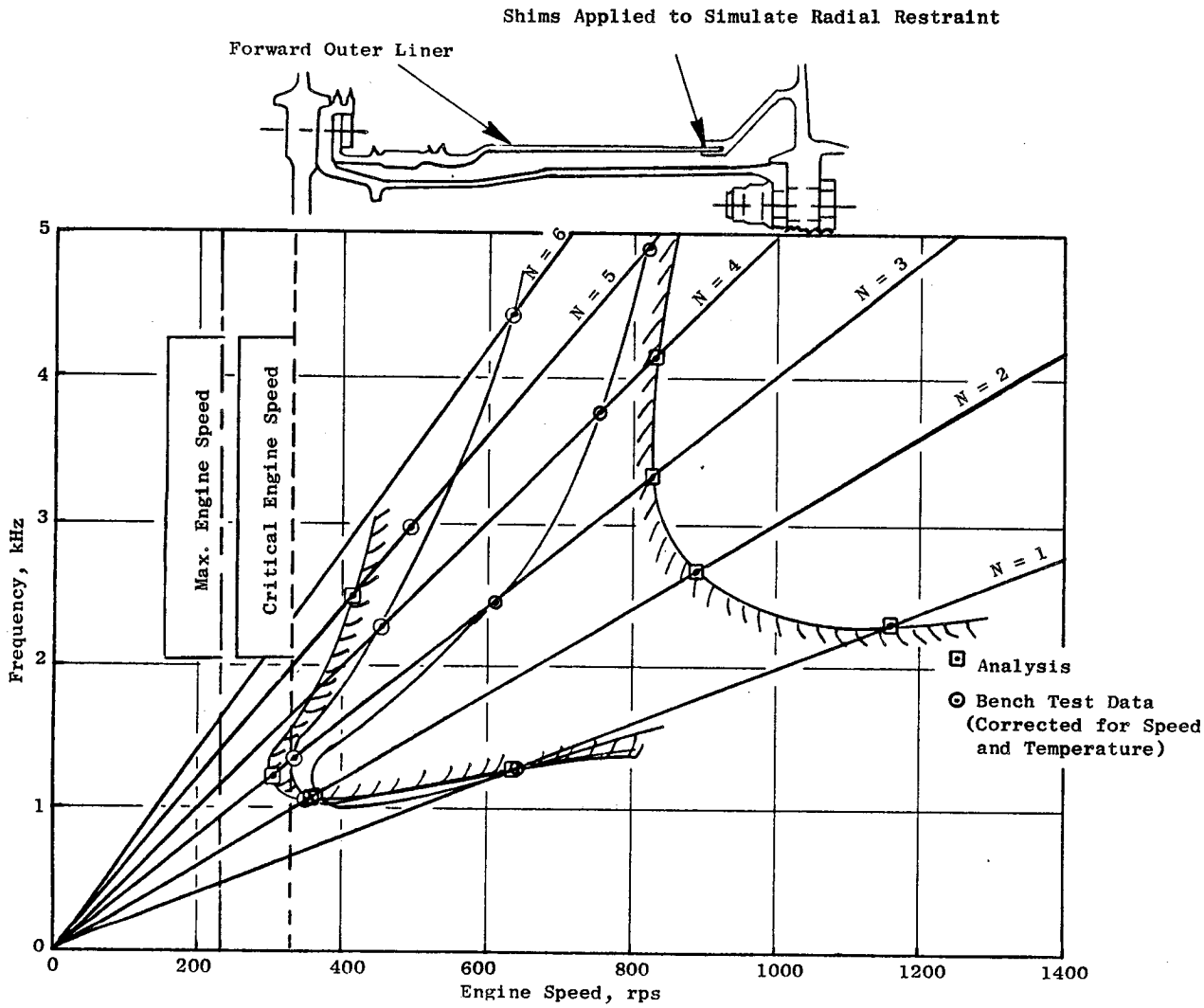

Figure 61. Campbell Diagram for HPT Forward Outer Liner.

required for safe engine operation. The forward outer-liner dynamic behavior at the aft end is similar to that described for the inner tube, and the safety margin is also higher than the requirements.

The Stages 1 and 2 blade vibration frequency characteristics have been examined in a bench test, and the results of the frequency investigations are shown in the Campbell diagrams of Figures 62 and 63. The bench tests were conducted without damper effects because they are believed to have little influence on the blade natural frequency levels.

Figure 62 shows the Stage 1 blade to have some degree of dynamic coupling for the first-axial (1A) and first-torsional (1T) frequency modes near the flight idle and ground idle engine conditions, respectively. The 1A frequency stimulus could be caused by the number of Stage 2 segments (24); the blade platform dampers are expected to moderate vibration response to this condition. Core engine strain gages will be monitored, and active vibratory stress levels will be evaluated throughout the engine operating-speed range.

Figure 63 shows the Stage 2 blade to have potential dynamic coupling for the first-flexural (1F) and 1T vibration modes. The level of vibratory stresses during core engine testing will be monitored and the effects evaluated. GE experience with similar coupling characteristics indicates that the blade dampers will provide adequate damping and result in significant vibratory stress reduction.

Work Planned

- Complete Stages 1 and 2 blade vibratory strain gage mapping tests
- Complete Stages 1 and 2 hot HCF tests
- Complete Stages 1 and 2 blade damping tests

2.4.5 High Pressure Turbine Cooling Development Testing

Technical Progress

During this reporting period, data from the cascade film-effectiveness test was reduced, and a technical report was prepared. A discussion of the results will follow. Final data reduction and report writing are in progress

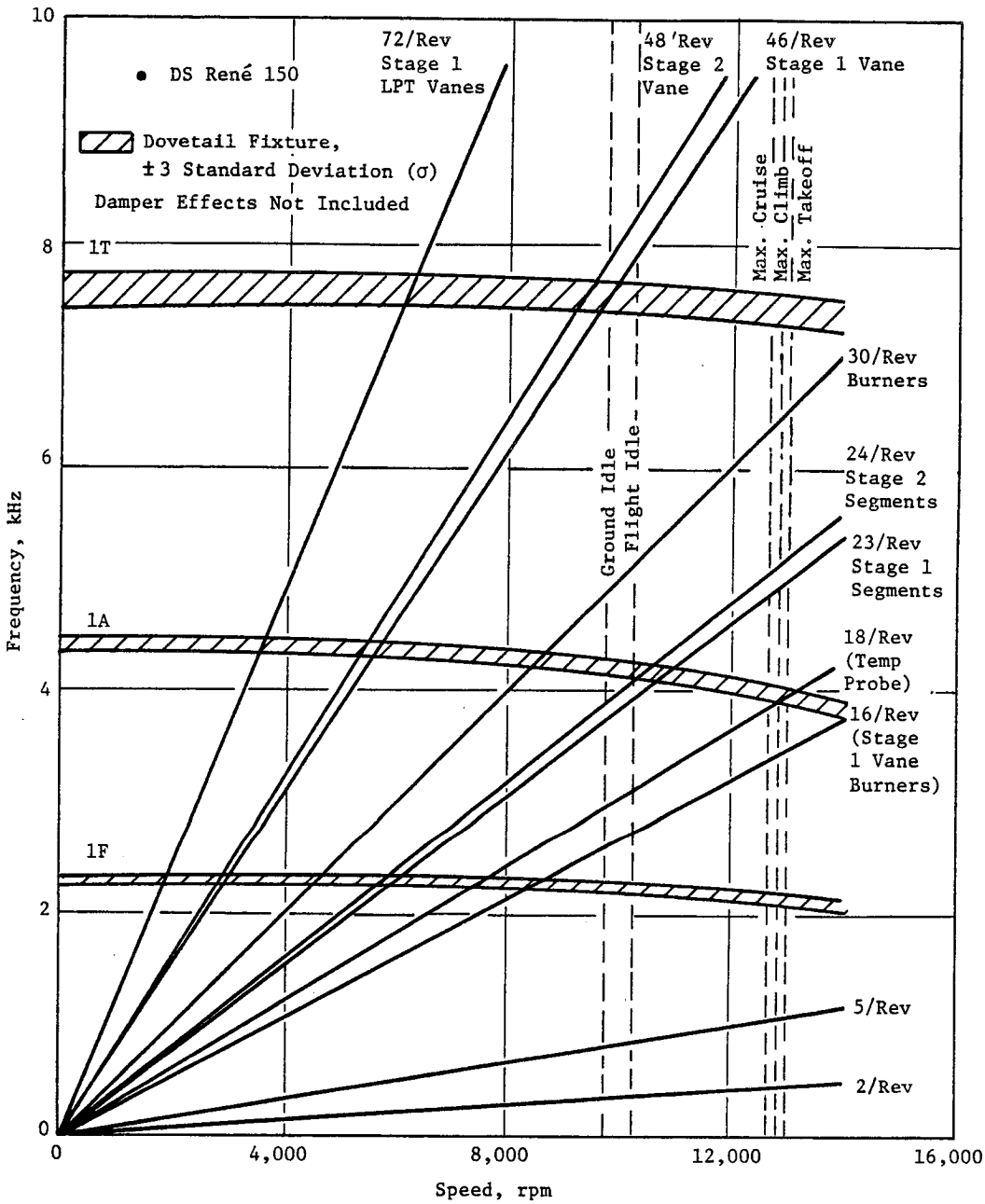

Figure 62. HPT Stage 1 Blade Campbell Diagram.

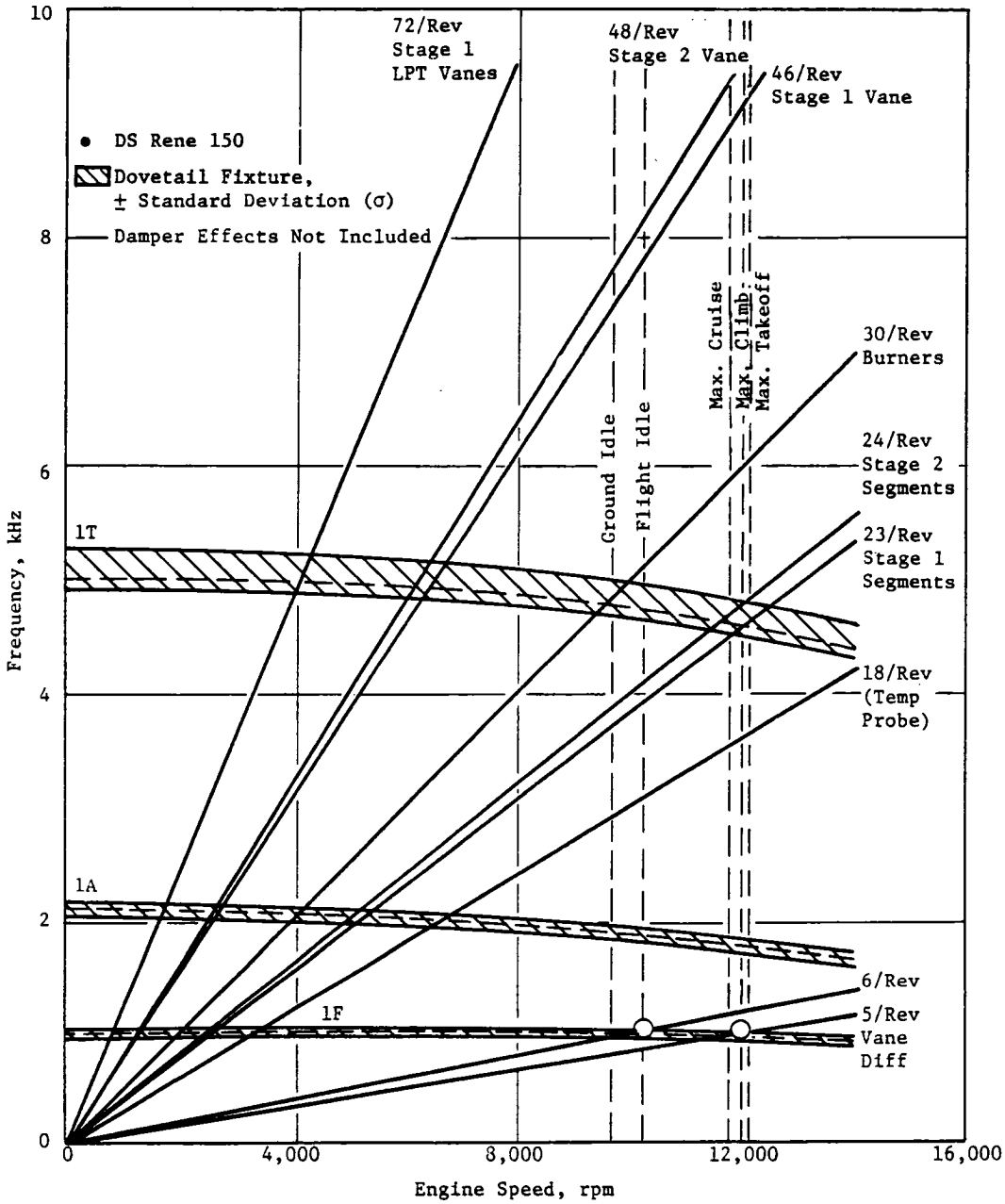

Figure 63. HPT Stage 2 Blade Campbell Diagram.

for both the ACC scoop system and the vane trailing-edge-slot, heat-transfer tests.

As stated above, the film and cooling-effectiveness data obtained from the cascade tests of low-solidity airfoils are presented in a report. The film-cooling configurations were representative of advanced, high-temperature-turbine, cooling designs. The film data represent various configurations of suction-surface shaped and round holes, pressure-surface round holes with compound angles, and pressure-surface round holes with axial orientation in the trailing-edge region. Full-scale models of the E^3 HPT Stage 1 vane with internal impingement inserts were employed. The cooling-effectiveness data include local measurements around the airfoil as well as the trailing-edge slots with boundary-layer restart cavities. Both film and cooling-effectiveness tests were run at a constant mainstream pressure ratio of 1.68, simulated E^3 design temperature ratio, inlet Mach number, and approach Reynolds number. Cooling flow rates varied from 30% to 150% of design values.

The film and cooling-effectiveness tests may be summarized as follows:

1. Suction-side-gill, shaped-hole and round-hole film effectivenesses of the E^3 low-solidity vane generally are higher than those of a conventional vane at similar operating parameters.

2. The suction side of the low-solidity vane, with a double row of round gill film holes, exhibits "blow-off" tendency at blowing parameter (M) greater than about 1.2, but the corresponding shaped-hole configuration did not.

3. For the E^3 low-solidity vane tested, both shaped and round suction-side-gill-hole configurations, a hole spacing of 3.34d shows a faster decay of film effectiveness aft of the vane throat compared to a conventional-design vane with a single row of shaped holes and a hole spacing of 3.61d.

4. Pressure-side-gill and pressure-side, trailing-edge, round-hole film effectiveness on the low-solidity vane is generally higher than that of the conventional-design vane for values of X/M_s of design interest. However, the low-solidity-vane, pressure-side film data show a "blow-off" effect as M goes to values higher than about 0.5.

5. The measured gross cooling effectiveness and local distribution for the E^3 Stage 1 vane are in good agreement with the design calculated values. This confirms that the Stage 1 vane cooling design meets requirements.

6. The E^3 Stage 1 vane has a boundary-layer-restart cavity in the trailing slots. This cavity produces a higher gross cooling effectiveness compared to the downstream section with conventional slots.

Work Planned

- Complete the ACC scoop report
- Complete the vane trailing-edge-slot, heat-transfer report.

2.4.7.1.1 Ceramic Shroud Process

Technical Progress

The previous semiannual reported the thermal cycle results of two ZrO_2-8 wt% Y_2O_3 coated E^3 superpeg shroud castings. These two shrouds underwent 40 furnace cycles to produce delamination. Microstructural examination of the ZrO_2 coated shroud which had shown indications of delamination after furnace cycling has now been completed. Delaminations were evident within the ZrO_2 top coat immediately adjacent to the bond coat. After progressive polishing to remove 0.060 in., examination revealed the continuation of these cracks. This indicates that the cracks were generated during thermal cycling. This also confirms the adequacy of the infrared nondestructive evaluation (NDE) technique for identifying delaminations.

Infrared NDE was conducted on the first lot of 28 Stage 1 HPT ceramic shrouds. The infrared NDE technique consists of heating the shroud to 65° C in a furnace for at least 30 minutes, individually removing the shroud from the furnace and placing it in a fixture, and then taking an infrared photograph of the ceramic-coated shroud surface. An oscilloscope is utilized to reduce operator-induced variability by establishing a controlled intensity for the photograph. The infrared NDE technique detects minor differences in the shroud surface-temperature profile resulting from thermal-conductivity variations. Variations in the shroud surface temperature have been correlated to delaminations at the bond-coat-to-top-coat interface.

The 28 ceramic-coated shrouds of Lot 1, engine quality level, were NDE inspected prior to and after a laboratory-thermal-cycle, quality-control check.

The laboratory thermal cycle consisted of heating the shrouds to 1800° F for 15 minutes in a static air furnace followed by rapid cooling to about 150° F in 3 minutes by an 90-psi air stream. This cycle is done once for each shroud. All shrouds passed the laboratory-thermal-cycle test, NDE, and flow check. Twenty shrouds were selected for core engine testing while two were selected for a 1000-cycle, thermal-shock test. The remaining shrouds will be held in reserve.

The cyclic thermal-shock conditions imposed on the test shrouds are reported in WBS 2.4.7.1.2. Both shrouds successfully completed the 1000 thermal-shock cycles. Posttest NDE analysis did not detect any delamination.

Work Planned

None - posttest inspection and analysis of the 1000-cycle, thermal-shock-test results will be reported in WBS 2.4.7.1.2 along with final lot shroud fabrication.

2.4.7.1.2 Component Test of Ceramic Shrouds

Technical Progress

Two ceramic shrouds of the E^3 design were successfully tested at the GE Thermal Shock Flame Tunnel at Lynn, Massachusetts. The thermal-shock tests were conducted for 1000 cycles. Each test cycle consisted of rapid heating for three minutes followed by a three-minute rapid cooling cycle (i.e., total of six minutes per cycle).

Figure 64 illustrates the test sequence for the six-minute cycle. Ceramic shroud surfaces were heated to an average of 2550° F by a combustor flame directed normal to the ceramic surface. The measured temperature at the ceramic surface rose to 2500° F within one minute. The temperature rise on the metallic backing material was more gradual and reached the desired 1450° F temperature at the end of the heating cycle. Impingement cooling was used on the shroud metallic backing, similar to the method to be used for cooling the ceramic shrouds in the E^3.

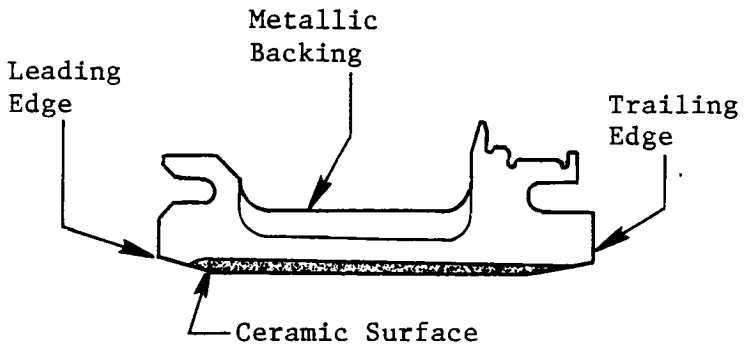

Note: After 3 Minutes of Cooling,
Shroud Temperature is 400 ° F

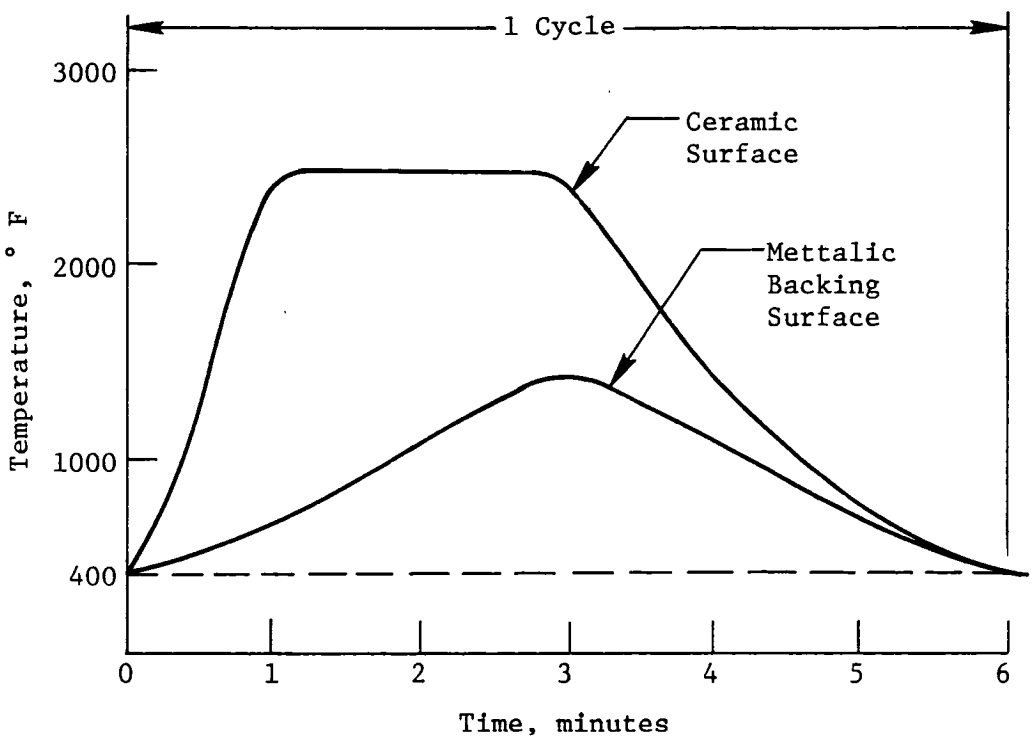

Figure 64. Ceramic Shroud, Thermal-Cycle Test.

Figure 65 shows a shroud being subjected to high-temperature gas during the heating cycle. Shop air (approximately 70° F) was directed normal to the ceramic surface during the cooling-cycle sequence while the backing structure was continuously cooled using shop air.

Visual examinations of the shrouds after completion of the test showed them to be in extremely good condition. The ceramic layer was found to be intact with minimal loss of coating. Figure 66 shows the condition of the ceramic shrouds before and after completion of the 1000 cycle-test.

Planned posttest evaluation of the shrouds includes examination of infra-red-signature characteristics for comparison with those prior to test. One shroud will also be inspected by cut-up and macroanalysis of the cross-sectional layer between the ceramic and metallic structure interface.

Completion of this successful test further substantiates the E^3 ceramic shroud design concept and provides an additional experience base for ceramic shrouds as a concept for reducing cooling flow to this type of turbine component.

Work Planned

- Complete metallurgical evaluation of the ceramic shrouds after the successful completion of the flame tunnel test
- Continue engineering coordination with the lab in the evaluation of these shrouds.

2.4.7.2.1 Thermal-Barrier Processes

Previous reports have described the progress of earlier tasks that led to the selection of a coating system, development of processes for applying the coating to engine components, qualification of the coating through mechanical-property tests, laboratory and component fatigue tests and a cascade rig test, application of the coating on HPT components for factory engine testing, and preliminary posttest evaluation results from the engine-tested coatings. This report briefly reviews the previously reported data and presents the remainder of the data from posttest evaluations of the engine-tested components.

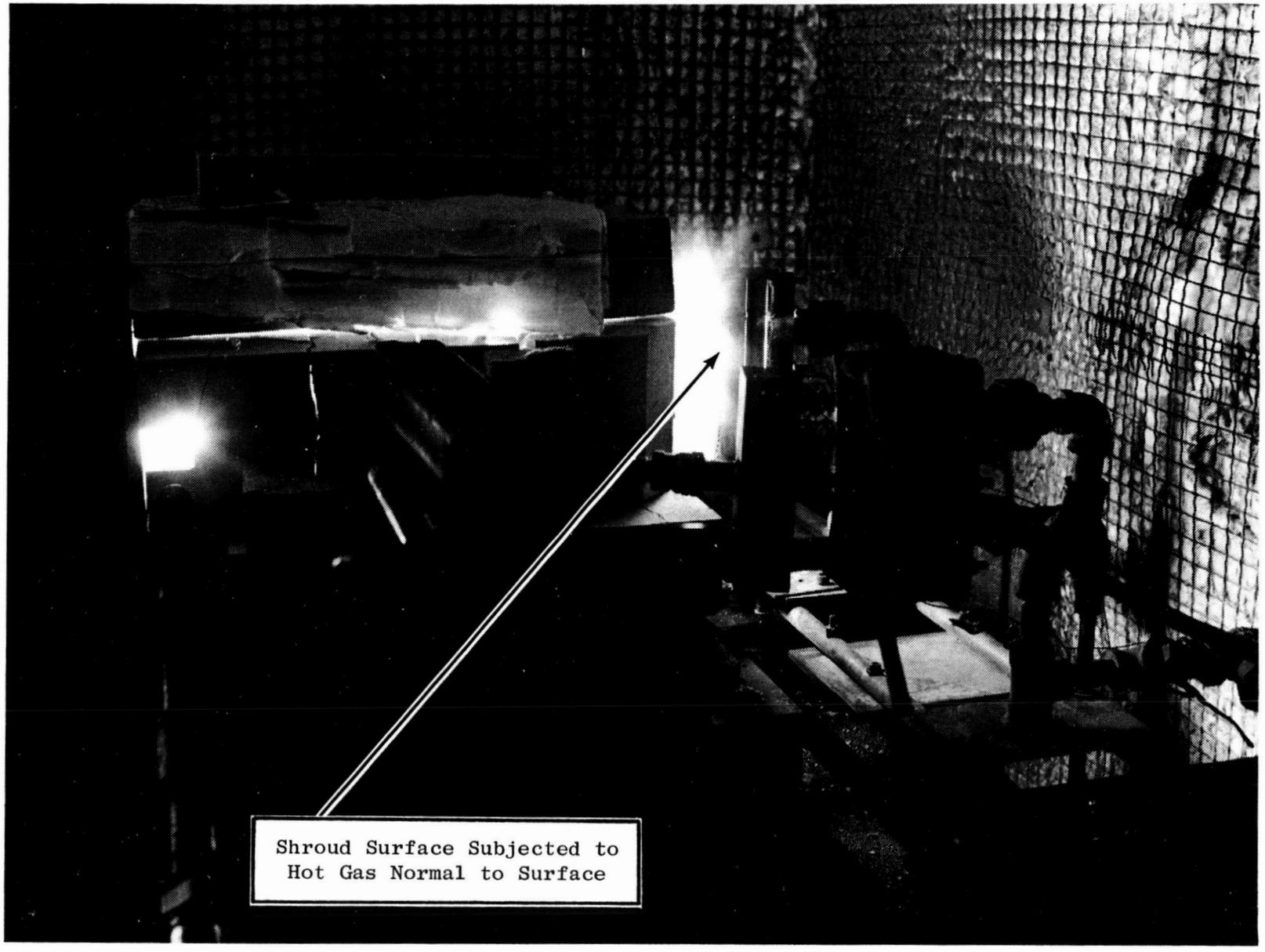

Figure 65. HPT Ceramic Shroud in Thermal-Shock Test Facility.

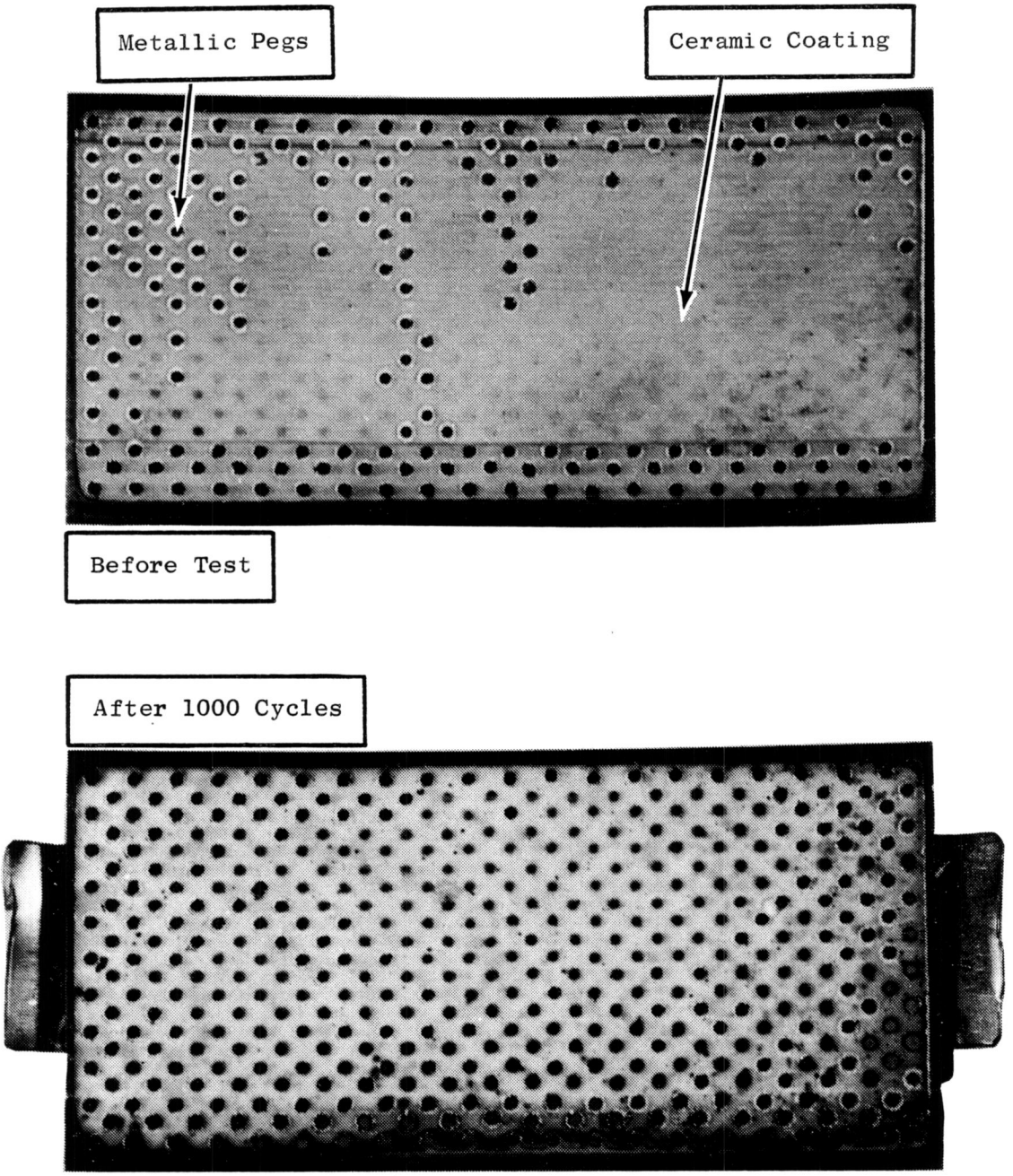

Figure 66. HPT Ceramic Shroud after 1000 Cycles.

Engine Test

A number of TBC HPT components were run for 1000 "C" cycles in CF6-50 factory engine 455-508/21. The HPT components tested were Stage 1 vanes, Stage 2 vanes, and Stage 2 blades. Four Stage 1 vane pairs and seven Stage 2 vane pairs were coated in selected areas of the airfoils and bands with a TBC consisting of a NiCrAlY bond coat layer and a ZrO_2-20%Y_2O_3 top coat. Both coating layers were applid to vanes by manual spraying in air. The Codep environmental coating was removed, from the areas which were coated with TBC, to enhance adherence of the conventionally plasma-sprayed bond coat to the component. The areas which were coated on the vanes have been reviewed in prior reports. Ten Stage 2 blades were coated with NiCrAlY bond coat and ZrO_2-Y_2O_3 top coat. The NiCrAlY bond coat was applied to the blades over the Codep environmental coating in a low-pressure, inert-gas environment (vacuum plasma spraying, VPS) using automated manipulation. Five of the blades had a top coat of ZrO_2-20%Y_2O_3, and the other five had a top coat of ZrO_2-8%Y_2O_3. Three of the blades with ZrO_2-8%Y_2O_3 were coated at GE Corporate Research and Development Center (CRD) under NASA Contract NAS3-21727; all other parts were coated at GE Aircraft Engine Business Group (AEBG). There were several differences between the material and coating-process variables of the coatings applied at GE-AEBG and GE-CRD.

Some minor pretest coating damage (small chips from the edge of the coating at the tip on the pressure side of the blades) occurred during tip grinding of the blades in engine assembly. A borescope examination of the blades after 27 hours of engine check-out revealed that some of the ceramic layer was missing in localized regions on the leading edge near the tips of the TBC blades. Three additional borescope inspections during the test showed the damage still to be limited to the area from about 75% span to the tip in the leading-edge region, but the damage appeared to progress slightly during the course of the testing. Difficulties were encountered in inspecting the vanes during the test.

Posttest Analysis - Blades

Visual examination of the engine-tested blades showed the TBC to be in excellent conditon on the pressure side of the airfoils and over the greater

part of the suction side of the airfoils, as shown in Figures 67 and 68. Some localized coating loss occurred from the leading edge above midspan and also from the forward part of the suction side of the airfoils adjacent to the leading edge. All of the blades had a similar pattern of coating damage confined to the leading edge on the suction side although the extent of damage varied from blade to blade. In small areas of the leading edge of the blade tip, ranging in size from 0.03 in^2 to 0.16 in^2 and averaging 0.1 in^2, the entire thickness of the ceramic layer was missing. In other areas of the forward part on the suction side, the damage was characterized by a roughened coating surface, the presence of pock marks and small craters, and isolated loss of ceramic coating. In these latter areas, a thin layer of the ceramic coating was still present. A tabulation listing the areas of the two extents of damage for each blade is given in Table XXIV. The damage appeared to be the result of impact and erosion caused by particulate impingement. Blades without a TBC (Codep only) also showed signs of particulate impingement at the leading edge on the suction side. This area appeared rougher than the rest of the airfoil and showed a greenish, foreign material adhered to the surface at the leading edge. Analysis (EDAX) showed the greenish deposits to be mostly Ni-Al with the amount of aluminum varying from 5 to 40 percent. Other minor elements detected were Co, Fe, Cr, and Ca. Although the exact source of the material in the observed deposits is not known because of the many possible sources of Ni and Al in the engine, it is known that some nickel-aluminum material was lost from the Stage 1 shrouds during the engine test and possibly was the particulate matter that damaged the TBC.

Microstructural examination of three blades (one with each type of ceramic layer) at 40, 70, and 90% span and in the platform region showed the TBC on all three blades to be in excellent condition in all areas except the leading edge on the suction side where the ceramic layer had been damaged. Figure 69 shows optical photomicrographs of one of the TBC blade cross sections at the three span heights and at the platform. Photomicrographs show the blade material (René 80) with Codep coating followed by the NiCrAlY bond coat and the ZrO_2-20%Y_2O_3 ceramic top coat. The bond coat was intimately bonded to the Codep layer. The microstructure, porosity, and thickness uniformity were typical of VPS applied bond coats on Blades 38 and 41, but the structure of the coating

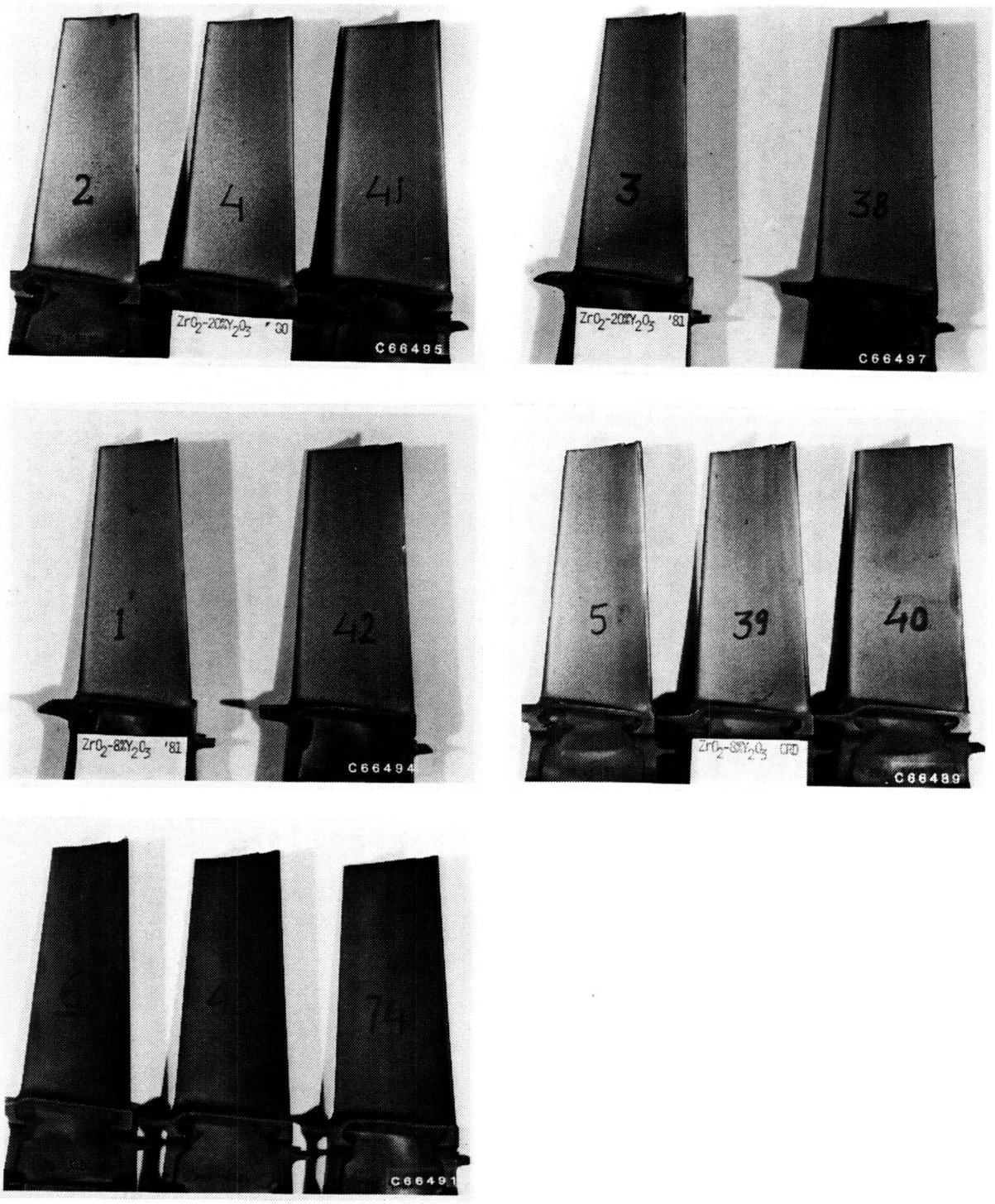

Figure 67. CF6-50 Stage 2 HPT Blades after 1000 Cycles With and Without TBC, Pressure Side.

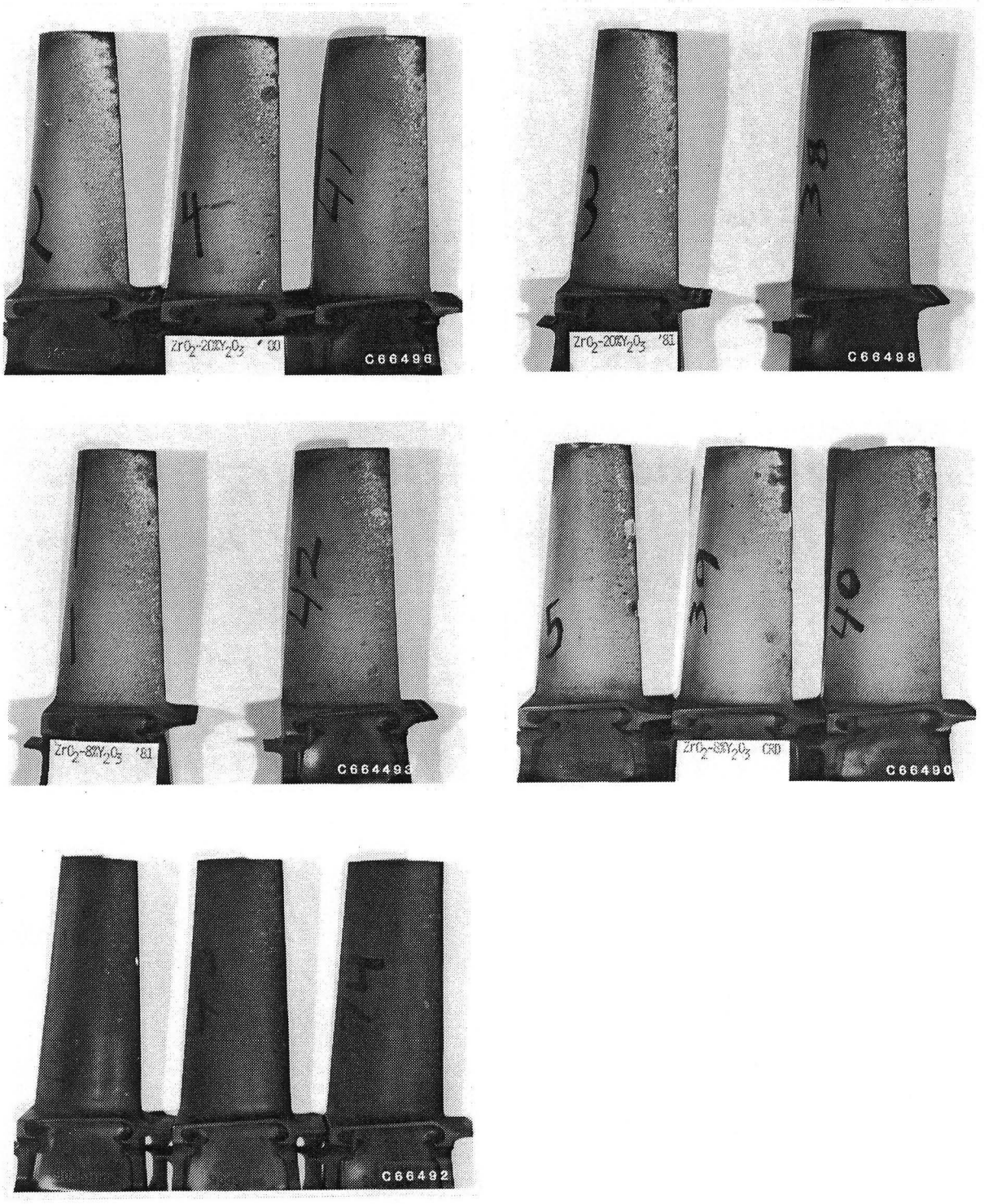

Figure 68. CF6-50 Stage 2 HPT Blades after 1000 Cycles With and Without TBC, Suction Side.

Table XXIV. Amount of Damage to TBC Blades in 1000-Cycle Test.

Blade No.	Top Coat Composition	Area of Damage, $in.^2$		
		Top Coat Missing	Some Top Coat Remaining	Total
2	ZrO_2-20%Y_2O_3	0.06	0.11	0.17
3	ZrO_2-20%Y_2O_3	0.09	0.20	0.29
4	ZrO_2-20%Y_2O_3	0.08	0.02	0.10
38	ZrO_2-20%Y_2O_3	0.14	0.13	0.27
41	ZrO_2-20%Y_2O_3	0.10	0.05	0.15
1	ZrO_2-8%Y_2O_3	0.09	0.08	0.17
42	ZrO_2-8%Y_2O_3	0.12	0.14	0.26
5	ZrO_2-8%Y_2O_3 (NAS3-21727)	0.03	0.04	0.07
39	ZrO_2-8%Y_2O_3 (NAS3-21727)	0.16	0.06	0.22
40	ZrO_2-8%Y_2O_3 (NAS3-21727)	0.04	0	0.04

Note: Total coated area = 14.6 $in.^2$

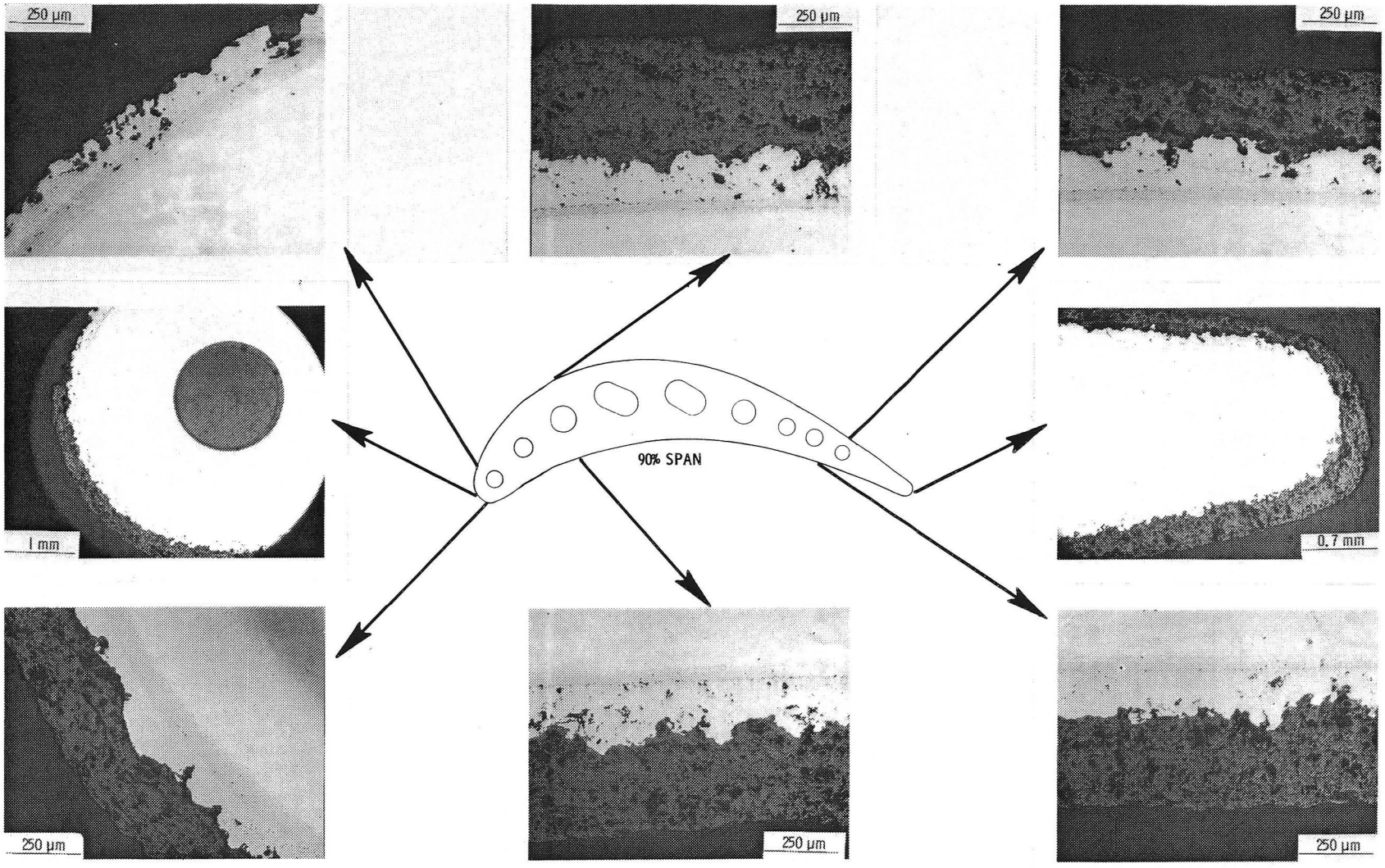

Figure 69. Photomicrographs of Blade with TBC after 1000 Cycles.

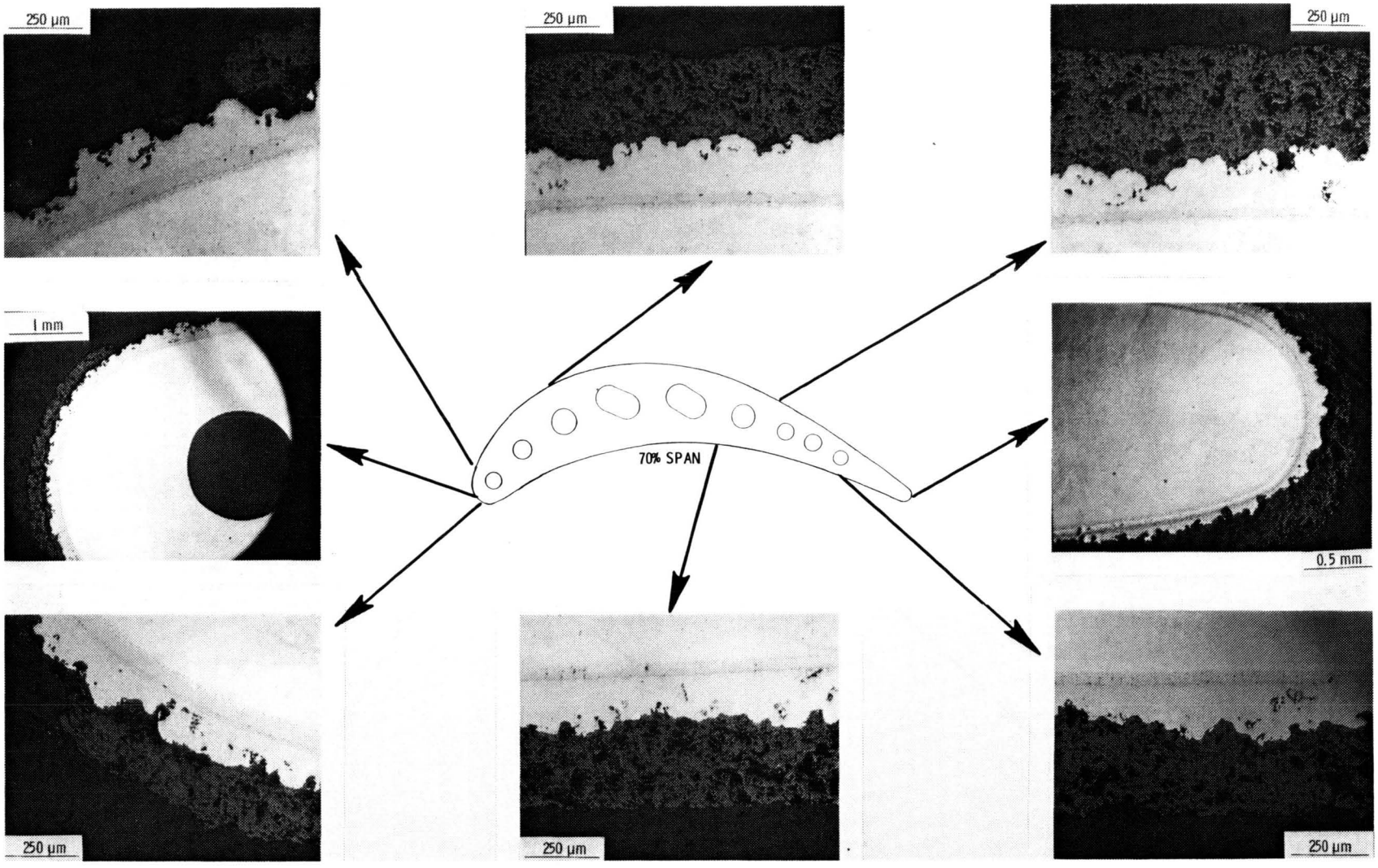

Figure 69. Photomicrographs of Blade with TBC after 1000 Cycles (Continued).

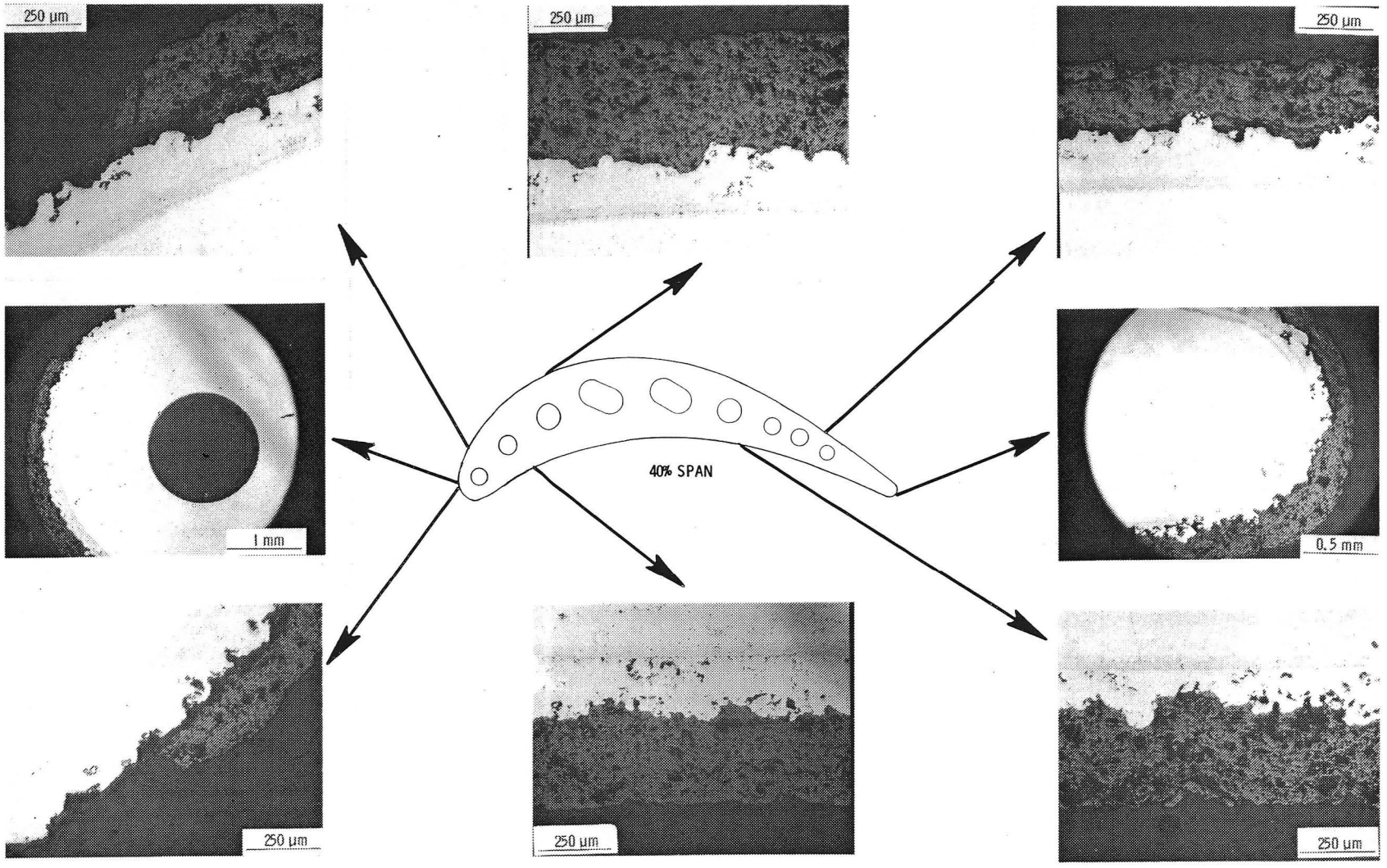

Figure 69. Photomicrographs of Blade with TBC after 1000 Cycles (Continued).

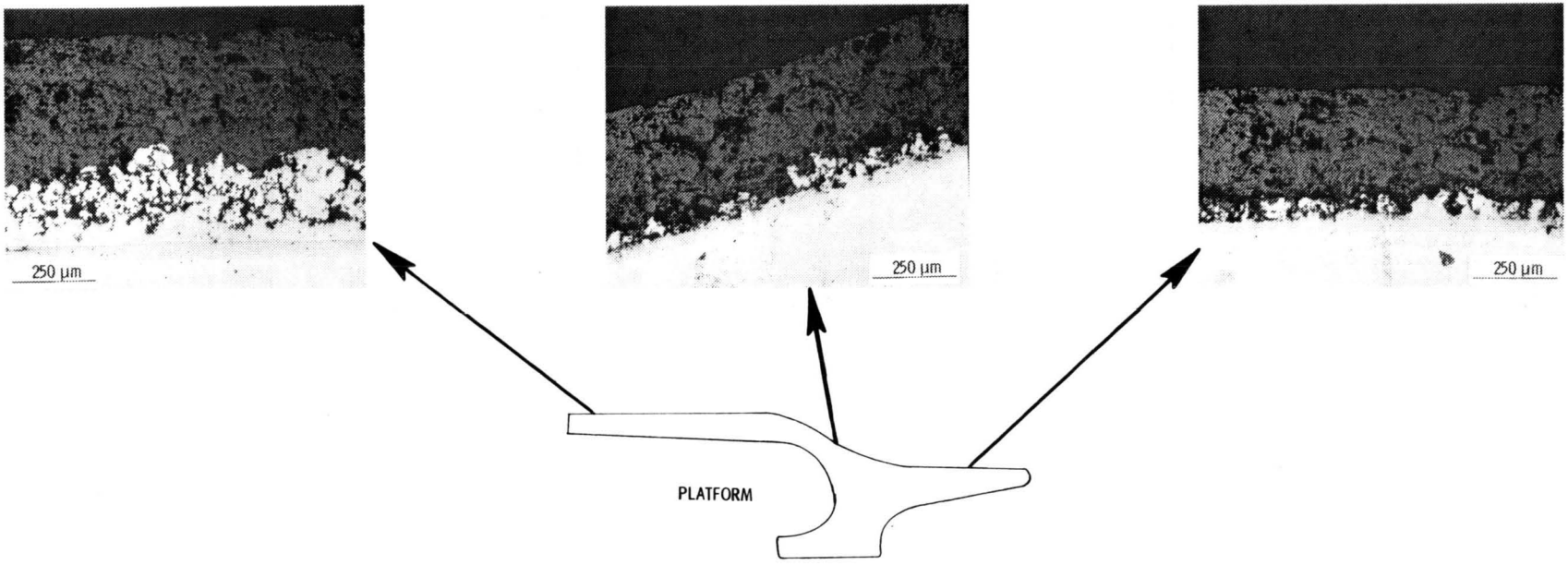

Figure 69. Photomicrographs of Blade with TBC after 1000 Cycles (Concluded).

on Blade 42 was unusually porous and nonuniform for low-pressure-plasma-sprayed bond coats. There was no loss or separation of the bond coat from the airfoil surface, including areas where the ceramic layer was damaged. Very little oxidation of the bond coat was observed on any of the blades. The ceramic layer on all three blades also appeared to be in excellent condition over most of the airfoil surface with the exception of the leading edge on the suction side where impact damage had occurred. The ceramic layer was adherent to the bond coat and showed no evidence of cracking or separation; microstructure was typical of conventionally plasma-sprayed ceramic coatings. Overall, the thermal-barrier coatings on all three blades appeared in sound condition microstructurally.

Electron microprobe analysis was performed at the 80% span to determine interaction and interdiffusion between the TBC and the substrate. X-ray density maps of Ni, Cr, Al, Zr, and Y showed that no interaction or extensive interdiffusion occurred between the ceramic layer and the metallic bond-coat layer. A thin scale (4 to 5 μm) of Al_2O_3 was present at the top-coat/bond-coat interface, which is normal, but there was no further oxidation of the bond coat. Interdiffusion between the bond coat and Codep layer, and the Codep layer and the René 80 substrate, was minimal. Bond-coat elements Ni, Cr, and Al were uniformly distributed, and no depletion of Al was observed.

X-ray diffraction analysis on the ceramic layer of the three blades showed the ZrO_2-20%Y_2O_3 coating to be mostly cubic phase with a small percentage of monoclinic phase; the ZrO_2-8%Y_2O_3 coating consisted of a mixture of cubic/tetragonal phases with a small percentage of the monoclinic phase. Before test, the ZrO_2-20%Y_2O_3 coating is essentially all cubic, and the ZrO_2-8%Y_2O_3 coating is mostly cubic with small amounts of tetragonal and monoclinic phases. The presence of a small amount of the monoclinic phase in the ZrO_2-20%Y_2O_3 coating after the engine test indicates that some phase transformation had taken place. This is consistent with observations from the previous engine test and laboratory cyclic thermal-exposure testing. There was an increase in the amount of tetragonal phase in the ZrO_2-8%Y_2O_3 during the engine test; this is also consistent with previous observations. The surface roughness of the engine-tested TBC blades was similar to that of untested blades except on leading edges where impact damage had occurred.

Posttest Analysis - Vanes

Figure 70 shows a closeup view of one of the engine-tested, TBC, Stage 2 vanes. The TBC was damaged fairly extensively on the outer one-third to two-thirds of the airfoil leading edges. Some pretest damage to the TBC on the leading edges (pitch line) of the airfoils had occurred during shroud grinding, and this may have contributed to the extent of damage observed after the test. Erosion of the TBC was rather severe at the forward edge of the outer bands just aft of the airfoil leading edge; local penetration of the TBC had occurred as indicated by the oxidized vane surface in that area. The TBC was in good condition on the trailing edges of the airfoils and on the aft edges of the inner and outer bands. Minor loss near the trailing edge on the suction side of some of the airfoils had taken place during the engine test. The TBC on the pressure side appeared to be in good condition, generally, although some thinning of the coating had occurred near the outer band.

Microstructural examination of one of the engine-tested Stage 2 vanes (paired), sectioned at 15, 50, and 95% span and in the outer and inner band regions, showed that the Codep layer had been removed successfully by grit blasting in areas where the bond coat and ceramic top coat were applied by conventional plasma spraying. Figures 71 and 72 are optical photomicrographs of a TBC airfoil at 15 and 95% span cross sections. The TBS was severely damaged at 95% span near the outer band; the ceramic layer had spalled, and local penetration and oxidation had taken place at the leading edge (0.005-in. maximum penetration of René 80 in localized region about 0.040 in. long). The TBC was in better condition at the trailing edge, but thinning of the ceramic layer was observed. The bond coat, wherever remaining on the airfoil surface, had provided adequate oxidation protection to the underlying substrate. The TBC was in much better condition at the 15% span although thinning of the ceramic layer was observed on the suction as well as the pressure side of the airfoil. The bond coat and top coat were not nearly as uniform in thickness on the Stage 2 vanes as they were on the blades. This is due to the difficulty in manually coating a complex shape such as a Stage 2 vane. The four Stage 1 vane pairs remained in the engine for additional testing, accumulating a total of 1230 "C" cycles. The coating generally was in good condition on the suction side of the airfoils, as shown in Figure 73. There were three very small,

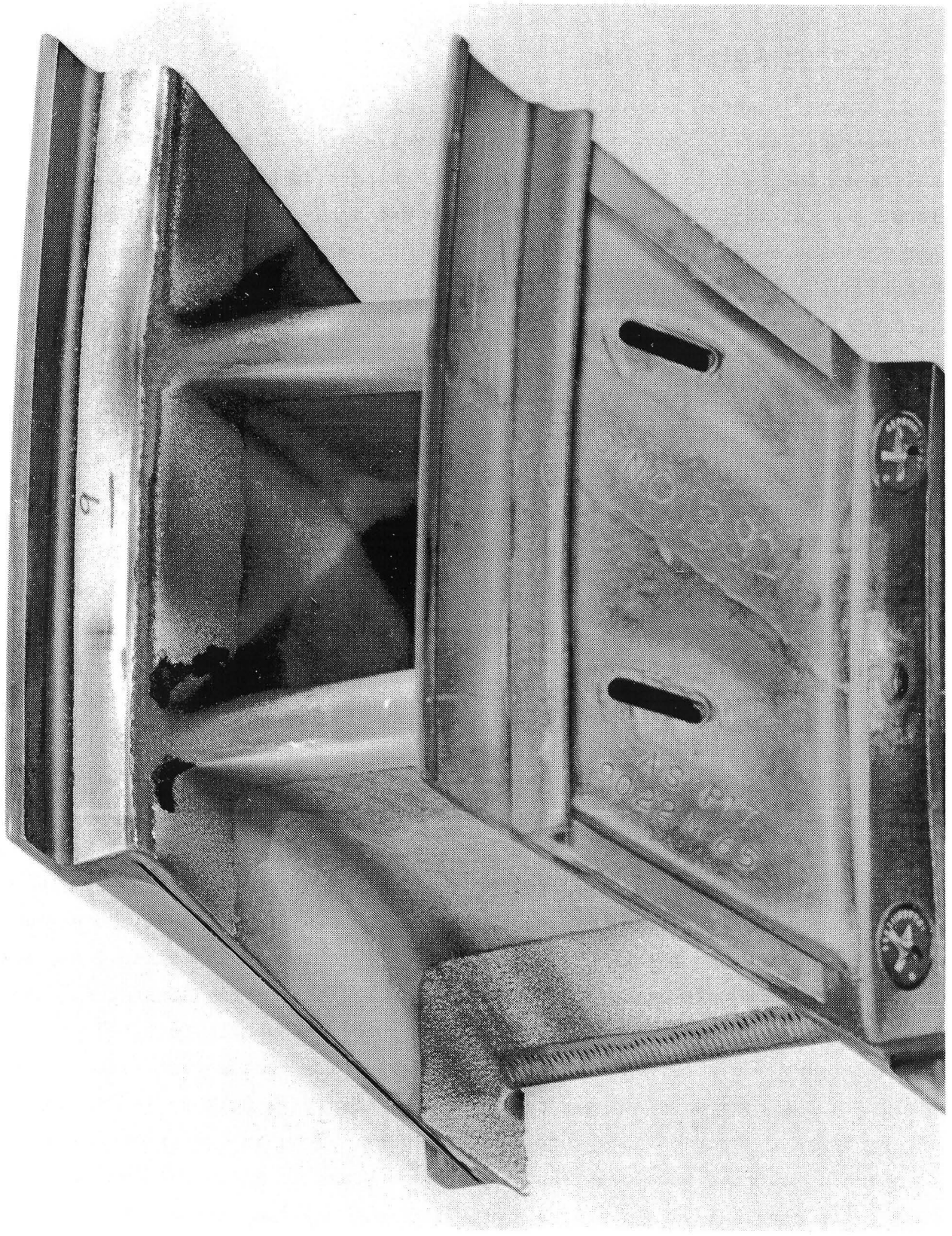

Figure 70. TBC CF6-50 Stage 2 Vane after 1000 Cycles.

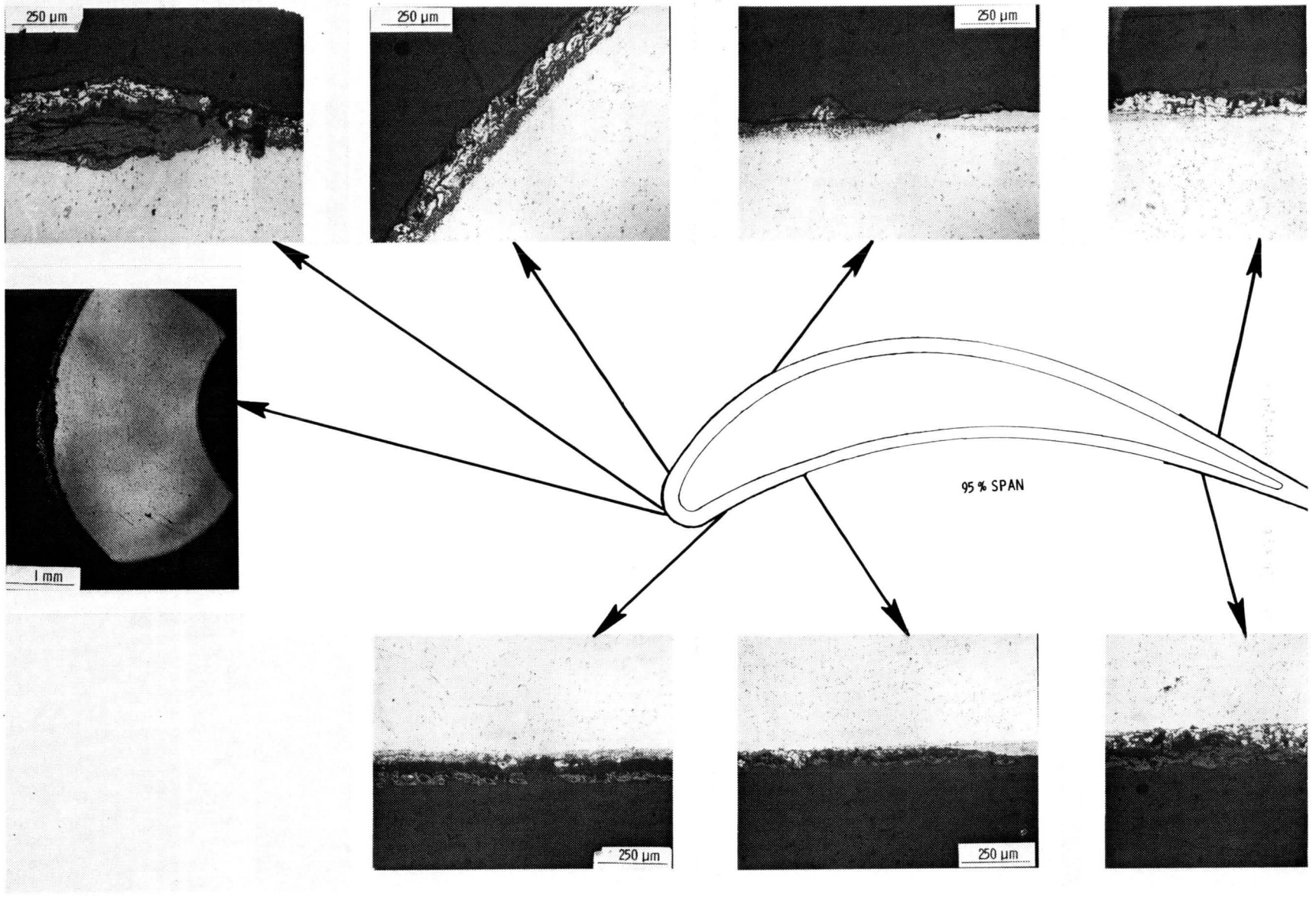

Figure 71. Photomicrographs of Stage 2 Vane with TBC after 1000 Cycles, 95% Span.

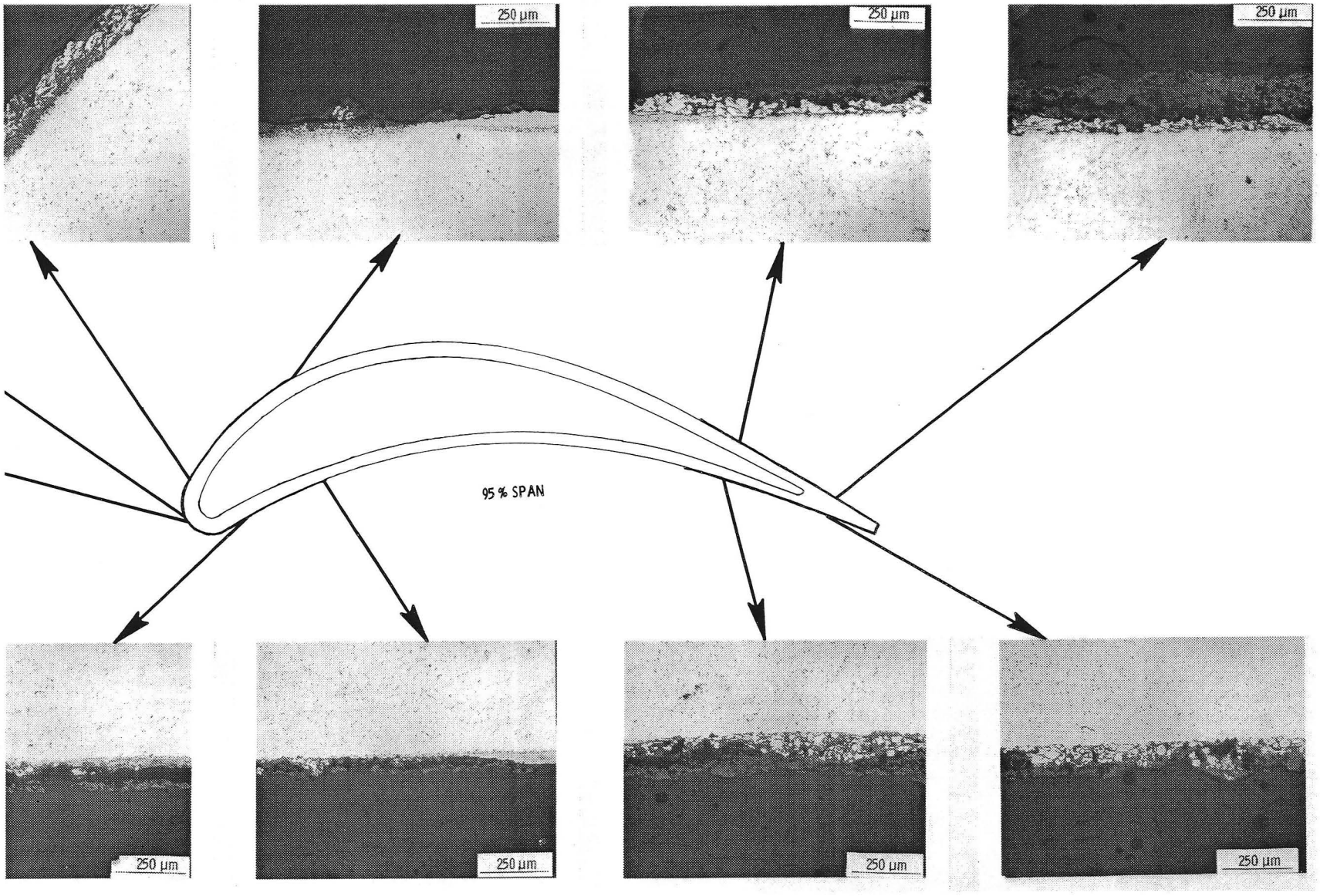

Figure 71. Photomicrographs of Stage 2 Vane with TBC after 1000 Cycles, 95% Span (Concluded).

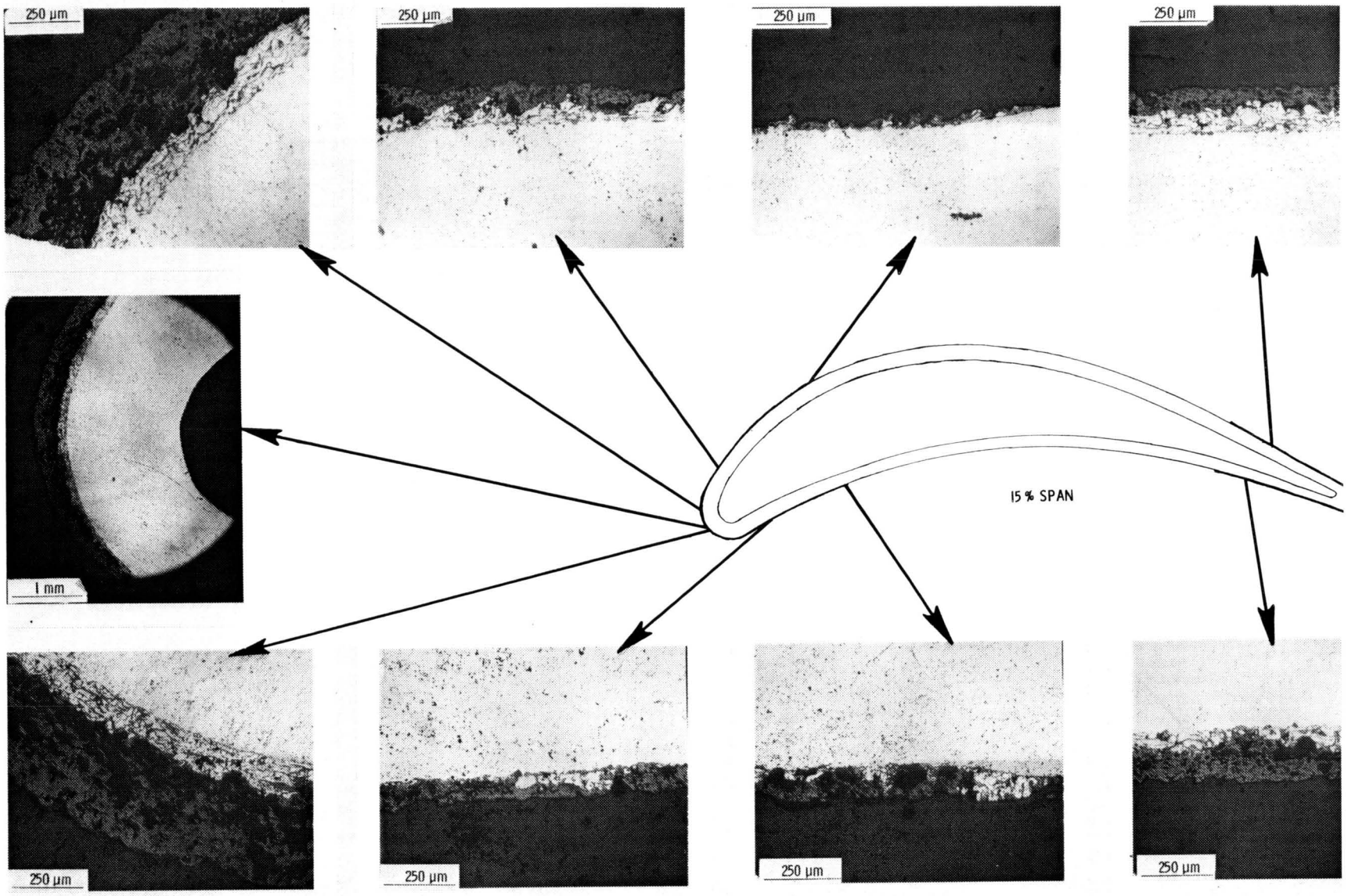

Figure 72. Photomicrographs of Stage 2 Vane with TBC after 1000 Cycles, 15% Span.

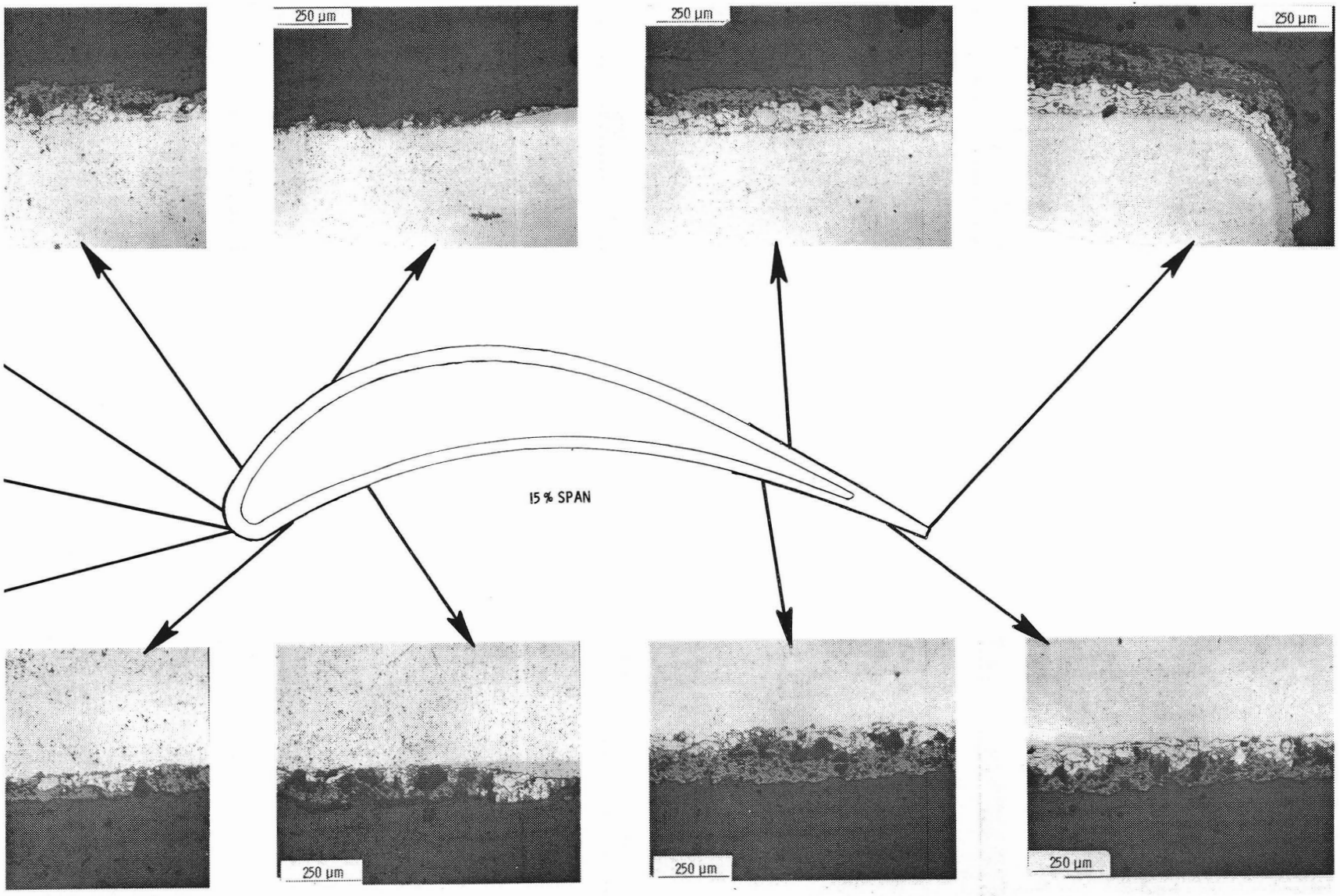

Figure 72. Photomicrographs of Stage 2 Vane with TBC after 1000 Cycles, 15% Span (Concluded).

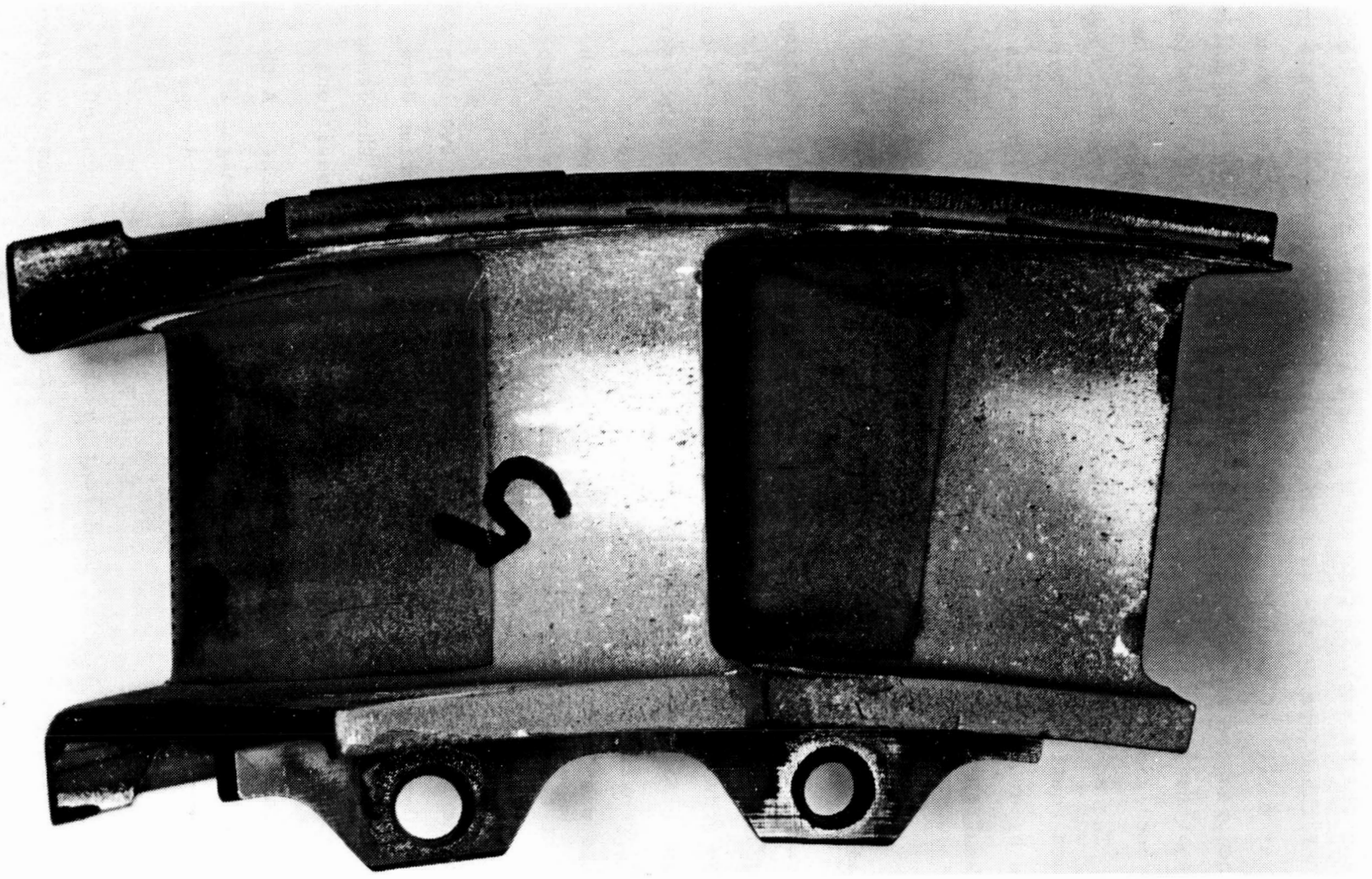

Figure 73. Condition of TBC on Suction Side of Stage 1 Vanes after 1230 Cycles.

localized areas on the suction side of the airfoils where the coating had spalled; two of these are on the vane shown in Figure 73 and are visible on the trailing airfoil. It was not possible to verify visually the presence of the TBC on the pressure side of the airfoil because of the heavy iron oxide scale that deposited during the test. On the inner bands, the TBC was in good to excellent condition except for a few isolated areas of coating loss, mostly by spalling. The condition of the TBC on the outer bands was generally good. There were some scattered areas of coating loss by spalling near the forward edge and more by erosion at the aft edge of the outer band. The results of the factory engine testing of CF6-50 blades and vanes with TBC may be summarized as follows:

Blades

The overall behavior of the TBC on the blades was very good. Coating damage was localized and limited to the leading edge and forward one-third of the suction side of the airfoil above midspan. There was no loss of coating from the pressure side of the airfoils or from the platforms with the exception of one spot (approximately 0.06 in^2) on one platform. The damage to the TBC on the airfoils was caused by impact of particulate matter present in the gas stream. Some of the particulate matter was Ni-Al in composition and probably came from the Stage 1 turbine shrouds.

There was no significant difference in the behavior of the two top-coat compositions, ZrO_2-20%Y_2O_3 and ZrO_2-8%Y_2O_3. The pattern of coating damage was similar on all TBC blades, and the amount of damage and size of the damaged area were not significantly different for the two top-coat compositions.

The adherence of the top coat to the bond coat was excellent. A thin layer of top coat remained adhered to the bond coat even in damaged areas except at the top of the leading edge where the severest impact damage had occurred.

Adherence of the VPS NiCrAlY bond coat to the aluminided René 80 substrate was excellent. No unbonded areas were found. Only minimal oxidation of the bond coat occurred, and interdiffusion of bond coat and substrate elements was minor.

The overall durability of the TBC was very encouraging, but the need for improvement of the impact and erosion resistance of the ceramic layer was demonstrated.

Vanes

The loss of the ceramic layer of the TBC from the outer one- to two-thirds of the leading edge of Stage 2 vane airfoils was by spalling. Severe erosion damage to the TBC occurred near the leading edge of the outer bands adjacent to the airfoil/outer-band juncture. The TBC survived well in other coated areas on the Stage 2 vanes. Oxidation of the NiCrAlY bond coat was considerably more extensive on Stage 2 vanes than on the blades. This is partially due to the higher operating temperature of the vanes and partially due to the more porous structure of the bond coat (conventional plasma sprayed on vanes, VPS on blades).

The greater variations in thickness of the coating layers on the vane bands and airfoils indicate the need for automated application processes for coating this type of complex-shaped part.

Work Planned

The final report on the TBC development effort will be completed.

2.4.7.2.5 TBC Design and Application

Technical Progress

Two successful engine tests with TBC applied to Stage 1 nozzle segments were run for 1300 and 750 "C" cycles in CF6-50 engines.

Four nozzle vane segments were coated on portions of the bands and airfoils for the first engine test and accumulated a total of 1300 "C" cycles in CF6-50 engine 455-508/21. Figures 74 and 75 show a segment after the tests. Visual examination indicated some local spallation on the front flange, specifically in front of the airfoil leading edge and also on the pressure side upstream of the trailing-edge cooling slots. Other areas of applied TBC were on the airfoil suction side and bands. No observable spallation was noted, and the coating was intact in these locations.

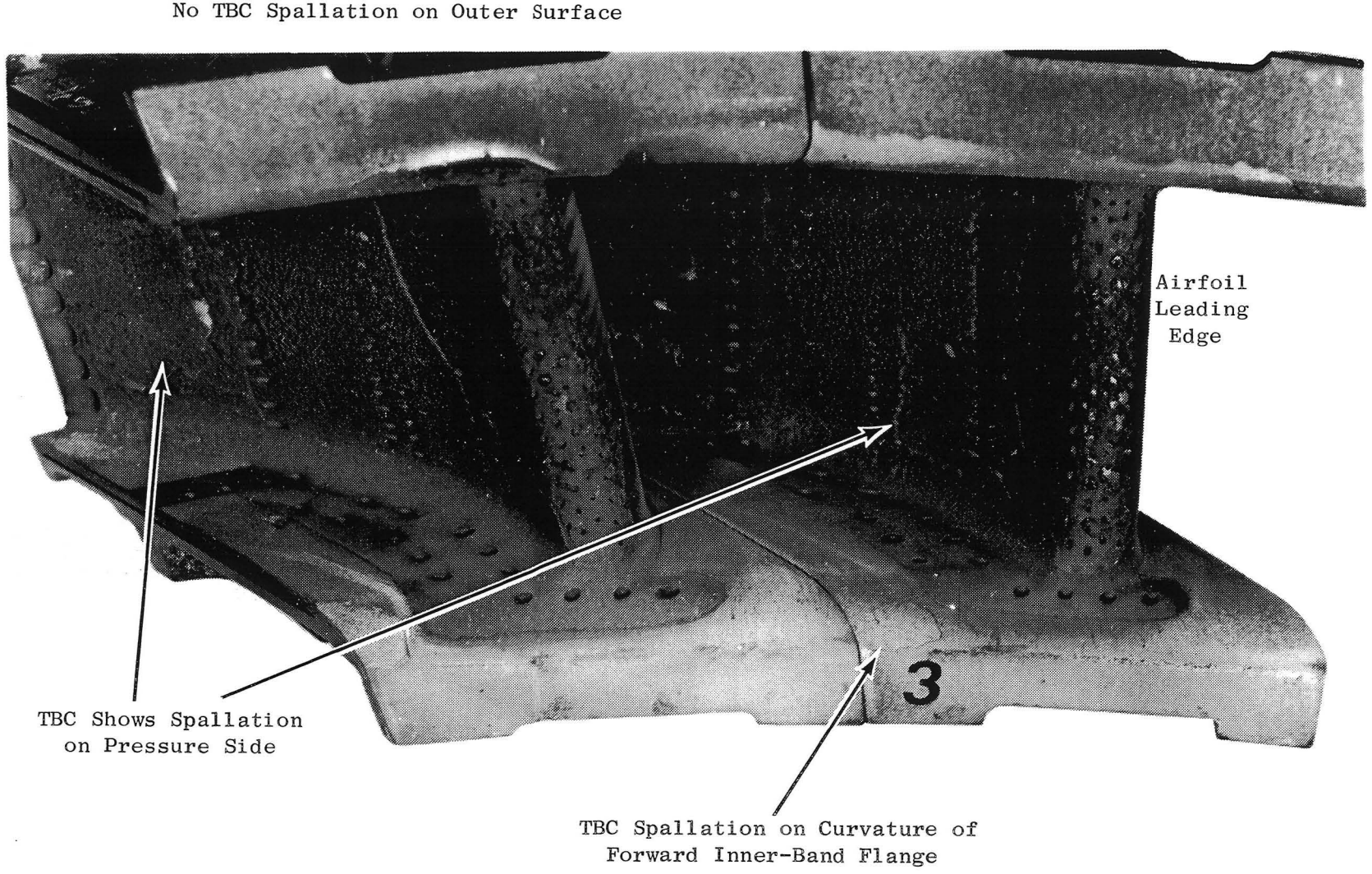

Figure 74. HPT Stage 1 Vane Segment with TBC after 1300 Cycles, Forward Looking Aft.

No TBC Spallation Observed on Airfoil Suction Sides or Inner Band

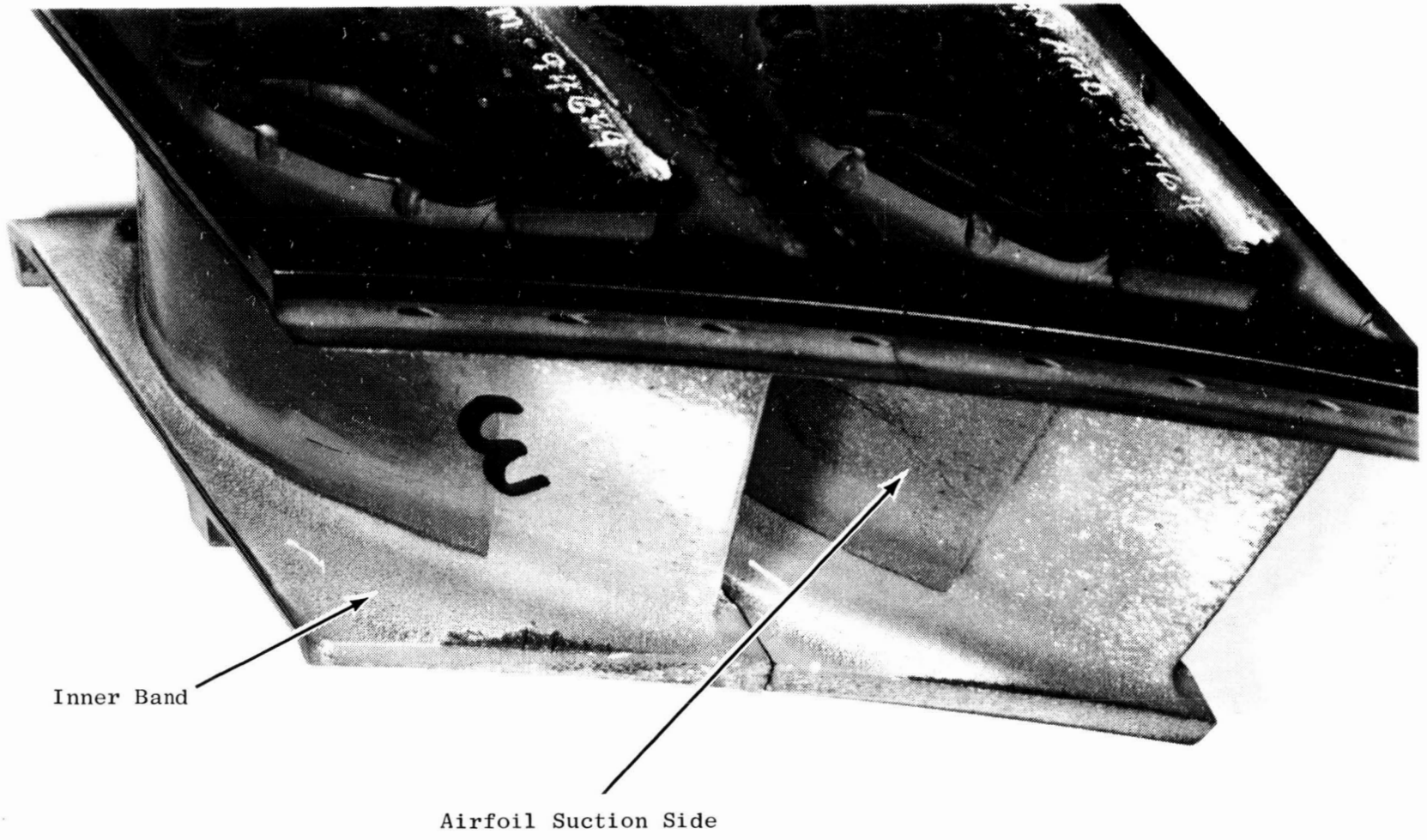

Figure 75. HPT Stage 1 Vane Segment with TBC after 1300 Cycles, Aft Looking Forward.

Two nozzle vane segments were also coated with TBC for the second engine test. One vane segment was coated in the same locations as the first engine test parts. TBC areas for the second vane segment were similar except on the bands. The TBC was applied over the entire band surfaces, and the film-cooling holes were mechanically opened to the original sizes.

The two segments were tested in a CF6-50 for 750 "C" cycles. Visual inspection of the condition of the airfoils indicated the TBC on the pressure side to be intact (see Figure 76). However, some local spallation and local cracks were observed on the inner band which had been completely coated. The vanes are in process of disassembly from the nozzle support after which they will be metallurgically examined to determine possible cause for the local spallation. Note that in the same nozzle segment (to the left in the photograph) the fully coated band surface experienced no distress.

Work Planned

Continue coordination with Materials Engineering on the evaluation of the TBC nozzle segments.

2.4.8.1 Stage 1 Blade Manufacturing

Technical Progress

The first set of completely manufactured Stage 1 blades was delivered in January 1982. The delivery of these blades represents an important milestone in advanced turbine design technologies. Figure 77 illustrates some of the features of the casting and final-machined blades.

The blade configuration breakdown for the core engine was established as follows:

	PVD	Noncoated (Instrumented)		
	Coated	Thermocouple	Strain Gage	Total
Blade Quantity	59	6	11	76

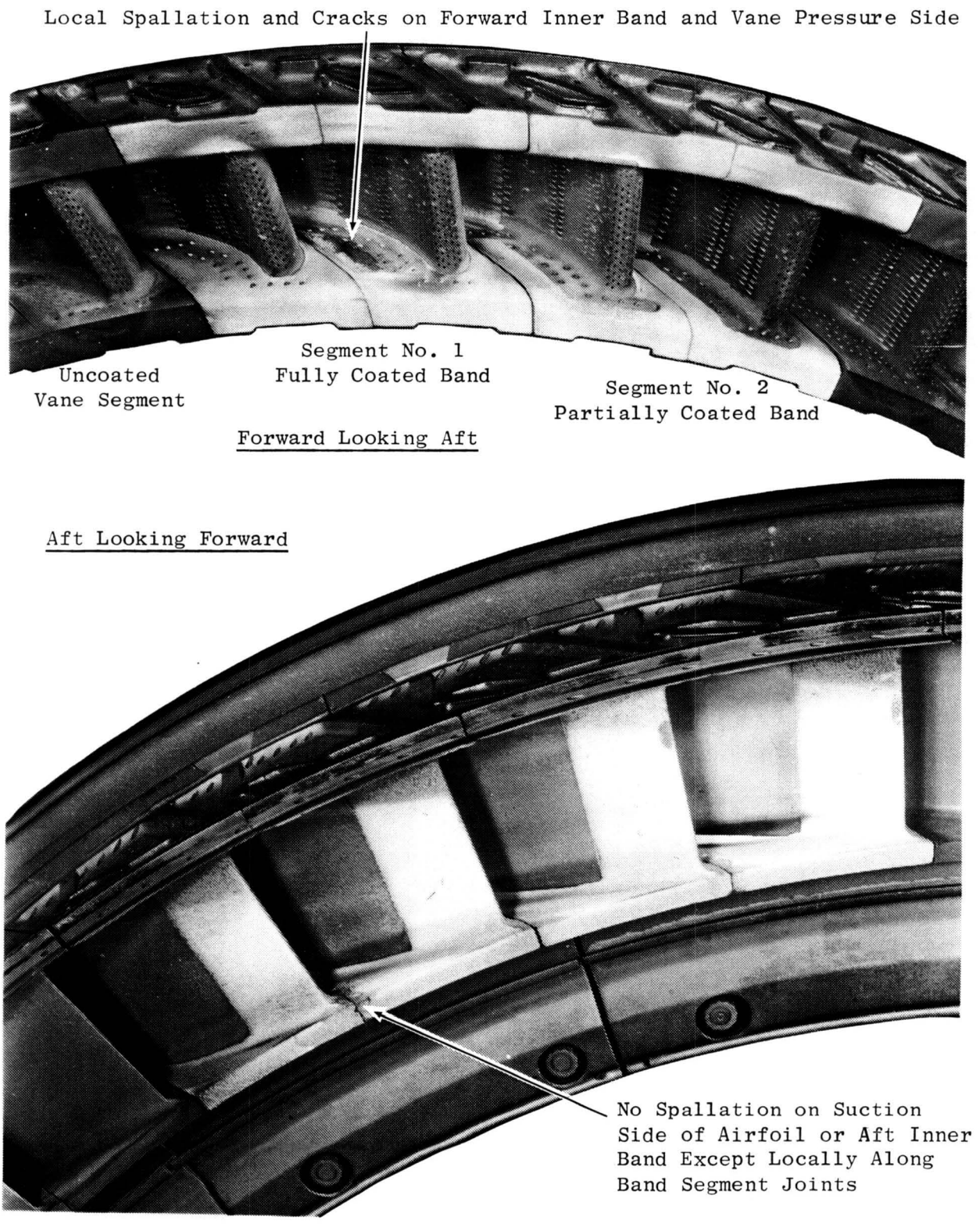

Figure 76. Stage 1 Nozzle Segments with TBC after 750 Cycles.

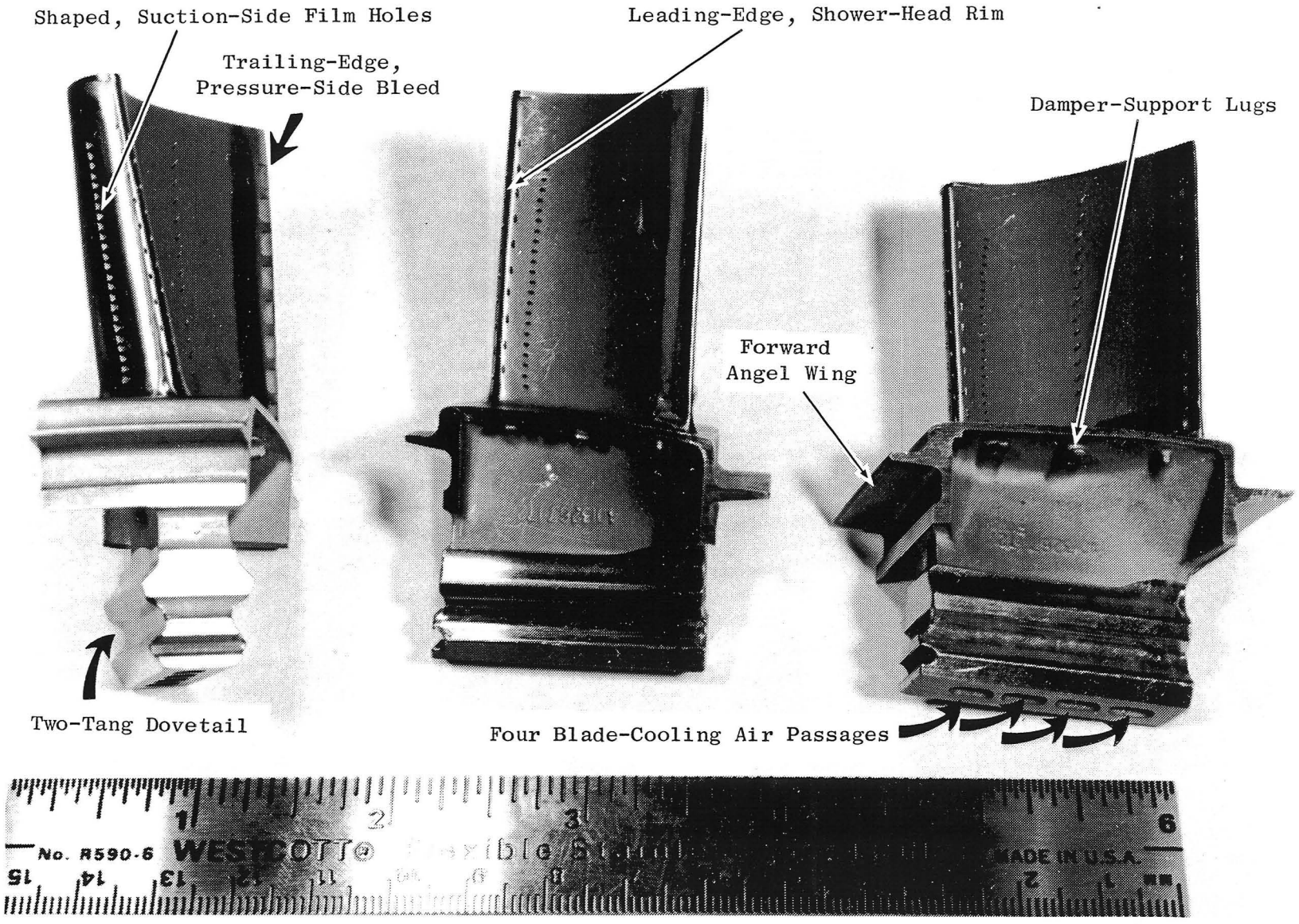

Figure 77. Stage 1 HPT Blades.

In addition to the first set of delivered blades, an additional 1-1/4 sets are in process of manufacture for use as spares and for component tests. The current status of the additional blades is as follows:

- Eighteen blades have been processed through the machining cycle and shipped to a vendor for PVD coating application.
- One hundred and twenty-four castings have been processed through the tip-cap braze cycle and returned to the casting vendor for final casting inspections and further airfoil-finishing operations.

The total blade-manufacturing costs are projected to be within the planned program funding.

Work Planned

Continue engineering support of manufacturing and production control for the balance of the blades in process.

2.4.8.2 Stage 2 Blade Manufacturing

Technical Progress

The balance of the first set of machined Stage 2 blades was delivered in January 1982. The blade incorporates design features based on the latest advanced technologies in aerodynamics, heat transfer, and mechanical design. Figure 78 shows some of the design features of the blade.

The blade configuration breakdown for the core engine was as follows:

	PVD Coated	Noncoated (Instrumented) Thermocouple	Strain Gage	Total
Blade Quantity	55	7	8	70

In addition to the blades already delivered, an additional 134 blade castings are in process of finish-manufacturing operations. The processing of these blades should yield an additional 1 to 1-1/4 blade sets for use as spares. Presently, the castings are in preparation for the tip-cap braze cycle.

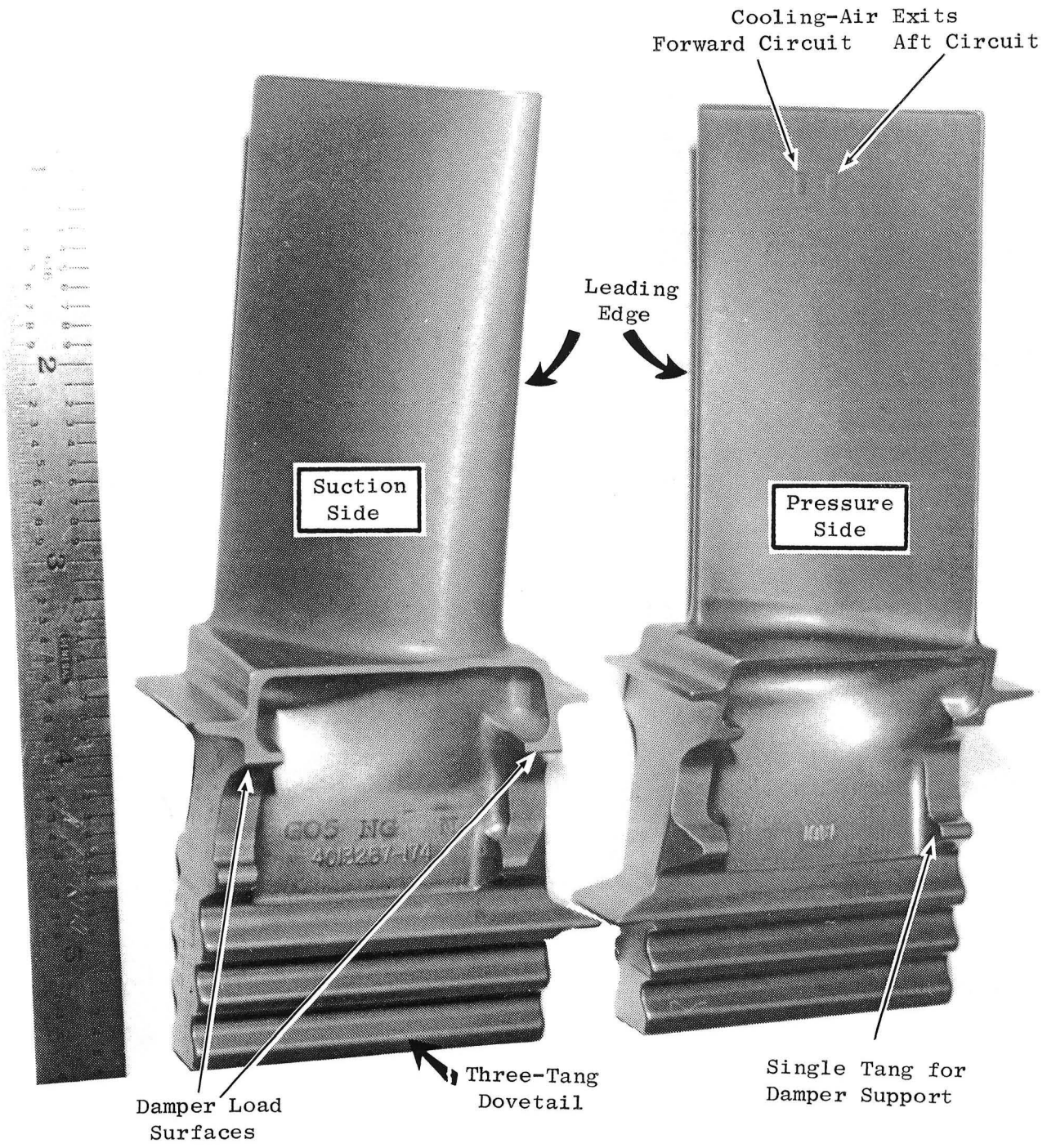

Figure 78. Stage 2 HPT Blades.

The total blade-manufacturing costs are projected to be within the planned program funding.

Work Planned

Continue engineering support during the manufacturing cycle for the second set of blades.

2.4.8.3 Stage 1 and 2 Disk Manufacturing

Technical Progress

The Stage 1 and 2 HPT disk rework for instrumentation was completed. Rework consisted of adding 0.04-in. diameter holes on the aft arm for both stages. Flame spraying was also applied on the webs (aft side) for attachment and egress of the instrumentation leads. Figures 79 and 80 show disk features, for Stages 1 and 2 respectively, after completion of the disk-machining operations.

The manufacturing costs and delivery for both disks were within the program funding and schedule.

Work Planned

All disk work has been completed.

2.4.8.4 Rotating Shafts and Seals

Technical Progress

All rotating components required for the core and ICLS engine tests were delivered. The necessary rework for instrumentation lead routing on these components was also completed. The rework consisted of drilling 0.04-in. diameter holes at specific locations and metal flame spraying areas where tack welding of the instrumentation leads will be required.

The quantity of hardware under this program was planned to be one of each with spares for the impeller and interstage disk. Both spares are planned for delivery in March 1982.

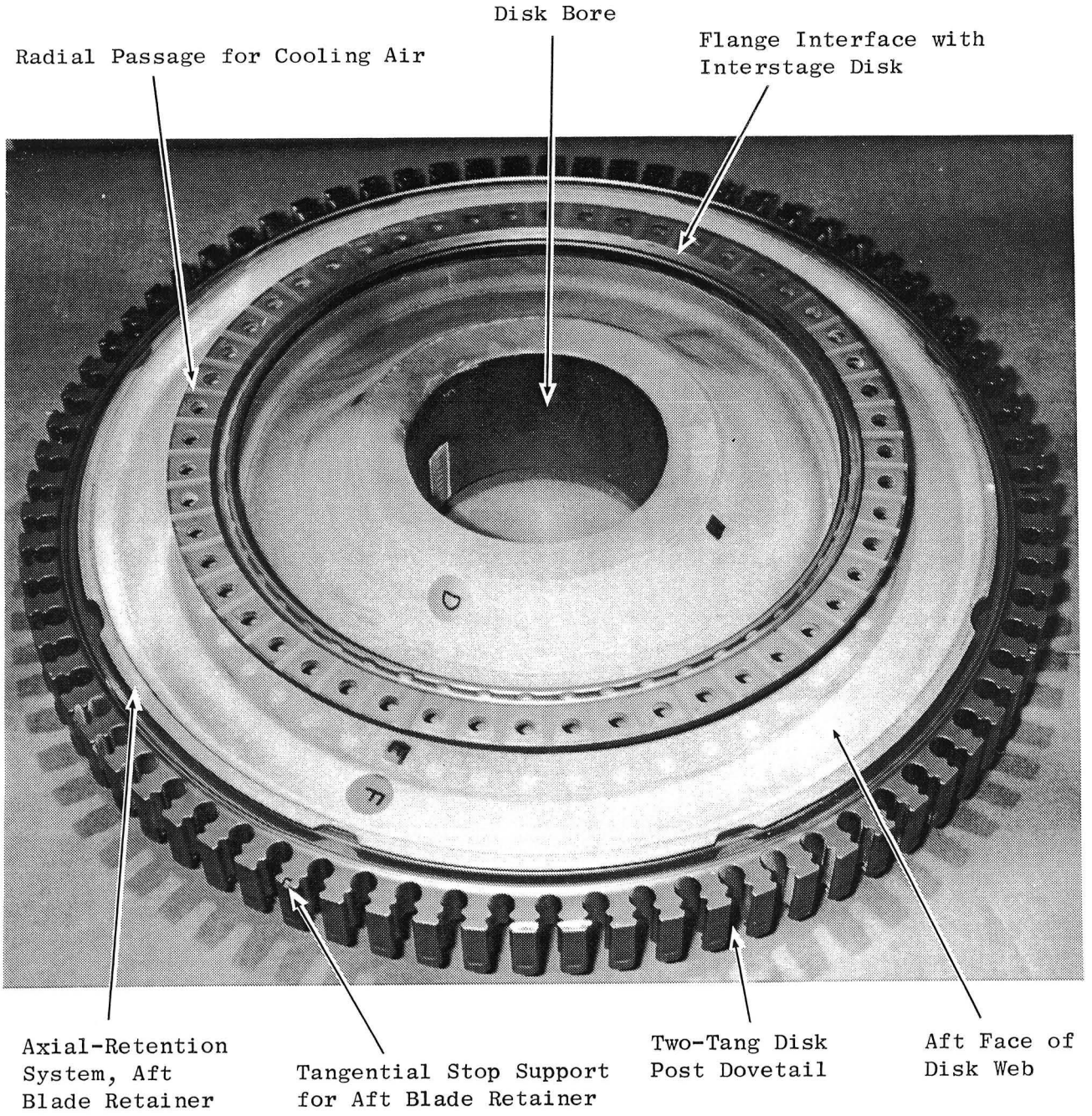

Figure 79. Stage 1 Disk.

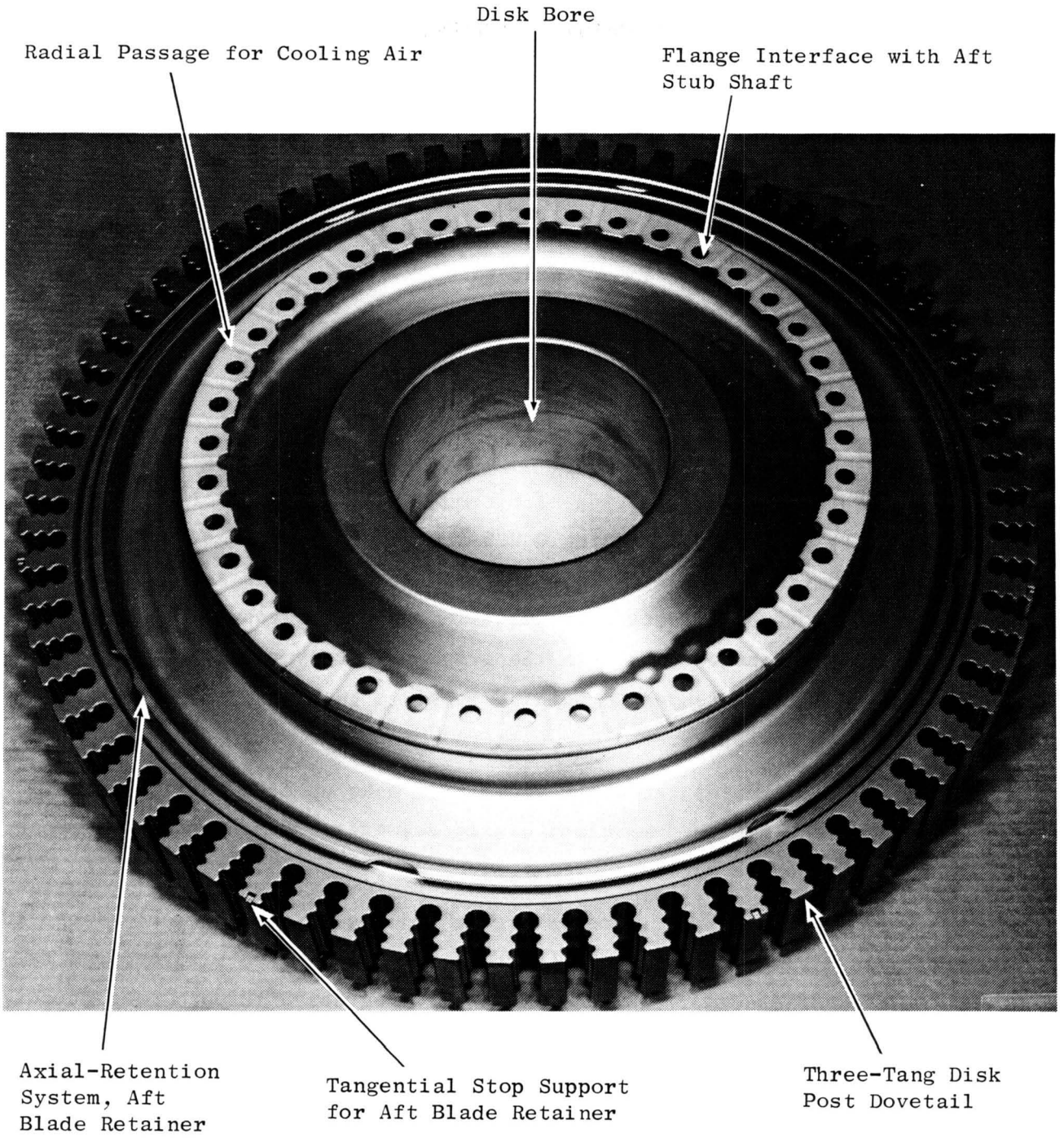

Figure 80. Stage 2 Disk.

Figures 81 through 92 illustrate the completed, machined parts and some features of the major rotating components in the HPT. Total hardware costs are projected to be within the planned funding.

Work Planned

Continue engineering support of manufacturing during the final machining and delivery of the impeller and interstage disk.

2.4.8.5.1 Stage 1 Nozzle Fabrication

Technical Progress

The fabrication of the first set of Stage 1 nozzle segments was completed. All rework required for application of thermocouples was accomplished. The rework primarily consisted of adding 0.026 x 0.025 inch grooves by electrodischarge machining (EDM) on the airfoil and band surfaces (gas side). Imbedded thermocouples and wire leadouts were installed in these grooves, covered with nichrome wire, and benched smooth to the original aerodynamic contour. Three nozzle segments were instrumented with 28 imbedded thermocouples: 20 on the airfoils and 8 on the bands.

Figure 93 illustrates the major items that make up each nozzle segment. Figure 94 shows the finished-machined nozzle segments. Twenty-three segments are required per engine set.

An additional 10 nozzle segments are in process of fabrication. These 10 segments, plus 3 completed segments (part of the first set), will be used as spares. The manufacture of these segments has progressed through completion of the EDM drilling for all the inner- and outer-band film holes. Preparation of the component parts for EDM of the airfoil contour into the bands is in process.

Work Planned

- Continue engineering coordination with manufacturing for completion of the remaining segments of the Stage 1 nozzles
- Deliver spare segments to Engineering stores after completion of nozzle fabrication

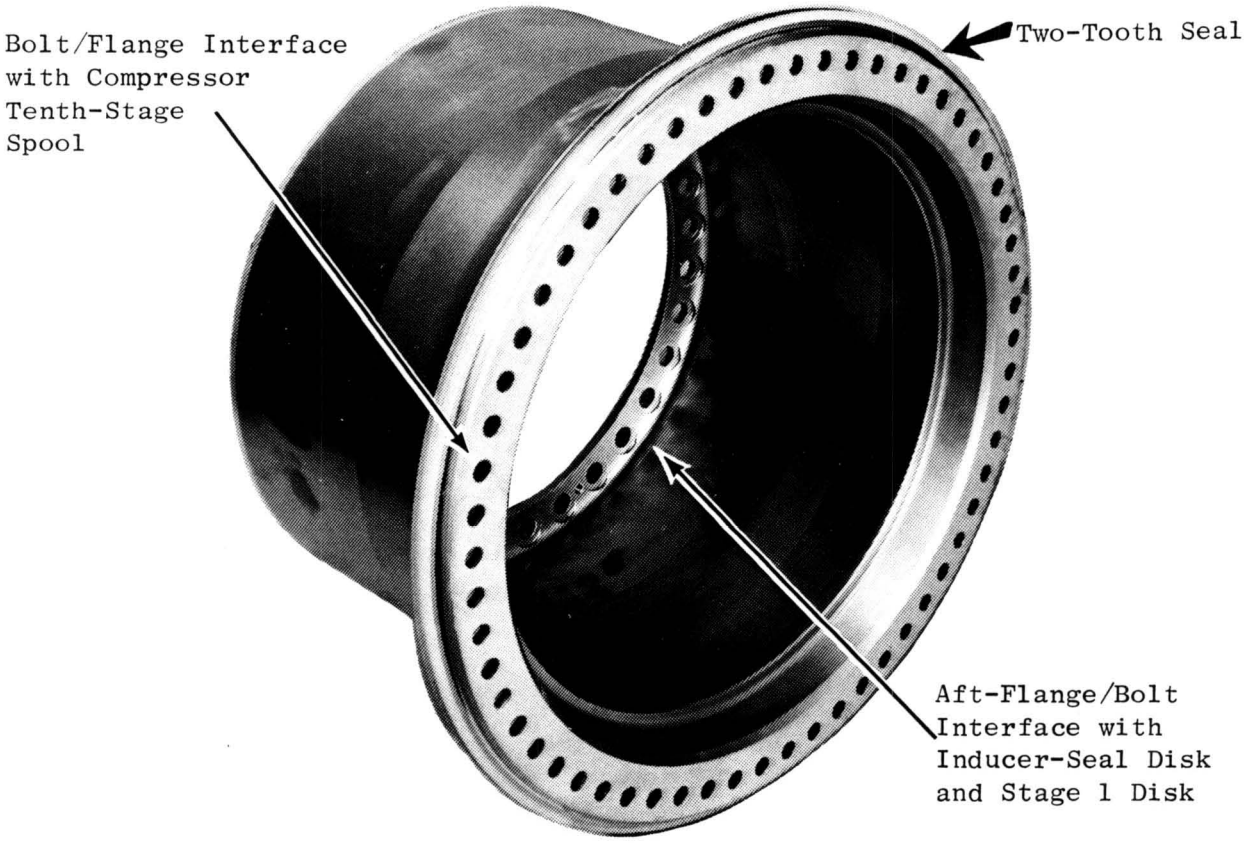

Figure 81. HPT Shaft.

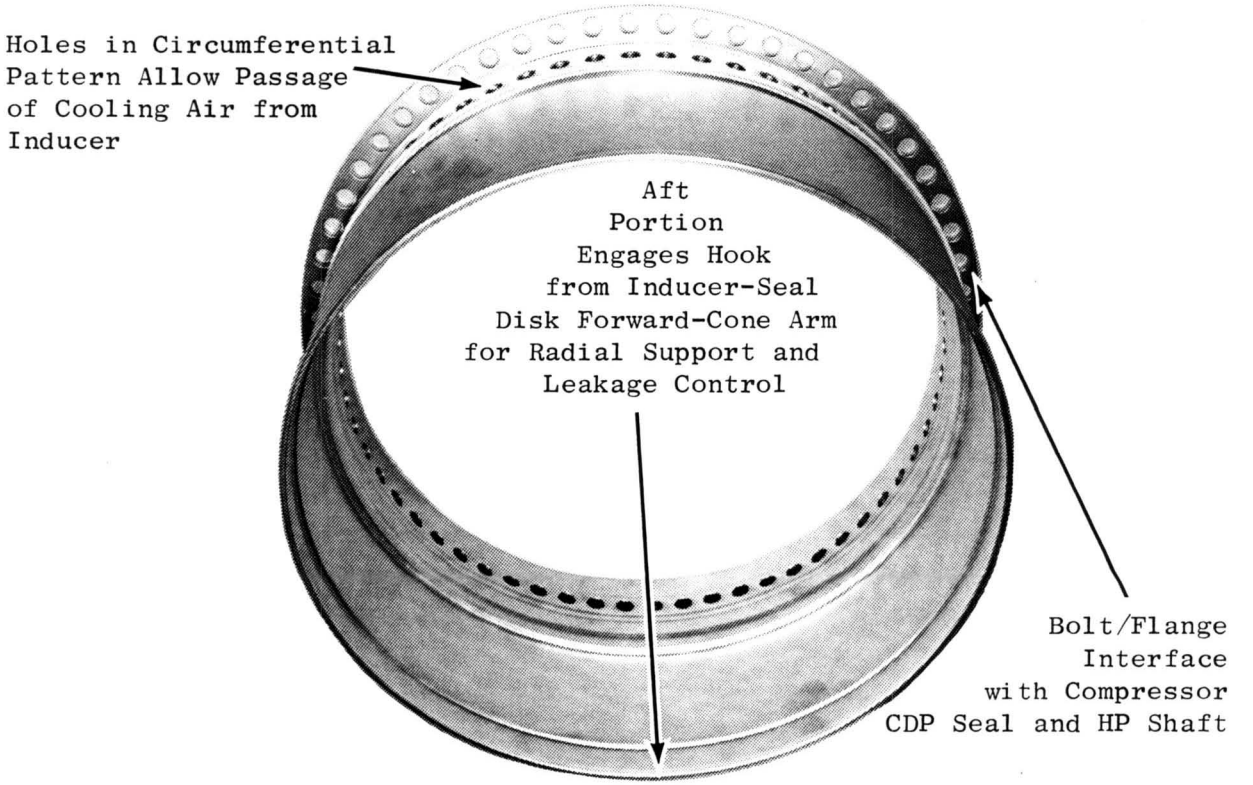

Figure 82. HPT Forward Outer Liner.

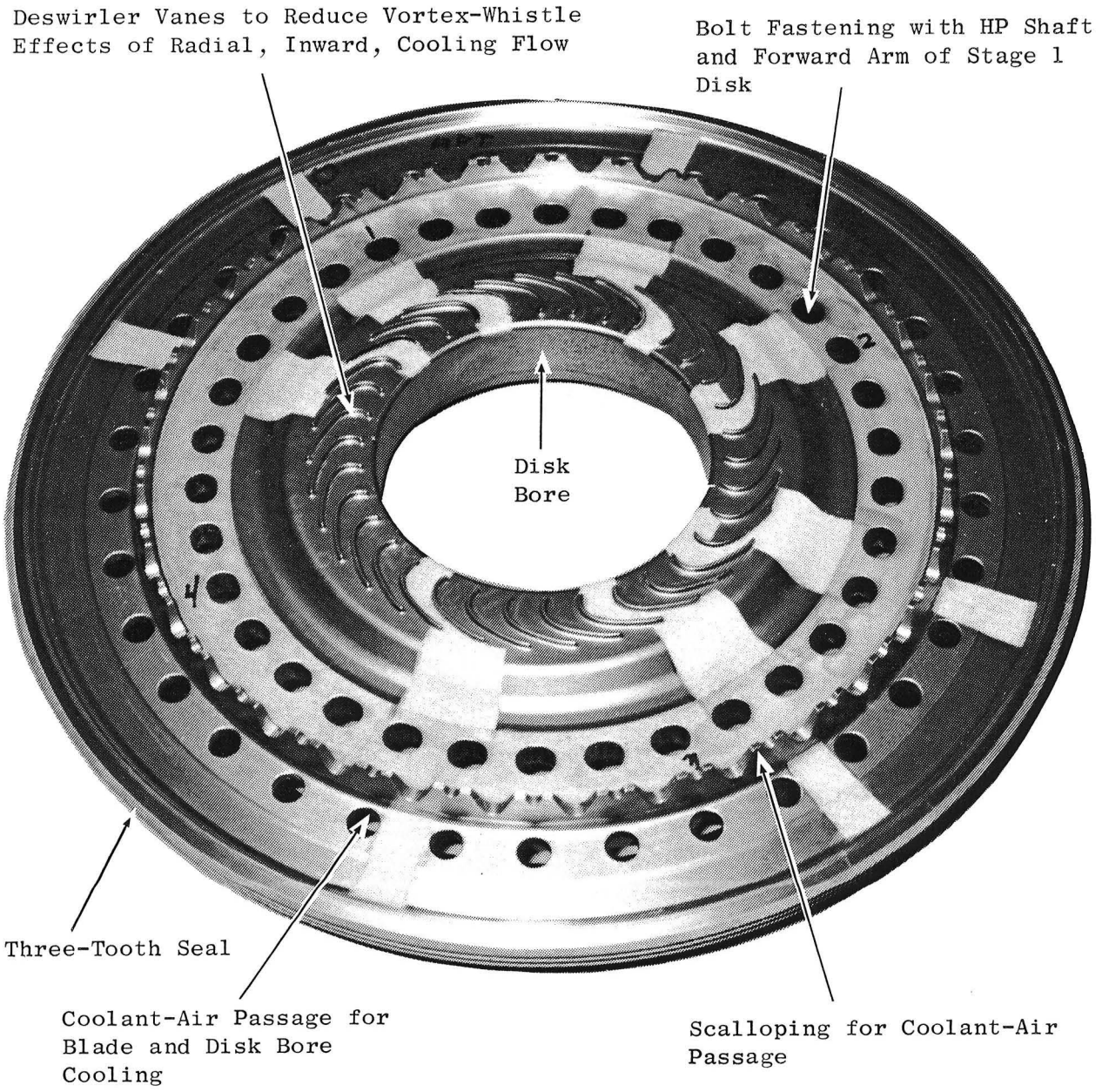

Figure 83. HPT Inducer Seal Disk.

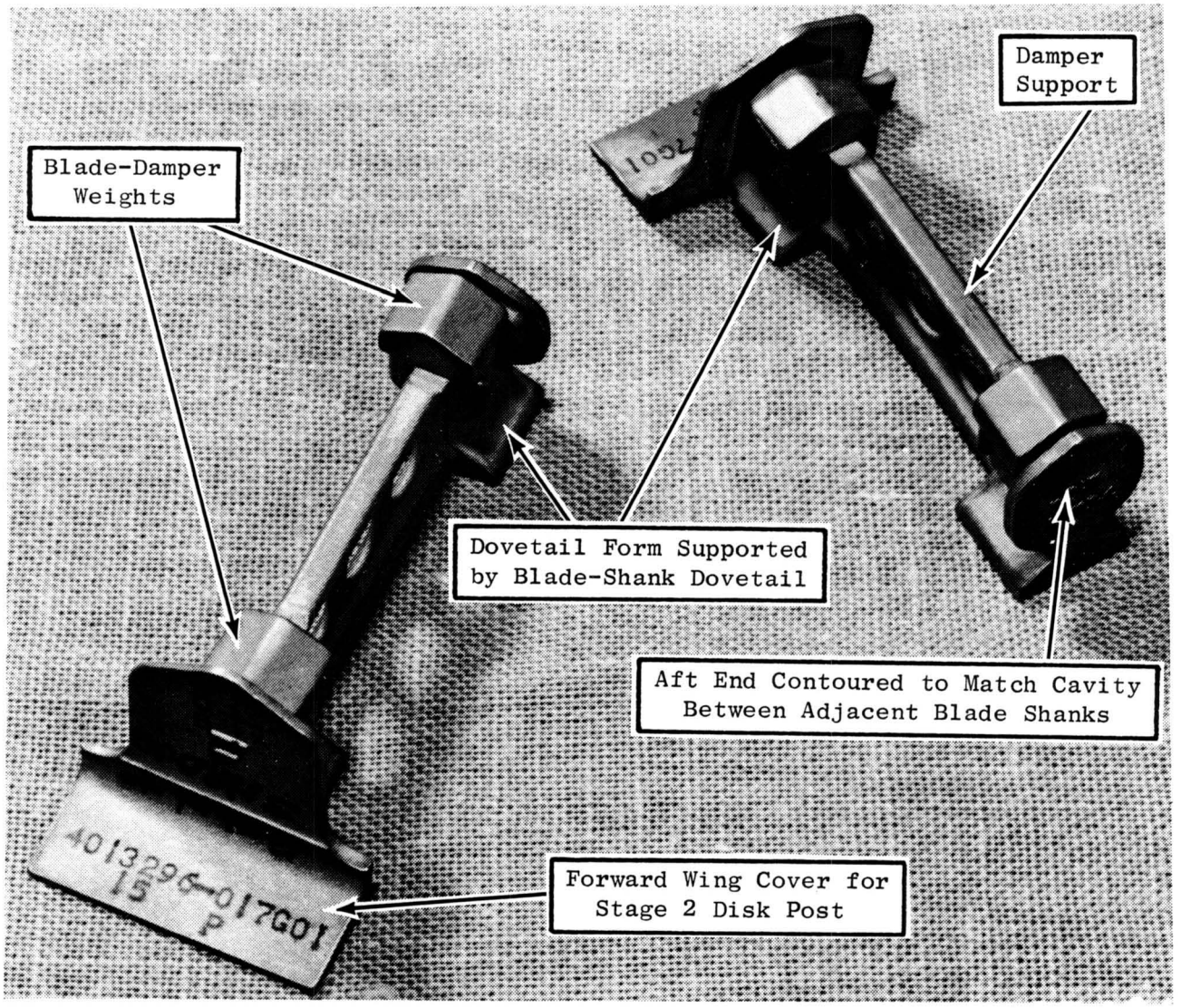

Figure 84. HPT Stage 2 Blade Damper.

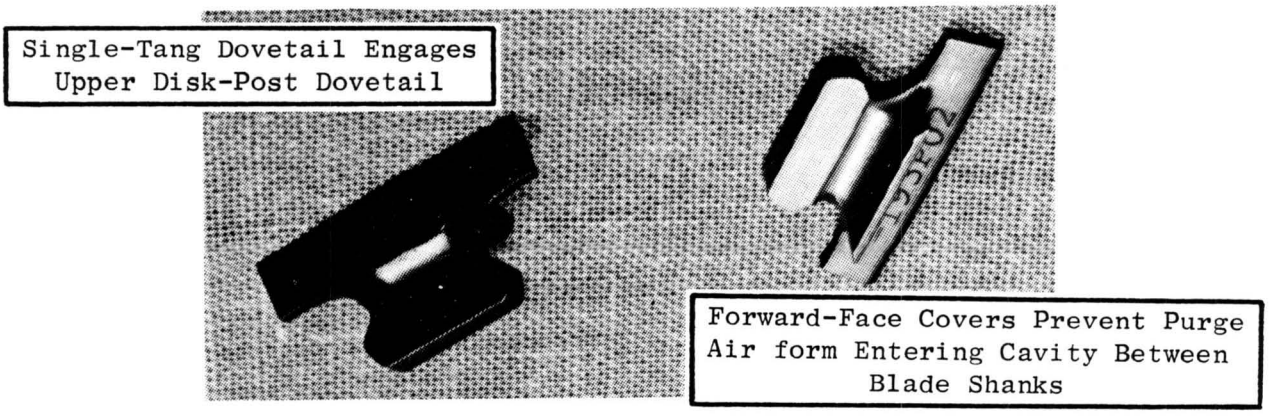

Figure 85. HPT Stage 1 Blade Forward Seal.

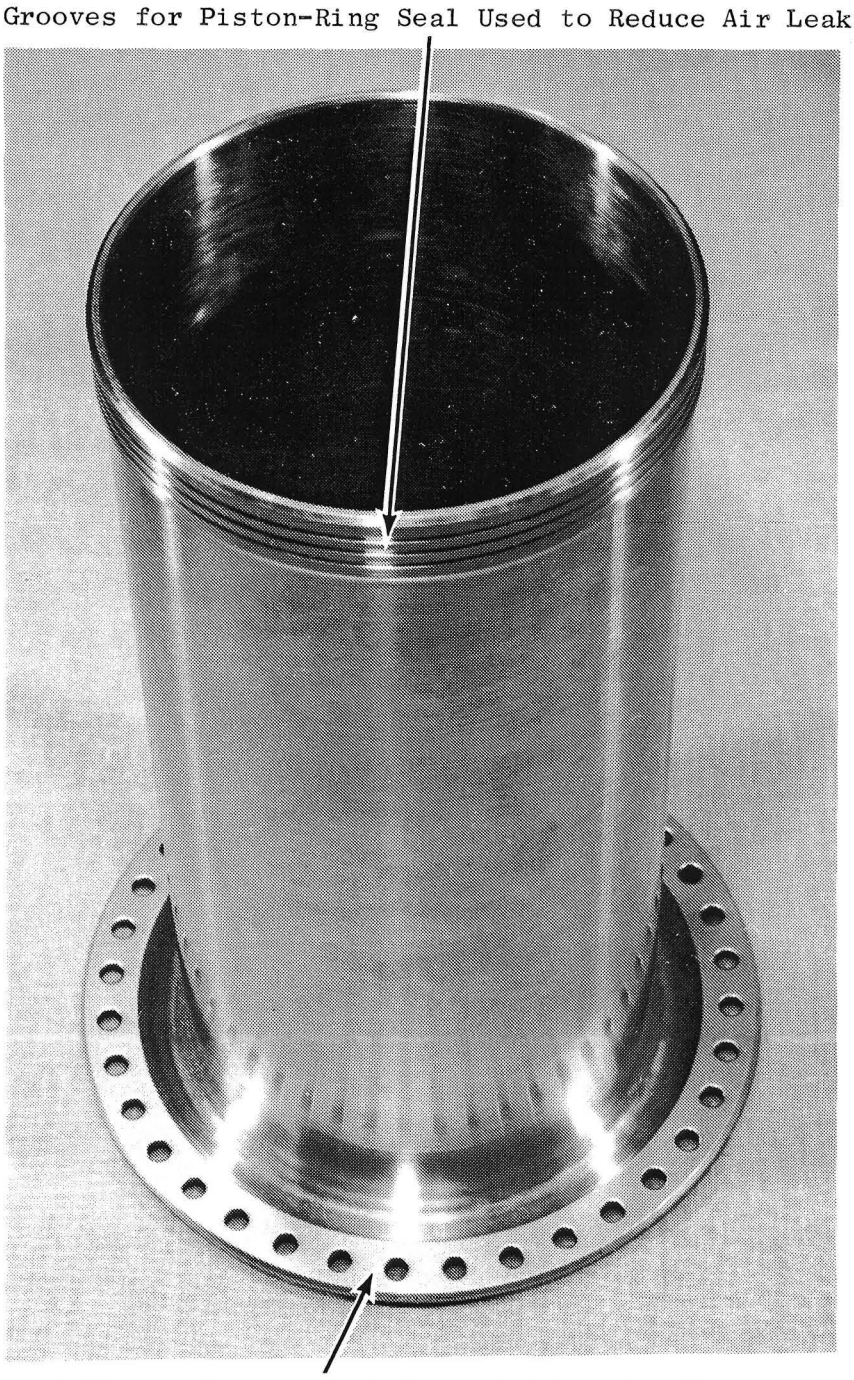

Figure 86. HPT Inner Tube.

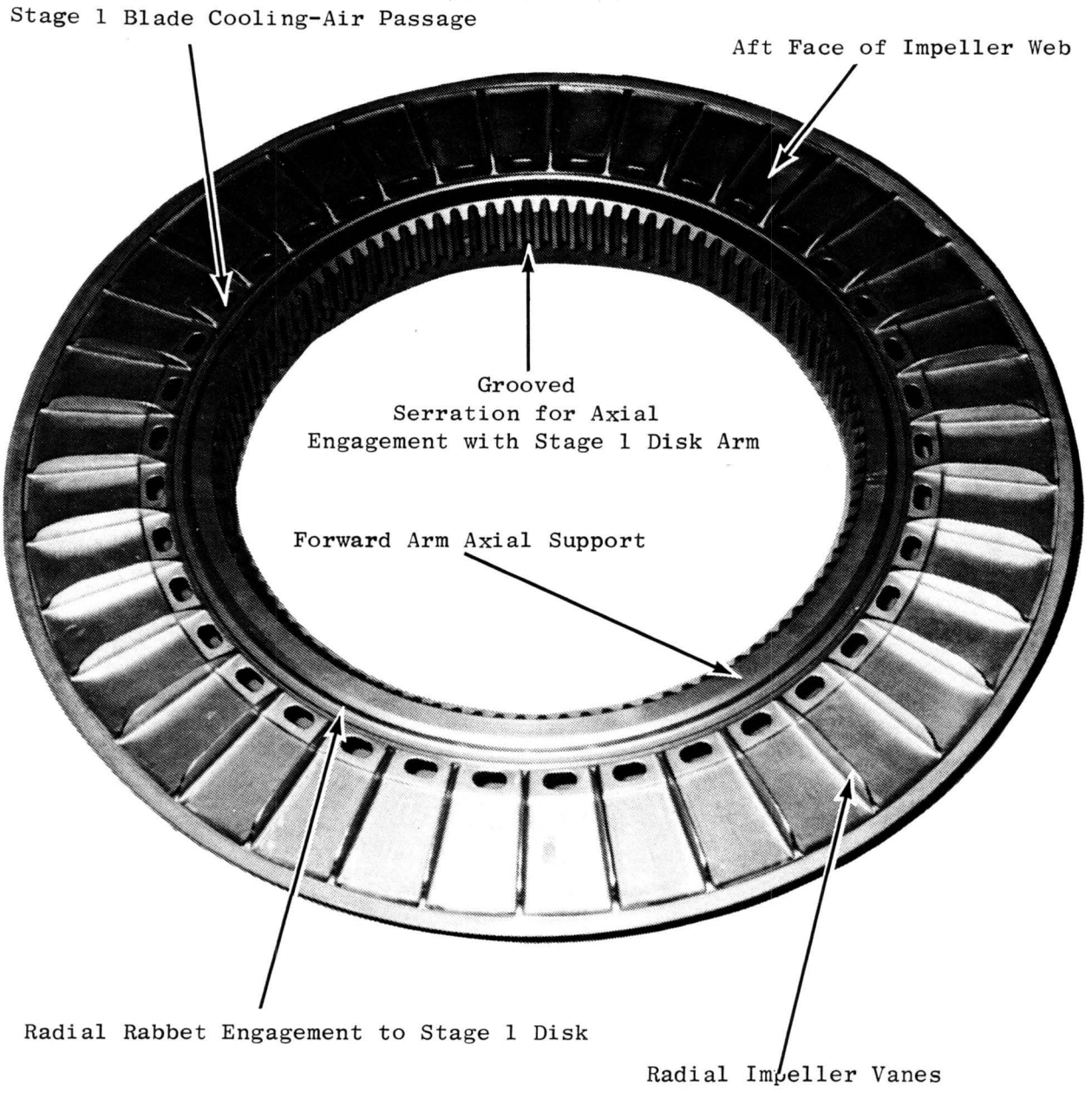

Figure 87. HPT Impeller.

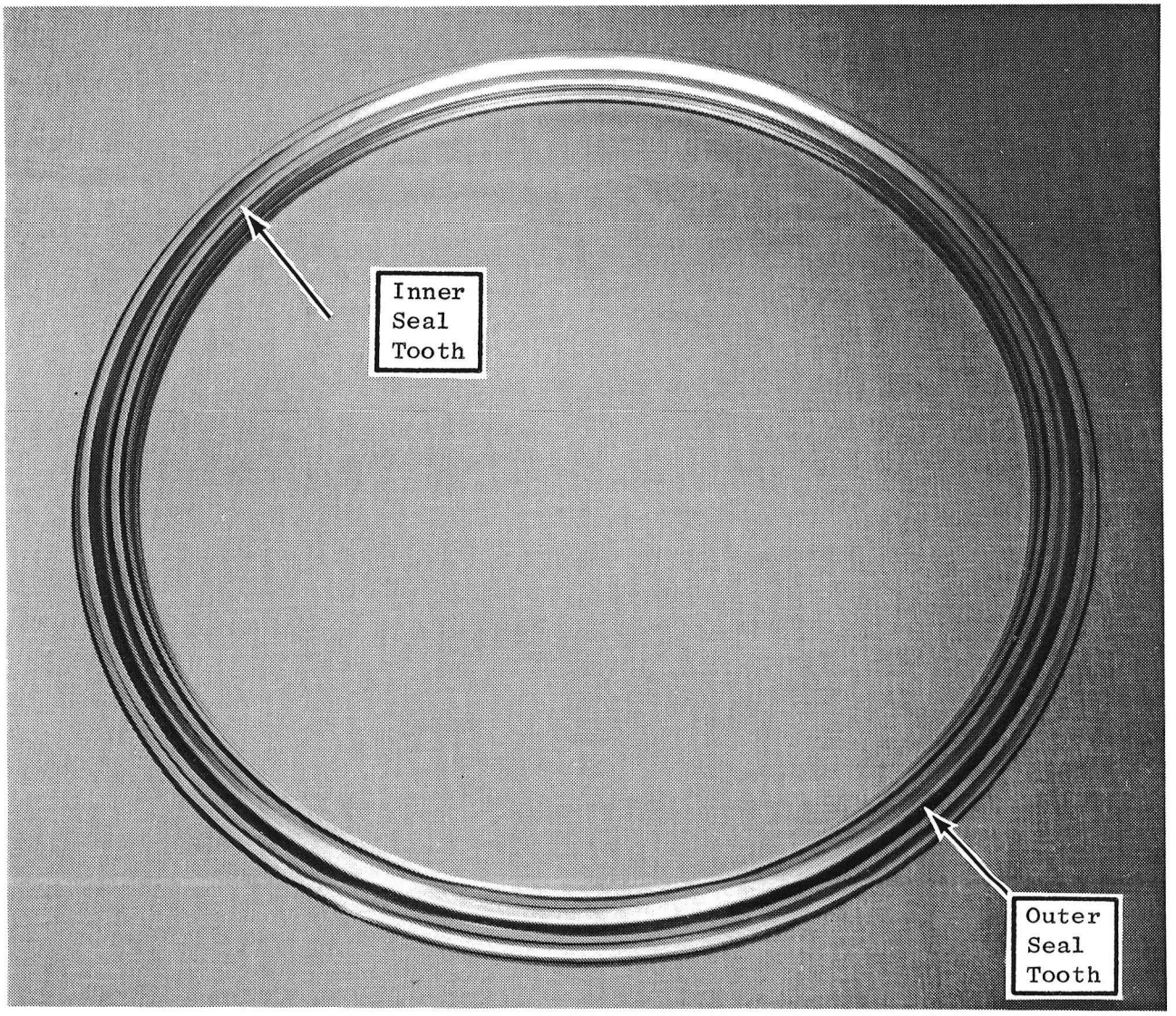

Figure 88. HPT Stage 1 Aft Blade Retainer.

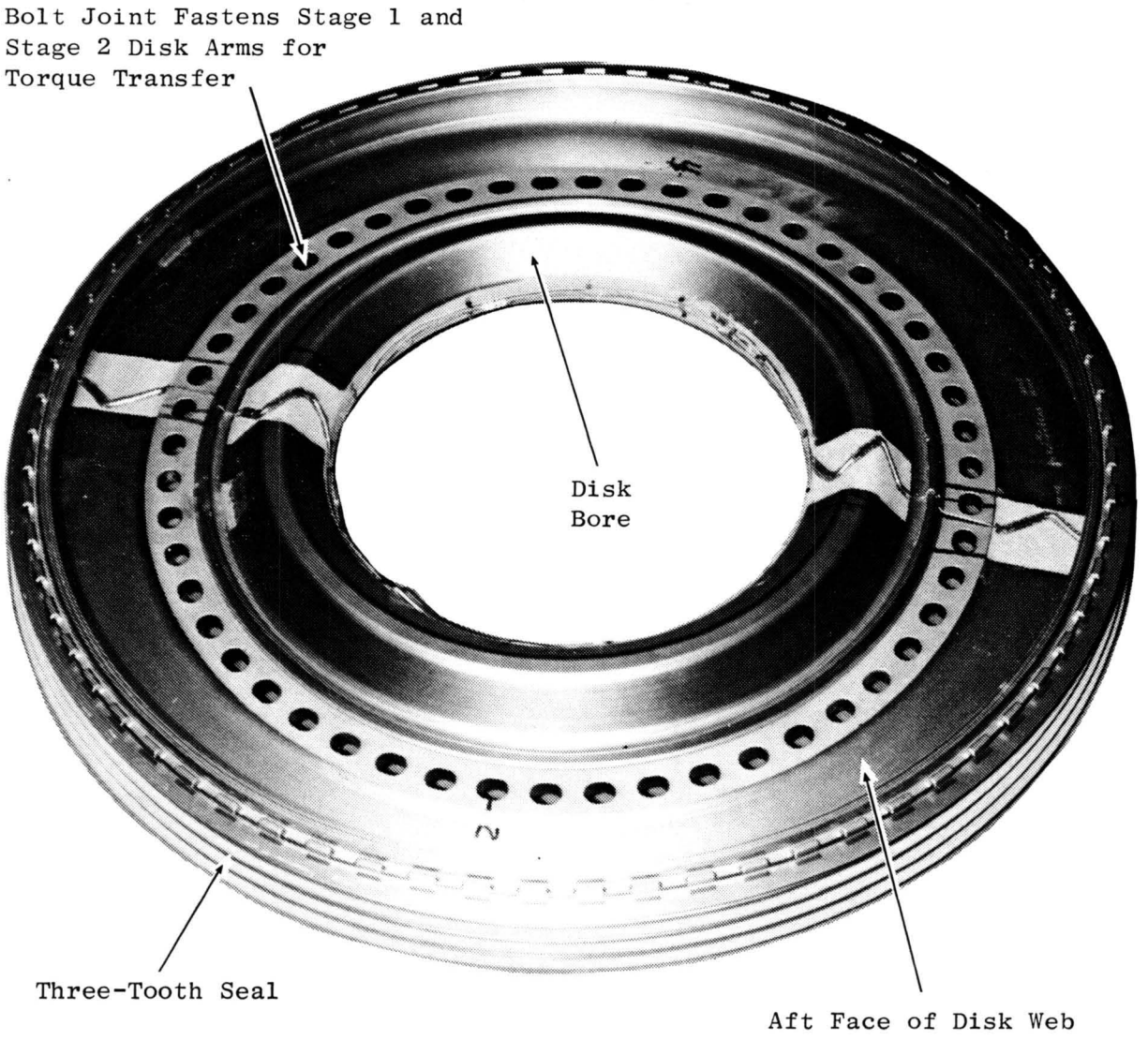

Figure 89. HPT Interstage Disk.

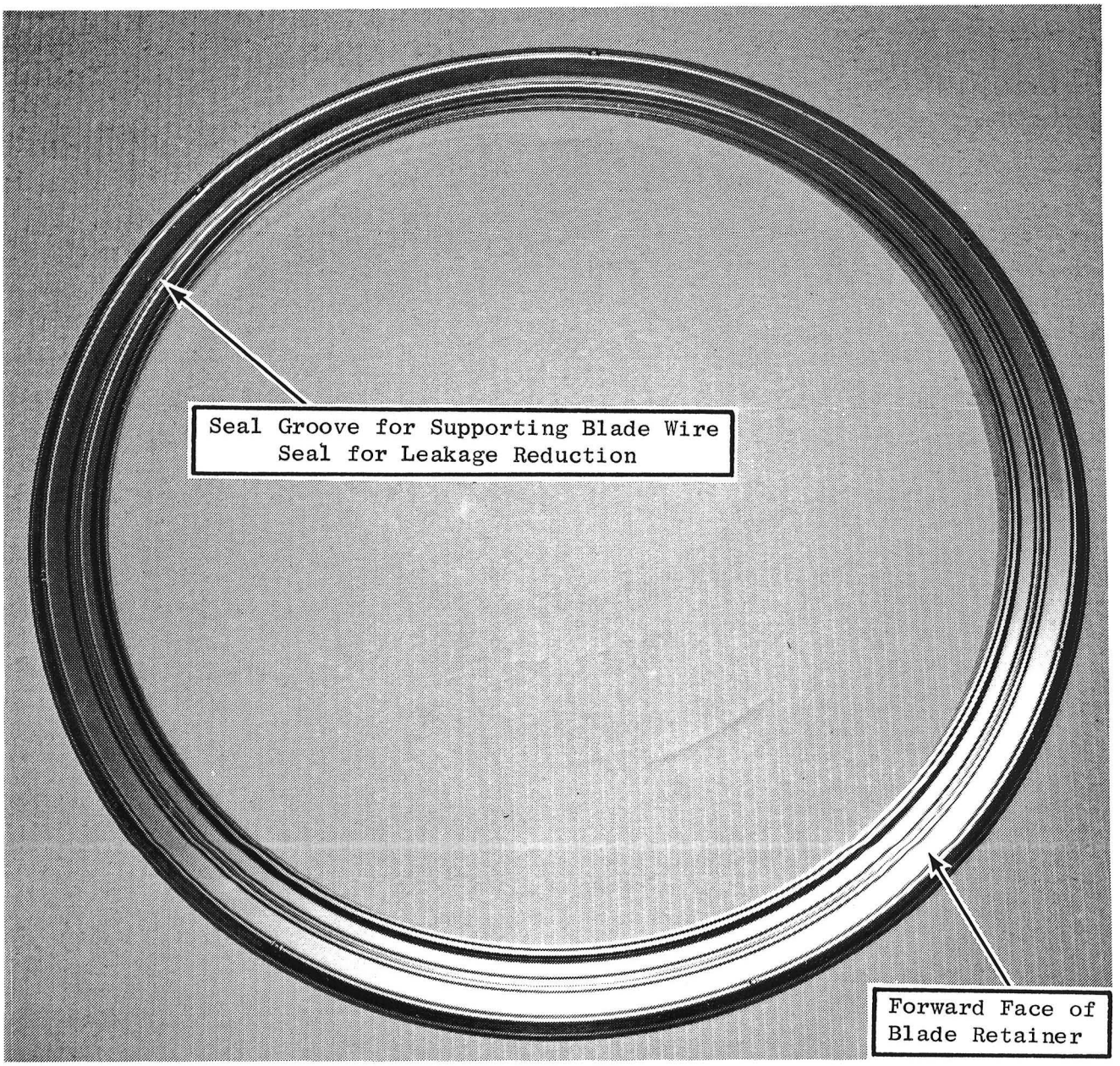

Figure 90. HPT Stage 2 Aft Blade Retainer.

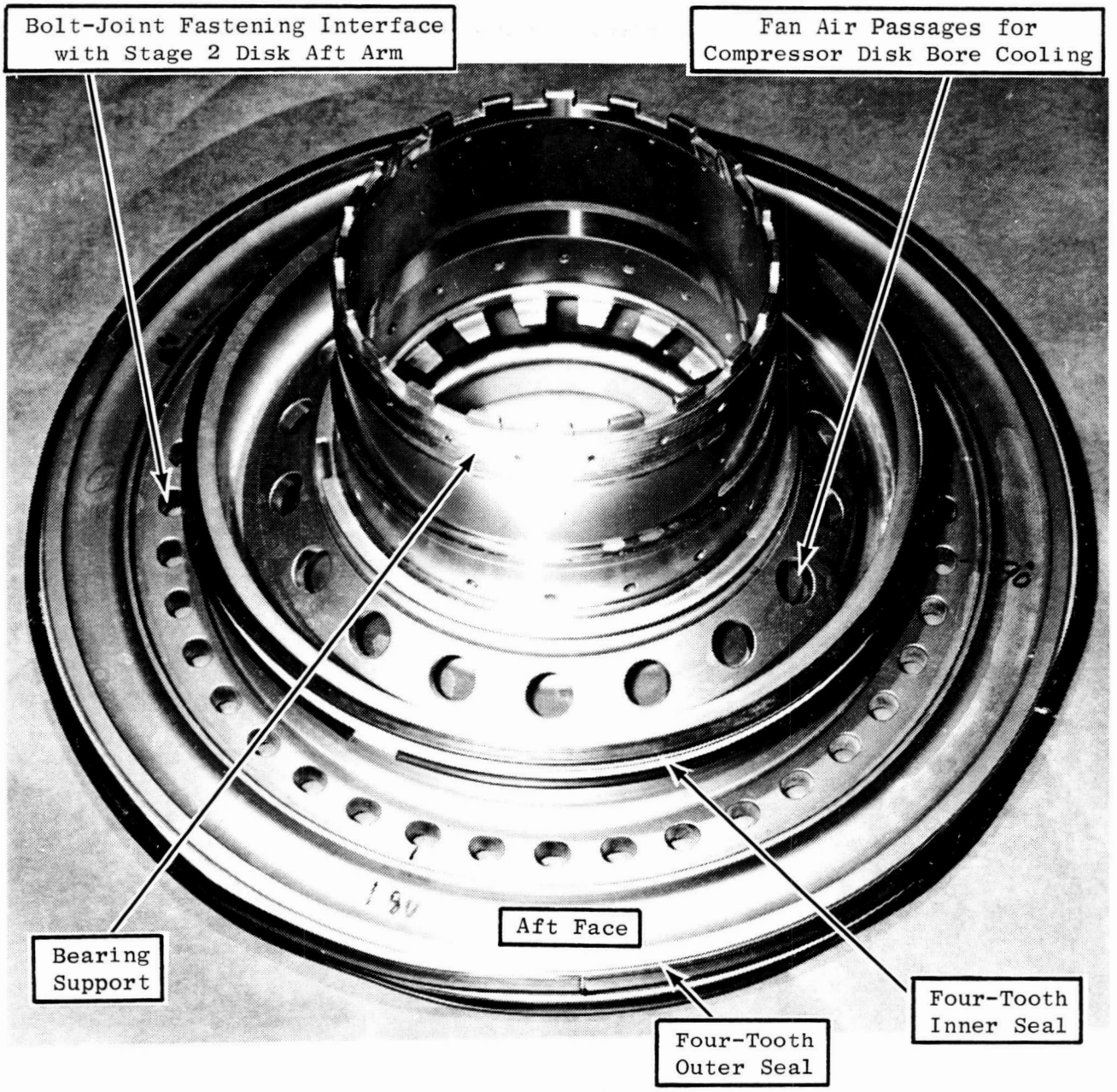

Figure 91. HPT Aft Stub Shaft.

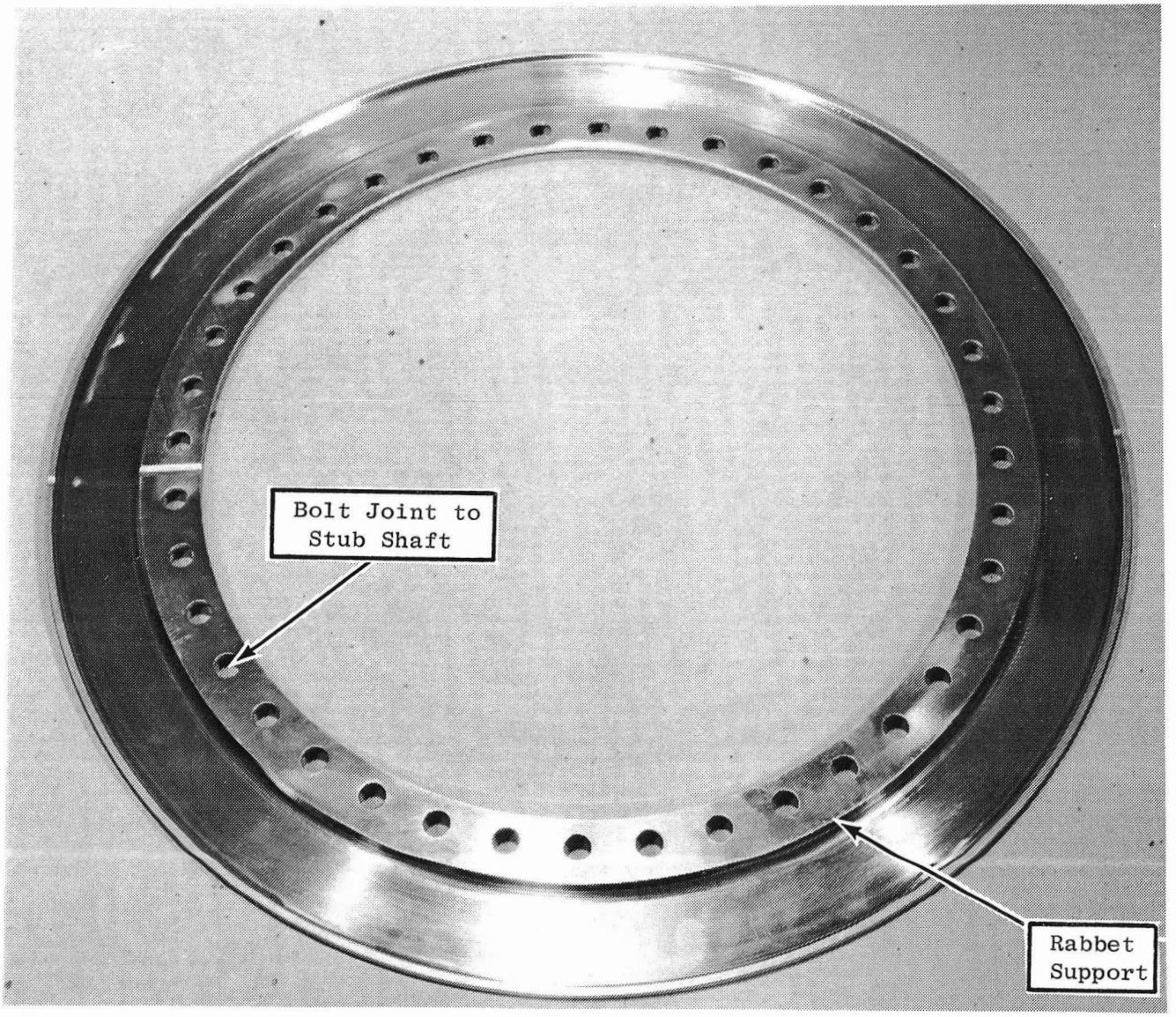

Figure 92. HPT Aft Shaft Axial Damper.

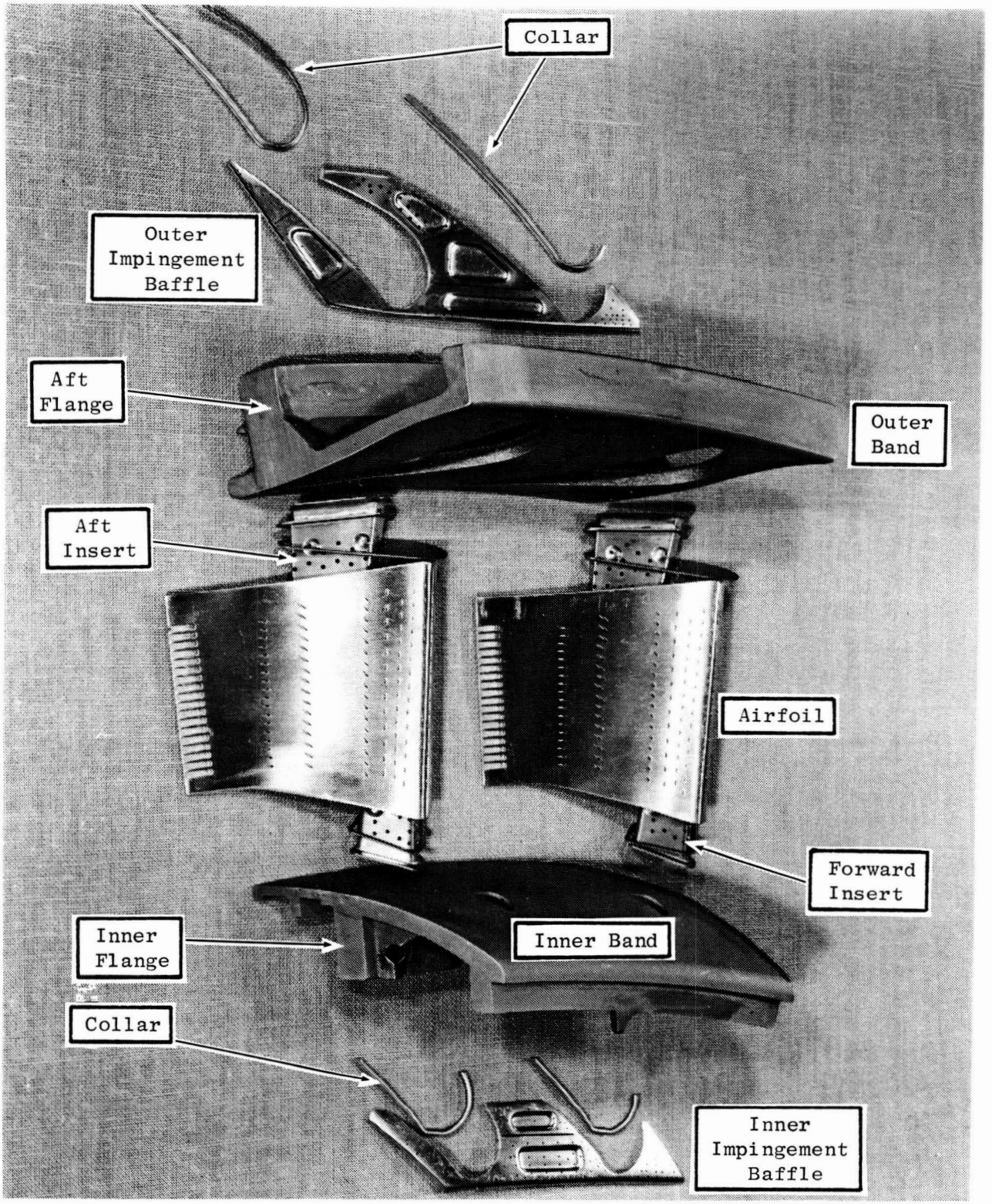

Figure 93. HPT Stage 1 Vane Major Components.

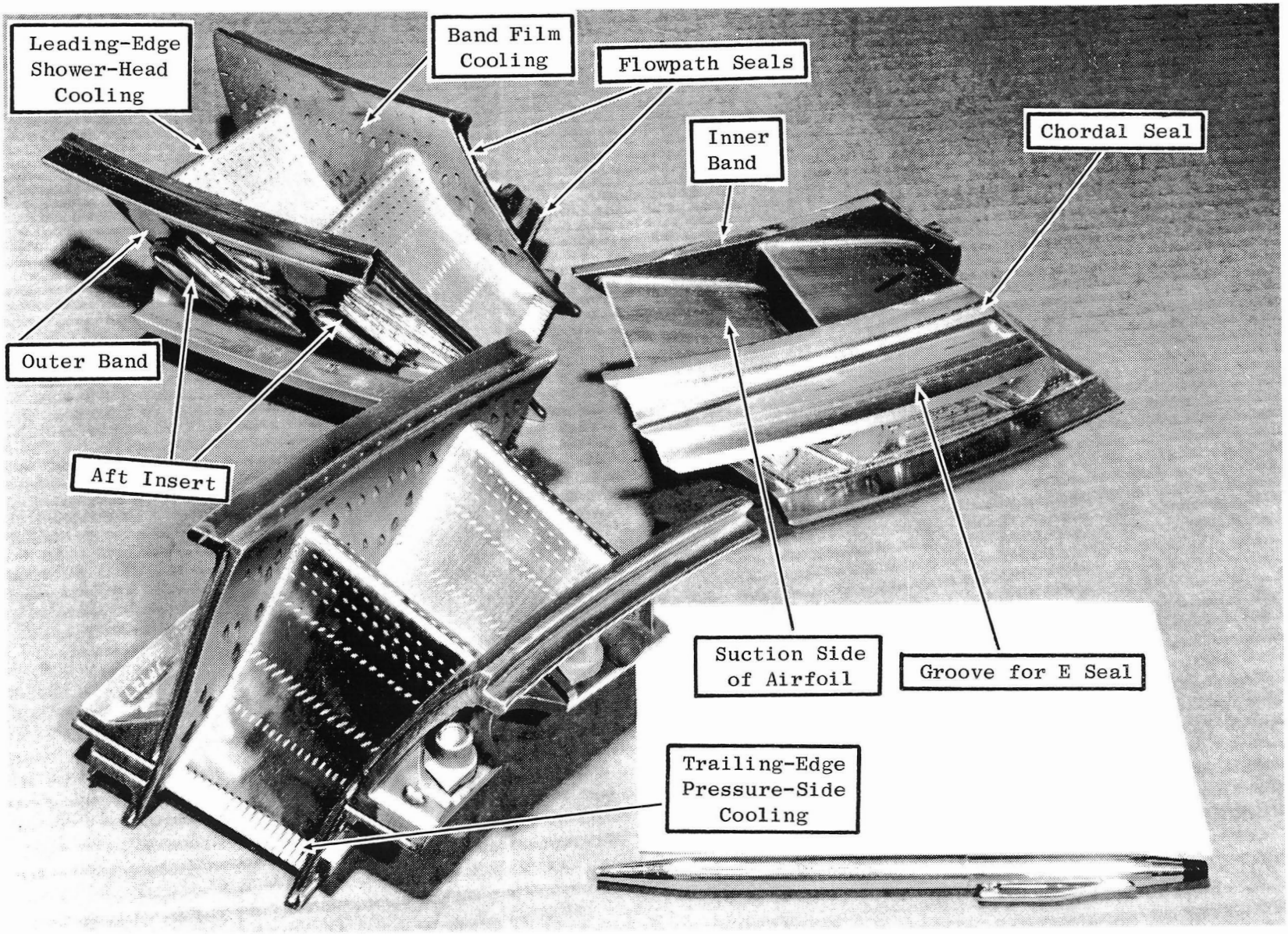

Figure 94. Fabrication of HPT Stage 1 Nozzle Segment.

2.4.8.5.2 Stage 2 Nozzle Fabrication

Technical Progress

The first set of Stage 2 nozzle segments required for the core engine was completed in January 1982. A total of 26 segments (24 required for set) were reviewed by Engineering and found to be acceptable for engine use. Figure 95 shows the nozzle parts prior to fabrication (insert not shown), and Figure 96 shows the nozzle after fabrication.

An additional 12 segments are planned to be manufactured, bringing the total number of Stage 2 nozzle segments to 1-1/2 engine sets. Sufficient airfoil and band castings are available to complete the required segments. Figure 97 shows the cast airfoil after completion of the machining process. Machine operations primarily consisted of precisely trimming the inner and outer material contour to allow the vane ends to enter an airfoil-shaped hole in the bands.

Airflow checks of the trailing edge indicated that the flow was about twice the design value. The condition was a result of oversize casting cores (i.e. core die error). A rework procedure was developed to reduce the overflow to the required level, but it could not be incorporated in the first set. The advanced state of the nozzle segments in the manufacturing cycle precluded the rework for these parts. The rework will be completed on the remaining segments on order.

Three nozzle segments were reworked for imbedded thermocouple application. The rework consisted of 0.026 x 0.026 in. EDM slots in the airfoils and bands. Similar to the Stage 1 nozzle segments, the thermocouples were applied and the grooves filled with nichrome wire and blended to a smooth surface matching the original aerodynamic contour. There were 15 thermocouples in the segments: 12 on the airfoil and 3 on the bands.

The manufacturing of the 10 additional nozzle segments has progressed through the initiation of the airfoil machining.

Work Planned

Complete the fabrication of the 10 nozzle segments.

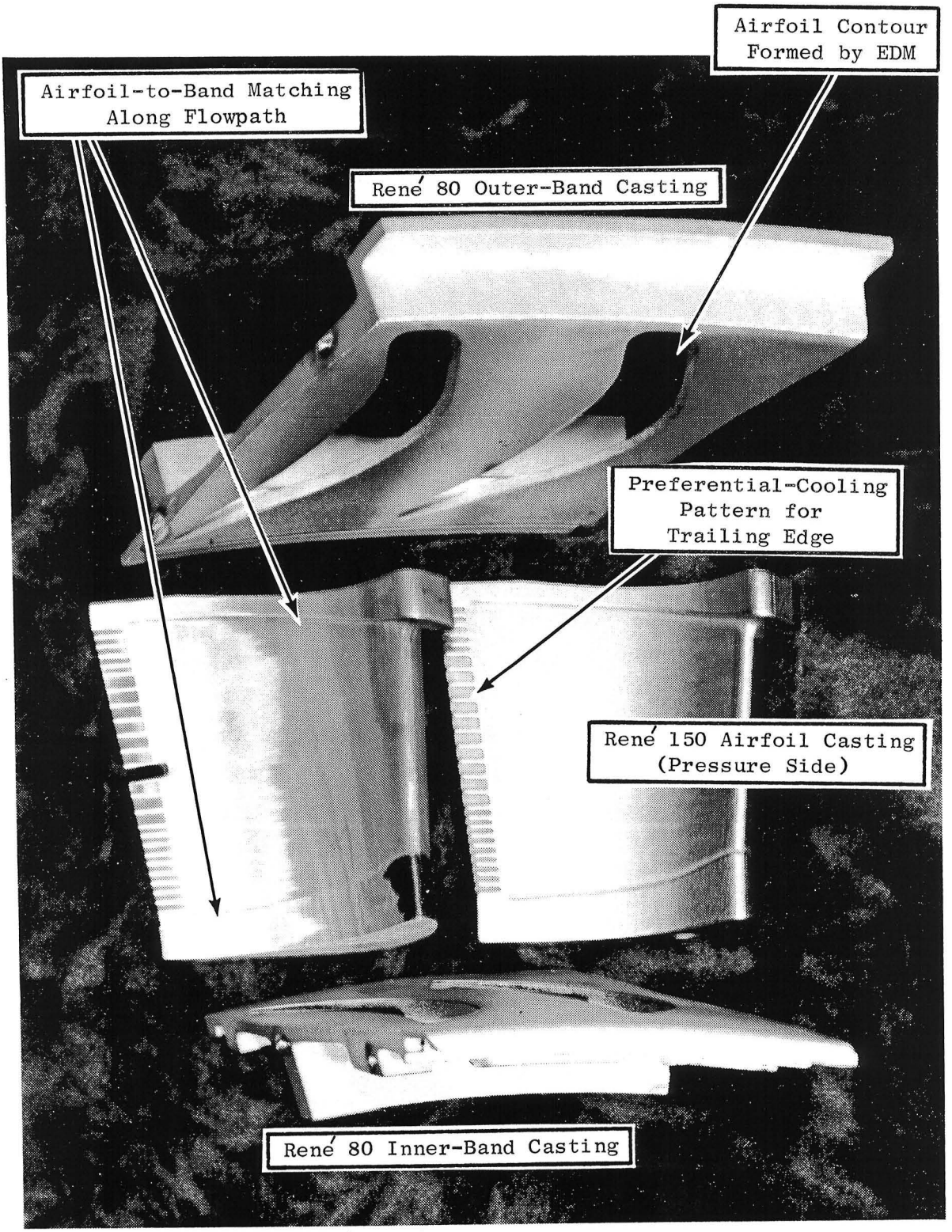

Figure 95. HPT Stage 2 Nozzle Segment Components.

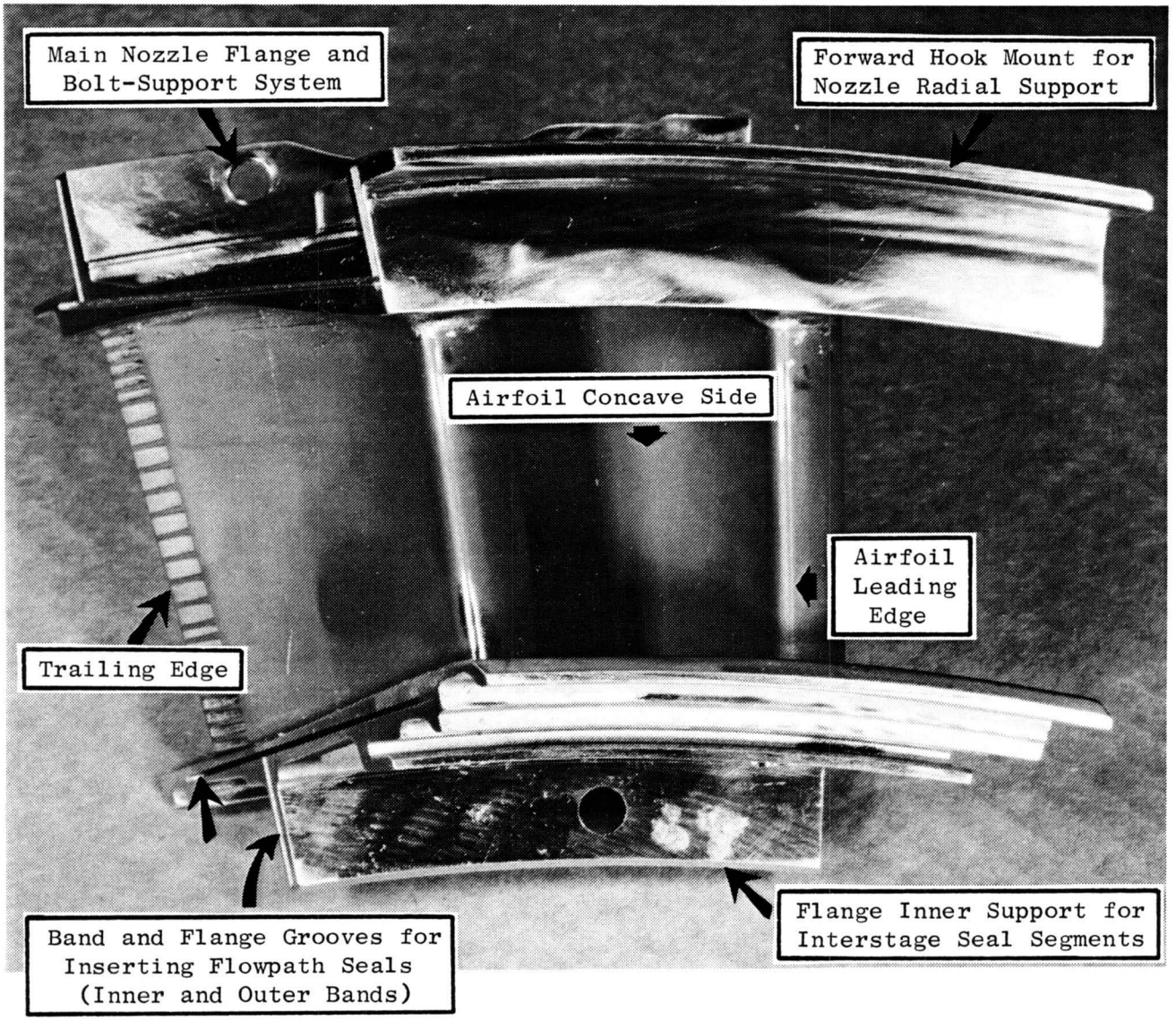

Figure 96. HPT Stage 2 Nozzle Segment after Fabrication and Machining.

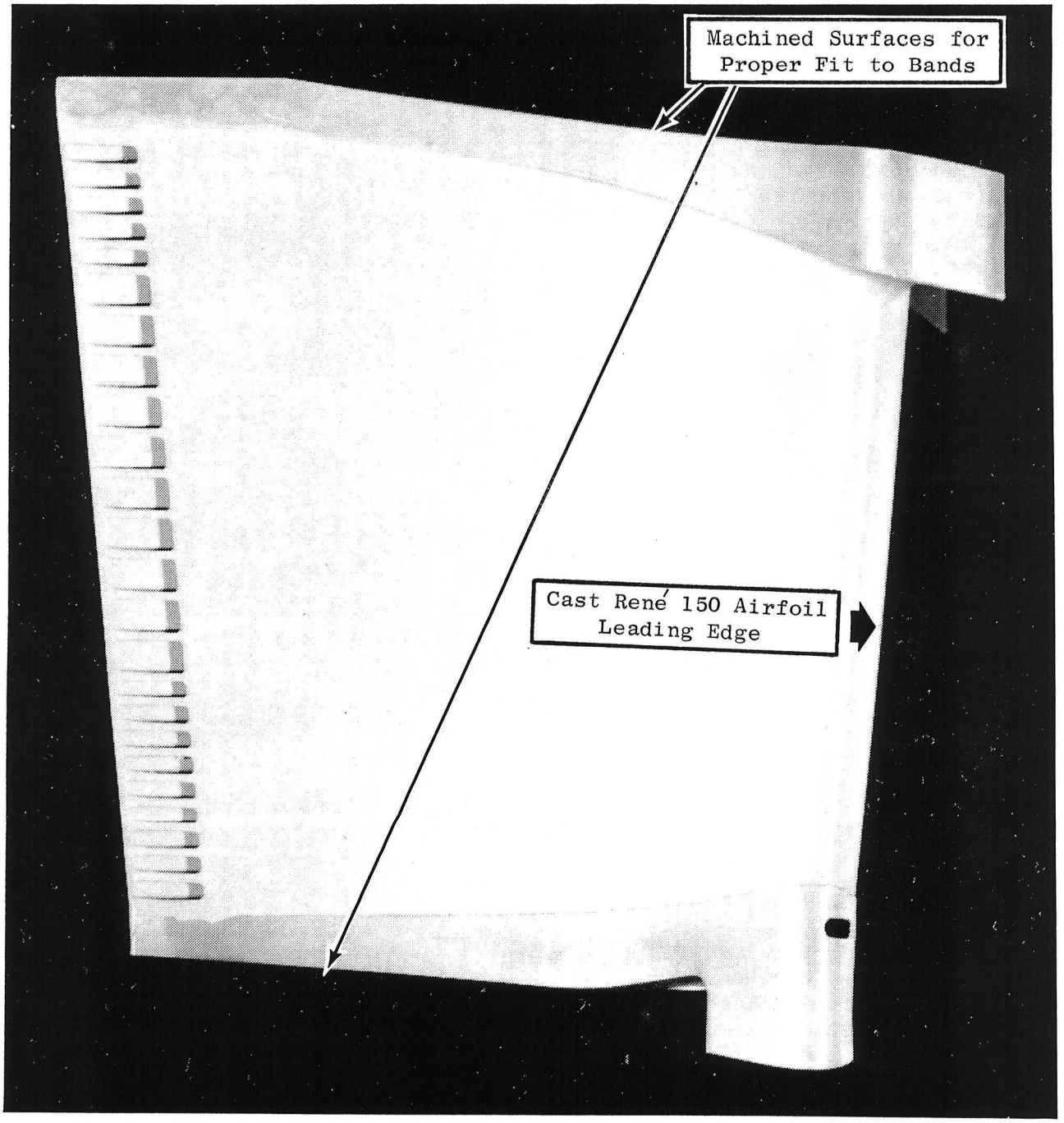

Figure 97. HPT Stage 2 Nozzle Airfoil.

2.4.8.6 Support Structures and Inducer Fabrication

Static Structures

All static structures required for the core turbine build-up were delivered. Rework drawings for instrumentation application and the actual rework were also completed. All requested instrumentation was applied to these components.

Figure 98 shows the forward casing with the ceramic and solid shrouds assembled, and Figure 99 shows the major features for the aft casing. Figure 100 is a picture of the Stage 1 shroud impingement manifold.

Active Clearance Control (ACC)

The first of two sets of ACC manifolds was delivered. Rework was completed on each of the four manifolds (four sectors per stage) for plenum pressure-measurement sensors. Figures 101 and 102 show the Stage 1 and 2 manifold sectors respectively; Figure 103 shows the Stage 1 and 2 manifold assemblies.

Ceramic Shrouds

The manufacturing and processing of 29 ceramic shrouds were completed. Twenty ceramic and four solid shrouds are required per engine set. The four solid shrouds are used to provide the mounting system for the clearance-measurement probes. Figure 104 shows the Stage 1 ceramic and solid shrouds.

An additional 26 ceramic shrouds were partially completed in preparation for spraying the ceramic coating.

Stage 1 Solid Shrouds

In addition to the ceramic shrouds, a total of 26 Stage 1 solid shrouds are also in process of manufacture. These shrouds are planned as back-up parts in addition to providing the clearance-probe mounting support. Currently, the shrouds are in process of preparation for spraying the gas-path surface with CoNiCrAlY.

Rework for instrumentation was also completed as required.

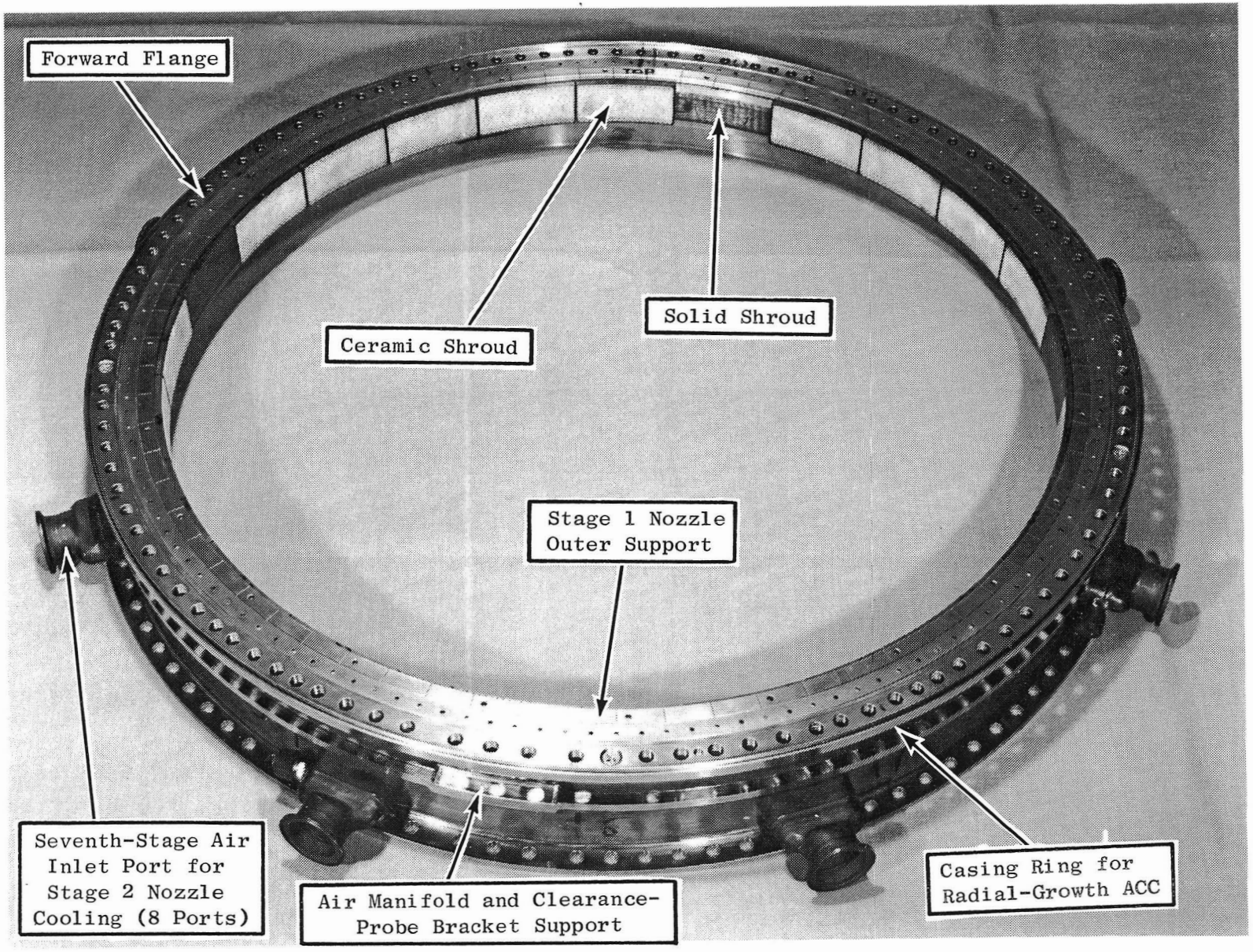

Figure 98. HPT Forward Casing Features.

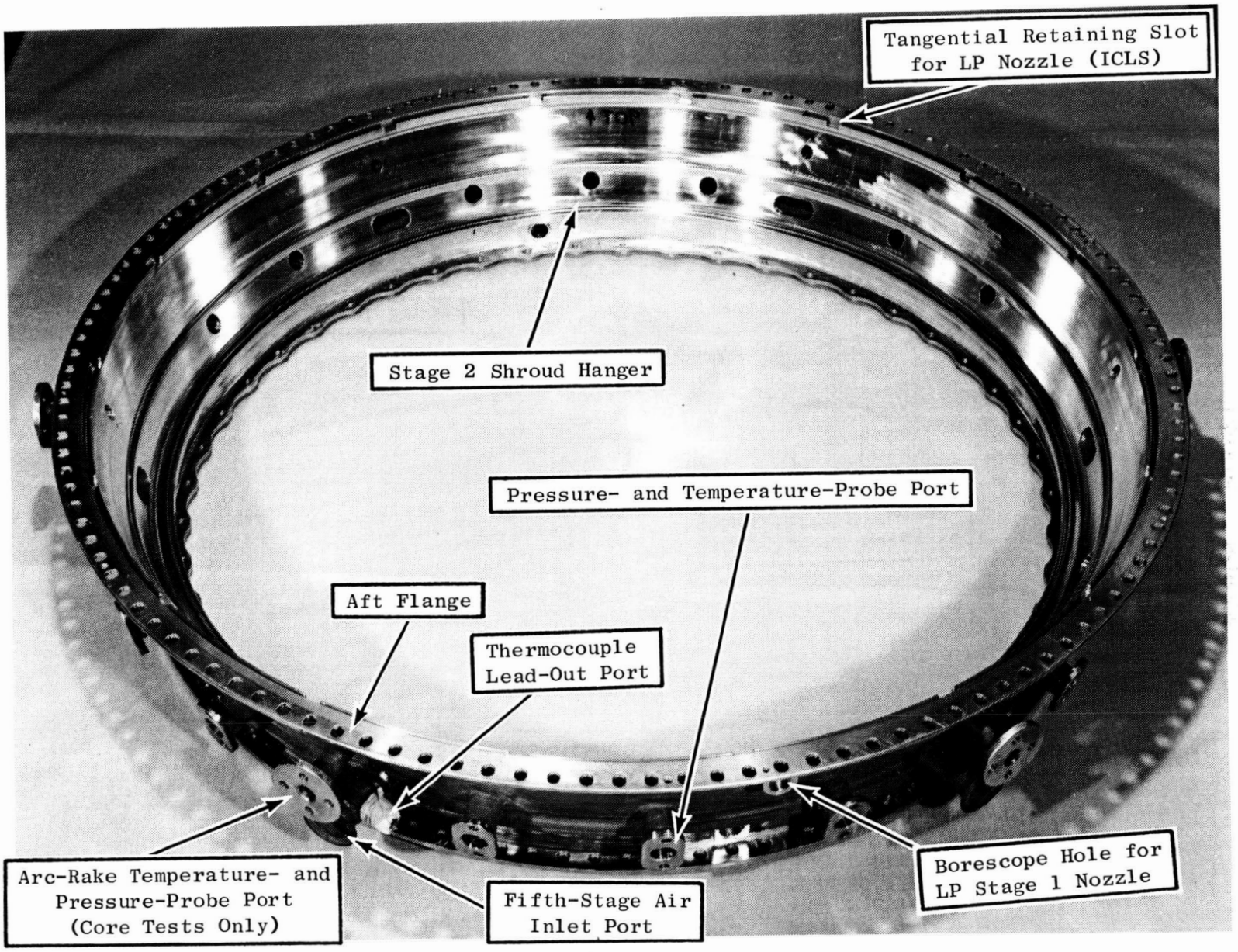

Figure 99. HPT Aft Case Features.

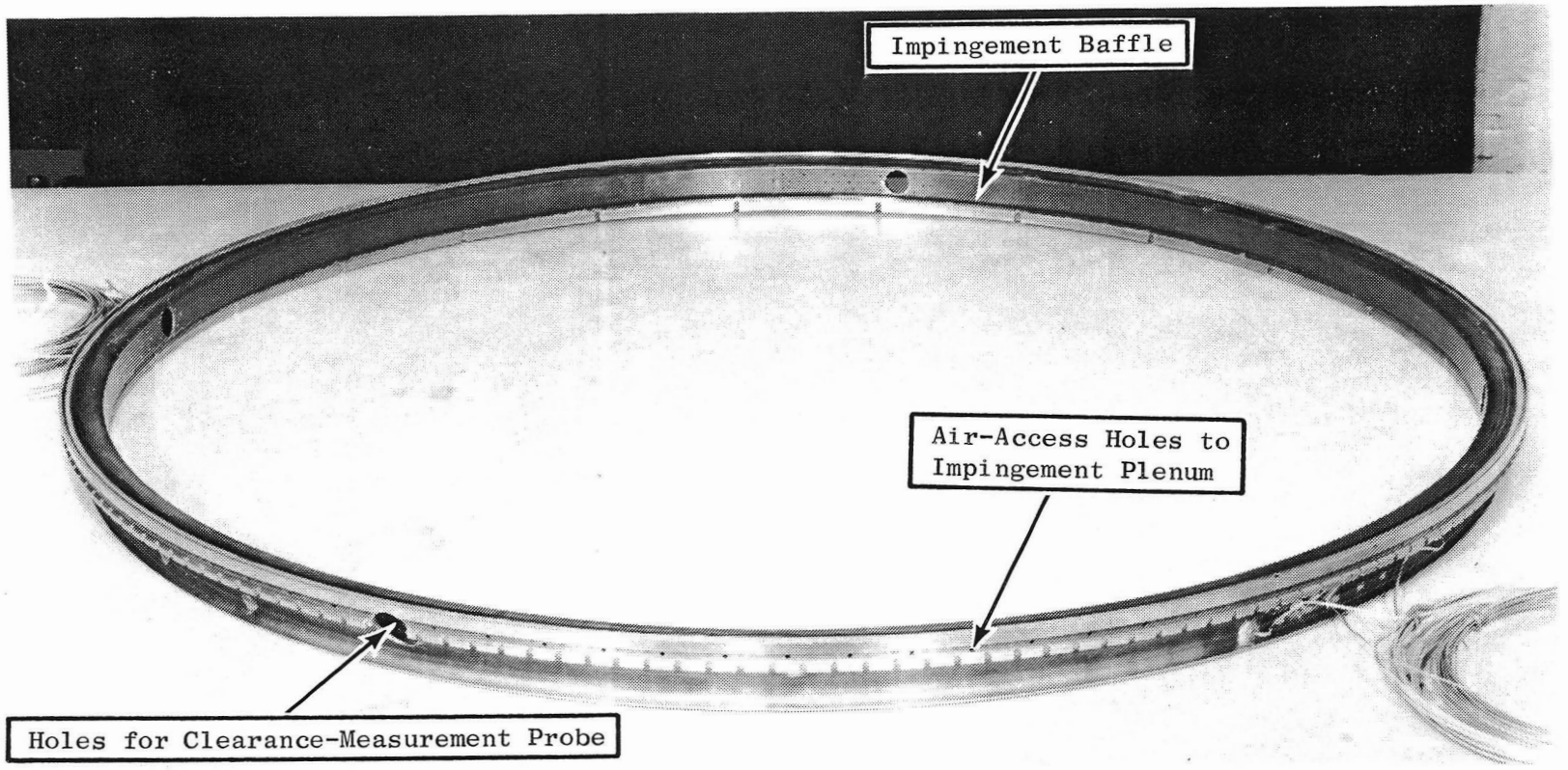

Figure 100. HPT Stage 1 Shroud Impingement Manifold.

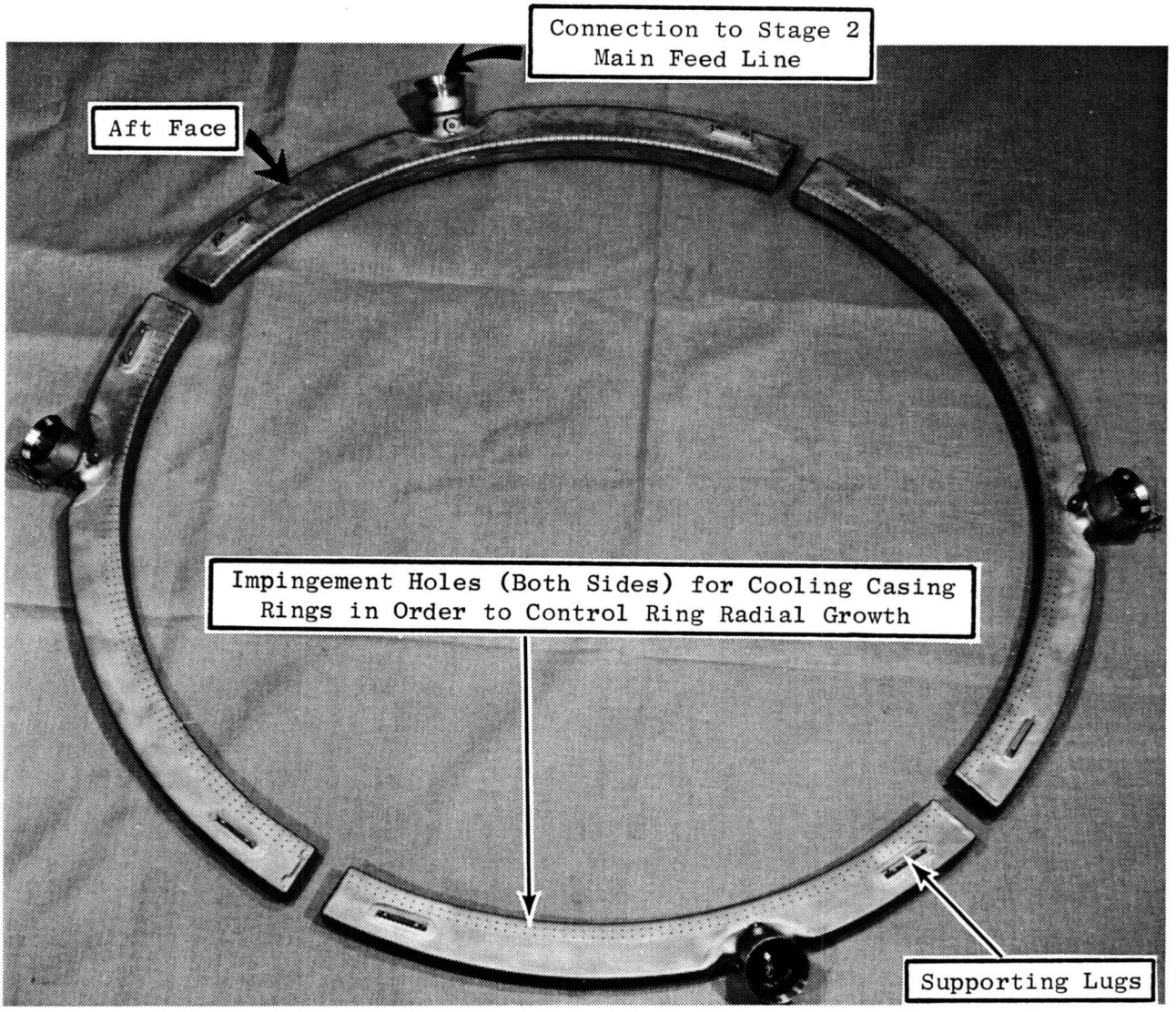

Figure 101. HPT Stage 1 ACC Manifold.

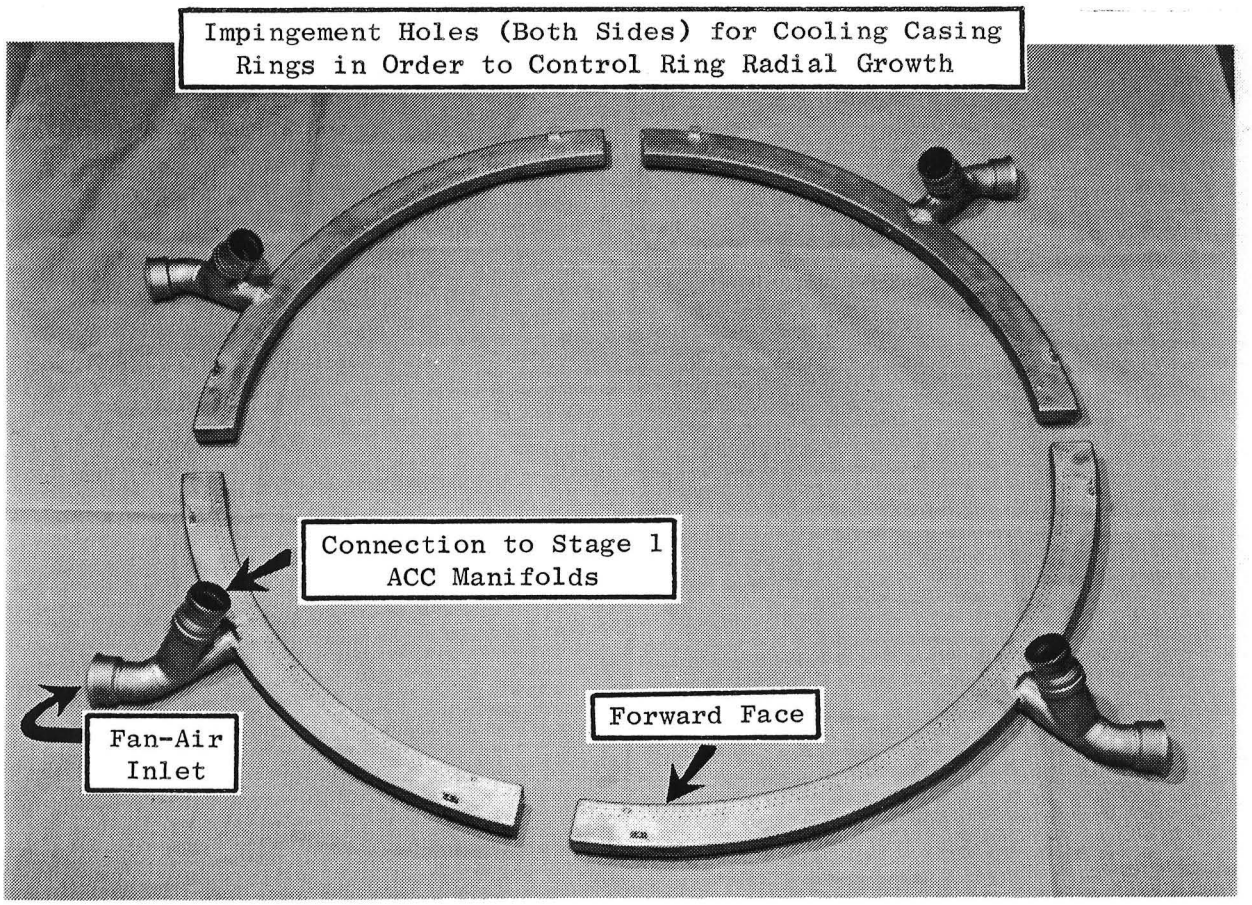

Figure 102. HPT Stage 2 ACC Manifold.

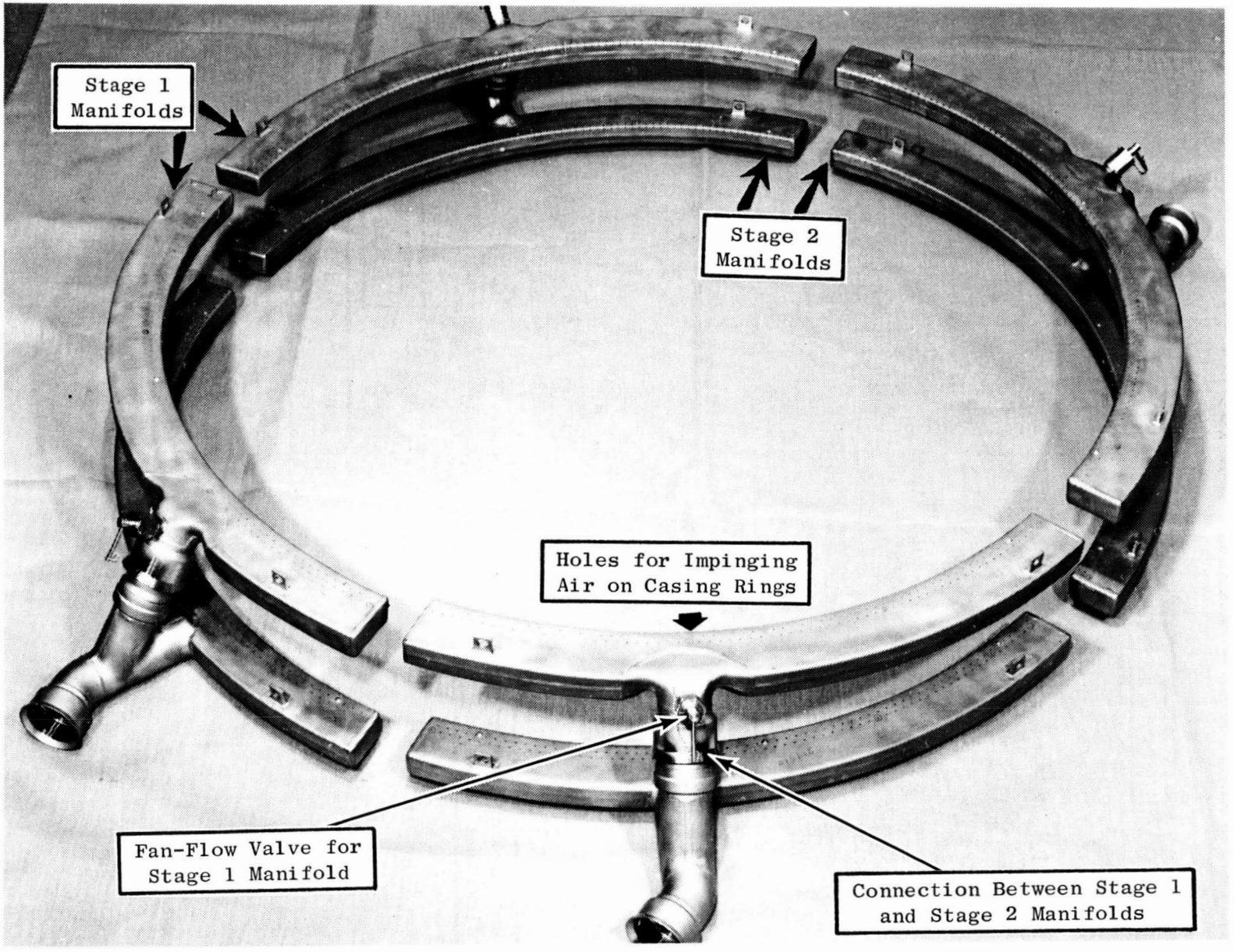

Figure 103. HPT ACC Assembly.

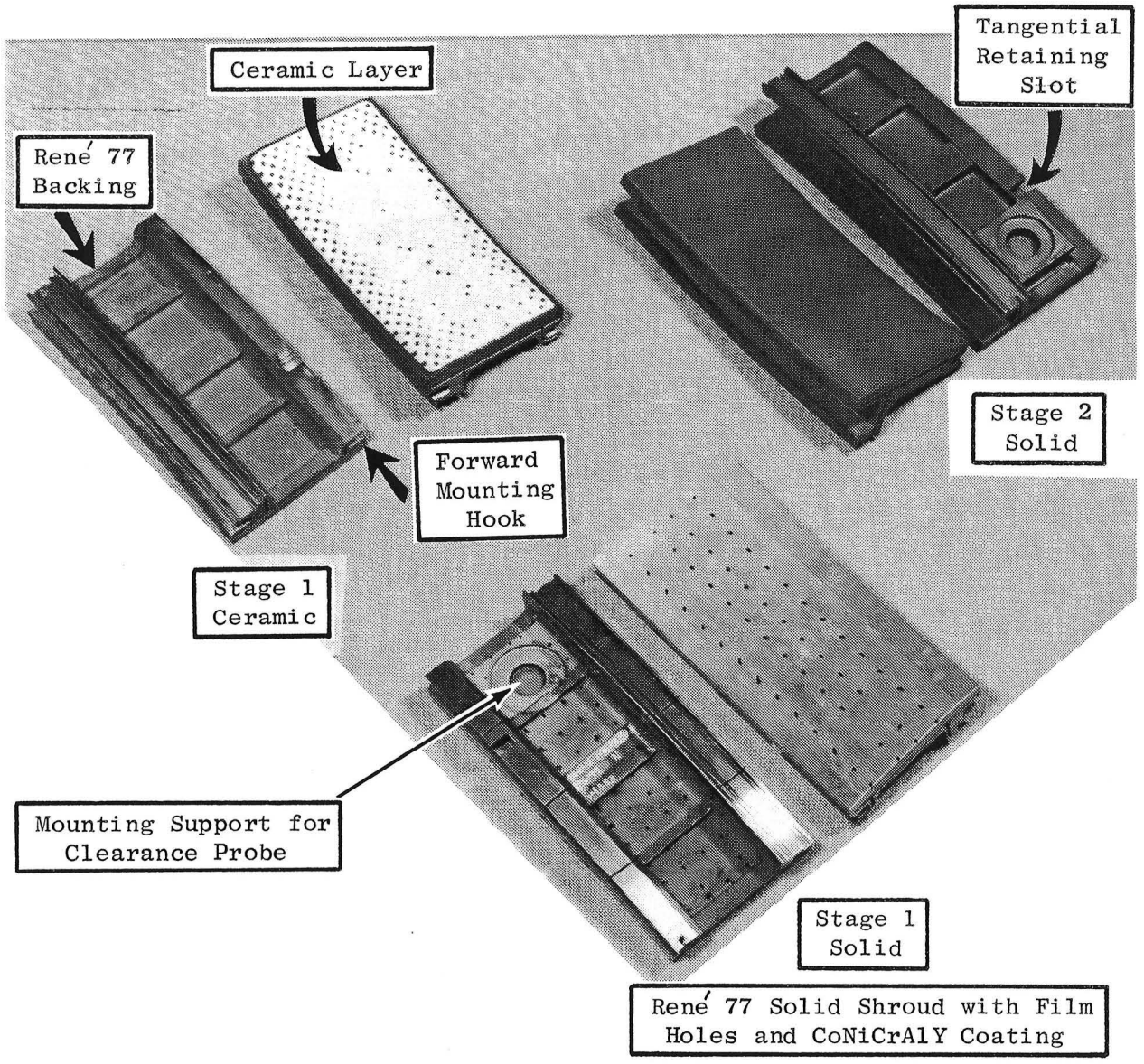

Figure 104. HPT Ceramic and Solid Shrouds.

Stage 2 Solid Shrouds

Manufacture of 26 Stage 2 solid shrouds was also completed. A total of 24 shrouds are required for an engine test. Instrumentation was applied to three shroud segments. Also shown in Figure 104 are features of the Stage 2 solid shroud.

An additional 26 shrouds are being processed for use as spares. These shrouds are presently in preparation for surface spraying with CoNiCrAlY coating.

Stage 2 Inner Seals

The Stage 2 inner seals comprise three separate parts. Each of these three components is manufactured as a six-segment component to provide one engine set. Figure 105 shows the inner-seal arrangement and relative position within the assembly. All parts have been completed.

Work Planned

Continue engineering support during the manufacture of the remaining shrouds.

2.5 LOW PRESSURE TURBINE

Overall Objectives

The objective of the low pressure turbine (LPT) development effort is to provide a highly efficient LPT having material and configuration features that provide maximum opportunity for mechanical success.

Performance improvements will be aimed at achieving the highest possible turbine efficiency compatible with moderate-to-high turbine aerodynamic loading. The FPS low pressure turbine efficiency goal is 0.917 at Mach 0.8, 35,000 feet, standard day, maximum climb power setting. Also considered are off-design operating points in order to ensure a viable system throughout the operating regime of the engine.

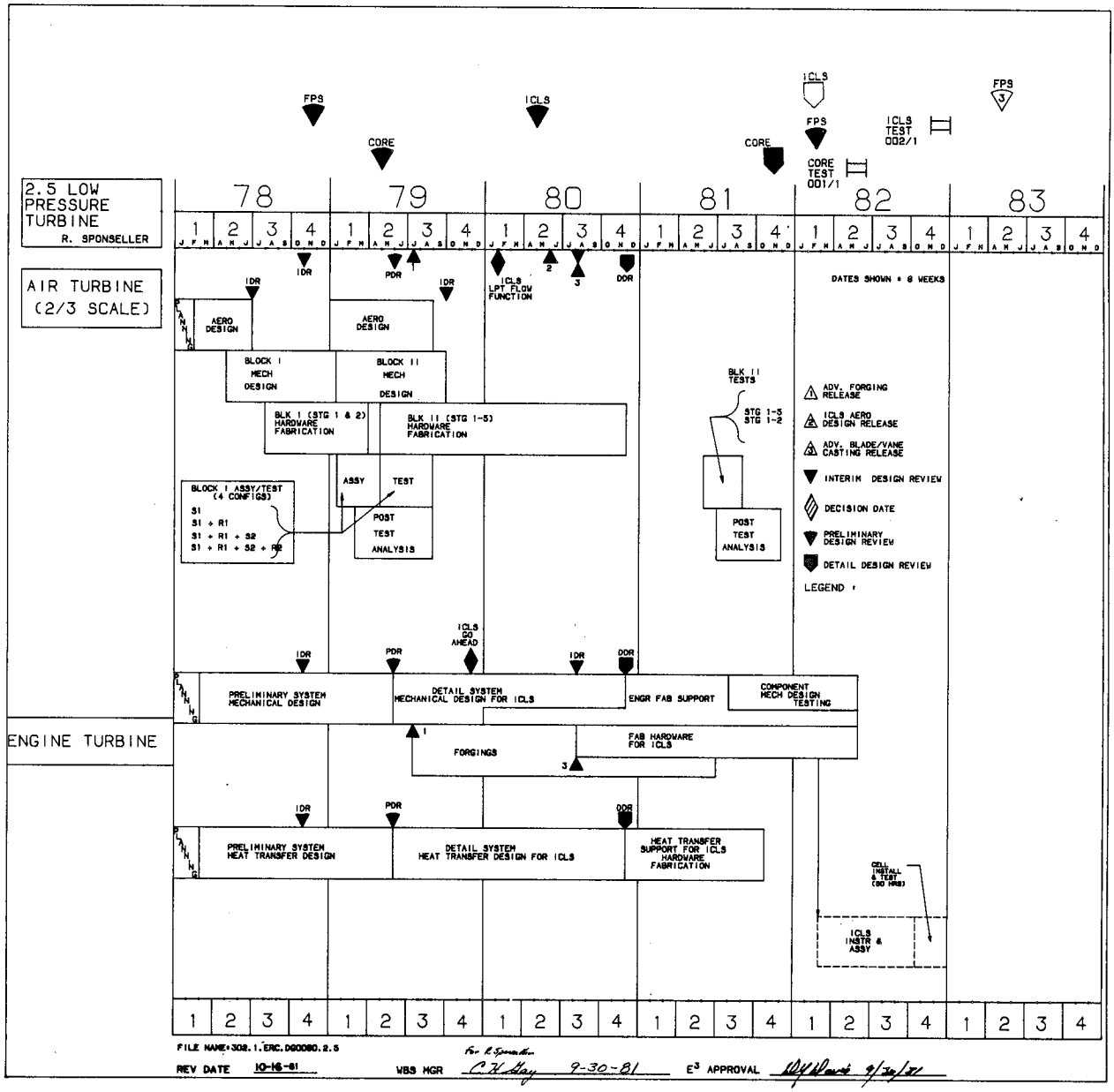
2.5 LOW PRESSURE TURBINE
R. SPONSELLER
AIR TURBINE (2/3 SCALE)
ENGINE TURBINE
78
79
80
81
82
83
FPS
CORE
ICLS
FPS
CORE
ICLS TEST 002/1
CORE TEST 001/1
FPS
IDR
PDR
ICLS LPT FLOW FUNCTION
DDR
DATES SHOWN ± 6 WEEKS
AERO DESIGN
BLOCK I MECH DESIGN
BLOCK II MECH DESIGN
BLK I (STG 1 & 2) HARDWARE FABRICATION
BLK II (STG 1-5) HARDWARE FABRICATION
BLOCK I ASSY/TEST (4 CONFIGS)
S1
S1 + R1
S1 + R1 + S2
S1 + R1 + S2 + R2
ASSY
TEST
POST TEST ANALYSIS
BLK II TESTS
STG 1-5
STG 1-2
ADV. FORGING RELEASE
ICLS AERO DESIGN RELEASE
ADV. BLADE/VANE CASTING RELEASE
INTERIM DESIGN REVIEW
DECISION DATE
PRELIMINARY DESIGN REVIEW
DETAIL DESIGN REVIEW
LEGEND :
ICLS GO AHEAD
PRELIMINARY SYSTEM MECHANICAL DESIGN
DETAIL SYSTEM MECHANICAL DESIGN FOR ICLS
ENGR FAB SUPPORT
COMPONENT MECH DESIGN TESTING
FORGINGS
FAB HARDWARE FOR ICLS
PRELIMINARY SYSTEM HEAT TRANSFER DESIGN
DETAIL SYSTEM HEAT TRANSFER DESIGN FOR ICLS
HEAT TRANSFER SUPPORT FOR ICLS HARDWARE FABRICATION
CELL INSTALL & TEST (60 MNS)
ICLS INSTR & ASSY
FILE NAME=308.1.ERC.060080.2.5
REV DATE 10-16-81
WBS MGR for R. Sponseller C.H. Gay 9-30-81
E³ APPROVAL W.H. Ward 9/30/81

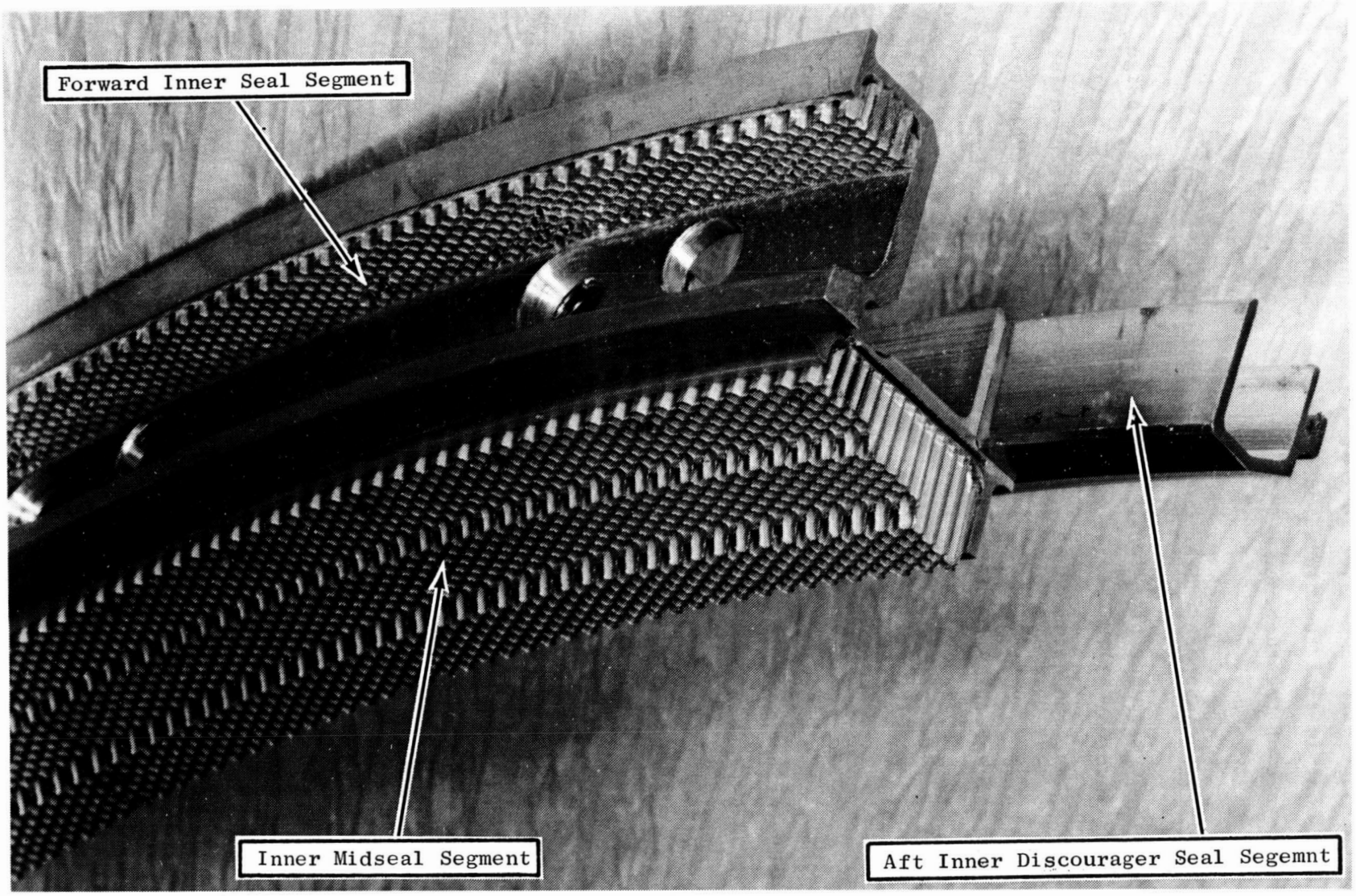

Figure 105. HPT Stage 2 Nozzle Inner Seal Arrangement.

Mechanical integrity is a major goal of the LPT mechanical design. The aeromechanical goal is that the blades and vanes have no instabilities within the operating range of the turbine.

Development Approach (Reference WBS 2.5 Schedule Sheet)

The overall development plan for the LPT provides a systematic design approach. This involves (1) early identification of critical areas and (2) component design that can accommodate the critical requirements. The major LPT development areas are (1) aerodynamic design and air turbine evaluation, (2) system and mechanical design (which is carried out concurrently with the aero work), (3) hardware fabrication, (4) component bench tests, and (5) instrumentation, assembly, and engine test.

Preliminary aerodynamic blade and vane design for the initial flowpath was the major initial effort. Other mechanical and heat-transfer design paralleled this effort, and an overall LPT IDR was held in November 1978 and followed by the LPT PDR in May 1979. Block I air turbine testing of Stages 1 and 2 was completed in August 1979. Aerodynamic modifications were factored into Block II blading and sequentially released over the period from January through March 1980. An IDR of this work was held in March 1980. Procurement of Block II hardware has been completed. Air turbine tests of all five LPT stages and two-stage air turbine testing have been completed, and data analysis is underway.

Detailed mechanical design of the engine turbine was initiated in June 1979 after the PDR milestone. The next major milestone was the ICLS go-ahead decision given in November 1979, ahead of the scheduled January 1980 date. Continuing detail mechanical design, incorporating the Block II airfoil configurations, was summarized for an August 1980 IDR, and a DDR was held in December 1980. Release of fabrication orders began in September 1980 with cast parts, although advanced forging releases had been made as early as June 1979. All ICLS engine hardware has been released for procurement, and initial finished parts are starting to be received. The earliest manufactured blades and vanes will be uitilized for bench testing. Bench testing will allow identification of responsive locations where instrumentation will be

applied on the airfoils. All components will then be assembled into the ICLS demonstrator; testing is scheduled for the last quarter of 1983.

2.5.1 LPT Aerodynamic Design

Technical Progress

During this reporting period all Block II data reduction and analysis were completed. A detailed performance map based on five-stage rig test results was prepared and fitted for inclusion into the ICLS cycle deck, and work began on the Block II Test Memo.

Block II data analysis revealed some minor problems that have necessitated reprocessing some of the test results. The two most prominent items affecting data quality which were corrected during the course of this reprocessing were: (1) erratic rig-inlet temperature, which for some off-design points had exhibited a level shift of about 1.5 degrees, and (2) a drift in primary-pressure transducer zero (signal at no load) for some off-design points.

The shift in primary-transducer zero required that all data be reprocessed using pressures measured by the redundant scanivalve transducers. The effect of this reprocessing on design-point data was to slightly raise the level of efficiency from an average of 91.93% to 92.0%.

Results of the Reynolds number excursion on the five-stage rig have now been fully assimilated and affirm the 0.7% loss in design-point efficiency expected for altitude-climb operation.

Final ICLS performance for the LPT at the equivalent of the Mach 0.8/ 35,000-ft, max-climb condition, based on rig test results, is as follows:

η_{TT} base	92.0%
$\Delta\eta$ purge air	0.1%
$\Delta\eta$ Reynolds No.	-0.7%
	91.4%

This is relative to program goals of 91.1% for the ICLS and 91.7% for the FPS.

Work Planned

During the next reporting period the Block II Test Memo and the Test and Performance (formal) Report will be issued.

2.5.3.4 LPT Hardware and Test Support

LPT Assembly Drawings and Balance Requirements

The assembly drawings were completed in October 1981 for the LPT rotor/stator assembly (P/N 4013296-305) and the LPT Stage 1 nozzle assembly (P/N 4013296-304). Balance requirements have been specified on the LPT rotor/stator assembly.

A stack-up drawing of the LPT has been made and is in engineering review. All major clearance values between adjacent LPT components will be defined.

LPT Instrumentation Rework

Instrumentation rework requirements for the ICLS LPT were defined after coordination between Design, Evaluation, and Instrumentation Engineering.

Eight blades per stage for each of the five stages will be instrumented with thermocouples and strain gages. The rework will consist of simple holes and slots through the blade platforms. No material rework is required on the airfoil regions of the blade.

Each of the rotor disks as well as the two forward-most rotor seals will be instrumented with thermocouples. The rework geometry was determined after a study of the lead paths required and the potential effects on component life. The final rotor rework consists of simple holes located in low-stressed regions such that the calculated LCF life of the rotor will not be reduced.

On the static parts, locations were identified for the placement of thermocouples on the transition ducts and seals, the nozzles, the casing, and the ACC manifold. This instrumentation will be used primarily for clearance/cycle

correlation with pretest predictions although selected locations will be monitored for safety/life engine test data.

Shop modification drawings which define instrumentation rework hardware have been issued for all LPT components that require rework and have been incorporated into the respective hardware orders. Rework has been completed on the forward and aft inner-seal supports, the four rotor disks, and the two rotor seals.

Instrumentation bosses have already been included in the fabrication of the LPT casing and will require no further instrumentation rework on the LPT casing.

Work Planned

- Continue to provide engineering support to the vendors
- Follow the hardware through ICLS engine build
- Review and sign-off on assembly/instrumentation drawings
- Complete and issue assembly clearance drawings
- Complete instrumentation rework of the LPT blades and stator hardware

2.5.4 LPT Mechanical Design Testing

Bench Blade Tests

Blade fixtures for both the hot-fatigue and the vibration testing have been received. Testing will begin after machined blades are received. Delivery is planned for April 30, 1982.

Several Stage 5 blades with machined dovetails were trial fitted into the hot-fatigue and vibration fixtures. They fit very well; all the blade dovetail pressure faces contacted the fixtures.

Nozzle Bench Tests

Planning continues for bench testing of the LPT nozzles. Due to the complexity involved in simulating nozzle-casing system modes of vibration, a

decision was made to test only for nozzle airfoil and overhang material frequencies. This will be accomplished by casting the nozzle support hooks in a rigidizing material (Kirksite).

A test project sheet (TPS) is now being formulated to initiate detail planning of the nozzle tests.

Work Planned

- Receive machined blades and complete blade bench testing
- Complete nozzle TPS and frequency testing

2.5.6.1 LPT Rotor (Bench Blades and Tooling)

Technical Progress

The majority of the work during this reporting period has been related to hardware procurement. All blade castings have been received, and machining of the castings has been initiated.

Castings

The full order of blade castings for all five stages was completed during this reporting period. The quality of the castings was very good. Airfoil contours were smooth, continuous, and met drawing tolerance requirements. Minor die dimensional errors were identified in the early castings and corrected in time to pour good parts for the full order. One and one-half sets of castings per stage were delivered to the machining vendors. One set of completed blade castings is being held in reserve.

Machining

Machining is progressing on all five stages with completion scheduled for the end of April 1982. Some chipping of the edges of the Triballoy T800 hard coat on the tip shroud occurred while grinding the Stage 5 blades (see Figure 106). The suspected cause of the chipping is vibration and/or shearing of the coating when the grinding wheel starts cutting, as shown in Figure 107. Discussions with the machining and thermal-spray vendors plus bonding checks of the coating have led us to believe that the remaining coating is good.

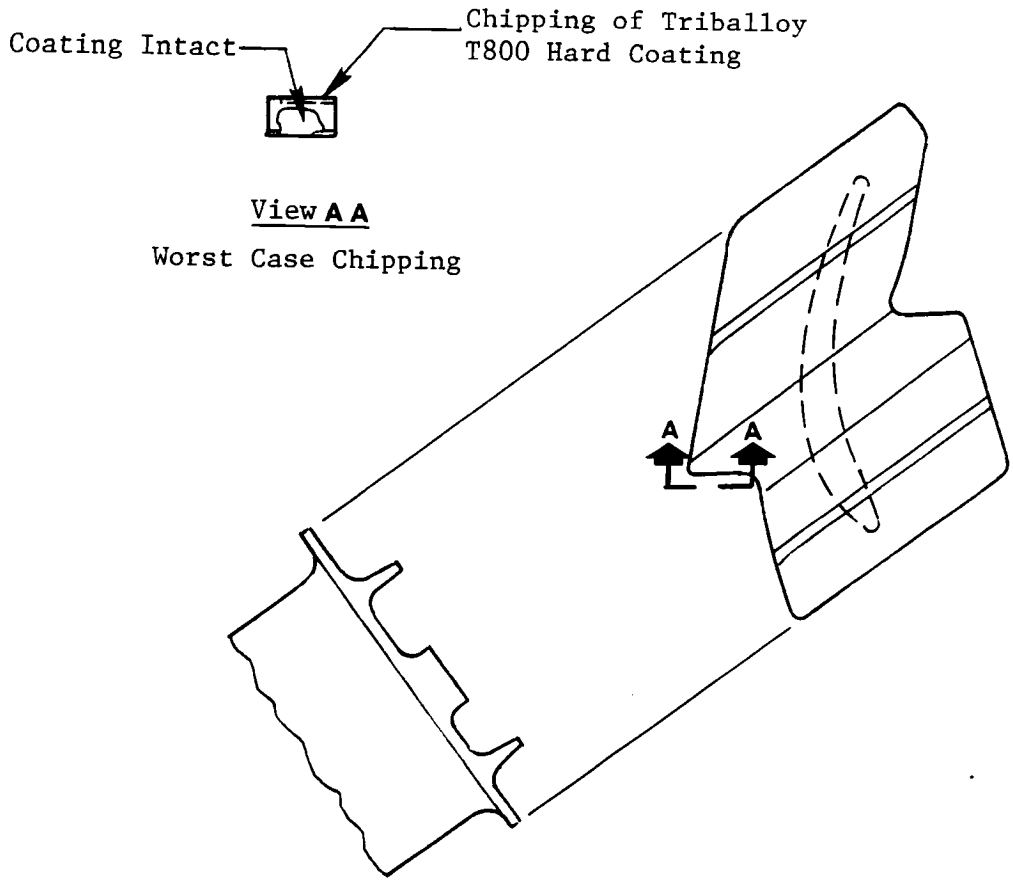

Figure 106. Top View of Stage 5 LPT Blade Tip Shroud.

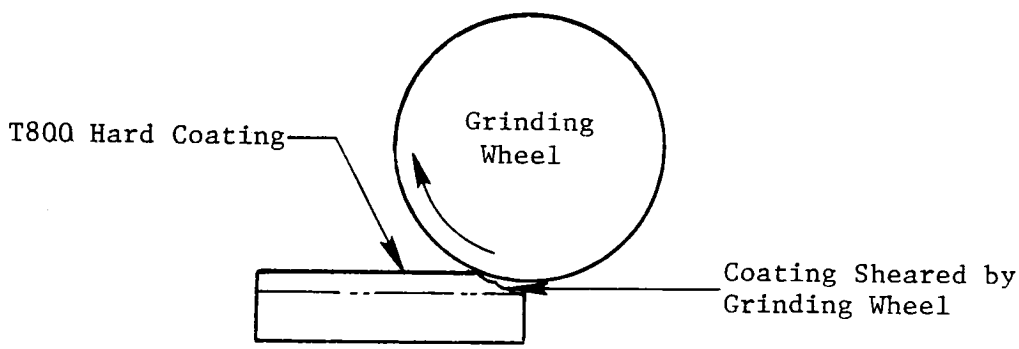

Figure 107. Chipping of Triballoy T800 Hard Coating when Grinding.

Projected engine operation of these blades shows that the contact stress in the hard coat will be increased somewhat by the reduction of contact area (30% max) caused by chipping. The original contact stress was calculated to be 60% of the maximum allowable values. Therefore, even with the most reduced contact area, the contact stress will be within the design limit, and Stage 6 blades are acceptable for engine testing. In addition, the 16 worst blades will be used for bench testing and will not be used in ICLS engine evaluation.

Machining and thermal-spray vendors of the other stages are aware of the chipping incident and will resolve it before the other stages are machined.

The Stages 1 and 4 blade dovetails have been machined, and the tip shrouds have been thermal-sprayed with Triballoy T800. They are now ready for final grind of the hard-coat area of the tip shroud.

Tooling for the Stages 2 and 3 blades is being completed.

Work Planned

- Continue to monitor vendor progress
- Finish machining of the blades
- Follow hardware through instrumentation and engine build

2.5.6.2 LPT Stage 1 Nozzle

Technical Progress

The review of the first Stage 1 nozzle casting at TRW in mid-November revealed dimensional discrepancies in the inner rail and booking faces, but they appeared very good under metallographic examination. Production was deferred while wax dies were reworked to correct the dimensional problem. A verification review of a new casting from the modified dies was held in mid-January and provided sufficient data to release 25 nozzle castings to be shipped by March 31, 1982. This timing is necessary to meet our commitment.

TRW cast 16 Stage 1 nozzle segments in February 1982 and had another 22 shells ready for pouring before discovering a new problem: hot tearing in the nozzle inner band. The vendor has now developed a procedure to eliminate the

problem. Ten castings without tears are now in process, and another 18 shells are ready for pouring.

The Stage 1 nozzles will be machined in AEMO (in-house Advanced Engine Machining Operation). Fixturing required to machine the castings is on schedule for delivery ahead of the March 31 casting shipping date.

Work Planned

- Work with casting vendor to supply Stage 1 nozzle castings on schedule
- Provide engineering support during nozzle machining and instrumentation rework
- Trial fit-nozzle machinings with attaching hardware
- Flow-test machined nozzle
- Follow hardware through instrumentation and engine build

2.5.6.3 LPT Stages 2 Through 5 Nozzle Fabrication

Technical Progress

The Stages 2 through 5 nozzle castings order has been completed at Misco and has been shipped to Johnson Mold for machining. Machining has been initiated on all four stages. No problems have been experienced to date at the machining vendor. Completed nozzles, including nozzles reworked for instrumentation, have been promised well in advance of the required date for instrumentation and engine assembly.

Work Planned

- Continue to provide hardware support to the Stages 2 through 5 machining vendor
- Deliver parts for frequency tests of Nozzles 2 through 5
- Trial fit completed nozzles in attaching hardware
- Follow hardware through instrumentation and engine build

2.6 TURBINE FRAME AND MIXER

Overall Objectives

While the E^3 design is based on experience with proven engine frames to ensure a long-life and maintainable structure, the E^3 frame has been specifically designed with improvements to meet the FPS requirements.

Performance improvements in engines with confluent exhaust nozzles can be achieved by forced mixing of the core and fan flows. A convoluted mixer is planned for the FPS to mix effectively the hot, high-velocity, core gas with the relatively lower velocity fan air to produce a more uniform velocity at the nozzle throat and improved thermodynamic cycle efficiency. The FPS mixer effectiveness goal is 0.75 at Mach 0.8, 35,000-ft altitude, standard day, maximum-cruise power setting.

Development Approach

Current technology related to the aerodynamic design of high-bypass mixers is not fully developed. Excellent computer techniques are available which allow good aerodynamic flowpath design in terms of low pressure losses with no separation. However, adequate design criteria that provide guidance for selecting a mixer with high mixing effectiveness and low pressure loss do not exist. Thus the first step in the development of a high-performance mixer for the E^3 was to establish a data base from which an advanced-technology, high-performance mixer may be designed.

A scale-model mixer parametric test was conducted early in the E^3 program. The models, 12% scale, were tested in a static thrust stand at both cold-flow and simulated hot-flow conditions. Selected mixer geometric parameters were systematically varied and tested in order to identify those parameters which significantly impact mixing effectiveness. The mixer models selected were consistent with the E^3 thermodynamic cycle and were within practical mechanical and installation constraints. Results of this test identified initial mixing effectiveness and pressure-loss design criteria.

Following the parametric test, five of the scale models were evaluated for noise characteristics. Results of the acoustic tests indicated a 2 to 4

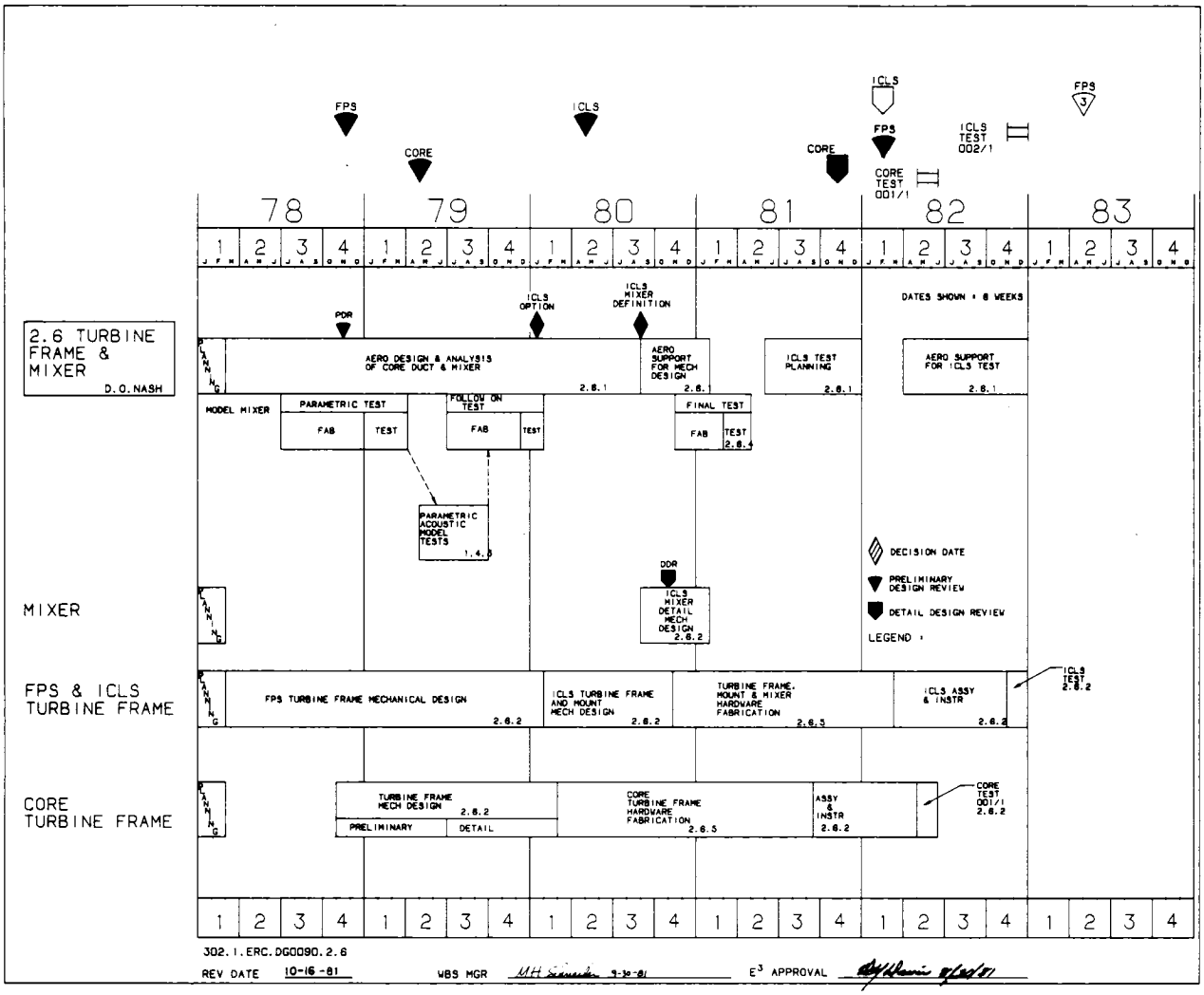
FPS
CORE
ICLS
ICLS
FPS
CORE
ICLS TEST 002/1
II
CORE TEST 001/1
II
FPS 3
78
79
80
81
82
83
1 2 3 4 J F M A M J J A S O N D
DATES SHOWN + 6 WEEKS
PDR
ICLS OPTION
ICLS MIXER DEFINITION
2.6 TURBINE FRAME & MIXER
D.O. NASH
PLANNING
AERO DESIGN & ANALYSIS OF CORE DUCT & MIXER
2.6.1
AERO SUPPORT FOR MECH DESIGN
2.6.1
ICLS TEST PLANNING
2.6.1
AERO SUPPORT FOR ICLS TEST
2.6.1
MODEL MIXER
PARAMETRIC TEST
FAB
TEST
FOLLOW ON TEST
FAB
TEST
FINAL TEST
FAB
TEST
2.6.4
PARAMETRIC ACOUSTIC MODEL TESTS
1.4.3
DECISION DATE
PRELIMINARY DESIGN REVIEW
DETAIL DESIGN REVIEW
LEGEND :
MIXER
PLANNING
DDR
ICLS MIXER DETAIL MECH DESIGN
2.6.2
FPS & ICLS TURBINE FRAME
PLANNING
FPS TURBINE FRAME MECHANICAL DESIGN
2.6.2
ICLS TURBINE FRAME AND MOUNT MECH DESIGN
2.6.2
TURBINE FRAME, MOUNT & MIXER HARDWARE FABRICATION
2.6.3
ICLS ASSY & INSTR
2.6.2
ICLS TEST
2.6.2
CORE TURBINE FRAME
PLANNING
TURBINE FRAME MECH DESIGN
2.6.2
PRELIMINARY
DETAIL
CORE TURBINE FRAME HARDWARE FABRICATION
2.6.3
ASSY & INSTR
2.6.2
CORE TEST 001/1
2.6.2
1 2 3 4 1 2 3 4 1 2 3 4 1 2 3 4 1 2 3 4 1 2 3 4
302.1.ERC.DG0090.2.6
REV DATE 10-16-81
WBS MGR
9-30-81
E3 APPROVAL

PNdB noise reduction relative to the separate-flow exhaust nozzle. Additionally, no discernible difference in noise level was observed for the various mixers tested. Thus noise generation did not affect the selection of the final mixer design.

Results of the mixer parametric test have been used to design and fabricate scale models for a follow-on mixer performance test. This test was aimed at evaluating overall mixer/exhaust-system variables with more emphasis on the total E^3 exhaust system. The follow-on test was added to the original program and was intended to provide the design information necessary to achieve an additional 10% mixing effectiveness (75%) relative to the original program goals (65%). Results of the follow-on tests identified significant exhaust-system-performance characteristics leading to performance improvements and also pointed out the significance of mixer sidewall shape on mixer performance.

Because of the discovery of the significance of mixer sidewall shape on performance in the follow-on test, the verification test was expanded to investigate mixer shape. Additionally, it has been determined that a change to the flowpath in the last several stages of the turbine and turbine frame can improve the mixer performance by an estimated 0.2% sfc at Mach 0.8 maximum cruise. This change was called the flared turbine design, and it was decided that it would be desirable for an FPS design but not timely for the ICLS flowpath. Thus the verification test included a selected best design of the ICLS flowpath based on the previous tests and analytical studies and a continued mixer investigation on the flared turbine FPS flowpath design. The 12-lobe ICLS mixer was tested over a range of operating conditions covering low-power sea level static (SLS) to maximum-power altitude cruise. Three FPS flared turbine mixers and three additional mixer cutbacks were tested at the cruise condition. Several of the FPS designs met or exceeded the 75% goal mixing effectiveness. One of the FPS mixers was selected for simulated-reverse-thrust testing. Phase III test results were factored into the ICLS performance predictions and final FPS design selection.

After the successful completion of the mixer verification tests, the detailed mechanical design of the mixer for the ICLS test vehicle was conducted. This design included an acoustic-excitation analysis to establish

that no acoustic vibration conditions exist which would result in fatigue life less than the design life of the part. The analysis was carried out by determining the elastic and dynamic characteristics of the panel in question by use of the MASS computer program. These results, together with a damping factor based on the type of construction and the predicted or measured acoustic-pressure levels, were entered into RANDEX, a computer program for predicting the response of structures to random excitation. From RANDEX, the expected root mean square (RMS) cyclic panel stress levels were obtained.

The design of the E^3 turbine frame initially involved preliminary layouts and analysis to ensure an adequate radial spring constant. The detail design of the turbine frame involved detailed stress analysis under limiting frame-load conditions such as flight-maneuver extremes, rotor imbalance, and transient start-up conditions. Analysis of these load and thermal-stress conditions was accomplished by use of a three-dimensional, finite-element computer program: Mechanical Analysis of Space Structures (MASS). By using enough nodes in setting up the analytical model, the elastic behavior and stress levels existing under any combination of loading and thermal stress can be determined. Metal temperature distributions, for use in the MASS analysis, were determined by a transient heat transfer analysis computer program.

The NASA Project Manager has approved the detailed design, and the full-scale turbine frame and mixer are being fabricated. After completion of the manufacture, the hardware will be available for engine assembly.

2.6.1 TRF/M Aerodynamic Design

Technical Progress

The mixer/exhaust-system flowpath for the FPS was selected based on analysis of the Phase III mixer test results, WBS 2.6.4. The configuration has 18 lobes with scalloped sidewalls and a mixer penetration of 45%. The performance at Mach 0.8, 30,000-ft, max cruise is summarized and compared against the program goals and the ICLS engine demonstrator projection in the following tabulation:

	Goal	ICLS	FPS
% Mixing Effectiveness	75	72	79
% Mixer Pressure Loss	0.2	0.66	0.57
% SFC Improvement*	3.07	2.22	2.62

*Relative to no mixing

The FPS mixer definition was provided to mechanical design and drafting for incorporation into the hot flowpath drawing.

The FPS mixer aerodynamics DDR was completed and presented at NASA Lewis on November 19, 1981.

Work Planned

Provide aerodynamics support for the turbine rear frame and mixer as required.

2.6.2 Turbine Frame and Mixer Mechanical Design and Analysis

Technical Progress

A cross section of the ICLS engine exhaust system is shown in Figure 108. One significant design change has been incorporated into the turbine frame/mixer hardware during the subject reporting period. This change involved increasing the length and diameter of the center vent tube. The center vent tube consists of a tubular extension on the aft end of the centerbody; it projects far enough aft to provide an ambient pressure sink for the engine vent air. The vent tube system for the ICLS engine was simulated in the Phase III scale-model mixer tests. Three vent tube lengths were tested, and the static pressure inside the exit of the tube was measured at the simulated maximum SLS power conditions. Test results indicated that the exit pressure was 5% above ambient pressure for the status vent tube. Since the vent system is designed to operate with ambient exit pressure, a design change was required. The model test results indicated that the vent tube needed to be increased in diameter by 1.5 inches, and the length needed to be increased by 12.9 inches. This change provided the desired vent tube base pressure and flow area for the estimated vent gas flow.

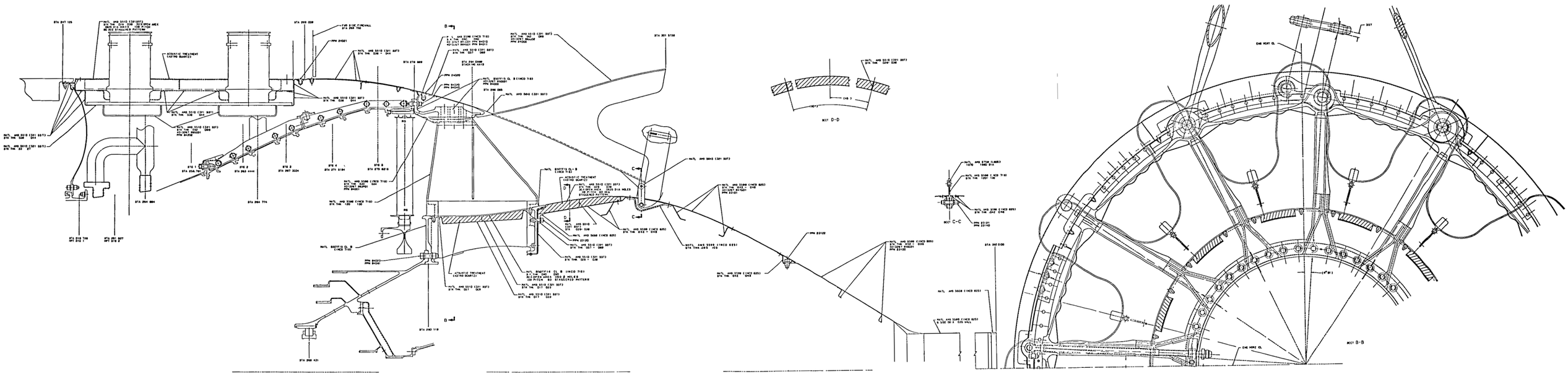

Figure 108. ICLS Engine Exhaust System.

Work Planned

- Support manufacturing through the completion of the ICLS hardware manufacture

- Provide engineering coverage of core engine assembly

2.6.4 Scaled Mixer Performance Testing

Technical Progress

Analyses of the Phase III test results have been completed including the integration of the nozzle exit survey data to determine mixing effectiveness. A description of the various test configurations was provided in the seventh Semiannual Report. The mixer pressure loss, mixing effectiveness, and calculated sfc gain are summarized in Figures 109, 110, and 111.

The mixing effectiveness obtained from the exit survey data is, in general, higher than that obtained from the thrust data. Detailed analysis of all the model data indicates the exit survey data provide a more accurate assessment of the mixing effectiveness, as concluded in the Phase II mixer test. The overall range of mixing effectiveness and sfc gains is essentially the same as previously reported. The survey data indicated a mixing effectiveness of 72% for the ICLS mixer, giving a 2.2% sfc gain. As anticipated, the flared turbine flowpath mixer improved the mixing effectiveness and reduced the pressure loss to give a 0.2% sfc improvement relative to ICLS. The best FPS mixer was an 18-lobe design which gave 79% mixing effectiveness and 2.6% sfc gain with a pressure loss of 0.57%.

Overall, the ICLS mixer fell short of expected performance. The 72% mixing effectiveness and 0.66% pressure loss yielded a 2.2% sfc gain; it was hoped to achieve 2.6% sfc gain for the ICLS configuration. Performance improvements were achieved with the flared turbine flowpath and 18 lobes for the best FPS mixer resulting in a 2.6% sfc gain. It is concluded that additional improvements are achievable, based on analysis of the nozzle exit profiles. An 85% mixing effectiveness with no change in pressure loss is feasible, resulting in a 2.9% sfc improvement. Achievement of this goal would

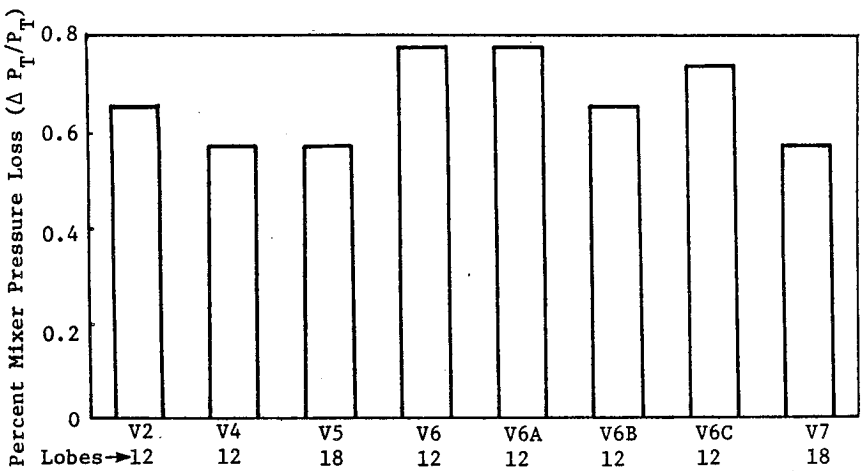

Figure 109. Mixer Pressure Loss Summary.

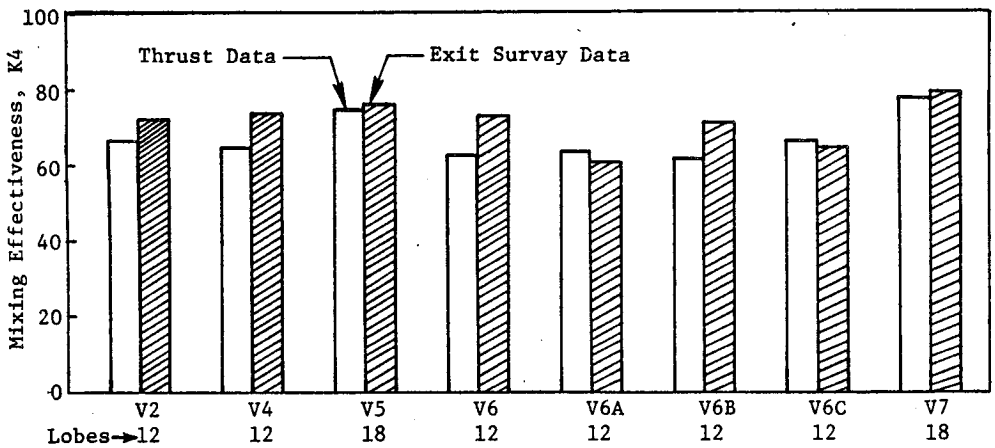

Figure 110. Mixing Effectiveness Summary.

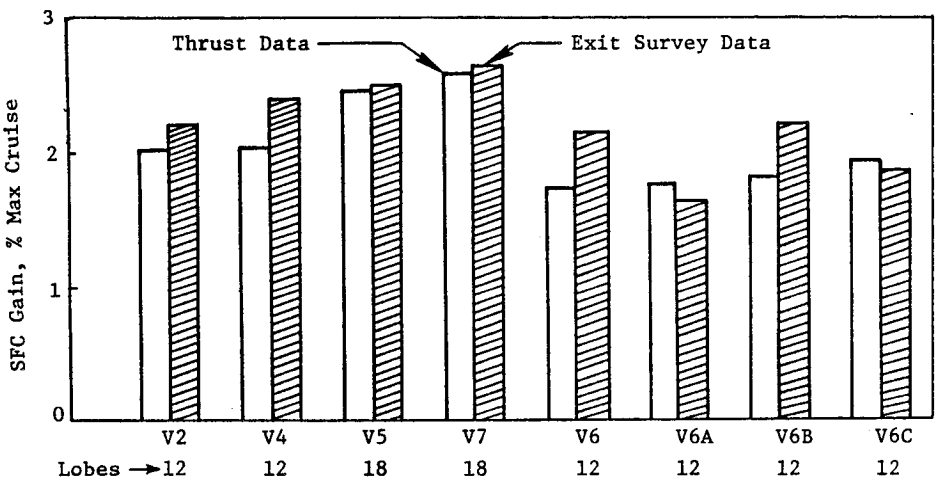

Figure 111. SFC Gain Summary.

require the development of a good analytical tool for fine-tuning studies followed by a scale-model test.

Analysis of the reverse-thrust operation data was completed, and revised performance characteristics were developed for incorporation into the engine cycle deck. A core "spoiled" thrust coefficient of 0.45 will be used versus the previously estimated value of 0.49. This will result in a slight increase in overall reverse thrust.

FluiDyne Engineering completed a recalibration of the scale-model test stand to determine low-pressure-ratio thrust coefficients more accurately for the ICLS mixer configuration. Revised data were provided by FluiDyne, and the data were analyzed to recalculate low-pressure-ratio mixing effectiveness, mixer pressure loss, and nozzle exit coefficients. Since both hot- and cold-flow testing are adjusted by similar amounts, the data revision did not change the mixing effectiveness or mixer pressure loss. However, the nozzle exit coefficients are more typical of a converging nozzle and have been provided for the cycle deck.

Preparation of the final detailed report covering the entire mixer development program was begun during this reporting period; the initial draft is nearly completed.

Work Planned

Complete the final mixer report and close-out this work package.

2.6.5 Turbine Frame/Mixer Fabrication

Core Engine Exhaust System

A cross section of the core engine exhaust system is shown in Figure 112. All core engine exhaust system hardware is complete and ready for assembly.

ICLS Engine Exhaust System

Considerable progress has been made on the ICLS engine exhaust system hardware. The fabrication of the turbine frame is nearing completion and can be seen in Figure 113. The strut halves have been welded together and then

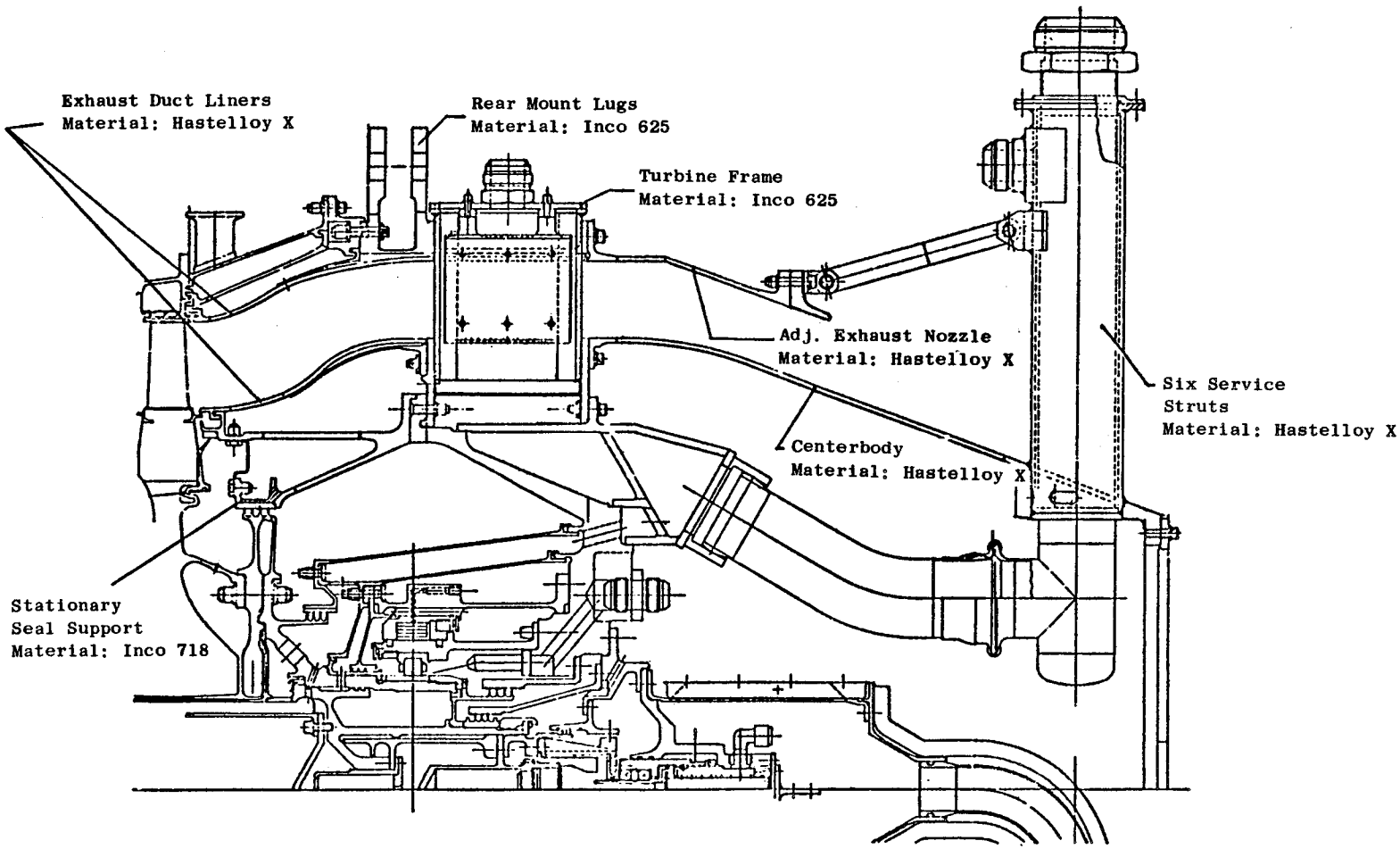

Figure 112. Core Engine Exhaust System Cross Section.

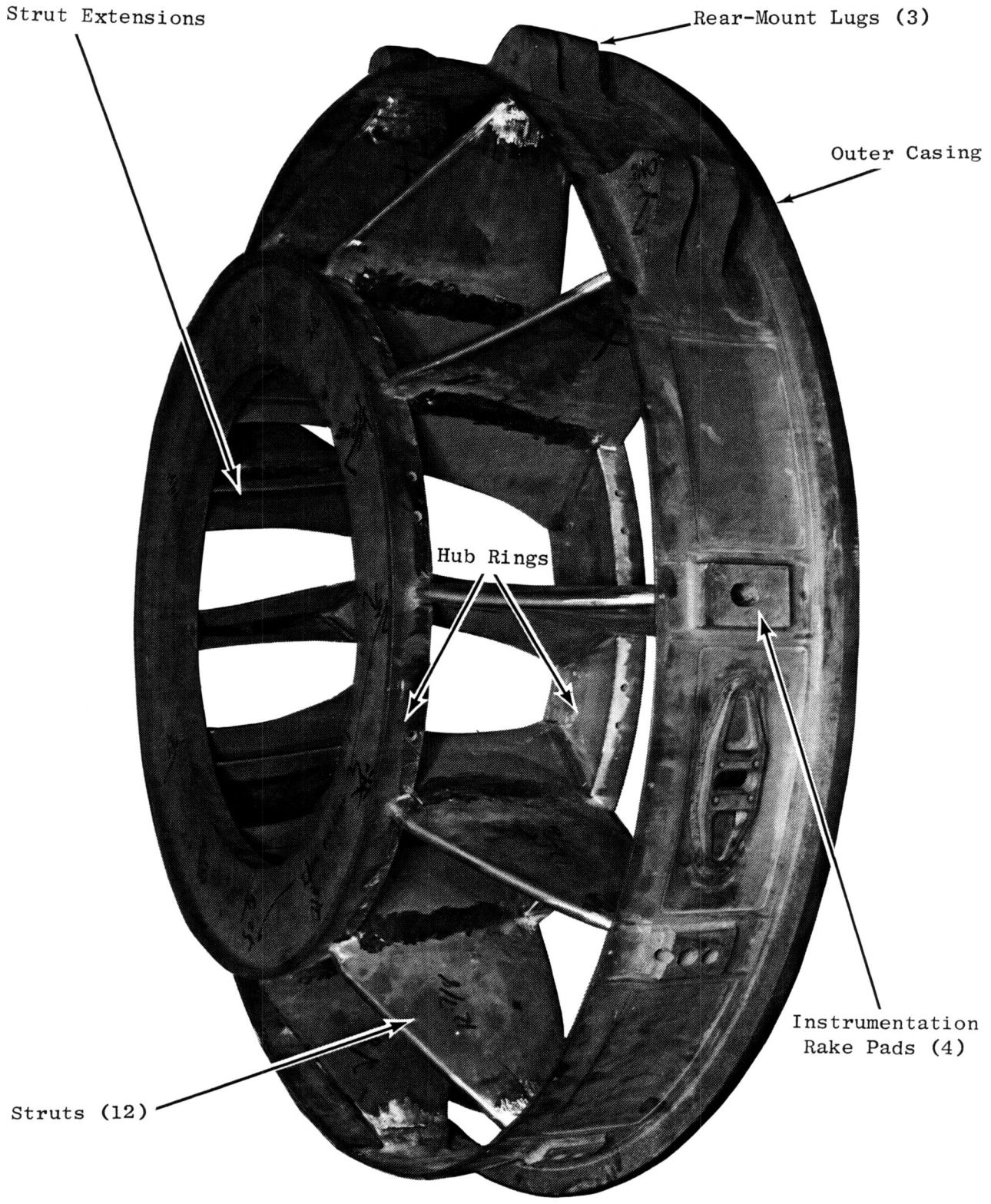

Figure 113. ICLS Engine Turbine Rear Frame.

welded to the hub rings and the outer casing. The strut extensions, which provide stabilization of the hub rings, have also been welded in place. The panels forming the inner flowpath surface are currently being welded in place between the struts. When fabrication of these panels is complete, the frame will begin final machining. The outer casing has been chem-milled between struts to provide local thinning and, therefore, the desired strain distribution. Also, pads for mounting the Plane 5 pressure/temperature instrumentation rakes have been incorporated into the casing.

The exhaust mixer is well into the fabrication cycle as can be seen in Figure 114. The chutes were hydroformed individually and then welded into an assembly. Twelve chutes were welded axially along the top of the hot chutes to form the mixing duct. The support clevises have been welded into the bottom of the cold chutes at the trailing edge. These clevises provide a means of supporting the trailing edge of the mixer with links to the centerbody. The sidewall cutouts have been incorporated into the mixer chutes. Also, the trailing edge of the mixer has been benched to provide a metal thickness of approximately 0.030 inch rather than the parent-stock thickness of 0.090 inch.

Fabrication of the forward centerbody has been completed, including the acoustic-treatment panels. The only item yet to be accomplished is the installation of the acoustic bulk absorber medium - Astroquartz. The Astroquartz sheets are scheduled for delivery in April. The aft centerbody is nearing completion. The spinning and Z-ring stiffeners have been spot-welded and back-brazed, and the center vent tube has been rolled and welded. After the vent tube is welded to the conical section, final machining will take place.

All hardware necessary for fabrication of the aft inner core cowl is in house. This includes the sheet metal spinnings, stiffeners, ACC air manifolds, and self-aligning adapters which join the ACC manifolds on the cowl to those on the turbine casings. The instrumentation plate at the top of the cowl and the split flanges have been machined and are ready for fabrication. Assembly of the aft cowl has recently been initiated.

Work Planned

Complete ICLS exhaust system hardware manufacture.

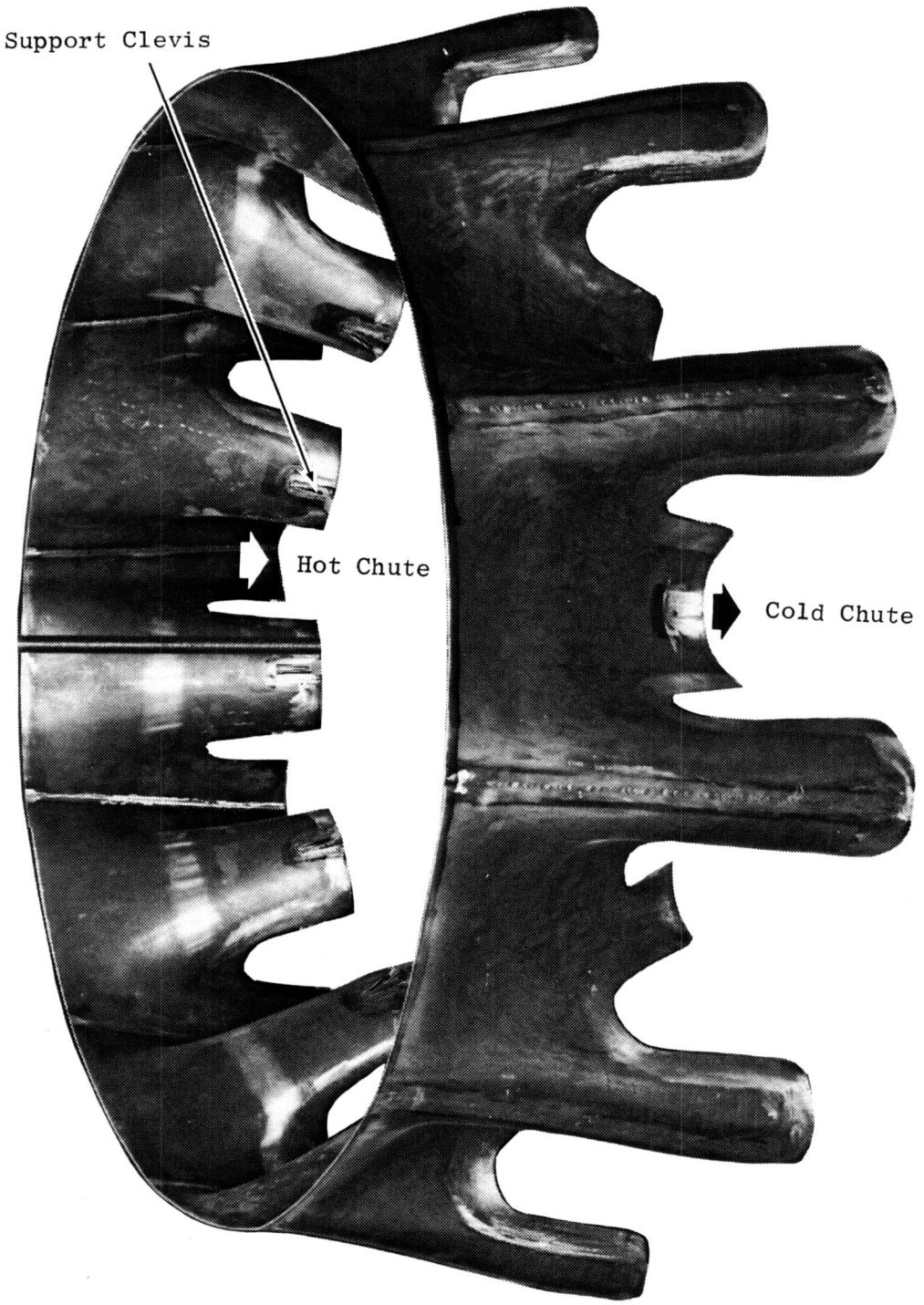

Figure 114. ICLS Engine Exhaust Mixer.

2.7 BEARINGS, SYSTEMS, DRIVES, AND CONFIGURATIONS

Overall Objectives

Bearings, systems, drives, and configuration components encompass the following:

- Main shaft support bearing and seal components
- Accessory drive system
- Lube system, including rotor thrust balance
- External piping and wiring configuration of the engine

The main-shaft bearings will be designed to properly support the engine rotor systems. These bearings will meet the design requirement for engine life considering fatigue and skidding criteria. They will operate with minimum heat rejection and within specified limitations.

The accessory drive system will provide the means to drive the engine-required accessories. Adequate horsepower capability, the proper pad speeds, and direction of rotation are the primary design objectives. Provision for two starter pads will be provided on the core/ICLS accessory gearbox. Critical speeds of all gearbox shafting will be kept at least 20% above the engine operating speed. The internal configuration of the accessory gearbox will be designed so that lubricating and cooling oil will be easily scavenged from it. During engine operation, the gearbox will operate within specified temperature limits.

The lube system will be designed to provide a flow network that will deliver and remove specific amounts of oil from various areas of the engine while maintaining predetermined pressure drops in the individual circuits. The rotor thrust balance will be determined as part of the lube system activity, and the thrust load on the fan and core thrust bearings will be established to be compatible with the life requirements of the bearings.

The objective of the configuration design is to provide the required external wiring and piping between various components of the engine. Piping is sized to meet specified flow velocities. The piping and wiring array will

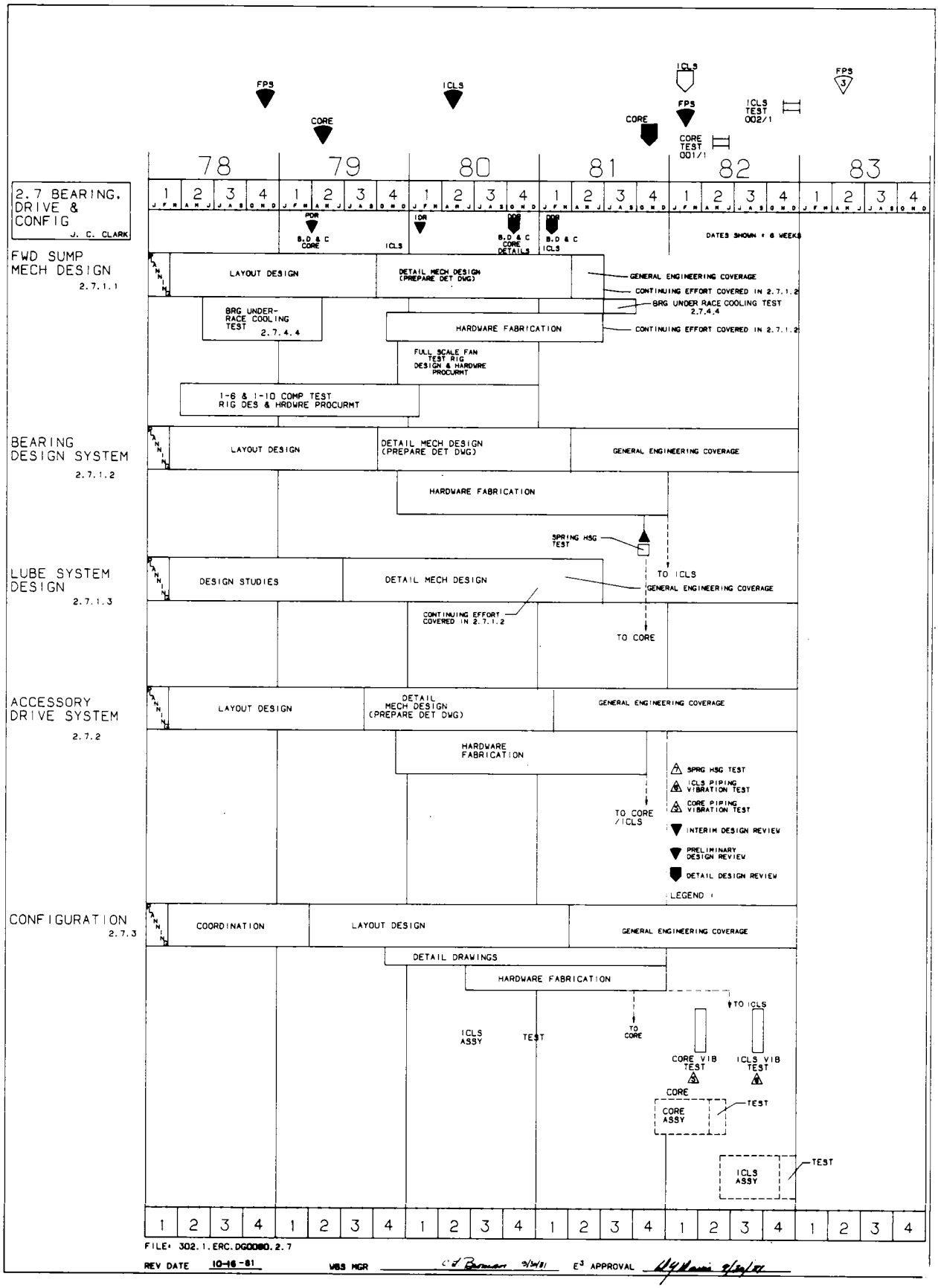

FILE: 302.1.ERC.DG00080.2.7

REV DATE 10-16-81 WBS MGR C. J. Barnum 9/24/81 E³ APPROVAL W. G. Morris 9/24/81

be capable of operating in the temperature and vibration environment of the engine.

Development Approach

To achieve the foregoing objectives, a development program has been established that consists of five subprograms defined as follows:

- Forward Sump Mechanical Design (WBS 2.7.1.1)
- Aft Sump Design (WBS 2.7.1.2)
- Lube System Design (WBS 2.7.1.3)
- Accessory Drive System (WBS 2.7.2)
- Configuration (WBS 2.7.3)

The major layout design of the forward and aft sumps was accomplished during 1978 through the third quarter of 1979. Preliminary design work was aimed at obtaining a viable design for the FPS. Studies have been made integrating the sumps with the core (high pressure) and low-spool (low pressure) rotor systems. Bearing and support housing designs are being analyzed in terms of rotor speeds, loads (including blade-out), cost, weight, and maintainability.

During the replanning activity of June 1981, Subprograms 2.7.1.1 and 2.7.1.3 were combined into Subprogram plan 2.7.1.2. This consolidation was made because the major design and analysis work had been completed, and reporting would be more efficient.

The Core PDR was held in the second quarter of 1979, and an integrated core/low-spool IDR was held in the third quarter of 1979. With NASA approval, the detail mechanical design was initiated with planned completion in the fourth quarter of 1980. With the exception of the configuration drawings, all design drawings were issued the first quarter of 1981. The core and ICLS bearing and sumps DDR's were held in the fourth quarter of 1980 and the second quarter of 1981, respectively. The ICLS bearings and sumps IDR was held in the first quarter of 1980.

Following NASA approval, hardware procurement and fabrication proceeded.

Two bearing tests have been planned to establish lubrication methods, provide heat-rejection data, and establish other design parameters for the core thrust bearing and the intershaft bearing. The thrust-bearing underrace cooling test (WBS 2.7.7.4) will be completed in two phases. The first phase was completed during the second quarter of 1979, and the second phase (which will test an E^3 core thrust bearing) was completed in the fourth quarter of 1981. The intershaft bearing test simulating the aft intershaft bearing arrangement of the E^3 design (WBS 2.7.4.3), scheduled to run in the fourth quarter of 1979, was run in the first quarter of 1980. During the replan of June 1981, further testing under this WBS was terminated. Bearing IRC will be determined by analytical means.

The lube-system preliminary and detail design efforts support the mechanical design work in such areas as lube-system network, main-shaft seal-pressurization networks, and rotor thrust. The PDR for the lube system was scheduled and completed as part of the core and ICLS PDR's. During the detailed mechanical design effort, the lube-system activity concentrated on finalizing such parameters as (1) lube flow and pressures, (2) seal ΔP's at various operating conditions, and (3) updating the rotor thrust-balance status.

While preliminary mechanical studies were continuing on the sump systems, a parallel effort went on in the accessory drive area. The design effort was in support of the FPS being designed under Task I. Attention was centered on the power takeoff (PTO), accessory gearbox (AGB), and the connecting shafting. The PDR for the accessory drive system was scheduled and completed as part of the core PDR. Detail design work has now been completed for the core/ICLS engine.

During 1978 and running through the first quarter of 1979, the configuration effort was concentrated on coordination with all the interfacing units and design layouts of all external wiring and piping. All detailing was completed by the fourth quarter of 1981. Vibration tests were also planned as a supporting effort for the scheduled core and ICLS tests.

In addition to the aforementioned effort, design and procurement of specific test rig hardware has been provided in support of the 1-6 and 1-10 compressor tests and the full-scale fan test (FSFT).

2.7.1.2 Bearing System

Forward Sump Mechanical Design (Formerly 2.7.1.1)

During this reporting period, design effort has been applied in the following areas:

- FSFT forward sump
- 1-10 compressor rig forward sump
- Core engine forward sump design
- Forward sump for ICLS engine

FSFT Forward Sump - The FSFT forward sump configuration is shown in Figure 115. The design is described in Semiannual Report No. 5, and all testing has been completed. All hardware functioned without any problems during testing. At rig disassembly, no hardware distress was seen. The seal housing will now be reworked for the ICLS assembly.

1-10 Compressor Rig Forward Sump - The compressor test rig forward sump is functioning well during -10B testing. There is still a problem with oil leakage at the sump carbon seal. The problem has been diagnosed as damper oil getting into the seal-pressurization cavity and blowing-out the seal into the compressor flowpath. The problem has been solved by maintaining seal air pressure higher than the damper oil pressure.

Core Engine Forward Sump Design - The core forward sump is shown in Figure 116. The design is the same as reported in Semiannual Report No. 4. Detail drawings have been completed, and hardware is now ready for assembly. A spring test has been completed on the No. 3 bearing housing, and the measured value of total spring rate is within 10% of the calculated value. Assembly work has started in the No. 3 bearing area.

Forward Sump for ICLS Engine - The ICLS forward sump is shown in Figure 117. Semiannual Reports 4 and 5 describe design features of this sump. All hardware is in the manufacturing process or awaiting assembly. Rework will be required to the air-seal housing that will be used from the FSFT. Major emphasis during this reporting period has been engineering support.

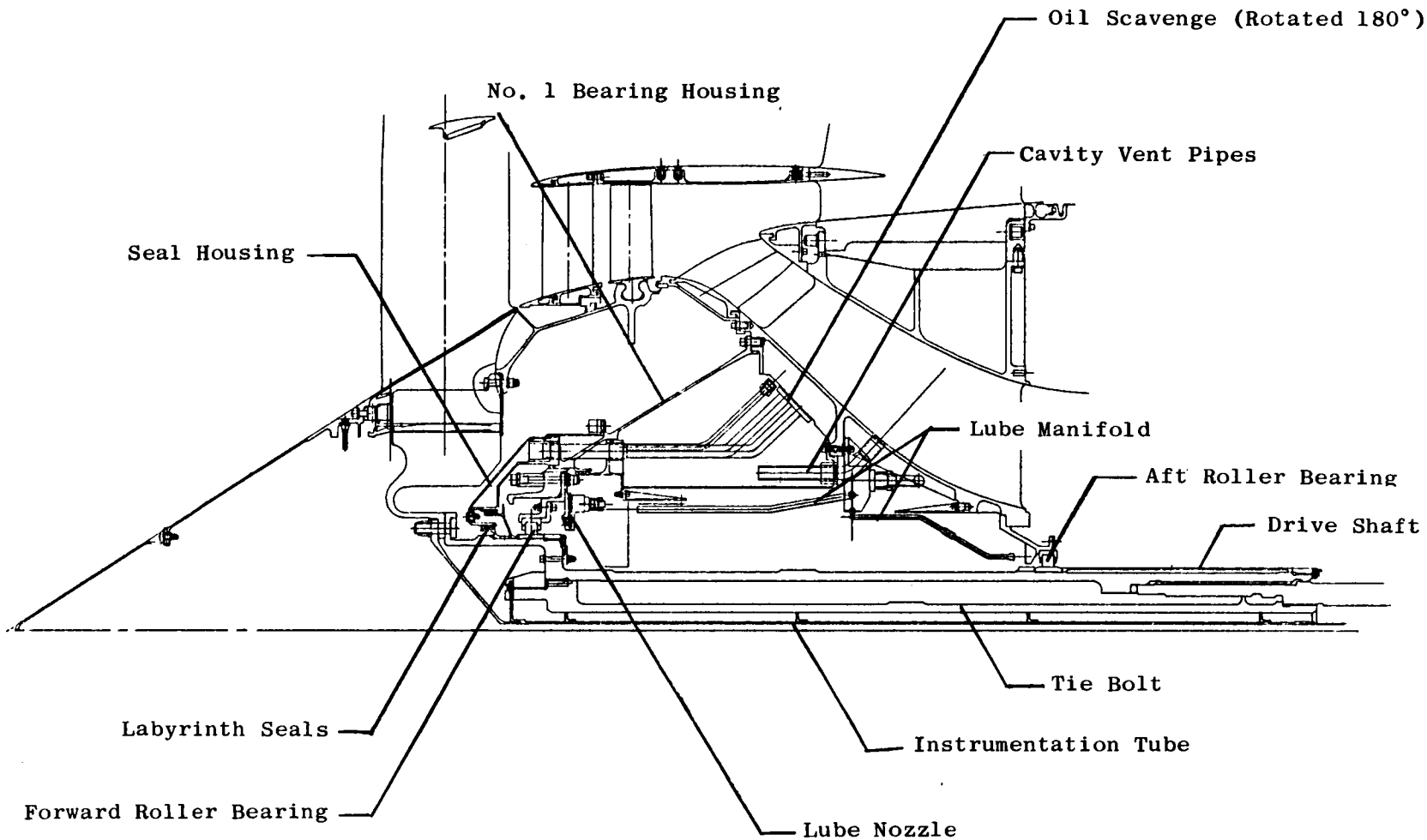

Figure 115. Forward Sump for Full-Scale Fan Test.

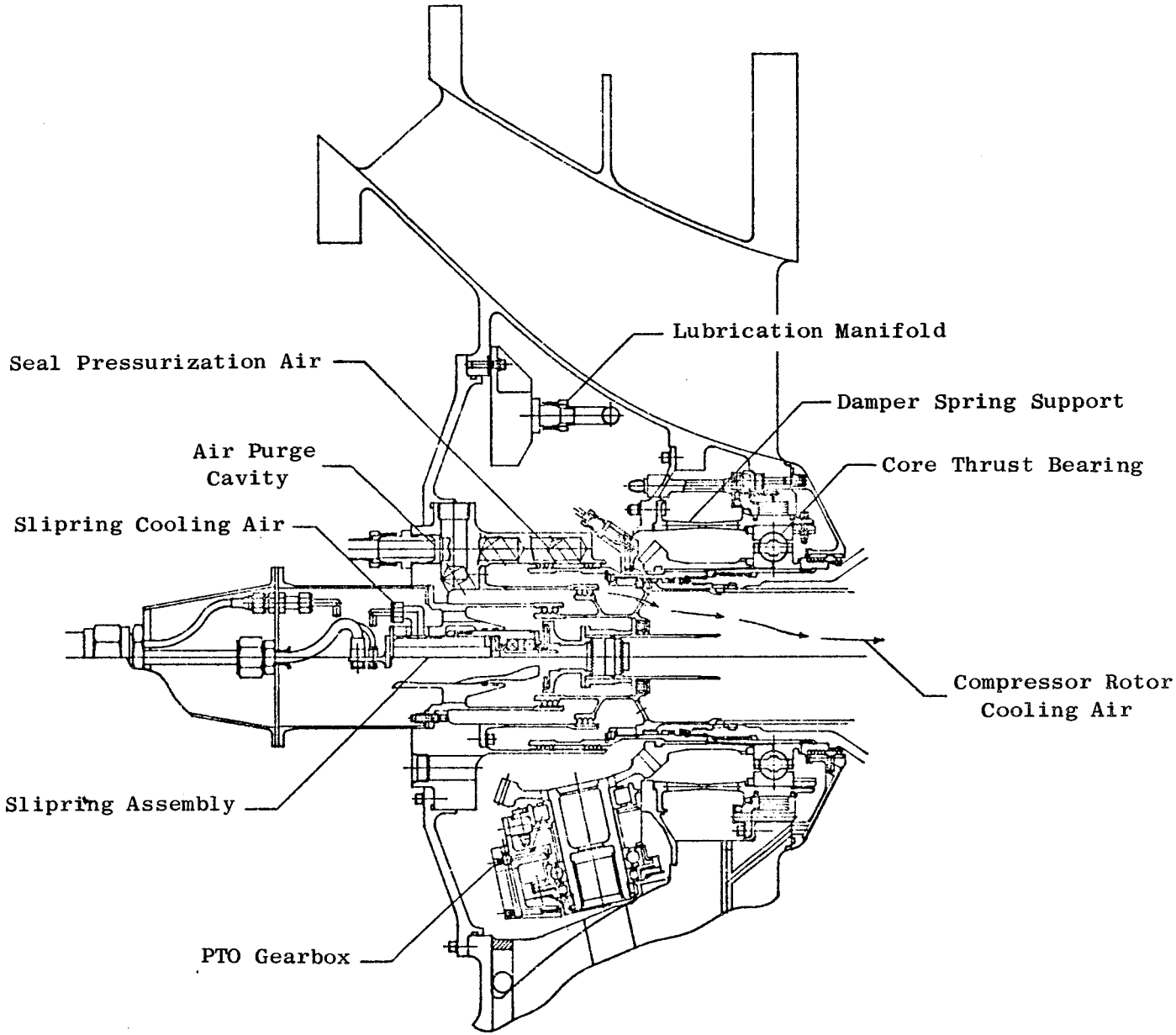

Figure 116. Core Engine Forward Sump.

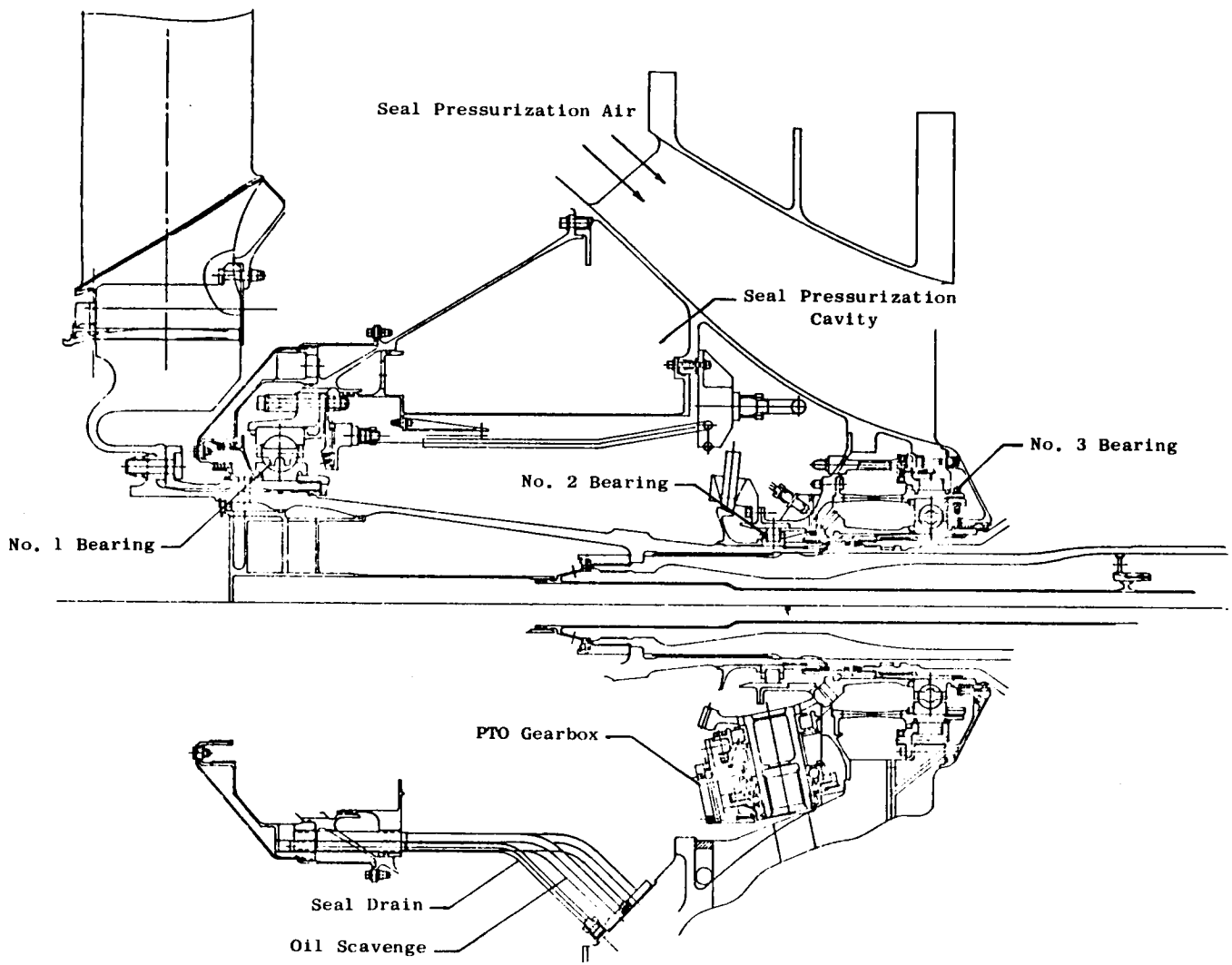

Figure 117. ICLS Forward Sump.

Work Planned

- Complete procurement of hardware for the core and ICLS engines
- Provide engineering coverage during the core and ICLS engine buildups
- Continue engineering coverage during the 10B compressor test

Aft Sump Mechanical Design

During this reporting period, design effort has continued in the following areas:

- Aft sump for the core engine
- Aft sump for the ICLS engine
- ICLS LPT shaft design

Aft Sump for the Core Engine - The Core engine aft sump is shown in Figure 118. All hardware is in the manufacturing cycle or awaiting assembly. The aft bearing support spring housing has been tested, and the overall spring rate is within 23% of the calculated value. This is the housing which had some manufacturing discrepancies in the area of the beams; after analysis and confirmation by spring rate test, it will be acceptable for the core engine. The hardware required for the 200-point instrumentation slip ring has been ordered and is in the manufacturing cycle.

Aft Sump for the ICLS Engine - The aft sump for the ICLS engine is shown in Figure 119. Hardware is in the manufacturing cycle or awaiting assembly. The No. 5 bearing housing, a major piece of hardware in the aft sump, is proceeding well through the manufacturing cycle and should be available next quarter.

ICLS LPT Shaft Design - Manufacture is proceeding on schedule for the ICLS LPT shaft. Modifications have been made to the shaft diameter to allow assembly of the shaft through the HPT duct without removing instrumentation. Changes also have been made to the aft air seals, and the vendor is proceeding with these.

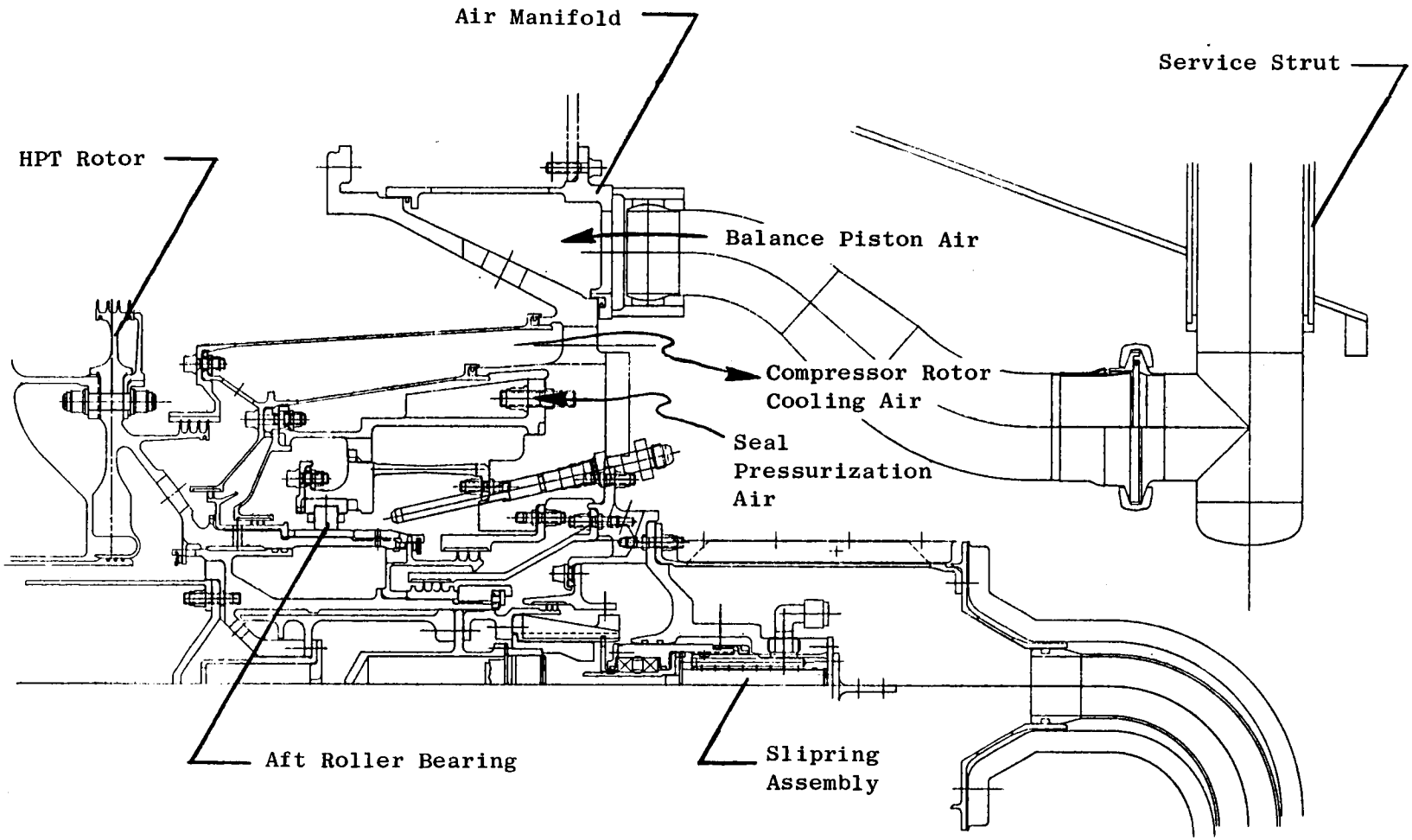

Figure 118. Core Engine Aft Sump.

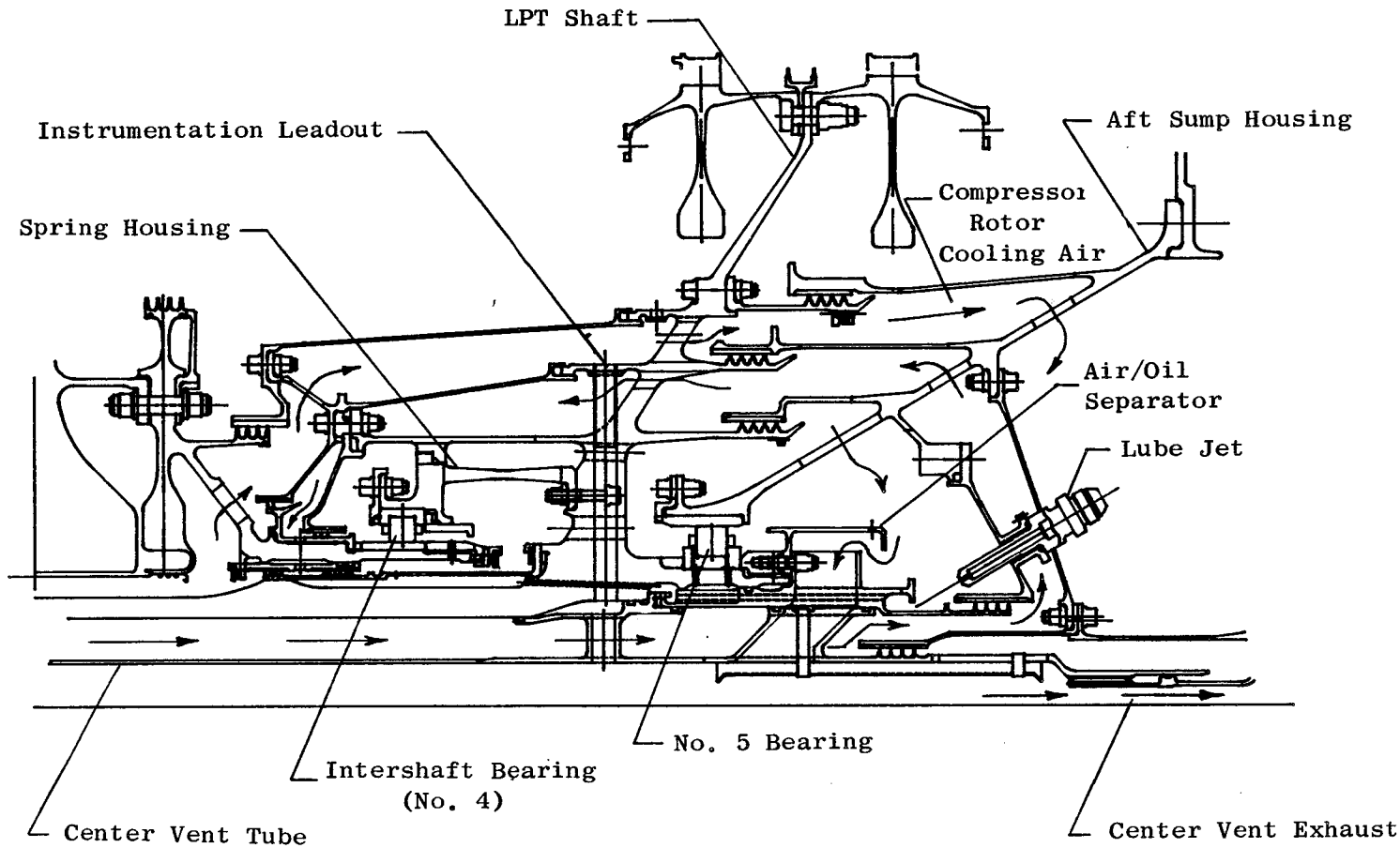

Figure 119. ICLS Aft Sump.

Work Planned

Continue engineering coverage during manufacturing and assembly.

Lube System Design (Formerly 2.7.1.3)

Work during this reporting period has consisted of minor coverage to ensure proper interfacing with other design disciplines. No problems have been encountered.

Work Planned

Continue to coordinate lube system with other engine functions.

2.7.2 Accessory Drive System

Technical Progress

Figures 120 and 121 show cross sections of the PTO and AGB, respectively. All hardware is now available, and assembly is proceeding. An oil-flow check has been made on the AGB; the measured flow was 11.5% higher than calculated and should be no problem.

Work Planned

Continue engineering coverage during assembly.

2.7.3 Configuration Design

Technical Progress

All drawings have been completed for the core and the ICLS engines, and manufacturing is proceeding. Manufacturing is also proceeding on the pressure bulkhead and the core junction box. Assembly drawings for the configuring hardware are in process.

Work Planned

- Complete assembly drawings
- Provide engineering coverage during the manufacturing and assembly cycles

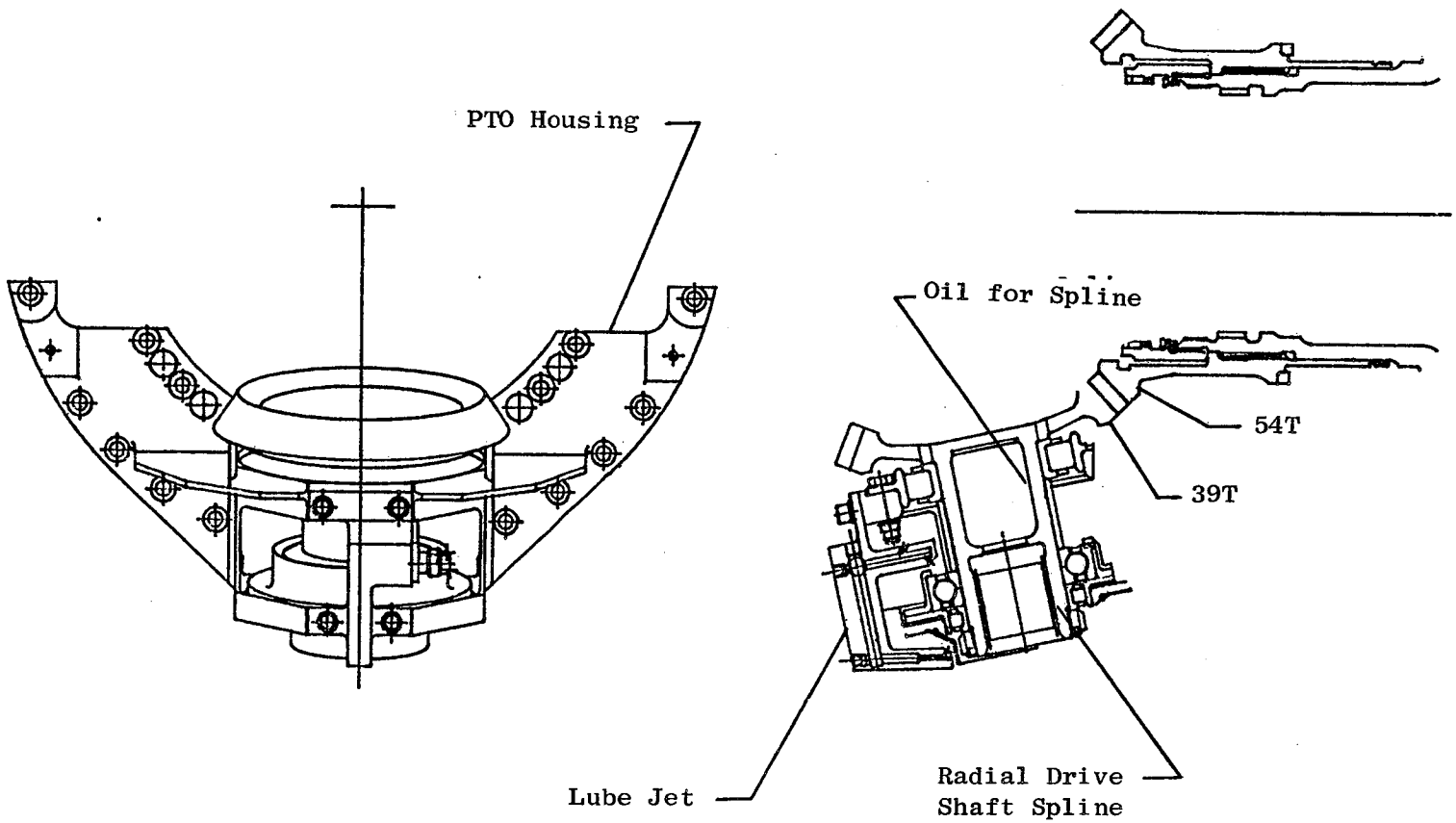

Figure 120. PTO Gearbox Assembly.

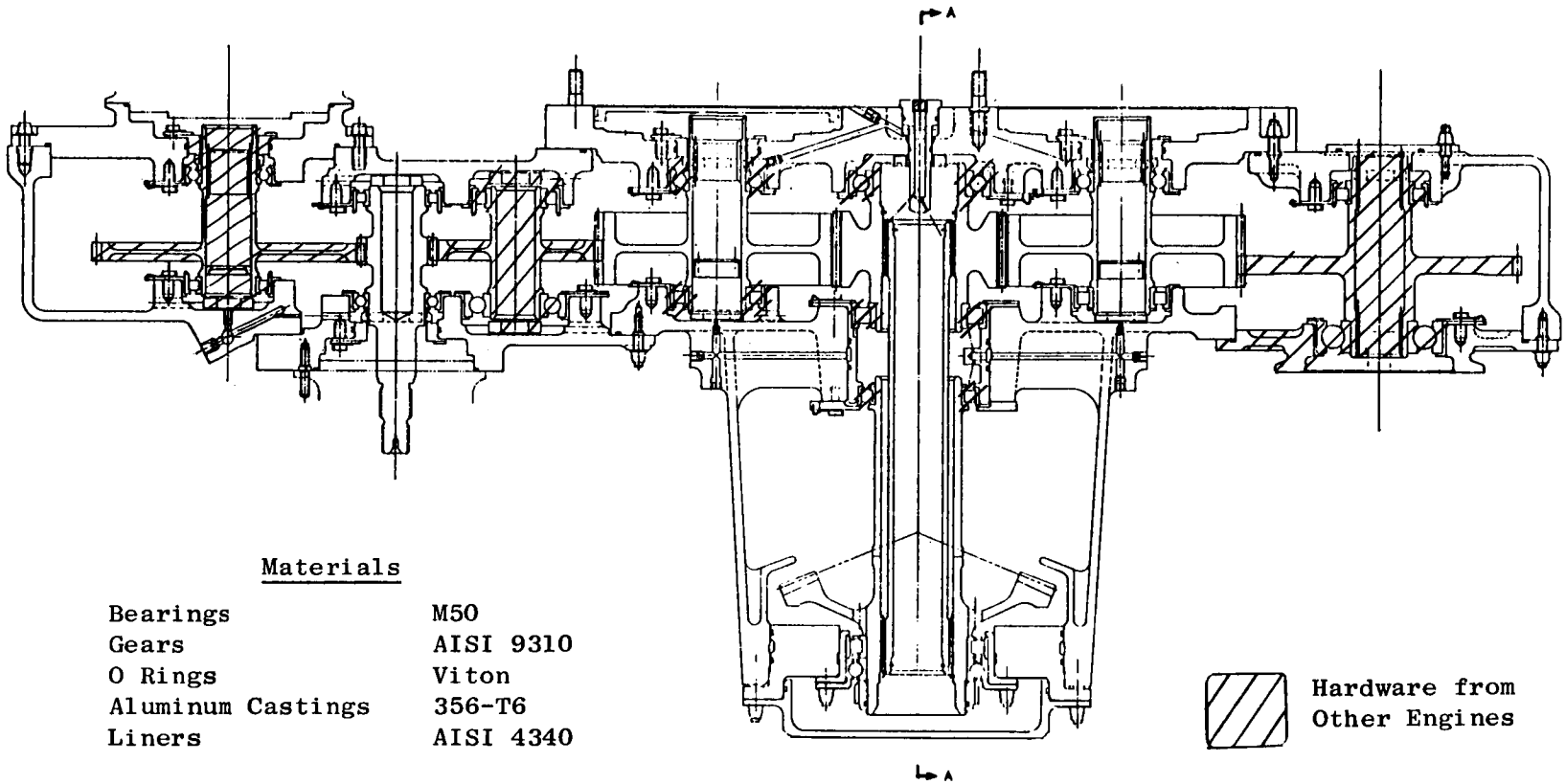

Figure 121. Core/ICLS Accessory Gearbox.

2.7.4.3 Intershaft Bearing Test

This program was cancelled in the June 1981 replanning effort. The bearing proposed for this test, although close in size to the E^3 intershaft bearing, is not the exact configuration. This, along with the inability to run core engine conditions (stationary outer race), influenced the decision to cancel further effort on the program. Bearing internal clearance will be established analytically.

2.7.4.4 Bearing Underrace Cooling Test

Figure 122 shows a cross section of the test rig with the test bearing in place. Testing was completed during this reporting period.

This test consisted of performance testing the core thrust bearing at axial loads of 200, 500, 1,000, 5,000, and 10,000 lbf with shaft speeds of 9,200, 10,500, 12,500, and 13,500 rpm. The test covered DN values of 1.5 to 2.23×10^6 and represent the speed range of the engine. Oil flows were varied between 0.5 to 2.3 gal/min with 180° F oil-in temperature. The test was performed for the purpose of determining the bearing heat-rejection rate and operating thermal performance at various oil-flow rates. Thermal stability was investigated at reduced oil-flow rates.

As a result of testing, no changes are being made to the engine bearings and the present oil delivery system.

2.7.5 Bearings, Systems, Drives, and Configuration Fabrication

Technical Progress

All hardware required for the accessory gearbox and PTO assembly is available and in various stages of assembly. Sump hardware is also available and awaiting assembly. Configuration hardware is proceeding on schedule.

We have identified areas where instrumentation rework is required, and rework is in process.

Work Planned

Follow hardware during assembly.

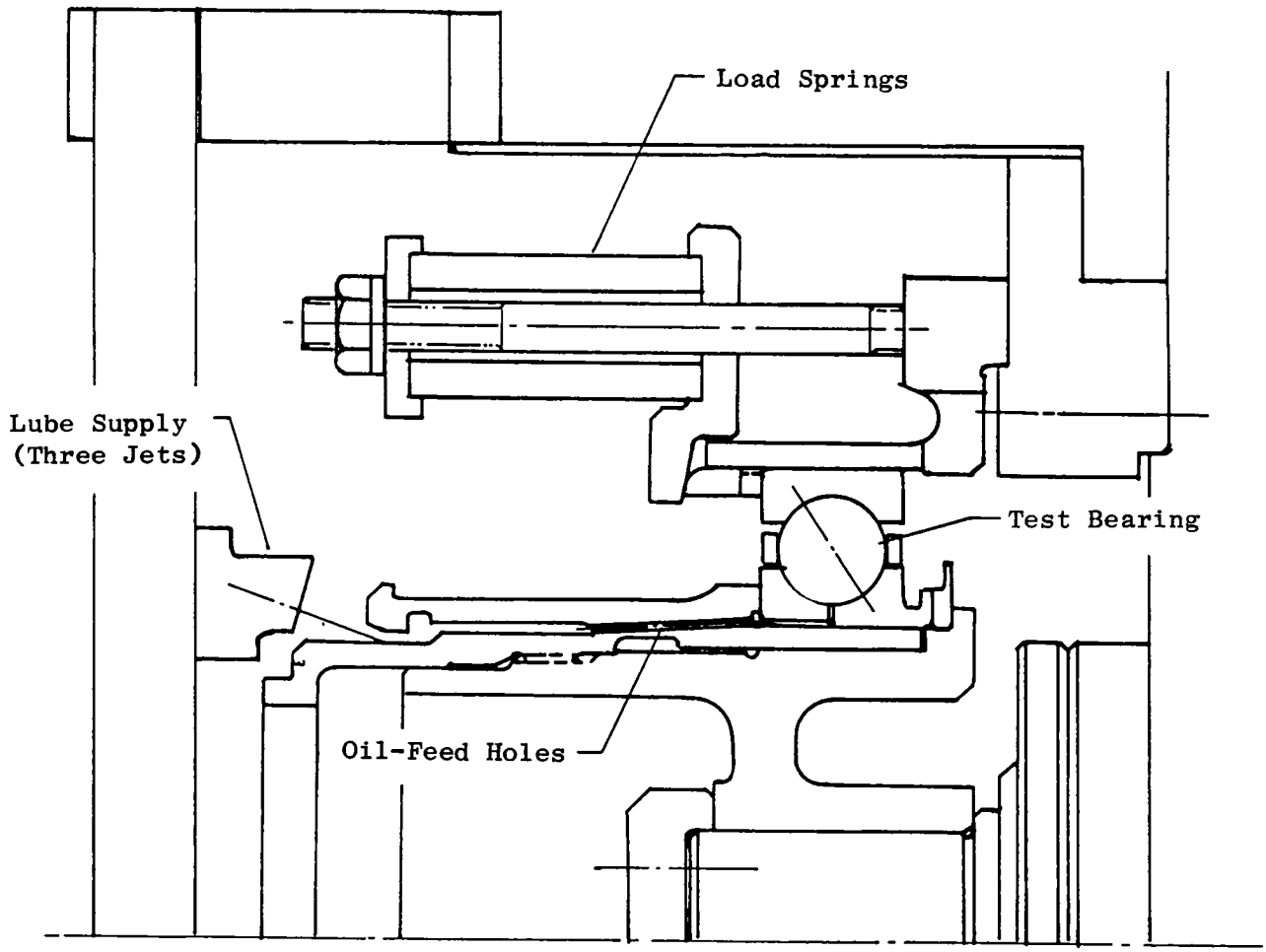

Figure 122. Underrace Cooling Test Rig.

2.8 CONTROL AND FUEL SYSTEM

Overall Objectives

The primary objective of the control and fuel system program is to define a system for E^3 that thoroughly exploits the fuel-conservation features, provides operational capability and reliability equal to or better than that provided by current transport-engine control and fuel systems, and employs digital electronic computation suitable for interfacing with an aircraft flight-control computer. An additional objective is to demonstrate the system functionally on the core and ICLS engines.

The proposed control and fuel system for the E^3 is based on many of the proven concepts and component designs used on the CF6 engine family. The major difference is in the addition of full-authority digital electronic computation; this provides significant improvements in control flexibility, accuracy, and aircraft/engine integration capability.

The digital control is expected to contribute to the low fuel consumption of the E^3 by providing automatic power management and optimum control of variable geometry on the engine over the full range of operating conditions. The control will also help reduce deterioration in engine efficiency by automatically preventing engine overspeed, overpressure, or overtemperature.

The E^3 employs fuel-handling concepts that are basically similar to the CF6 fuel system. In the flight design an engine-driven, positive-displacement, gear pump with an integral centrifugal boost element is used for pumping. A pump-mounted heat exchanger, downstream of the gear pump element but upstream of the system filter and fuel metering section, provides the dual functions of cooling the engine lube oil and heating the fuel to prevent filter icing. Fuel metering is accomplished by a fuel metering valve/bypass valve combination that sets engine fuel flow and returns excess fuel to the inlet of the gear pump element. Downstream from the metering valve, excess heat from the air being bled from the compressor for use in the aircraft environmental control system (ECS) is transferred into the fuel, thereby improving engine system efficiency by returning waste heat to the engine cycle and reducing the ECS air cooling requirements. After passing

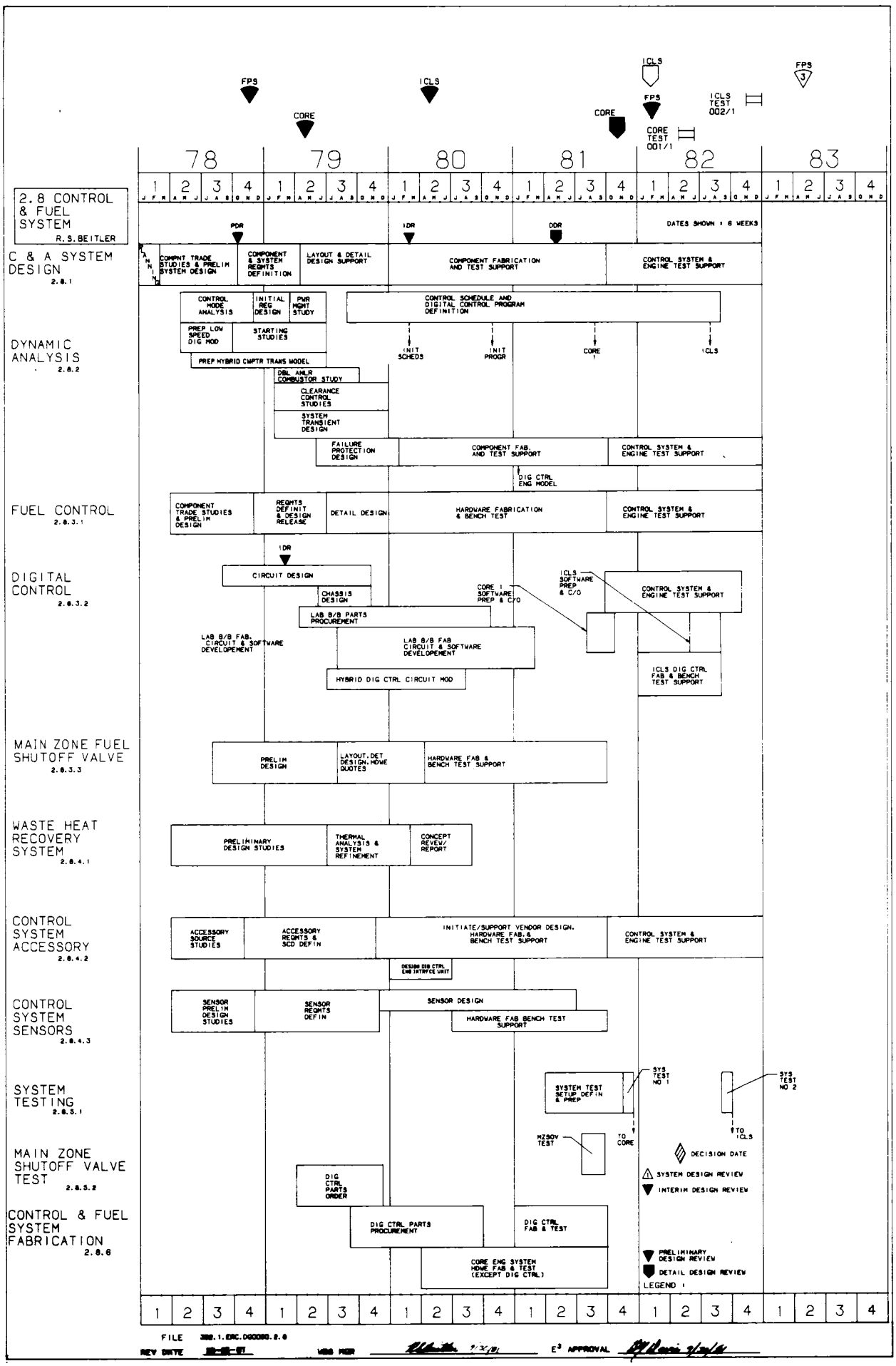
FPS
CORE
ICLS
CORE
FPS
CORE TEST 001/1
ICLS TEST 002/1
FPS
78
79
80
81
82
83
2.8 CONTROL & FUEL SYSTEM
R.S. BEITLER
C & A SYSTEM DESIGN 2.8.1
DYNAMIC ANALYSIS 2.8.2
FUEL CONTROL 2.8.3.1
DIGITAL CONTROL 2.8.3.2
MAIN ZONE FUEL SHUTOFF VALVE 2.8.3.3
WASTE HEAT RECOVERY SYSTEM 2.8.4.1
CONTROL SYSTEM ACCESSORY 2.8.4.2
CONTROL SYSTEM SENSORS 2.8.4.3
SYSTEM TESTING 2.8.5.1
MAIN ZONE SHUTOFF VALVE TEST 2.8.5.2
CONTROL & FUEL SYSTEM FABRICATION 2.8.6
PDR
IDR
DDR
DATES SHOWN + 6 WEEKS
COMPNT TRADE STUDIES & PRELIM SYSTEM DESIGN
COMPONENT & SYSTEM REQMTS DEFINITION
LAYOUT & DETAIL DESIGN SUPPORT
COMPONENT FABRICATION AND TEST SUPPORT
CONTROL SYSTEM & ENGINE TEST SUPPORT
CONTROL MODE ANALYSIS
INITIAL REG DESIGN
PWR MGMT STUDY
CONTROL SCHEDULE AND DIGITAL CONTROL PROGRAM DEFINITION
PREP LOW SPEED DIG MOD
STARTING STUDIES
PREP HYBRID CMPTR TRANS MODEL
INIT SCHEDS
INIT PROGR
CORE I
ICLS
DBL ANLR COMBUSTOR STUDY
CLEARANCE CONTROL STUDIES
SYSTEM TRANSIENT DESIGN
FAILURE PROTECTION DESIGN
COMPONENT FAB. AND TEST SUPPORT
CONTROL SYSTEM & ENGINE TEST SUPPORT
DIG CTRL ENG MODEL
COMPONENT TRADE STUDIES & PRELIM DESIGN
REQMTS DEFINIT & DESIGN RELEASE
DETAIL DESIGN
HARDWARE FABRICATION & BENCH TEST
CONTROL SYSTEM & ENGINE TEST SUPPORT
IDR
CIRCUIT DESIGN
CHASSIS DESIGN
LAB B/B PARTS PROCUREMENT
LAB B/B FAB. CIRCUIT & SOFTWARE DEVELOPEMENT
LAB B/B FAB CIRCUIT & SOFTWARE DEVELOPEMENT
HYBRID DIG CTRL CIRCUIT MOD
CORE I SOFTWARE PREP & C/O
ICLS SOFTWARE PREP & C/O
CONTROL SYSTEM & ENGINE TEST SUPPORT
ICLS DIG CTRL FAB & BENCH TEST SUPPORT
PRELIM DESIGN
LAYOUT, DET DESIGN, HDWE QUOTES
HARDWARE FAB & BENCH TEST SUPPORT
PRELIMINARY DESIGN STUDIES
THERMAL ANALYSIS & SYSTEM REFINEMENT
CONCEPT REVIEW/ REPORT
ACCESSORY SOURCE STUDIES
ACCESSORY REQMTS & SCD DEFIN
INITIATE/SUPPORT VENDOR DESIGN, HARDWARE FAB, & BENCH TEST SUPPORT
CONTROL SYSTEM & ENGINE TEST SUPPORT
DESIGN DIG CTRL ENG INTRFCE UNIT
SENSOR PRELIM DESIGN STUDIES
SENSOR REQMTS DEFIN
SENSOR DESIGN
HARDWARE FAB BENCH TEST SUPPORT
SYSTEM TEST SETUP DEFIN & PREP
SYS TEST NO 1
SYS TEST NO 2
TO CORE
TO ICLS
MZSOV TEST
DECISION DATE
SYSTEM DESIGN REVIEW
INTERIM DESIGN REVIEW
DIG CTRL PARTS ORDER
DIG CTRL PARTS PROCUREMENT
DIG CTRL FAB & TEST
CORE ENG SYSTEM HDWE FAB & TEST (EXCEPT DIG CTRL)
PRELIMINARY DESIGN REVIEW
DETAIL DESIGN REVIEW
LEGEND :
FILE
REV DATE
E³ APPROVAL

through this heat exchanger, the metered fuel is divided as necessary to accommodate the double-annular combustor.

The system also controls several variable-geometry elements on the engine including the variable stator vanes and starting bleed valves on the compressor and the air valves for controlling clearances in the compressor, HPT, and LPT.

Engine starting will be accomplished using a gearbox-mounted, air-turbine starter similar to that used on the CF6. Scheduling of fuel flow during the starting sequence will be done by the digital control; this will also provide ignition-sequencing logic by energizing the ignition as a function of a starting command input and deenergizing it when the engine has accelerated beyond the point where ignition is needed. The ignition will also be automatically energized if the digital control detects deceleration conditions that indicate a burner blowout has occurred.

Development Approach (Reference WBS Spread/Schedule Sheet)

The control and fuel system design and development effort began with a preliminary design phase in which various system and component design options were defined and evaluated. Particular emphasis was placed on the method of incorporating advanced-technology features such as the full-authority digital control, air/fuel heat exchange for waste-heat recovery, active clearance control, and fuel flow division for the double-annular combustor. The initial study work resulted in the definition of a preliminary control system design in late 1978. A preliminary design review of this system was held at NASA Lewis in October 1978, and the design was further reviewed as part of an overall engine preliminary design review in November 1978.

With the basic system design concepts established, the next task was to define detailed system and component requirements for the demonstrator engine program and proceed with detailed component design. This task, which was essentially completed in 1979, involved several different types of activity. In the system design area, the basic system and component requirements were established and documented. Concurrently, a number of supporting analytical activities were carried out under the Dynamic Analysis

subprogram using computer simulations to investigate engine and control characteristics and to define requirements, particularly those related to control stability and response. Meanwhile, component design and development activity was proceeding as described below.

Fuel control design and development are being done under WBS 2.8.3.1. For the core and ICLS, a modified F101 fuel control will be used. Detailed requirements for the control have been defined and transmitted to the control vendor. Control modifications were defined in detail, and the modifications were reviewed with NASA in March 1980. The first of two E^3 controls has been received and is being tested as part of the core engine control-system test. The second control, being procured under WBS 4.2.4, will be received in the near future.

Design of the digital control is being carried out under WBS 2.8.3.2. The basic control design process includes initial circuit design, experimental circuit refinement using a laboratory breadboard control, and chassis design. Because construction of the laboratory breadboard required procurement of electrical parts prior to the control-system DDR in early 1981, an IDR of the digital control was conducted in March 1979.

Construction of the breadboard was completed in March 1981, and it is being used to check out and refine control circuits and to check out control software.

The digital control resulting from the above design effort is an off-engine unit suitable both for the core engine and the ICLS engine. It has been built and tested under WBS 2.8.6. This control will definitely be used on the core engine, but it is planned that an on-engine unit, constructed under a separate program, will be used for the ICLS engine. The on-engine unit will incorporate an advanced, hybrid-electronic packaging concept.

The main-zone-fuel-shutoff valve covered by WBS 2.8.3.3 is a new valve designed to assist in the fuel flow division required by the double-annular combustor. Detailed design of this valve was completed and reviewed with NASA in early 1980. Fabrication and test of the valves for the engine test programs has been completed under WBS 2.8.6 and 2.8.5.2.

The air/fuel heat exchanger work under WBS 2.8.4.1 began with thermal model studies to examine, in detail, the potential fuel savings available by transferring heat from the compressor bleed air to the engine fuel. Early in the second quarter of 1980, the results of these studies were assessed by NASA and General Electric, and a decision was made to delete the hardware demonstration originally planned for the waste-heat recovery concept. This was done primarily because the concept, although unique in function, is implemented with standard components that do not represent new technology.

Design of control-system accessories and sensors is being carried out under WBS 2.8.4.2 and 2.8.4.3. These components do not represent advanced technology and consequently, for economic reasons, will be modifications of existing designs. Detailed component requirements were established in 1979 and transmitted to the appropriate design organizations (mostly outside vendors) to serve as a basis for detailed definition of component modifications. The designs were reviewed in a March 1980 IDR and released for procurement.

The system and component designs resulting from all of the effort described above were reviewed and approved in a DDR at NASA Lewis in April 1981, and the designs are being implemented in hardware. A full set of control-system components is currently undergoing a system bench test. Subsequently, the components will be installed for operation of the core engine.

Control system hardware from the core engine will be used on the ICLS except that an on-engine digital control will be used, as noted previously, and a fan speed sensor and LPT clearance-control subsystem will be added. The ICLS control system components will also be bench tested as a complete system prior to operation on the engine. A small amount of additional control-system hardware has been procured to provide a limited supply of spare parts.

2.8.1 Control System Design and Analysis

Technical Progress

A majority of the system design engineering effort during this reporting period was associated with preparing for, setting up, and running the bench test of the core engine control system (discussed under WBS 2.8.5.1). The only notable system design activity was the selection of a design approach

for the sensor-failure protection strategy to be provided in the ICLS control system and a minor change to the fuel flow-split control strategy. The sensor-failure strategy activity is discussed under WBS 2.8.2, and the fuel flow-split change is described below.

In early testing of the double-annular combustor it was found that the desired, steady-state, pilot-zone/main-zone fuel flow split did not provide enough fuel for ignition in the main zone during an engine start. A pilot-zone reset valve was therefore added to the fuel control system to provide temporary enrichment of the main zone during a start. Later, compressor and turbine component test results indicated that start-range gas temperatures would be lower than originally anticipated, so main-zone operation for smoother temperature profiles during a start wouldn't be necessary. Thus, it was thought that the pilot-zone reset function was no longer required. However, subsequent combustor tests indicate that main-zone enrichment is required for ignition even at the normal main-zone light-off point just above ground idle.

Thus the pilot-zone reset valve has been retained, but the operating characteristics were changed to reflect the fact that it will now operate at a higher fuel flow. Fuel distribution sequencing as the engine accelerates above ground idle (where only the pilot zone is burning) will be as follows:

1. Main-zone shutoff valve starts open and pilot-zone reset valve starts closed.

2. Main-zone valve holds at partially open point for approximately one second, to allow main nozzle tubes to fill without starting the pilot zone, then proceeds to fully open position in less than a second.

3. Pilot-zone reset reaches full-closed position (25/75 pilot/main flow split) approximately two seconds later and remains there until speed increases above flight idle indicating main zone is lit. If engine doesn't accelerate through flight idle in a reasonable length of time (adjustable 0 to 20 seconds on initial control), the pilot-zone reset opens.

4. Above flight idle both valves are open, and the fuel nozzles set the flow split (50/50 pilot/main at low speed, 40/60 at high speed).

A manual control mode for fuel distribution will also be included on the core and ICLS to allow the above sequence to be deactivated and the two valves to be positioned by means of potentiometers in the control room.

Work Planned

- Prepare core engine control system test report
- Support core engine assembly and test
- Prepare ICLS control systems test plan

2.8.2 Dynamic Analysis

Technical Progress

The design concept for digital-control-sensor failure indication and corrective action (FICA) was reviewed with NASA during this reporting period, and detailed design characteristics were mutually agreed upon.

The basic FICA concept involves the incorporation of a simplified engine model in the digital-control software. This model would control input-sensor signals and replace failed signals with model-generated signals. A preliminary FICA design was completed in 1980 before the current control strategy was completed. Subsequent experience with other GE digital controls and with other FICA's indicates that the preliminary E^3 FICA should be refined in order to enhance the probability of a successful on-engine demonstration. These refinements will include the following types of changes:

- Reduced complexity and improved robustness of the Kalman filter which updates the model to match real engine conditions
- Better integration of the FICA and the current control strategy

A diagram of the refined FICA is shown in Figure 123.

The original E^3 FICA Kalman filter had seven states, all of which were updated. They were the two rotor speeds, the fuel-metering-valve position, the high-pressure compressor stator position, and three temperature sensors. The high-pressure compressor stator position was included in anticipation of getting a good model of the effect of this position on compressor performance

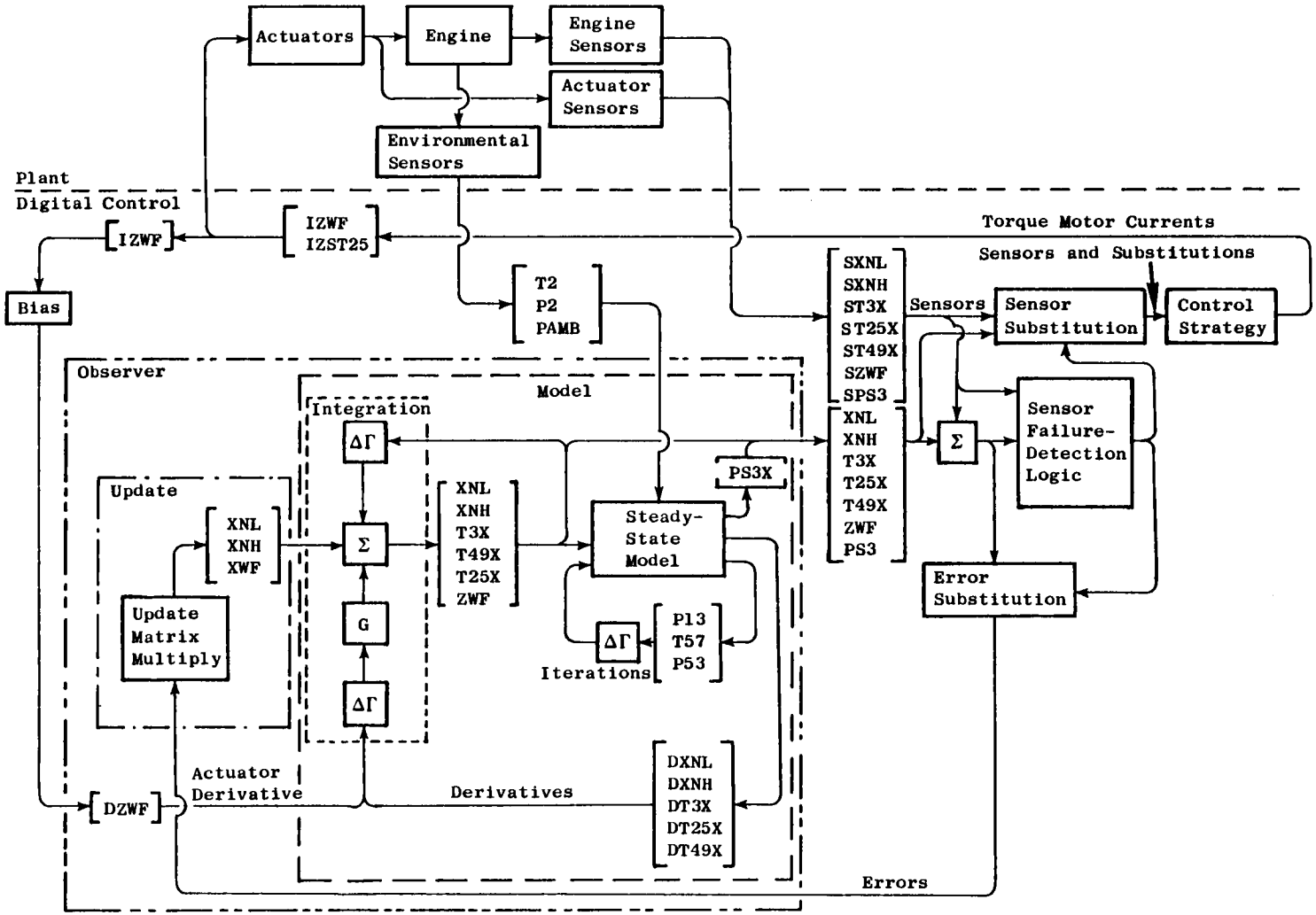

Figure 123. Sensor Failure Indication and Corrective Action.

and solving the problems of actuator sensor substitution. This state will be dropped for lack of this model and by agreement not to solve the actuator-sensor-substitution problem.

The temperature sensors are states in the sense that they are dynamic. They have, however, no effect on the engine thermodynamics. If the engine sensor fails, the state becomes unobservable. The temperature sensor dynamics are well understood, and the sensor model will track the actual sensor accurately. The error between the model sensor and the actual sensor will be used to update other states as shown in Figure 123. Since these temperature-sensor states do not affect the engine thermodynamics, the information useful for updating is in the nondynamic part of the signal, i.e., the gas temperature. The benefit to the filter of dropping the update of these states is reduced complexity and improved robustness. The filter tracking performance reduction without these sensor updates will be minimal. It should also be noted that the update of one of these temperature-sensor models would be suspended whenever the sensor is failed.

The FICA strategy will deal with sensor failures in the following ways. If either of the two rotor-speed sensors (SXNH, SXNL), the high-pressure compressor discharge pressure sensor (SPS3), or the three temperature sensors (ST3, ST25, ST49) fail, the lost sensor value will be replaced with the estimated value from the Kalman filter. If any other sensor including the metering-valve-position sensor fails, the FICA action will be subordinated to the failure provisions elsewhere in the control strategy.

The Kalman filter employs a multivariable feedback in which the filter response is made optimal in the presence of sensor and model noise. While the procedure to compute the feedback matrix guarantees stability at the design point, it does not guarantee robustness. Since the E^3 FICA preliminary design was done, some new multivariable control analysis methods (such as the principal-gain plots) have become available, and these should be applied to the filter feedback design to test for robustness. Other methods (such as the procedures of adjusting the sensor and model noise covariance matrices to recover robustness, as suggested by Doyle and Stein) will be used if the software becomes available in time.

The error criteria of the FICA need to be coordinated with the sensor-out-of-limits and rate-limit logic. These latter two failure-detection strategies have been employed upstream of the FICA in past designs. These strategies can mask certain types of sensor failures from the FICA. If however, the sensor failure detection of these is integrated with the FICA, then the FICA can detect the failures. This logic will need to be designed and integrated into the control strategy and FICA.

The control strategies for development or demonstrator engines usually include provisions for adjusting schedules or sensor output signals. The adjustments to accommodate engine performance differences from predicted should be placed so that the adjusted signal matches the predicted engine performance and is used by the control strategy and the FICA. These adjustments will need to be designed and integrated into the control strategy.

The plans to test the FICA software are basically unchanged from the original. The design will be tested and refined in the hybrid-computer simulation of the E^3. Following this, various tests will be performed in the hardware test stands. The final test will be on the ICLS engine. FICA will not be incorporated on the core engine because the limited control requirements limit the scope of FICA demonstration.

Another small but important task that was done recently under this subprogram was the assessment of the three air turbine starters that have been acquired for the core and ICLS engines. These are production starters, and torque characteristics were not mapped during acceptance testing. The only torque-related data available is a measure of time required to accelerate a test flywheel to 4750 rpm (67% core speed) with 50-psia air. To determine how this relates to E^3 starting, the starter torque characteristics used in E^3 starting studies, and judged to be satisfactory, were run with a simple model of the starter test rig. The E^3 starter torque characteristic accelerated the rig to 4750 rpm in 18.6 seconds compared to 18.4, 18.7, and 18.5 seconds for the three actual starters. Based on this result the E^3 starters are judged to be adequate.

Work Planned

- Complete FICA design and incorporate it into the ICLS digital control software
- Support core control system and engine testing

2.8.3.1 Fuel Control

Technical Progress

During this reporting period the first of the two modified F101 fuel controls which will be used on the E^3 demonstrators was completed, bench tested, and delivered for system testing. The control and new elements - namely the RVPT (rotary variable-phase transducer) metering valve position sensor, the fail-safe fuel servovalve, and the fuel transfer valve for electrical/hydromechanical fuel control mode selection - operated satisfactorily in all phases of the bench testing and are judged satisfactory for the core engine. A photograph of the control with the fuel-transfer valve installed (lower right on photo) is shown on Figure 124.

Also during this reporting period the stator transfer valve, which operates in conjunction with the fuel transfer valve, was successfully bench tested and delivered for core control system testing.

Work Planned

Support core control system and engine testing.

2.8.3.2 Digital Control

Technical Progress

The digital control for the core engine has been completed, bench tested, and delivered for core control system testing with other system hardware. This was the result of a considerable amount of effort during this reporting period, much of it devoted to the solution of problems discovered during hardware checkout and to the preparation and checkout of software.

The most persistent problem in the control has been electrical noise associated, primarily, with the internal power supply of the control. At the

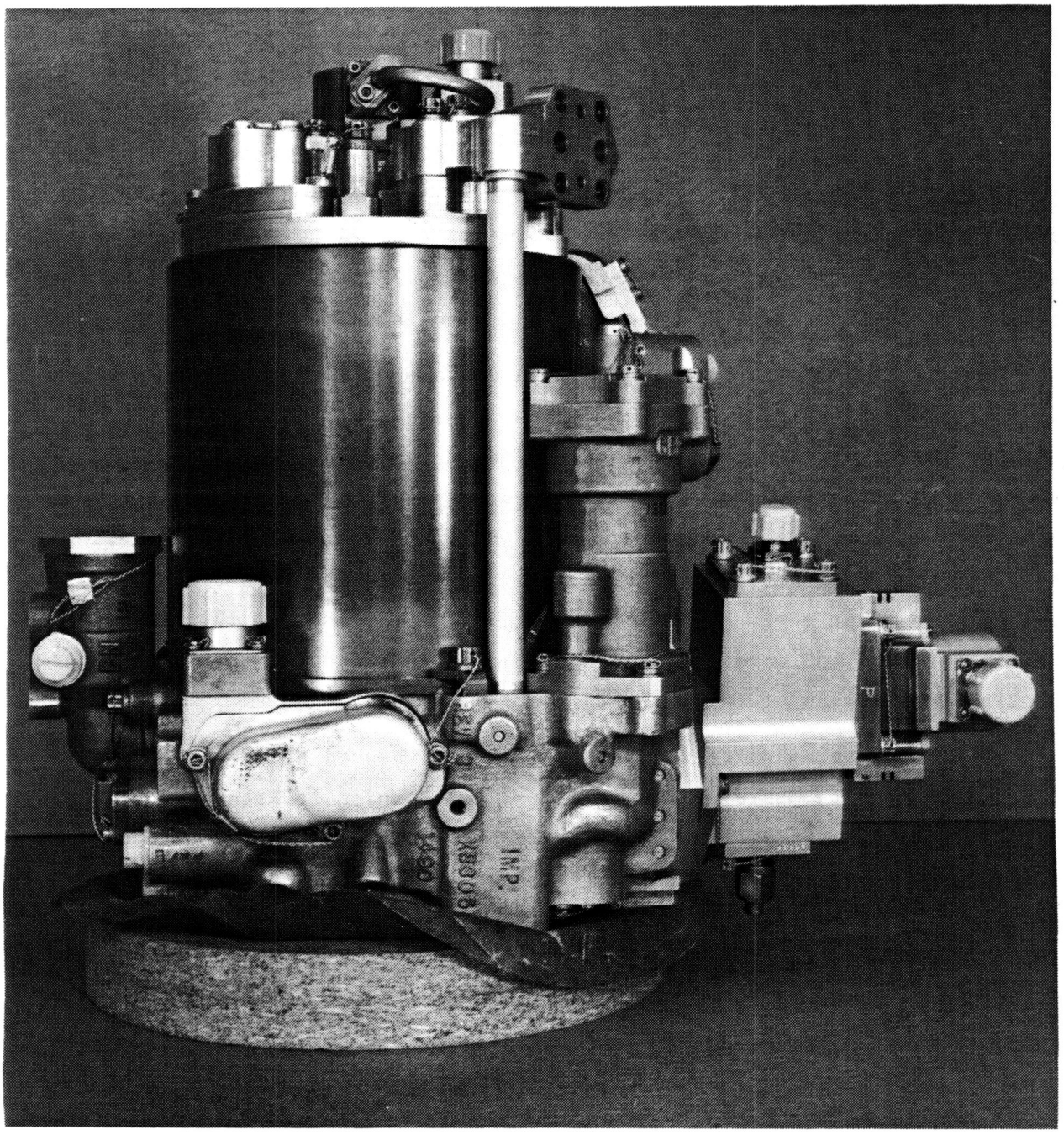

Figure 124. Main Fuel Control.

end of the last reporting period it was noted that the internal configuration of the control had been changed to provide better shielding between the power supply and other circuits. This proved to be an improvement, but noise continued to cause trouble; the most significant example was noise on the compressor inlet-temperature (T25) sensing channel equivalent to 20° F. This noise produced unacceptably erratic acceleration fuel scheduling and compressor stator scheduling. The noise was finally reduced to an acceptable level by rerouting wires in the analog-to-digital (A/D) converter section of the control. The T25 sensing noise was reduced to less than 0.4% of full scale.

The initial control software, which was prepared last year to represent preliminary ICLS control strategy, served as the basis for core engine control software. All of the ICLS-only elements were deleted, and updated versions of schedules such as the power lever angle (PLA) schedule and the acceleration fuel schedule were introduced along with a number of other refinements arising from component-test results and from experience with similar digital controls on other engines. The resulting software contains 4791 words of program memory and 458 words of constants memory, and it utilizes 368 of the available 512 words of read/write memory.

The core engine software was debugged and checked by incorporating it in a readily reprogrammable memory simulator and running it with the core engine control and a test simulator representing the core engine and other control-system hardware. Through this process, the software was refined until all functions were operating properly and within acceptable limits. Then it was introduced into a set of programmable, read-only memory (PROM) chips and the PROM's were installed in the control. A brief run was made with the engine/system simulator to verify that the software had transferred properly to the PROM set, and then the control was delivered for core engine control-system testing.

Work Planned

- Support core control system and engine testing
- Prepare and check software for ICLS digital control

2.8.3.3 Main-Zone Shutoff Valve

Technical Progress

The main-zone-shutoff valve and the derivative, pilot-zone-reset valve both were completed during this reporting period. Tests were run on both units verifying that they operate satisfactorily and in accordance with design requirements. Report R81AEG762 covering test of the main-zone shutoff valve was prepared and transmitted to NASA.

Work Planned

None; any further related work will be covered under WBS 2.8.3.1.

2.8.4.2 Accessory Design

Technical Progress

All of the accessories for the core engine have been received and most are currently involved in the control system test. The small amount of engineering during this reporting period has all been associated with acquisition of hardware and support of the system test.

Work Planned

- Support air valve calibration efforts
- Support core control system and engine testing

2.8.4.3 Sensor Design

Technical Progress

All of the sensors for the core engine have been received and are being tested as part of the core control-system test. This includes the T_3 sensor (a thermocouple probe designed specifically for the E^3 demonstrators), the linear variable-phase transducer (LVPT) position sensors installed in all air-valve actuators and in the main-zone shutoff valve, the compressor inlet-temperature detector (resistance type), and the rotary variable-phase transducer (RVPT) position sensor on the main fuel-metering valve.

Work Planned

None; any further work related to sensors will be covered under WBS 2.8.4.2.

2.8.5.1 Control System Testing

Technical Progress

The control-system components that will be used on the core engine have been installed in a bench test facility, and tests are underway. The only system components not included are the start-bleed valves, the compressor clearance-control valve, and the HPT clearance-control valve. These air valves will be flow-checked as part of the engine assembly process. The fuel-powered actuators for these air valves are included in the system test.

Figure 125 shows the digital control and associated components that will be set up in the control room, and Figure 126 shows the test-cell-mounted components that will be mounted on the engine.

The system test is in progress as this report is being written, and it is proceeding satisfactorily. The test is following the NASA approved test procedure described in Test Plan R81AEG708. Following satisfactory completion of the system testing, the components will be delivered for core engine assembly and test.

Work Planned

- Complete core engine system test
- Set up and run ICLS control-system test

2.9 NACELLE STRUCTURES

2.9.1 Nacelle Aerodynamic Design

Technical Progress

The pressure-loss predictions were completed for the ICLS exhaust system. These losses were combined with the ICLS mixing effectiveness, nozzle exit

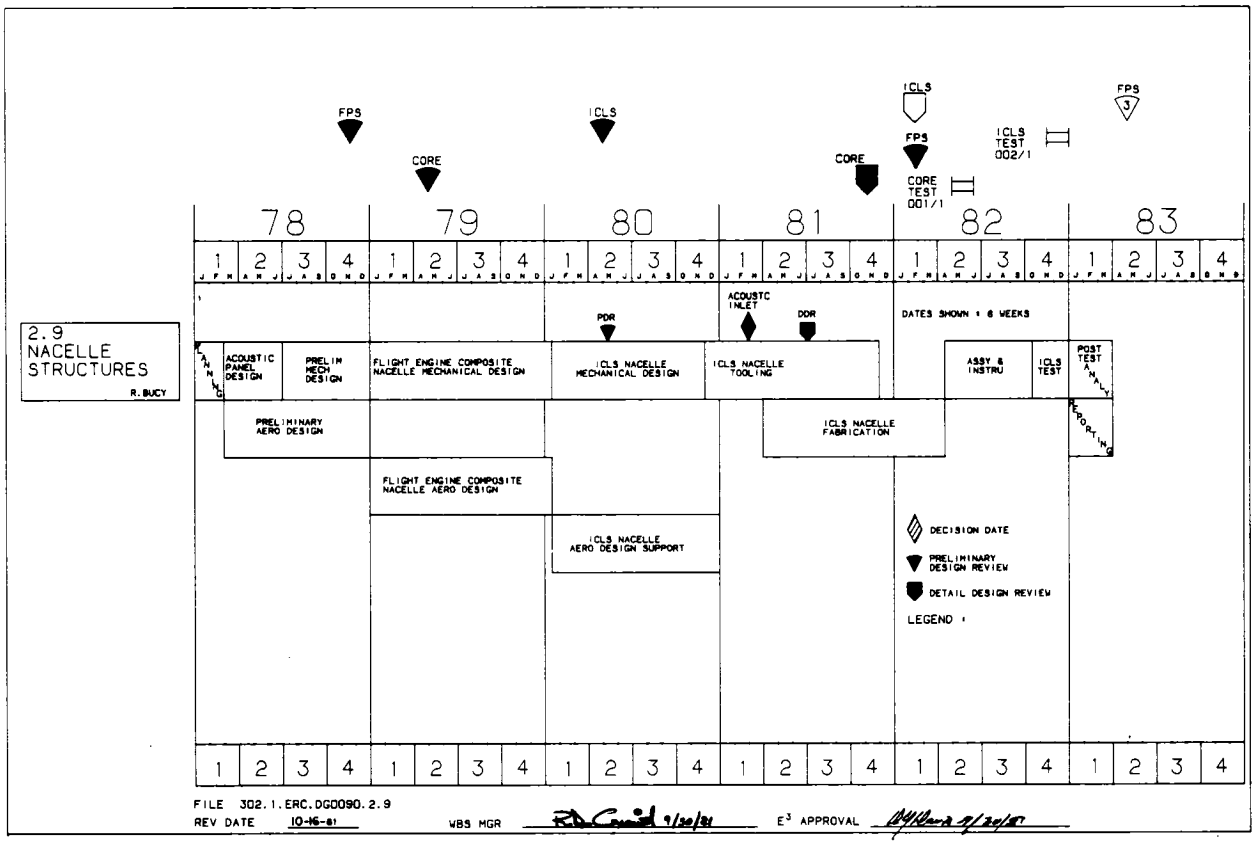
2.9
NACELLE
STRUCTURES
R. BUCY
FPS
CORE
ICLS
CORE
ICLS
FPS
CORE
TEST
001/1
ICLS
TEST
002/1
FPS
78
79
80
81
82
83
PDR
ACOUSTC
INLET
DDR
DATES SHOWN ± 6 WEEKS
PLANNING
ACOUSTIC
PANEL
DESIGN
PRELIM
MECH
DESIGN
FLIGHT ENGINE COMPOSITE
NACELLE MECHANICAL DESIGN
ICLS NACELLE
MECHANICAL DESIGN
ICLS NACELLE
TOOLING
ASSY &
INSTRU
ICLS
TEST
POST
TEST
ANALY
REPORTING
PRELIMINARY
AERO DESIGN
ICLS NACELLE
FABRICATION
FLIGHT ENGINE COMPOSITE
NACELLE AERO DESIGN
ICLS NACELLE
AERO DESIGN SUPPORT
DECISION DATE
PRELIMINARY
DESIGN REVIEW
DETAIL DESIGN REVIEW
LEGEND :
FILE 302.1.ERC.DG0090.2.9
REV DATE 10-16-81
WBS MGR
E³ APPROVAL

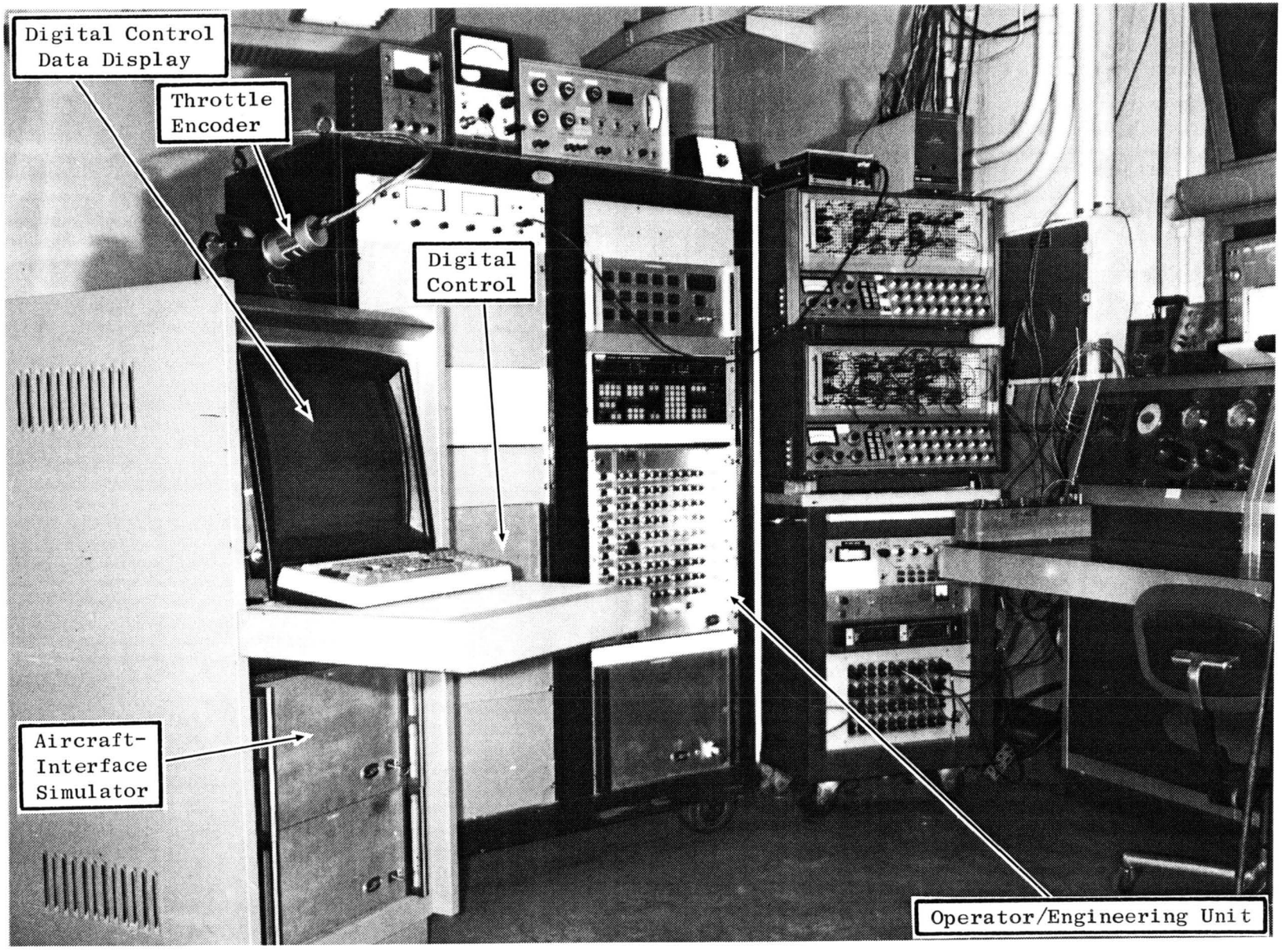

Figure 125. Control Room.

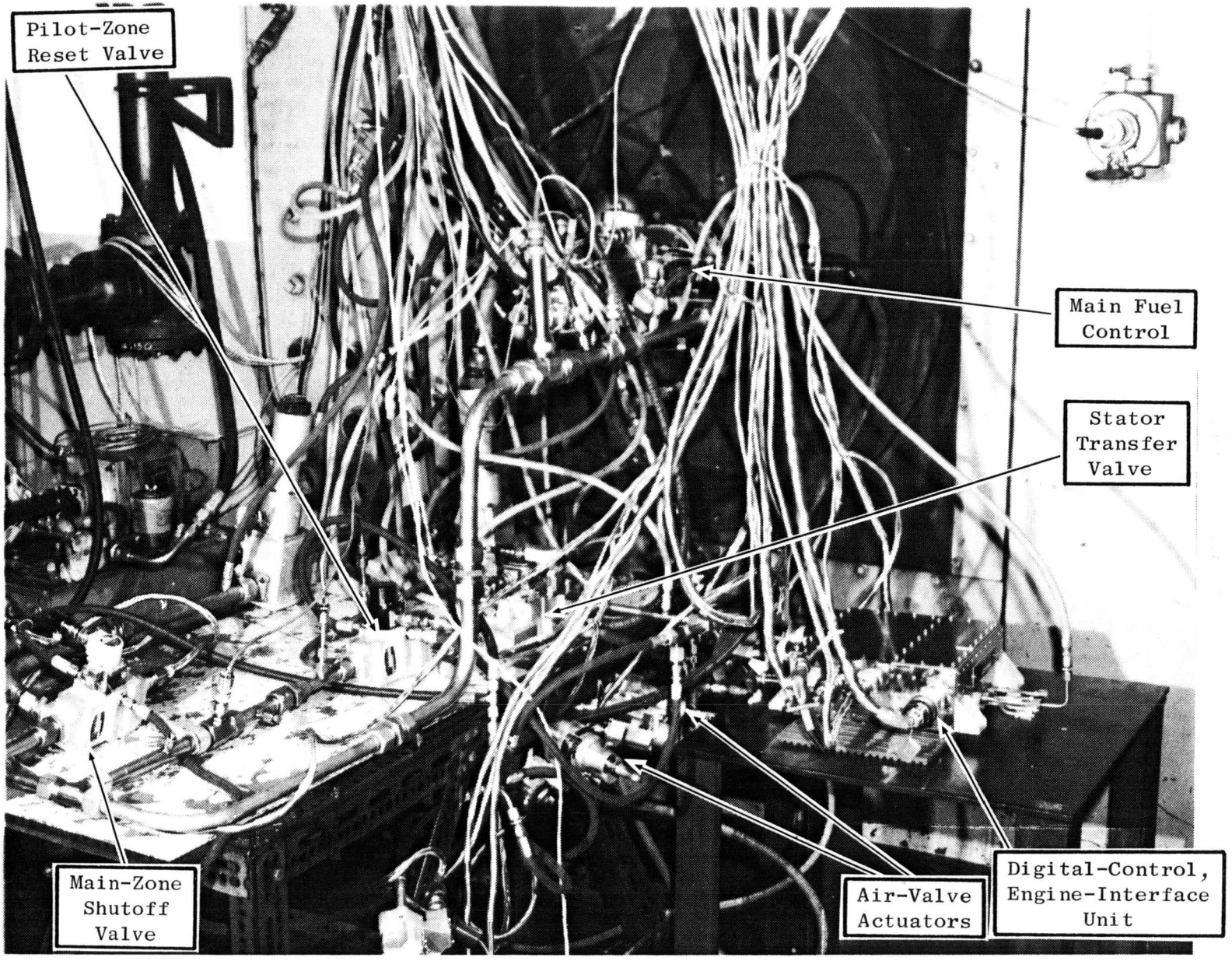

Figure 126. Control-System Test Cell.

coefficients, and mixer-matching characteristics determined from the scale-model test, WBS 2.6.4, to update the ICLS engine cycle deck. Analysis of the performance differences between FPS and ICLS was initiated but has not been completed.

Work Planned

Complete the FPS exhaust system performance predictions.

2.9.2 Nacelle Mechanical Design

Technical Progress

The objective of this task is to design and analyze boilerplate nacelle hardware for the ICLS engine test. The basic hardware to be designed includes the inlet, outer cowl doors, core cowl doors, fan nozzle, and pylon sidewalls. The design of these components has been discussed in previous semiannual reports and was described in detail at the ICLS Nacelle DDR given in July 1981.

The work performed under this WBS item during the current reporting period consisted of providing design support for the fabrication of the ICLS nacelle hardware.

Work Planned

Design support will be provided for the fabrication and procurement of the ICLS nacelle components being conducted under WBS 2.9.4. Support will also be provided for the assembly of this hardware at the Peebles test site.

2.9.4 Nacelle Hardware

Technical Progress

The objectives of this task are to perform the detail design of the boilerplate ICLS nacelle, fabricate the components, and perform a trial assembly of the nacelle for the ICLS engine test. The basic hardware to be fabricated includes the inlet, outer fan cowl doors (forward fan cowl) and outer apron, inner core cowl doors and inner apron, pylon sidewalls, ACC

scoop and plenum for the HPT and LPT, and fan exhaust nozzle (fan midcowl, fan aft cowl, and two exhaust nozzles).

All the required detail drawings have now been released, as have all except three of the assembly drawings. These three drawings are the overall nacelle assembly drawing, the core cowl assembly drawing, and the door hold-open assembly drawing.

All of the nacelle hardware is complete except for the acoustic panels for the fan and core cowl doors and the door hold-open assembly. This hardware is now being fitted to the mount beam and dummy engine assembly. All hinge fittings and attach angles will be line-drilled, once the fit-up is complete, to assure proper alignment of the nacelle hardware.

Work Planned

The fabrication of the ICLS nacelle will be completed and the hardware shipped to the Peebles test site.

3.0 TASK 3 - CORE TESTING

Overall Objectives

- Design, fabricate, assemble, and test a core engine and obtain experimental evaluation of E^3 components operating as a system
- Develop methods by which performance of the core can be measured as to suitability as a core for the projected Flight Propulsion System
- Evaluate performance and mechanical integrity of the core to identify changes required to meet program goals. Within program timing and cost constraints, incorporate design improvements identified from component and core testing into core and ICLS hardware.

Development Approach (Reference WBS Spread/Schedule Sheet)

The core engine will incorporate the individual components designed and tested in part or full scale in Task 2 (Component Analysis, Design, and Development). These components will include the high-pressure compressor, the combustor, and the high-pressure turbine. They will include clearance-control devices and a control system adequate to permit starting, steady-state operation, and slow transients. The purpose of the core test will be to evaluate the performance, stability, and mechanical integrity of the components as a system and to identify desirable changes for incorporation into the ICLS or the FPS.

The core test vehicle will be assembled with extensive performance and mechanical instrumentation, including:

- Gas-path, steady-state total temperature and pressure rakes at compressor inlet, compressor exit, and turbine exit
- Rotor mechanical speed measurement
- Fuel flow measurement
- Compressor rotor and stator strain gage instrumentation, based on FSCT results, sufficient to monitor mechanical integrity
- Turbine rotor and stator strain gage instrumentation sufficient to monitor mechanical integrity

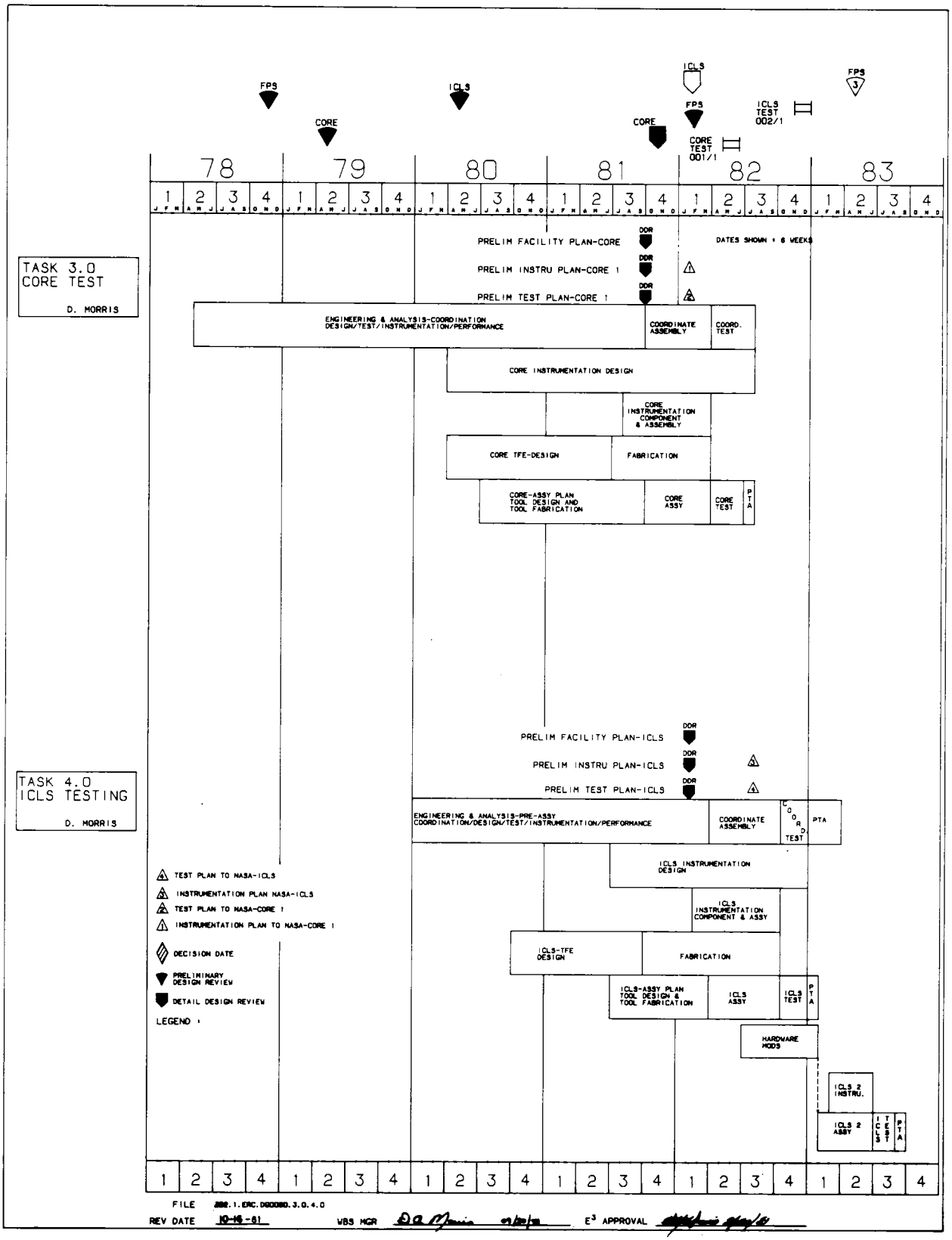
FPS
CORE
ICLS
FPS
CORE
ICLS
TEST
002/1
FPS
3
CORE
TEST
001/1
78
79
80
81
82
83
1 2 3 4 1 2 3 4 1 2 3 4 1 2 3 4 1 2 3 4 1 2 3 4
J F M A M J J A S O N D
DATES SHOWN + 6 WEEKS
TASK 3.0
CORE TEST
D. MORRIS
PRELIM FACILITY PLAN-CORE
PRELIM INSTRU PLAN-CORE 1
PRELIM TEST PLAN-CORE 1
DDR
ENGINEERING & ANALYSIS-COORDINATION
DESIGN/TEST/INSTRUMENTATION/PERFORMANCE
COORDINATE ASSEMBLY
COORD. TEST
CORE INSTRUMENTATION DESIGN
CORE INSTRUMENTATION COMPONENT & ASSEMBLY
CORE TFE-DESIGN
FABRICATION
CORE-ASSY PLAN TOOL DESIGN AND TOOL FABRICATION
CORE ASSY
CORE TEST
PTA
TASK 4.0
ICLS TESTING
D. MORRIS
PRELIM FACILITY PLAN-ICLS
PRELIM INSTRU PLAN-ICLS
PRELIM TEST PLAN-ICLS
ENGINEERING & ANALYSIS-PRE-ASSY
COORDINATION/DESIGN/TEST/INSTRUMENTATION/PERFORMANCE
COORDINATE ASSEMBLY
COORD. TEST
PTA
ICLS INSTRUMENTATION DESIGN
ICLS INSTRUMENTATION COMPONENT & ASSY
ICLS-TFE DESIGN
FABRICATION
ICLS-ASSY PLAN TOOL DESIGN & TOOL FABRICATION
ICLS ASSY
ICLS TEST
PTA
HARDWARE MODS
ICLS 2 INSTRU.
ICLS 2 ASSY
ICLS 2 TEST
PTA
TEST PLAN TO NASA-ICLS
INSTRUMENTATION PLAN NASA-ICLS
TEST PLAN TO NASA-CORE 1
INSTRUMENTATION PLAN TO NASA-CORE 1
DECISION DATE
PRELIMINARY DESIGN REVIEW
DETAIL DESIGN REVIEW
LEGEND :
1 2 3 4 1 2 3 4 1 2 3 4 1 2 3 4 1 2 3 4 1 2 3 4
FILE
REV DATE 10-16-81
WBS MGR
E³ APPROVAL

- Inlet airflow instrumentation
- Variable guide vane setting readout
- Measurement of compressor rotor tip clearances for Stages 3, 5, and 10
- Compressor interstage steady-state instrumentation; incorporated, as necessary, to determine compressor interstage conditions
- Measurement of HPT rotor tip clearances
- Parasitic flowpath instrumentation, included to help evaluate the design of sump venting and cooling systems and to establish the levels of parasitic flows under actual operating conditions; direct measurement of parasitic flows will be done wherever such measurements are practical in the hardware configuration
- Temperature measurements of the compressor and turbine casings for evaluation of ACC effectiveness
- Temperature measurements of HPT rotor, stator, and other hot structures

The core vehicle test program will be designed to exercise the components over a sufficiently wide range to cover operating requirements in the ICLS. This will include operation at SLS ambient inlet conditions and with inlet heat/ram operation. In addition to covering the ICLS operating range, the characteristics of the core engine will be explored up to the corrected airflow (120 lbm/sec) required for FPS operation throughout the flight envelope. This will provide an important part of the basis for extrapolating ICLS performance to altitude conditions outside the range of ICLS testing.

Prior to testing, a core engine computer model will be constructed on the basis of component rig tests and core engine configuration assembly measurements. This model will represent the anticipated performance of the core engine and will be used in the generation of pretest predictions and in the analysis of test results.

Using the core engine computer model as a base, a data-reduction program will be developed to analyze the measurements during testing. This will ensure consistency of calculation procedures between the core engine computer model and the data-reduction program, and it will substantially facilitate the construction of a status-performance model.

As the engine test results are obtained, the performance of the individual components and the overall core system will be compared to the performance of the pretest prediction model. Deviations in performance will be identified, and reasons for those deviations will be determined. As a result of this analysis, desirable changes will be identified for incorporation in the ICLS or the FPS design.

At the conclusion of the core test, a core test status-performance computer model will be established. This will be used to project ICLS performance on the basis of the demonstrated core engine performance. In conjunction with the ICLS test results plus improvements anticipated from further component development, it will provide the essential basis for FPS performance projections.

3.1.1 Core Engineering and Analysis

Technical Progress

Instrumentation application and buildup of the core engine subassemblies began in October. The major effort during this reporting period was to provide engineering support for these two activities. In addition, the facility hardware designs were finalized and parts placed on order. A summary of the work effort is listed below.

- Refined core assembly schedule
- Refined core instrumentation list
- Completed core instrumentation drawing
- Completed core centerline machining operations
- Finalized subassembly procedures and tooling lists
- Provided floor engineering coverage for assembly and instrumentation activities
- Finalized facility hardware list and placed parts on order
- Monitored hardware designs for assembly and maintainability ease
- Monitored assembly tooling design and procurement

- Held design reviews for subassembly procedures and tooling, instrumentation application drawings, and facility hardware
- Prepared and presented formal Core DDR in November for assembly and test functions
- Started work on Test Request

Work Planned

- Complete core engine buildup
- Prepare Test Request, finalize test plan
- Complete procurement of test and facility hardware
- Start and complete core test
- Continue to provide engineering coordination between Design and the supporting organizations

3.1.2 Core Instrumentation and Assembly

3.1.2.1 Instrumentation Design

Technical Progress

The major work efforts during this reporting period were in defining and finalizing methods for the application and leadout of instrumentation sensors according to the Instrumentation Plan and providing engineering support during the application and assembly process. The major activities are listed below.

- Completed all subassembly and main-engine-level application drawings
- Finalized all hardware rework requirements
- Completed design of turbine discharge rakes and started fabrication
- Completed design of forward and aft slipring hardware and started fabrication
- Completed design of clearanceometers for compressor Stages 3, 5, and 10. A prototype model was tested with excellent results, and fabrication of the probe hardware was initiated.

- Completed fabrication of compressor rotor instrumentation leadout duct
- Received all engine accelerometers and completed fabrication of brackets
- Received forward sump proximity probes and completed bracket fabrication

Work Planned

- Complete fabrication and assembly of sliprings
- Complete rake and clearanceometer fabrication
- Provide engineering support as required during assembly and test

3.1.2.2 Instrumentation Application

Technical Progress

- Completed thin-film strain gage application on compressor Stages 1 through 7 blades and IGV/Stage 6 stator vanes
- Completed application of leading-edge aerodynamics sensors on all stator vanes
- Completed sensor application on all components of the following subassemblies:
  - Compressor Rotor
  - Compressor Stator Vanes
  - Compressor Stator Cases
  - Combustor
  - Diffuser/OGV
  - CDN
  - Stage 1 HPT Nozzles
  - Stage 2 HPT Nozzles
  - Rear Frame/Aft Sump
  - No. 3 Bearing
  - Turbine Stator
  - Turbine Rotor

- Completed sensor routing and tiedown on the Stage 1 nozzle, Stage 2 nozzle, and CDN subassemblies
- Completed approximately 90% of leadout and tiedown on compressor and turbine rotors
- About 80% complete in fabrication of rakes for the compressor inlet, compressor discharge, and turbine discharge

Work Planned

- Complete application and leadout of engine sensors
- Complete final termination
- Provide assembly and test coverage as required

3.1.2.3 Core Assembly

Technical Progress

- Completed design and procurement of assembly tooling
- Completed written procedures for all subassemblies and main engine
- Completed centerline machining, compressor and turbine rotor tip grinds, compressor and turbine stator flowpath and interstage seal grinds, and CDN seal grind
- Completed buildup of compressor and turbine rotors
- Completed buildup of CDN, Stage 1 turbine nozzles, and Stage 2 turbine nozzles
- Approximately 90% complete on buildup of forward and aft stator cases
- Initiated buildup of accessory gearbox, inlet gearbox, and turbine frame

Work Planned

- Complete buildup of core engine
- Provide test cell support as required

3.1.2.4 Signal Conditioning

Technical Progress

- Completed optical assembly of all turbine-clearance probes (laser)
- Initiated work on signal processor
- Completed fabrication and fitup of probes in engine
- Completed programming on signal processor
- Provide engineering support during assembly and test

3.1.3 Core Test Facilities Engineering

Technical Progress

- Completed design and fabrication of buildup/transport dolly
- Defined engine installation and slave service systems
- Received about 80% of all facility hardware; the remainder is on order with all deliveries promised by 5/1/82
- Received components for inlet prefilter and initiated assembly
- Completed design reviews with Evaluation and Design Engineering
- Completed cell installation drawing

Work Planned

- Complete fabrication of remaining facility hardware items and slave systems
- Complete test cell installation of inlet hardware and slave systems
- Assist in installation of engine in the test cell
- Provide engineering support during cell installation and engine test

4.0 TASK 4 - ICLS TESTING

Overall Objectives

- Design, fabricate, assemble, and test a turbofan demonstrator engine and obtain experimental evaluation of E^3 components operating as a system
- Develop methods by which performance of the turbofan demonstrator engine can be measured as to suitability toward the projected Flight Propulsion System
- Evaluate performance and mechanical integrity of the turbofan demonstrator engine and identify changes required to meet program goals.

Development Approach (Reference WBS Spread/Schedule Sheet)

The turbofan engine will incorporate the individual components designed and tested in part or full scale in Task 2 (Component Analysis, Design, and Development). These components will include the high-pressure compressor, combustor, high-pressure turbine, fan, low-pressure turbine, and mixer including clearance-control devices and a control system adequate to permit starting, steady-state operation, and slow transients. The current plan is to use the applicable core test vehicle and full-scale fan test vehicle component hardware in the assembly of the ICLS. This assumes that there will be no major hardware modifications required as a result of the individual component tests. The purpose of the ICLS test will be to evaluate the performance, stability, and mechanical integrity of the components as a system and to identify desirable changes for the FPS.

The turbofan test engine will be assembled with extensive performance and mechanical instrumentation, including:

- Gas-path, steady-state total temperature and pressure rakes at the fan inlet, compressor inlet, compressor exit, HPT exit, LPT exit, and mixer exhaust.
- Rotor mechanical speed measurements
- Fuel flow measurement

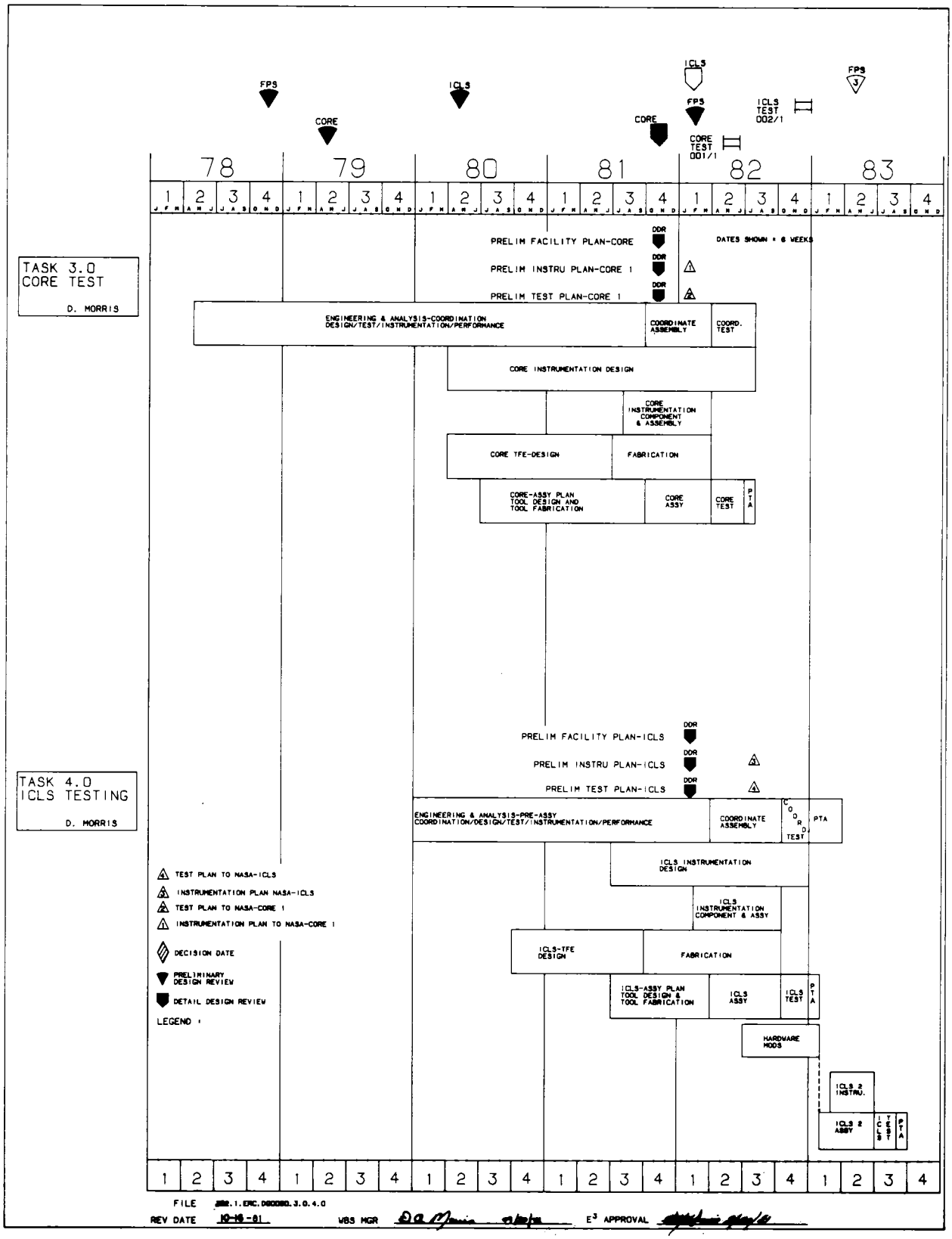
FPS
CORE
ICLS
CORE
FPS
ICLS
CORE TEST 001/1
ICLS TEST 002/1
FPS
78
79
80
81
82
83
DATES SHOWN = 6 WEEKS
TASK 3.0
CORE TEST
D. MORRIS
PRELIM FACILITY PLAN-CORE
PRELIM INSTRU PLAN-CORE 1
PRELIM TEST PLAN-CORE 1
DDR
ENGINEERING & ANALYSIS-COORDINATION DESIGN/TEST/INSTRUMENTATION/PERFORMANCE
COORDINATE ASSEMBLY
COORD. TEST
CORE INSTRUMENTATION DESIGN
CORE INSTRUMENTATION COMPONENT & ASSEMBLY
CORE TFE-DESIGN
FABRICATION
CORE-ASSY PLAN TOOL DESIGN AND TOOL FABRICATION
CORE ASSY
CORE TEST
PTA
TASK 4.0
ICLS TESTING
D. MORRIS
PRELIM FACILITY PLAN-ICLS
PRELIM INSTRU PLAN-ICLS
PRELIM TEST PLAN-ICLS
ENGINEERING & ANALYSIS-PRE-ASSY COORDINATION/DESIGN/TEST/INSTRUMENTATION/PERFORMANCE
COORDINATE ASSEMBLY
COORD TEST
PTA
ICLS INSTRUMENTATION DESIGN
ICLS INSTRUMENTATION COMPONENT & ASSY
ICLS-TFE DESIGN
FABRICATION
ICLS-ASSY PLAN TOOL DESIGN & TOOL FABRICATION
ICLS ASSY
ICLS TEST
PTA
HARDWARE MODS
ICLS 2 INSTRU.
ICLS 2 ASSY
ICLS TEST
PTA
TEST PLAN TO NASA-ICLS
INSTRUMENTATION PLAN NASA-ICLS
TEST PLAN TO NASA-CORE 1
INSTRUMENTATION PLAN TO NASA-CORE 1
DECISION DATE
PRELIMINARY DESIGN REVIEW
DETAIL DESIGN REVIEW
LEGEND :
FILE
REV DATE 10-16-81
WBS MGR
E³ APPROVAL

- Fan rotor and stator strain gage instrumentation, based on FSFT results, sufficient to monitor mechanical integrity
- LPT rotor and stator strain gage instrumentation sufficient to monitor mechanical integrity
- Inlet airflow instrumentation
- Variable guide vane setting readout
- Combustor static pressure (control pressure) measurement
- Compressor interstage static pressure instrumentation; incorporated, as necessary, to determine compressor interstage conditions
- Direct measurement of HPT rotor tip clearances
- Parasitic flowpath instrumentation, included to help evaluate the design of sump venting and cooling system and to establish the levels of parasitic flows under actual operating conditions; direct measurement of parasitic flows will be done wherever such measurements are practical in the hardware configuration
- Measurement of baseline and fully suppressed acoustical characteristics
- Exhaust emissions measurement
- Temperature measurement of the compressor, HPT, and LPT cases sufficient to evaluate ACC effectiveness
- Temperature measurements of LPT rotor and other bolt structures

The ICLS test program will be designed to test the components over the entire range of ICLS operating conditions. All testing will be at ambient inlet conditions. In addition to covering the ICLS operating range, the characteristics of the core engine will be explored up to the corrected airflow (120 lbm/sec) required for FPS operation throughout the flight envelope. This will provide an important part of the basis for extrapolating ICLS performance to altitude conditions outside the range of ICLS testing.

Prior to testing, an ICLS computer model will be constructed on the basis of component rig tests, core engine test, and the ICLS configuration assembly measurements. This model will represent the anticipted performance of the ICLS engine and will be used in the generation of pretest predictions and in the analysis of test results.

Using the ICLS computer model as a base, a data-reduction program will be developed to analyze the measurements during testing. This will ensure consistency of calculation procedures between the ICLS computer model and the data-reduction program and substantially facilitate the construction of a status-performance model.

As the engine test results are obtained, the performance of the individual components and the overall engine system will be compared to the performance of the pretest-prediction model. Deviations in performance will be identified, and reasons for those deviations will be determined. As a result of this anlaysis, desirable changes will be identified for the FPS design.

4.1.1 ICLS Preassembly Engineering and Analysis

Technical Progress

During this reporting period, the primary task continued to be the definition and engineering coordination effort between Design Engineering and the contributing support organizations. The major work efforts are listed below.

- Disassembled full-scale fan test vehicle. Rotor components were cleaned, inspected, and placed in storage. The fan frame is at a vendor undergoing machining required for ICLS assembly.
- Finalized instrumentation list, initiated work on the instrumentation drawing
- Refined assembly procedures and schedule, defined tooling list
- Defined hardware rework for instrumentation of the LPT
- Began fitup of cowling on a dummy engine at Mojave
- Prepared material for ICLS Detail Design Review

Work Planned

- Monitor design and procurement of assembly tooling
- Develop written assembly procedures and review with Design Engineering
- Complete fan frame rework
- Initiate instrumentation and buildup of ICLS subassemblies

4.2.2.1 LPT Rotor Hardware (For ICLS Tests)

All rotor hardware is on order. All the major structural hardware for the rotor has been received during this reporting period. The disks and rotor seals have been completed, including instrumentation rework. The rotor nuts and bolts have been received, and machining of the blades has been initiated.

Blades

Details on the blades are reported under WBS 2.5.6.1.

Rotor

All five stages of rotor disks and seals have been completed including instrumentation rework. Photos of the rotor components are shown in Figures 127 through 136. As finished parts are being received, they are being weighed for correlation with calculations. Actual weights of the disks and rotor seals are listed in Table XXV. These measured weights are within 5% of the earlier calculated weight.

Table XXV. LPT Disk and Seal Weights.

Item	Part Number	Weight, gram (lbm)	
Disk, Stage 1	4013205-784P02	14,687	(32.35)
Disk, Stage 2	4013205-785P01	19,840	(43.70)
Disk, Stage 3	4013205-786P01	26,627	(58.65)
Disk, Stage 4	4013205-787P02	26,219	(57.75)
Disk, Stage 5	4013205-788P01	22,201	(48.90)
Rotor Seal, Stage 1	4013205-968P02	2,297	(5.06)
Rotor Seal, Stage 1/2	4013205-969P01	3,927	(8.65)
Rotor Seal, Stage 2/3	4013205-983P01	4,327	(9.53)
Rotor Seal, Stage 3/4	4013205-970P01	2,197	(4.84)
Rotor Seal, Stage 4/5	4013205-970P02	1,870	(4.12)
Total		124,192	(273.55)

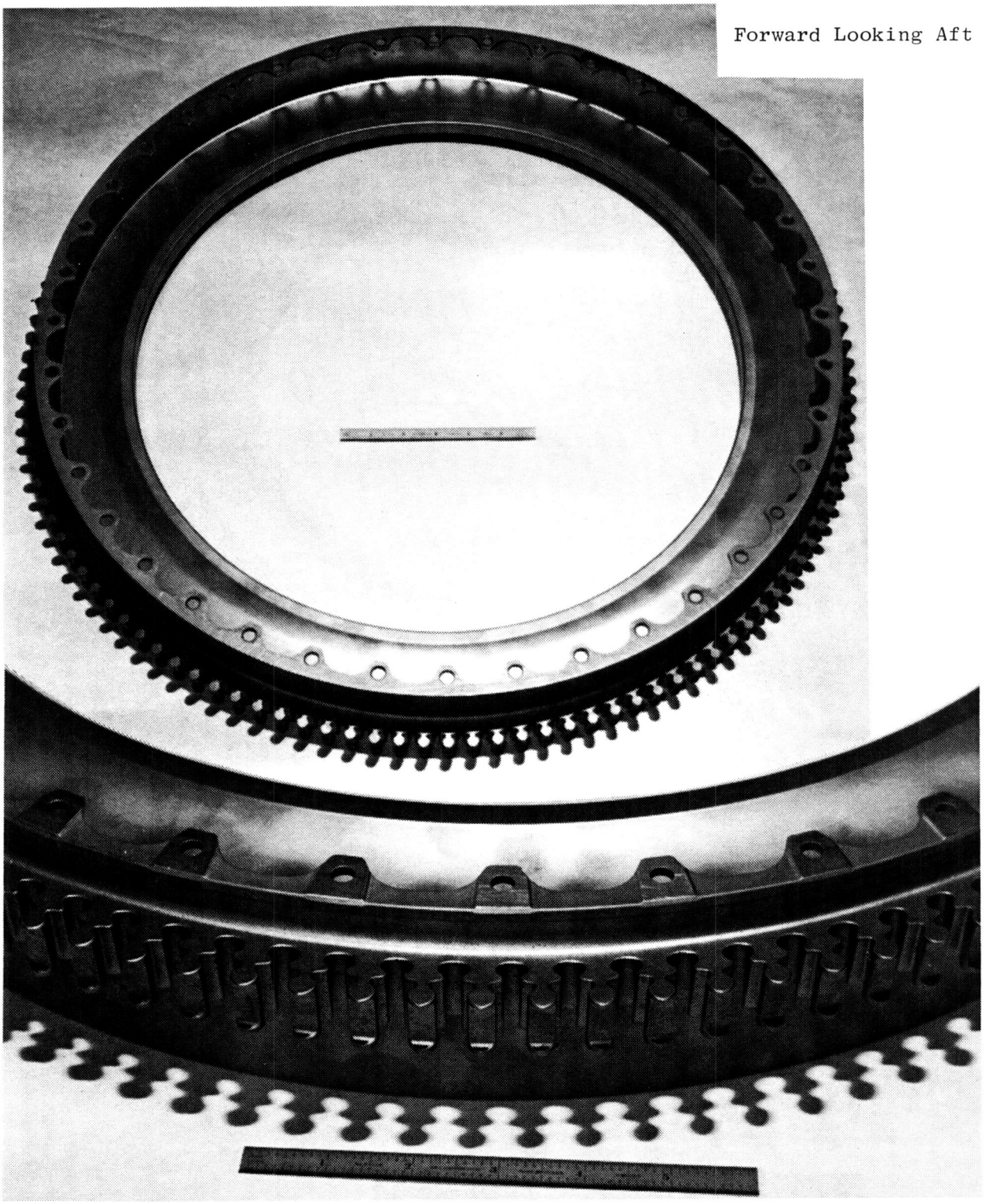

Figure 127. Stage 1 Disk.

Forward Looking Aft

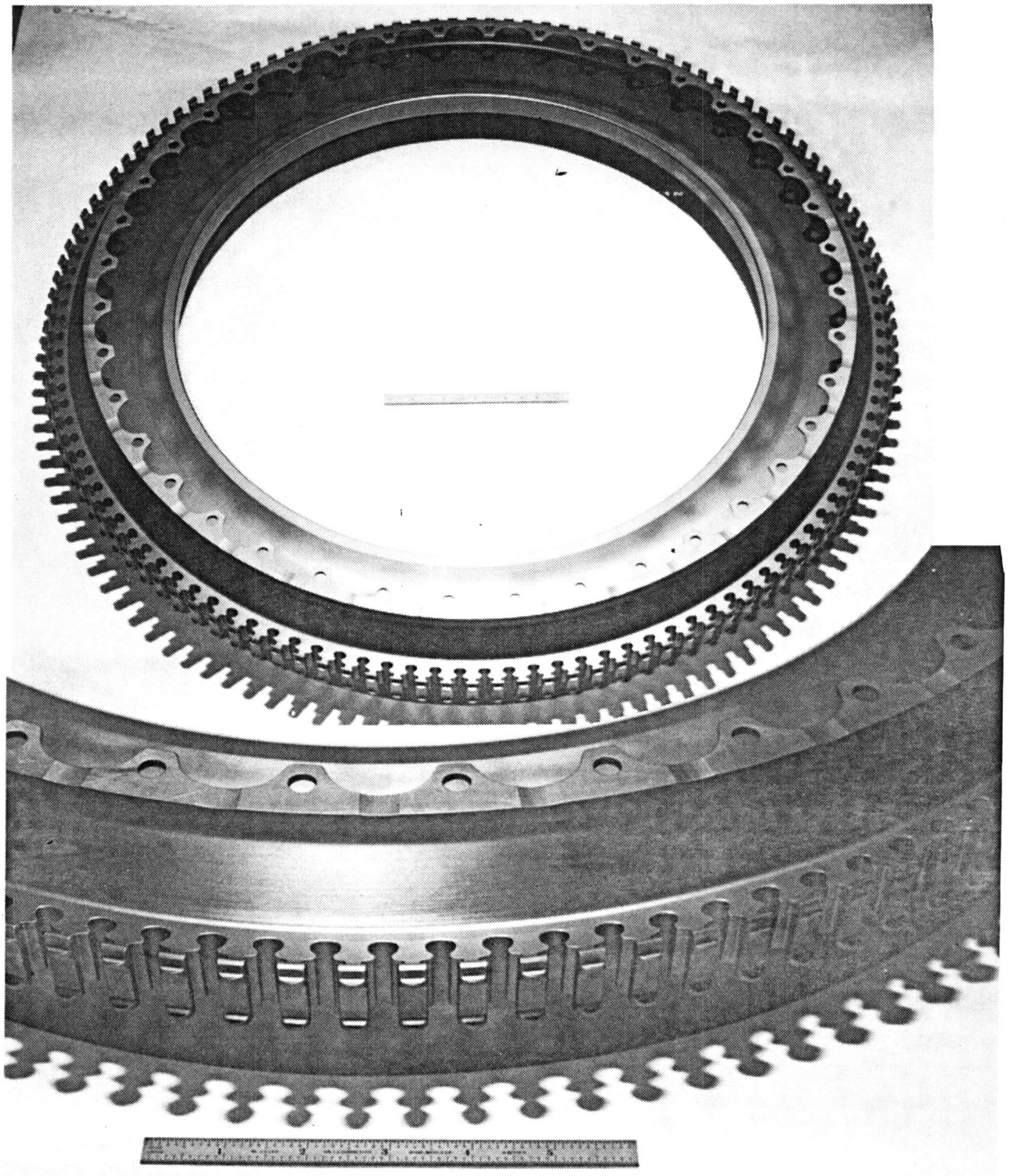

Figure 128. Stage 2 Disk.

Figure 129. Stage 3 Disk.

Figure 130. Stage 4 Disk.

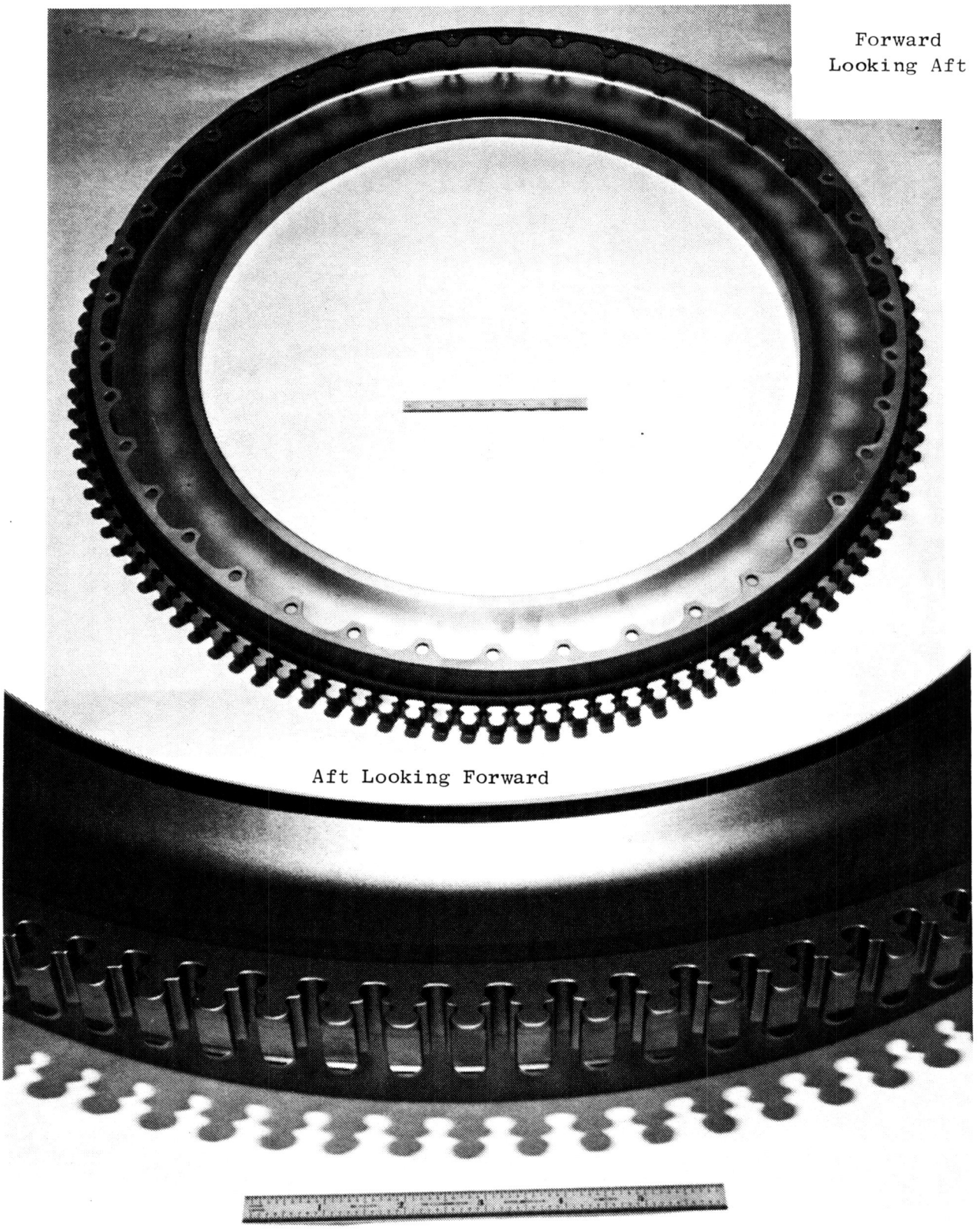

Figure 131. Stage 5 Disk

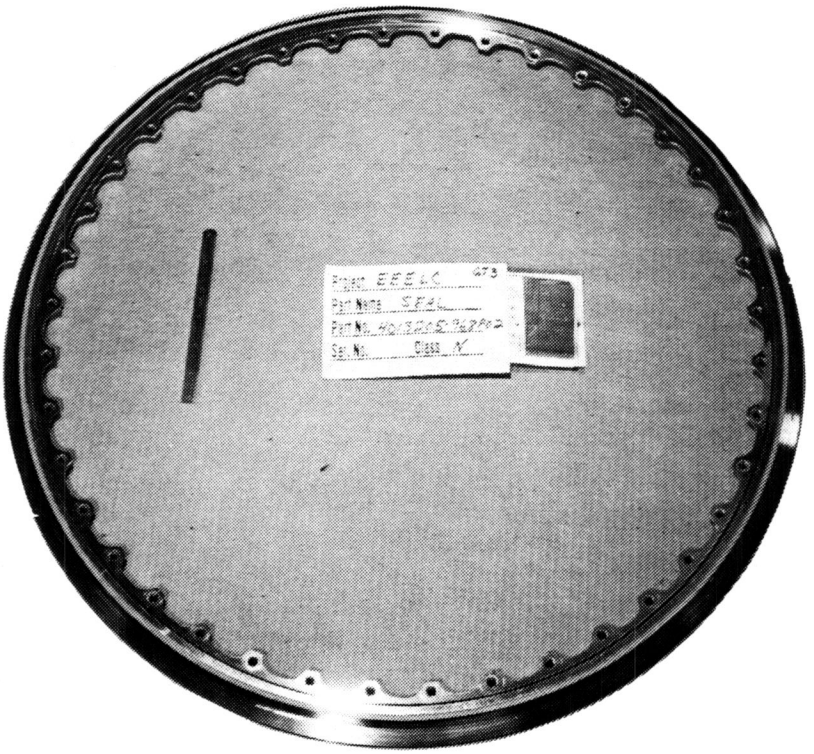

Figure 132. Stage 1 Rotor Seal.

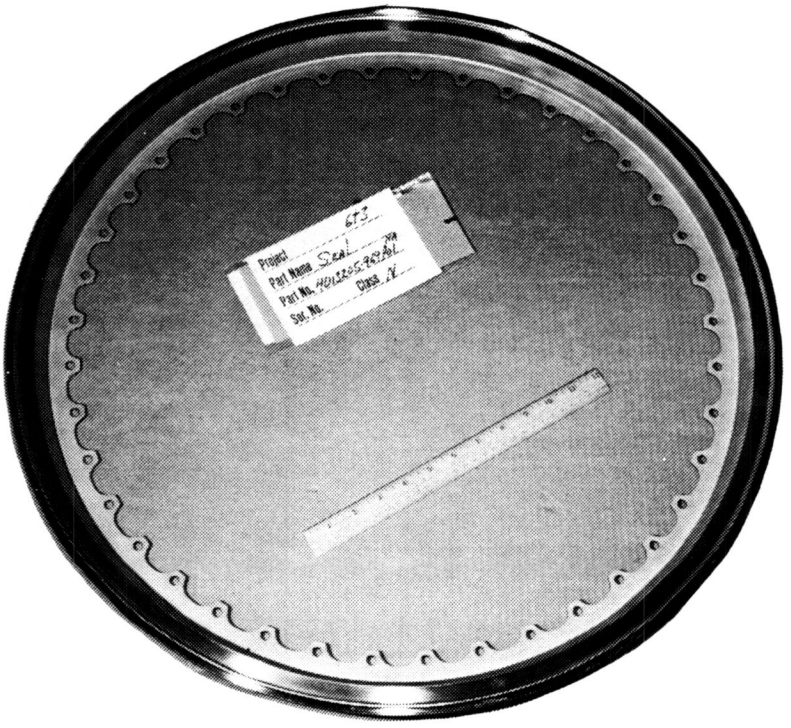

Figure 133. Stage 1/2 Rotor Seal.

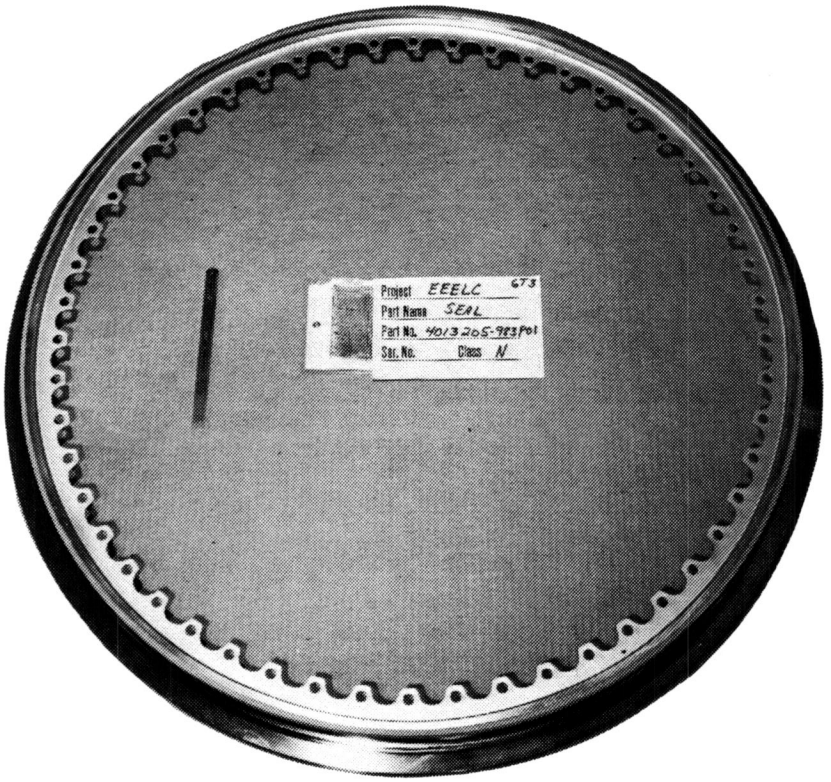

Figure 134. Stage 2/3 Rotor Seal.

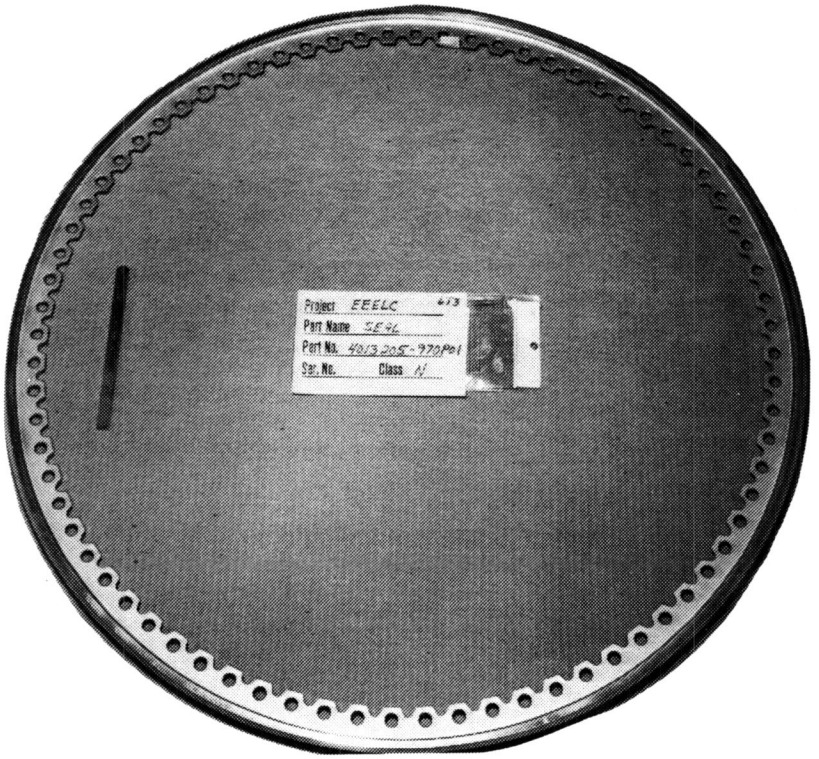

Figure 135. Stage 3/4 Rotor Seal.

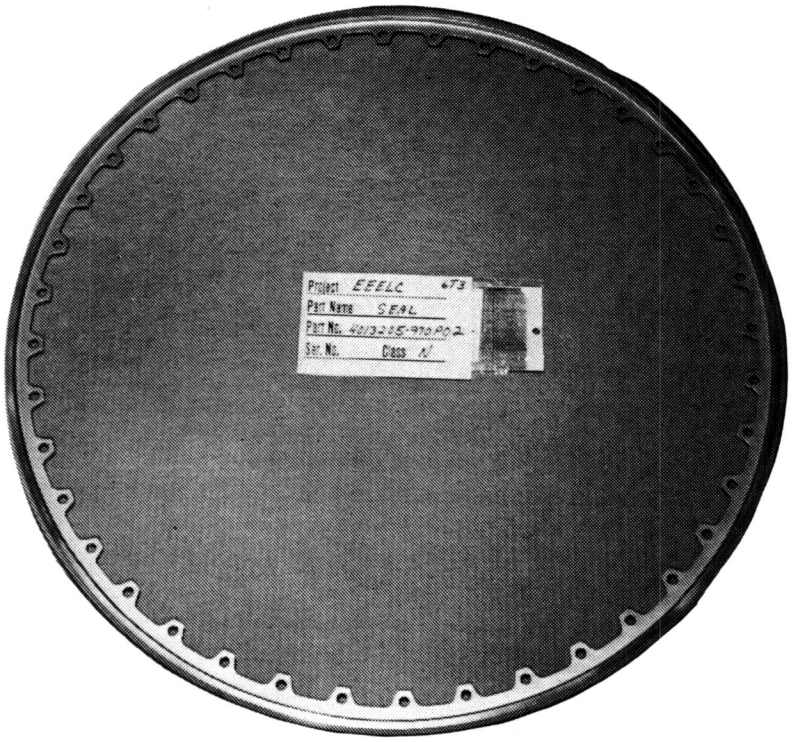

Figure 136. Stage 4/5 Rotor Seal.

Four Stage 5 blades with machined dovetails were trial fitted into the disk successfully. The blades were slid into the disk with the bent tab retainers in the disk dovetail slots. They fit snugly, and all the blade dovetail pressure faces contacted the disk.

Fasteners

All rotor nuts and bolts have been received. All that remains to be received are weights to balance the rotor at assembly and "C clips" to hold the rotor seals to the Stages 2 and 3 disks at assembly.

Work Planned

- Receive remaining fasteners
- Receive machined blades

4.2.2.2 LPT Nozzle Hardware

All nozzle hardware for the ICLS has been ordered, and scheduled deliveries meet the required dates for ICLS build-up.

Nozzles

See WBS 2.5.6.2 (for Stage 1) and WBS 2.5.6.3 (for Stages 2 through 5).

Inner Seal Supports

Both the forward and the aft inner seal supports have been completed, including instrumentation rework, and are in engineering stores. The aft inner seal support was flow checked and is within design limits (see Figure 137).

Work Planned

- Trial fit seal supports to attaching hardware
- Follow hardware through instrumentation and engine build

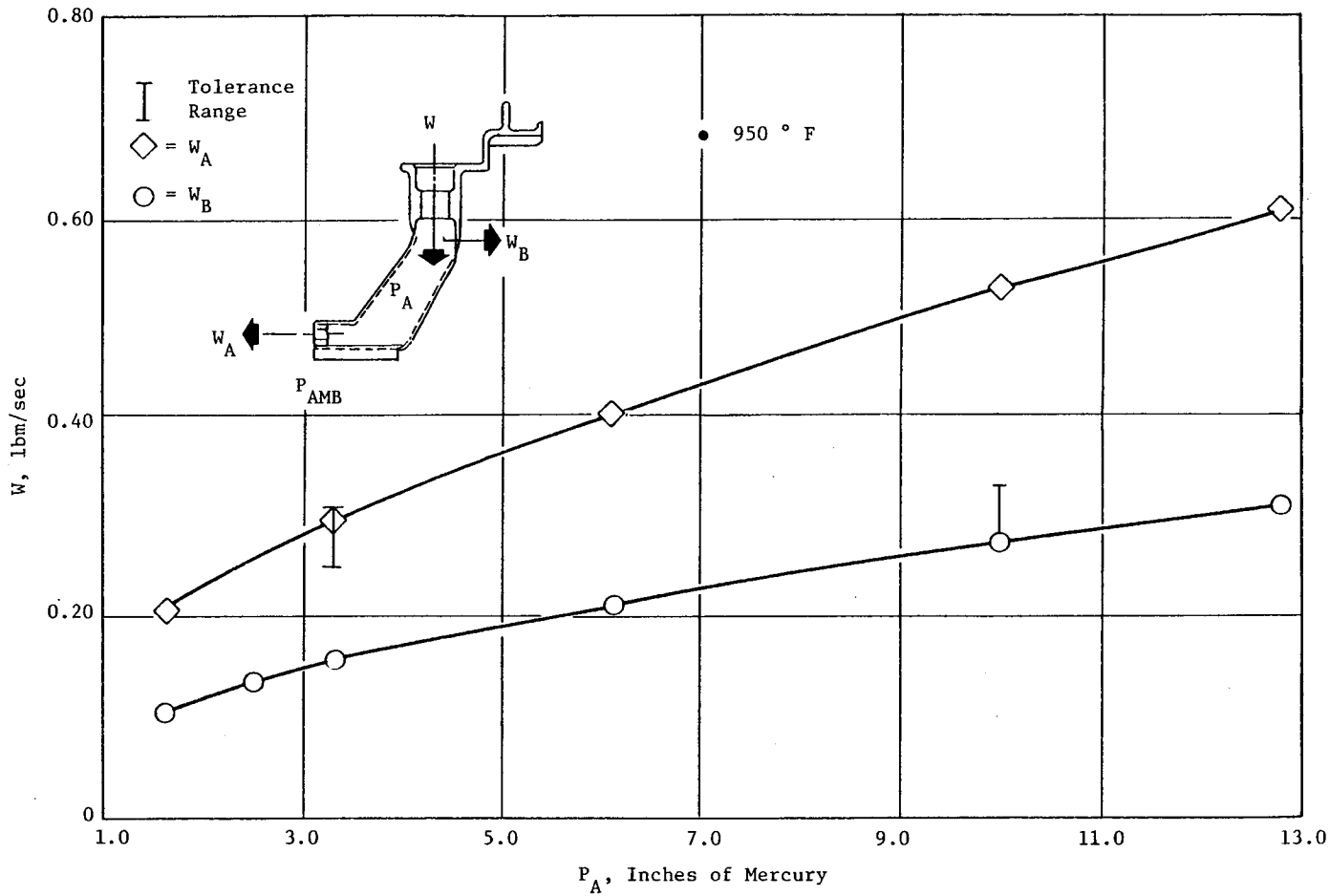

Figure 137. LPT Stage 1 Nozzle Stationary Air Seal.

4.2.2.3 LPT Static Structures Fabrication

All static-structure hardware items for ICLS have been ordered. Fabrication is in progress, and scheduled deliveries meet the required dates for ICLS buildup.

LPT Casing

The LPT case is very near completion, well in advance of the date required to meet ICLS buildup. A picture of the LPT casing about midway through the fabrication process is shown in Figure 138. At the time of this picture, the cylindrical front forging ring and the cylindrical aft forging ring had been welded together, heat treated, and all of the outside (OD) turning had been completed. The rings which stand out in the picture are still in the rough-machined state from which borescope and instrumentation bosses are to be machined. Since the instrumentation bosses were defined early enough to be included in the fabrication of the case, no additional rework of the case for instrumentation will be required. The photo shows the rings are being milled away to leave only material for each boss. The forward two rings (top of picture) have already been removed, leaving the bosses 180° apart, as can be seen at each side of the picture.

Since the time of the picture, the OD machining removal of the rings and the ID turning have been completed. The flanges have been turned, the bolt holes put in, and the bosses turned and blended with the casing shell.

All that remains to be completed are the machining of slots in the shroud hangers, holes in the bosses for lock wire, and finishing touches. Currently the slots are being added to the shroud hangers.

Outer Duct Support Machining

The outer duct support has two diameters that mate with the HP casing. These are flame sprayed during the machining operation for wear resistance during engine operation. Problems with the flame spray on one of those diameters have delayed completion of the support, but a wear coat has now been successfully applied. After this diameter is ground to final dimensions,

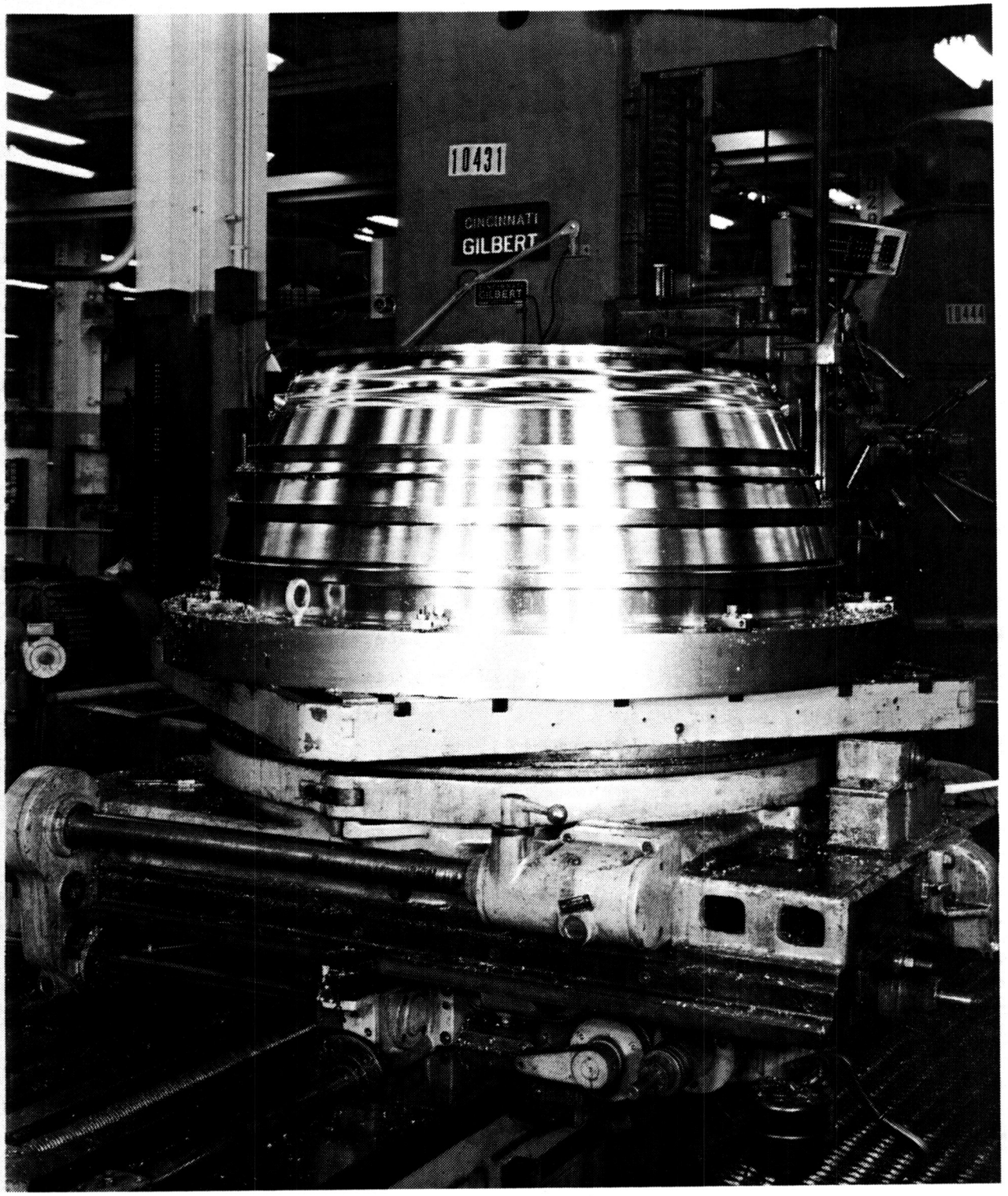

Figure 138. LPT Casing in Fabrication.

ample time remains to finish-machine the support before it is needed for engine assembly.

Instrumentation rework drawings have been issued for this part and have been released to AEMO for inclusion in the machining cycle.

Cooling Manifold for LPT Active Clearance Control

The aft portion of the manifold has been completed, but final inspection has identified minor discrepancies requiring local rework. The forward portion of the manifold has all detail parts fabricated and is ready to proceed into the welded and brazed assembly.

Instrumentation rework drawings have been issued and combined with the manifold order for inclusion in the fabrication cycle.

Adequate time remains for completion of the manifold assembly to meet ICLS assembly.

Work Planned

- Complete LPT casing
- Complete machining of outer duct support
- Complete fabrication of cooling manifold
- Trial-fit support with attaching hardware
- Follow support through instrumentation and engine build

4.2.2.4 LPT Shroud (and Seals) Hardware

All five stages of shroud segments, inner and outer transition-duct segments, insulation for the shrouds and transition ducts, and the strip seals for between the nozzle and duct segments have been ordered for the ICLS. Fabrication is in progress, and scheduled deliveries meet the required dates for ICLS build-up.

Shrouds For Stages 1 Through 5

All five stages of the LPT honeycomb shrouds are being fabricated. A temporary hold on manufacturing was released after the dimensional changes were implemented to relieve anticipated assembly problems. All outstanding drawing changes have been incorporated into the fabrication order. Material for the shrouds has been obtained by the vendor, and all the fabrication and assembly tooling for the shroud has been obtained.

The promised delivery date has been established well in advance of the date required to meet the ICLS buildup.

The insulation blankets for the ICLS LPT are essentially complete. This includes the insulation blankets over the Stage 1 nozzle, over the Stages 2 through 5 nozzles, Stages 1 through 5 shrouds, over the outer transition duct, and under the inner transition duct. Currently, parts are being inspected at the vendor's plant and are expected to be delivered ahead of the required date to meet the ICLS build-up.

Transition Ducts

Outer Ducts - During this reporting period, 38 outer-duct castings were received. Distortion was observed in all castings, to varying degrees, when an attempt was made to clamp castings into the machining fixture. The duct castings were returned to the vendor and were individually inspected for distortion. Inspection results were recorded by the vendor and were analyzed by GE personnel. Using the inspection results, the duct castings were separated into acceptable and unacceptable lots. The acceptable castings were returned to GE while the machining fixture was relieved to allow for part-to-part dimensional variation (within drawing requirements) in the castings.

Meanwhile the balance of the original-order, outer-duct castings were also inspected and the data transmitted to GE for analysis. All castings in the balance were determined to be acceptable, and the parts have been shipped.

The vendor has been instructed to provide additional castings to replace those rejected from the original shipment. These "replacement" castings are spares and are not required for the ICLS engine buildup.

Sixteen of the eighteen segments which compose an engine set of outer ducts are now being machined in the first setup. A second setup will follow to complete the full set of parts. Instrumentation rework drawings have been issued, released to AEMO, and will be incorporated into the machining cycle.

Inner Ducts - Nineteen inner-duct castings were received from the vendor (Bescast) during this reporting period, and machining was started immediately. During the machining process, 16 of these 19 castings set up for the first machining were inadvertently mismachined and had to be scrapped. The balance of the inner-duct casting order (25 pieces) was subsequently received, and machining was restarted. This provided a sufficient number of casting segments to machine a complete engine set. Replacement castings for the 16 scrapped parts have been reordered.

Inner-duct machined segments are scheduled to be completed well in advance of the deadline for engine assembly. Instrumentation rework definition has been issued and released to AEMO for incorporation into the machining cycle.

Strip Seals - The strip seal that fits between adjacent nozzle segments, and others that fit between the transition duct segments, remain on order. Partial deliveries of several seals have already been made. No problem has been identified concerning the fabrication of the remaining strip seals which are scheduled for delivery well in advance of the required date to meet ICLS buildup.

Work Planned

- Receive remaining seal strips
- Receive LPT shrouds and insulation blankets
- Trial-fit shrouds and insulation into LPT casing
- Follow inner and outer ducts through machining
- Trial-fit ducts into supporting hardware
- Follow ducts through instrumentation and into engine assembly

4.2.3 Bearings, Systems, Drives, and Configuration Fabrication

All hardware is proceeding through manufacturing cycles. Hardware from the FSFT is now available to be reworked for the ICLS engine. Rework will be accomplished during the next reporting period.

The manufacturing of the LPT shaft is proceeding on schedule with no major problems. The No. 5 housing has completed the welding cycle, and machining is proceeding.

4.4 ICLS TEST FACILITIES ENGINEERING

Technical Progress

- Completed design of inlet tooling for bellmouth and acoustic inlet
- Completed site installation drawing
- Completed fabrication of engine mount and dummy engine, initiated trial fit of engine cowling at Mojave
- Initiated work on definition of design requirements for slave systems

Work Planned

- Complete fit of engine mount and cowling to dummy engine and ship hardware to Evendale
- Finalize slave system requirements and start final design
- Complete fabrication of engine-mount links

5.0 TASK 5 - PROGRAM MANAGEMENT

5.2 CONFIGURATION MANAGEMENT

Technical Progress

Continued to release the E^3 Multiple Engine Buildup Parts List (MEBUL) and to provide buildup parts list to Assembly as scheduled.

Work Planned

Continue work schedule in accordance with contractural requirements.

EXHIBIT B - QUALITY ASSURANCE

Technical Progress

During this period, the following has been accomplished:

- Monitored the rebuild and check-out of the Phase II Stage 1-10 compressor at Evendale, the shipment to Lynn and set-up for test, and the mechanical check-out, and mechanical/aerodynamic performance testing to date. Special attention was given at the start-up of testing to ensure that Lynn test facility modification had corrected the questionable inlet icing problem.

- Maintained cognizance of the successful testing of the Full-Scale Fan Test in Lynn completed in November 1981

- Completed the upgrading of the last of the catalog hardware to be contractually required Engineering Class "N"

- Coordinated the on-site review at Evendale of hardware control and assembly practices and records by the NASA Product Assurance Office

- Continued close coordination between Design Engineering and the responsible quality control functions

Work Planned

- Monitor the assembly of the core engine modules and the final core engine assembly with target completion in late June. Audit the engine buildup record, the setup and check-out of the engine in the test cell, and the initiation of testing in late July.

- Follow the progress of the 10B Compressor Rig Test at Lynn and the shipment/receiving back at Evendale at the completion of testing

- Continue to monitor and review all aspects of the program participating in program and design reviews to ensure compliance with the Quality Assurance Program Plan. Also, maintain close contact with E^3 Engineering to assist in the expediting of hardware while maintaining the required quality-control discipline.

- Maintain continued interface with NASA Product Assurance Manager and designated AFPRO offices at Evendale